

MEASUREMENTS OF OCULAR COUNTERROLLING DURING LINEAR
ACCELERATIONS USING AN ELECTROMAGNETIC SCLERAL SEARCH COIL
SYSTEM

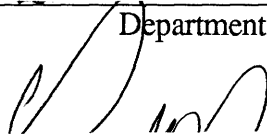
by
Glenn W. Law
B. S. A. E., University of Michigan, 1989

Submitted to the Department of Aeronautics and Astronautics
in Partial Fulfillment of the Requirements for the
Degree of Master of Science
in Aeronautics and Astronautics
at the
Massachusetts Institute of Technology
August, 1991

© Massachusetts Institute of Technology 1991
All Rights Reserved

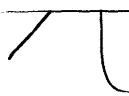
Signature of Author _____

Department of Aeronautics and Astronautics
July 31, 1991



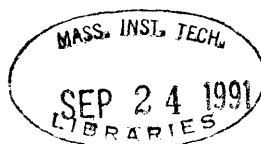
Certified by _____

Prof. Laurence R. Young
Thesis Supervisor
Professor of Aeronautics and Astronautics



Accepted by _____

Prof. Harold Y. Wachman
Chairman
Departmental Graduate Committee



**MEASUREMENTS OF OCULAR COUNTERROLLING DURING LINEAR
ACCELERATIONS USING AN ELECTROMAGNETIC SCLERAL SEARCH COIL
SYSTEM**

by
Glenn W. Law

Submitted to the Department of Aeronautics and Astronautics
in Partial Fulfillment of the Requirements for the
Degree of Master of Science
in Aeronautics and Astronautics

ABSTRACT

Lateral accelerations have been shown to elicit ocular counterrolling in human subjects in the direction of the acceleration. Past experiments of this type have used a photographic method of data acquisition which provided a data rate of 3 Hz. For the linear accelerations, this method is much too slow since it can not capture fast phase motions such as saccades.

The main purpose of this experiment was to record real-time, high bandwidth measurements of ocular counterrolling during linear accelerations. To perform this task, a scleral search coil system, which can monitor real-time eye movements, was mounted on the MVL linear accelerating sled. Six subjects were sinusoidally accelerated at 0.2 g and 0.6 g at four different frequencies. Each of these sessions was conducted twice. Data was taken at 200 Hz.

This experiment has shown that there are torsional saccades in the eye motion during linear accelerations, which result in discontinuities in the position trace. For this reason, the cumulative eye position trace, which neglects the saccades, is a much better indicator of ocular counterrolling than the position trace.

The ocular counterrolling responses were found to have decreasing gains and decreasing phase lags with increasing frequency. The trend of decreasing phase lag does not agree with the existing models of Hannen [1966] and Young and Meiry [1968].

Thesis Supervisor: Professor Laurence R. Young
Professor of Aeronautics and Astronautics

ACKnowledgements

There were a lot of people who helped me get through the last two years, which were not the best years of my life but were interesting nonetheless, and deserve thanks.

To my advisor, Professor Laurence Young, for inviting me into the MVL and allowing me the opportunity to work on a Shuttle mission. It was a pretty hectic two years because of the mission, but all in all it was very interesting. And it gave me a lot of frequent flyer mileage.

Other MVL employees who deserve thanks:

To Dan Merfeld for all his help on everything. It's hard to be a boss as well as a friend, but Dan could do both very well.

Sherry Modestino. How can I possibly thank her? It's like thanking your mother for bringing you up right. But thanks for making life much easier and for keeping us all well fed.

To Jim Costello, for saving my butt too many times to count. His knowledge of everything was greatly needed and appreciated at usually the worst possible times.

To Kim Tseko, for always providing a smile and a laugh even during the worst of times. Just talking to her brightened up a rotten day (of which I had many).

To Beverly Linton for handling all the paperwork stuff that I know I'd screw up.

And then there are the MVLers of past and present.

First and foremost, to Jock Christie for being my hero and role model during my stay here, as well as for the rest of my life. Also for giving me more nicknames than I care to remember and for making me feel guilty every time I try to throw away a ketchup packet or a piece of paper. Just knowing him has made me a better person, and I feel like I've come one step closer to Jockness.

To Keoki Jackson, for showing me that there are fun people at MIT and in Boston. If I hadn't met him, there is no doubt in my mind that I would have gone insane from boredom a long time ago. The roadtrips, beach trips, and parties broke up the monotony of life. Mardi Gras, Cape Cod, Rafting, the Jimmy Buffet party (I really am sorry for drawing on you), DC trips, the trip to Florida for the Space Shuttle launch.

To Brad McGrath, for making me ill for weeks after each of his return visits. He is the best bad influence I ever had. Mardi Gras, Rafting (Jock's car and bread crumbs to my face), the Florida trip.

To Cheryl Blanford, for everything. The long talks, the fig newtons, and those big pretzel things. If anyone deserves a good life, it's Cheryl.

To Tom Mullen, for all the basketball games and beach trips and for being a great all-around guy.

To Gail Standish for trying to bring a little culture into my life and trying to show me that there is more to life than just partying. (Which, for the most part, failed. But thanks for trying.) See you in Cali.

To Dava Newman for just being Dava (everyone who knows her understands what this means).

To Nick Groleau for his computer knowledge as well as all the computer games we played while waiting for our next astronaut subject.

To Mark Shelhamer, for giving me a very small portion of his vast knowledge before leaving.

And for the non-MVLers:

To Dave Darmofal for being the best roommate (mainly because we never saw each other) and for citing my one and only publication in his thesis.

To Caroline Kert, for being a great bud even though we don't talk for months at a time. Thanks also for bringing me to Boston and giving me a place to stay when I needed it.

To Eliot Young, for being a nut.

To Anthony Rodriguez, for bringing humor to the Houston and Edwards trips (like we needed any more).

To Joan Law, my mother. Who else did I have to call every two weeks or so and spew on about everything that's going wrong with my life, and have her laugh at it all? I guess that's what mom's are for.

To Budweiser and Burger King, for obvious reasons.

To Sam Malone and the rest of the cast of Cheers for bringing me laughter from 7:00 to 7:30 every weekday night (plus the bonus Thursday night at 9:00). For lines like "I'm not a sad guy, I'm a happy horny guy" and "Isn't it great that I can make my own fun."

Like I said earlier, it's been a very interesting two years. I've met some very interesting people that I hope to know for a very long time, and be able to call up someday and say "hey, can I sleep on your couch for a couple of days?"

Research funding has been provided by NASA grants NAG2-445 and NAS9-16523.

Table of Contents

Chapter 1	Introduction	11
	1.1 Purpose of Experiment	11
	1.2 Organization of Thesis	11
Chapter 2	Background	13
	2.1 Previous Ocular Counterrolling Experiments	14
	2.2 Data Acquisition and Analysis	35
	2.3 The Scleral Search Coil Method	43
Chapter 3	Equipment	46
	3.1 The MIT Sled	46
	3.2 The Scleral Search Coils	49
	3.3 The Magnetic Field Generating Coils	51
	3.4 The Sled Chair	53
	3.5 Controlling the Sled	56
Chapter 4	The Experiment	59
	4.1 Experiment Design	59
	4.2 Protocol	62
	4.3 Subjects	65
	4.4 Data Analysis	66
Chapter 5	Results	70
	5.1 Comparison to Previous Experiments	96
Chapter 6	Conclusions	102
	6.1 Suggestions for Further Research	103
Appendix A	Reconfiguring the Sled	105
Appendix B	Setup for Control of Sled with Function Generator	108
Appendix C	CNC Scleral Coil System Manual	110
Appendix D	Coil Calibration	125
Appendix E	Subject Preparation	128

Appendix F Scleral Coil Insertion/Removal	130
Appendix G Consent Statement	132
Appendix H Setup for Sled Run	143
Appendix I Program Listings	146
References	207

List of Figures

2.1	Miller ocular counterrolling tilt chair.	15
2.2	Counterrolling as a function of body tilt for Miller's experiments.	16
2.3	Counterrolling as a function of body tilt for Kirienko's experiments.	18
2.4	Slow rotating chair used by Diamond and Markham.	18
2.5	Counterrolling as a function of body tilt during constant velocity rotation from 0° to 360°.	20
2.6	Counterrolling as a function of body tilt during rotations from 0° to 90° right ear down to 90° left ear down and back to 0°.	20
2.7	Counterrolling response to sinusoidal linear accelerations.	22
2.8	Comparison of the effects of body tilt and centrifugation on ocular counterrolling.	24
2.9	Counterrolling responses for tilting and for centrifugation.	25
2.10	Counterrolling response as a function of the lateral force in tilt and centrifuge experiments.	25
2.11	The MVL Rotating Dome.	27
2.12	Parabolic flight path of the C131B.	30
2.13	Parabolic flight path of the KC-135.	30
2.14	Tilting device used in the C131B parabolic flight experiments.	31
2.15	Counterrolling as a function of the magnitude of gravitational force and the angle of tilt.	31
2.16	Counterrolling response versus lateral gravito-inertial force in weightlessness.	33
2.17	Projector system used by Diamond and Markham for analysis of ocular counterrolling.	37
2.18	Contact lens patterns used in SL-1 and D-1 Shuttle missions.	39
2.19	Torsion coil used by Malan.	44
3.1	The MIT linear accelerating sled and cart.	47
3.2	MIT sled operating range.	48
3.3	The two types of scleral search coils.	50
3.4	Coil system in lateral upright position.	57

4.1	Ocular counterrolling produced by the rotation of the force vector.	60
4.2	Comparison of the effects of rotation and linear acceleration on ocular counterrolling.	61
4.3	The four frequencies of sled motion for the present experiment.	64
4.4	Diagram of the steps involved in analysis of data.	67
5.1	The four channels that are monitored during the experiment.	71
5.2	Ocular counterrolling response during four frequencies at 0.2 g.	72
5.3	Ocular counterrolling response during four frequencies at 0.6 g.	73
5.4	Close up views of blinks and saccades.	74
5.5	Cumulative eye position versus OCR position.	79
5.6	Curve fits for OCR position and cumulative eye position.	80
5.7	CEP gains and phases for all runs for subject A.	82
5.8	Bode plot for Subject A.	84
5.9	Bode plot for Subject B.	85-88
5.10	Bode plot for Subject C.	89
5.11	Bode plot for Subject D.	90
5.12	Bode plot for Subject E.	91-94
5.13	Bode plot for Subject F.	95
5.14	Hannen model and Young and Meiry model.	100

List of Tables

4.1	Subject profiles.	65
5.1	Number of saccades before and during the sled motion for all subjects.	76-78
5.2	Counterrolling for each subject for each run at 0.26 Hz.	98
5.3	Counterrolling values from three static OCR studies.	98

Chapter 1

Introduction

1.1 Purpose of Experiment

Previous studies of ocular counterrolling during linear accelerations have used photographs of the eye to track the motion of the eye at 3 Hz. A smooth sine curve was then fit to this data. At a data acquisition rate of 3 Hz, the photograph method can not catch fast phase eye motions, such as saccades, if they exist. Another setback of these previous studies was that the analysis method, which involved locating natural landmarks on the eye, took a considerable amount of time and introduced errors involved in locating these landmarks. The purpose of this experiment is to conduct the first real-time, high bandwidth study of ocular counterrolling during lateral sinusoidal linear accelerations. A scleral search coil system was mounted onto the MIT linear accelerating sled to acquire ocular counterrolling data at 200 Hz. With the coil system sampling at 200 Hz, torsional saccades can be located and removed. Six subjects were used in the experiment, and a small coil embedded in silicone rubber was inserted in each subject's eye during the run. Each subject was run at four different frequencies and two different maximum accelerations. The response to these motions are studied and presented.

1.2 Organization of Thesis

Chapter 2 provides a review of past ocular counterrolling experiments and the methods of data acquisition and analysis. The chapter not only describes the past studies of ocular counterrolling during linear accelerations, but also the past studies of ocular counterrolling in any form. These past studies include ocular counterrolling during head

rotation, during full body rotation, during rotation in a centrifuge, during parabolic flight, and with the influence of a rotating field of view.

Chapter 3 describes the equipment used for the present study. This includes a description of the previously existing equipment as well as the equipment that was built by the author to replace most of the old equipment. The method of running the equipment and the data storage technique are also presented.

Chapter 4 describes the experimental design and protocol for the present study. The data analysis techniques are also presented.

Chapter 5 presents the results of this study and compares these results with past studies.

Chapter 6 presents the conclusions of the study and presents suggestions for future research.

The Appendices describe in detail the equipment used in this study. Listings of programs used for analysis are also presented.

Chapter 2

Background

Ocular counterrolling (OCR) is known to be a direct indicator of the otolith sensing function. Ocular counterrolling was defined by Miller as "the conjugate rolling movement of the eyes around their lines of sight opposite to the lateral inclination of the head" [Miller, 1966]. By measuring OCR in different states, the involvement of the otoliths in detecting gravitoinertial forces can be better understood.

Ocular counterrolling was first documented by John Hunter in 1786 in his Observations of Certain Parts of the Animal Economy. It did not get studied in depth, though, until the early twentieth century. In 1928, Kompanajetz observed OCR when the head was tilted and concluded that OCR was regulated by the otolith organs and not by the semicircular canals, as was then believed [Kompanajetz, 1928].

In the 1960's, with more humans going into space and the discovery of space motion sickness, the study of the otolith system became more important. The results from early experiments suggested that space motion sickness may be the result of a conflict between the otoliths and the visual system [Oman, 1987]. Since ocular counterrolling is the main measurement of the otoliths, the study of ocular counterrolling increased with the need to find a "cure" for space motion sickness. Preflight and postflight tests from the Spacelab missions have shown that there is generally a reduction in OCR and therefore a decrease in gain in the otolith system [von Baumgarten, 1986]. This decreased gain in the otolith system has surfaced as a possible cause of space motion sickness. Also, some experimenters suggest that an asymmetry between the left and the right otolith, which can be compensated for on the ground, is a possible cause of space motion sickness [von

Baumgarten, Thulmer, 1978; Lackner et al., 1987; Diamond et al., 1990; Diamond, Markham, 1991].

2.1 Previous Ocular Counterrolling Experiments

Early experiments for measuring OCR only involved the subject tilting his head a certain angle and then measuring the rotation of the eyes [Kompanejetz, 1928; Walton, 1948; Miller, 1961; Petrov, Zenkin, 1973; Fluor, 1975; Galoyan et al., 1976]. It was soon found that the action of tilting the head provides proprioceptive cues and reduces the OCR reaction [Wapner et al., 1951; Cohen, 1961]; and therefore the experiments called for whole body rotation with the head restrained from moving, usually with a biteboard. An ocular counterrolling tilt chair was designed by Miller at the U. S. Naval School of Aviation Medicine (now called the Naval Aerospace Medical Research Laboratory, NAMRL) which was capable of tilting the entire body through angles from -90° to $+90^{\circ}$ as shown in Figure 2.1 [Miller, 1961, 1966, 1969; Miller et al., 1965; Miller et al., 1968; Miller, Graybiel, 1971, 1972; Graybiel et al., 1967]. Velcro straps and a saddle mount were used to secure the subject in a standing position within the chair. The chair was rotated around the subject's line of sight, and the tilt position was read from an angle dial placed on the rear of the chair. The rotation angle as shown on the angle dial was accurate to 0.5 degrees. Miller's chair only measured static. The chair was rotated to each selected angle by means of a hydraulic pump operated by the investigator. Many photographs of the eye were then taken at each position, and the OCR angle was plotted against the tilt angle. Data from a typical subject is shown in Figure 2.2. Many tests were conducted using the Miller tilt chair including:

1. Measurement of OCR in normal subjects.
2. Measurement of OCR in labyrinthine-defective subjects.
3. Measurement of OCR in normal gravity and hypogravity.
4. Measurement of changes in amount of OCR as a function of duration of body

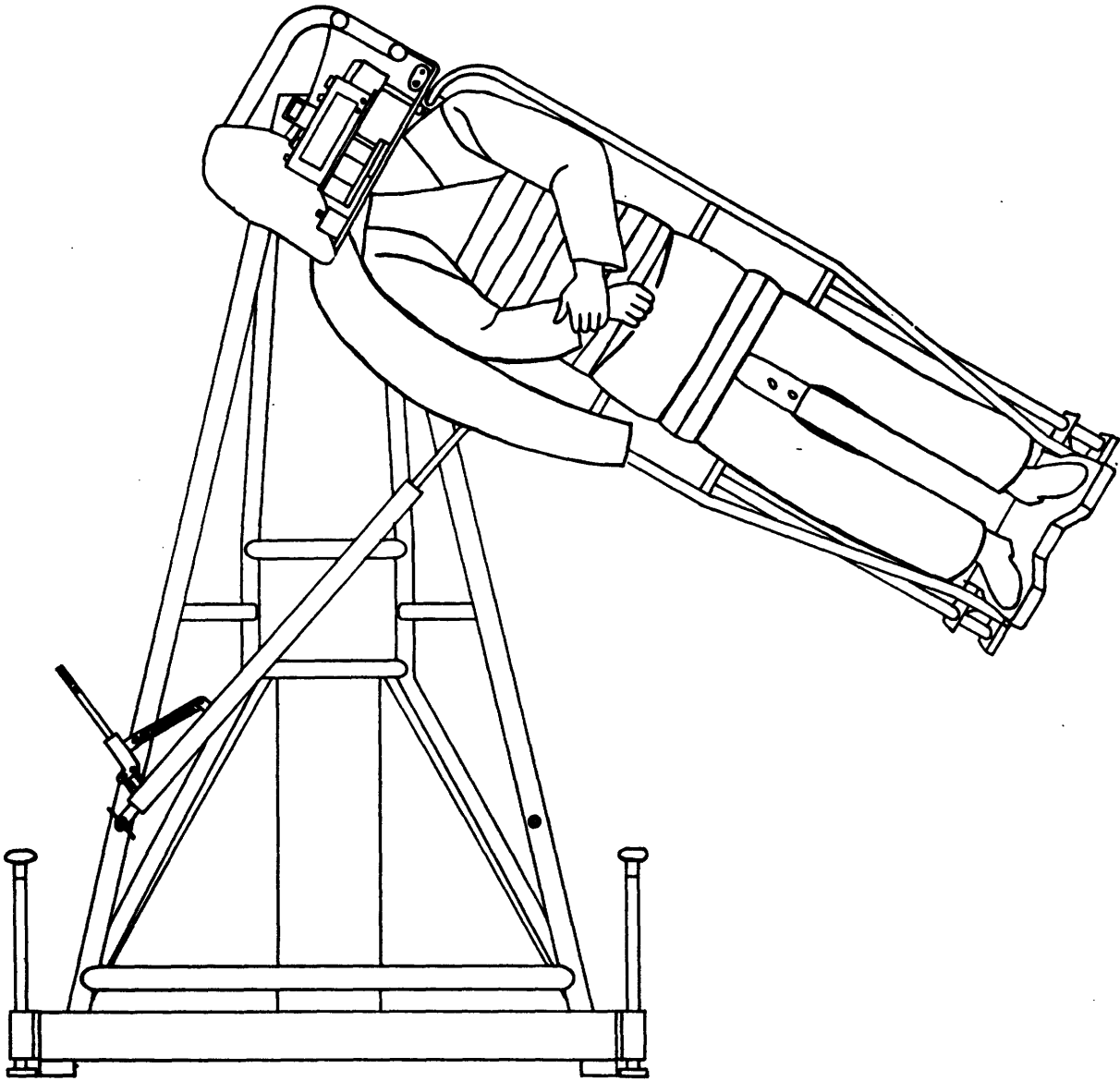


Figure 2.1 Miller ocular counterrolling tilt chair. The chair, shown in the 60° position, was capable of being rotated from -90° to $+90^\circ$. Notice the camera mounted in front of the subject's face. From Miller, Graybiel [1972].

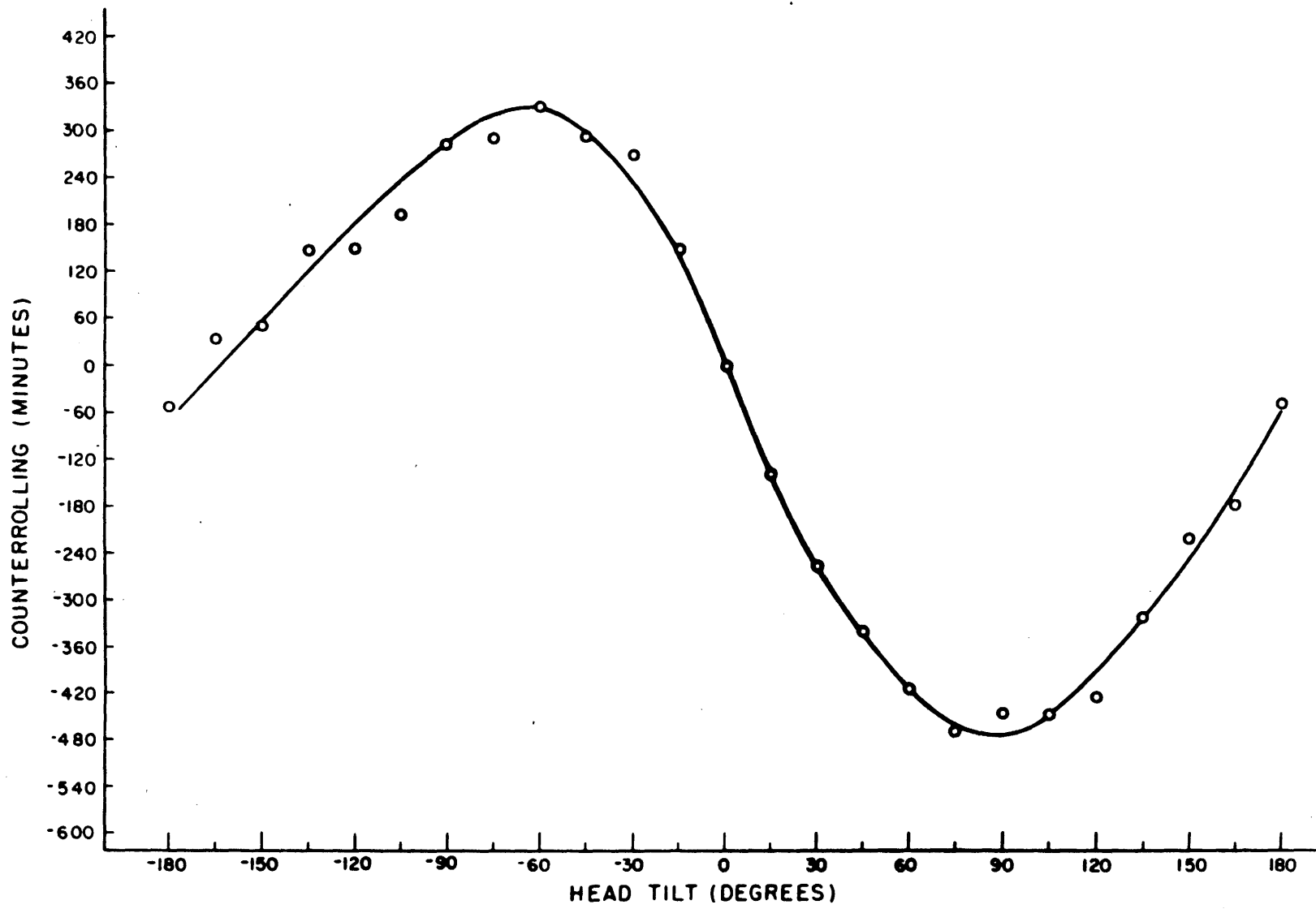


Figure 2.2 Counterrolling as a function of body tilt. This plot is from the average of many subjects. From Miller [1969].

tilt.

Some of the significant results from these experiments are:

1. Counterrolling was always found to occur opposite to the lateral component of head tilt and to increase rapidly up to maximum at a head tilt angle between 60° and 70° . Counterrolling decreased from this point on, but at a lesser rate than it increased (see Figure 2.2).
2. There is a relatively high ratio of counterrolling to body tilt in the first 50 to 60 degrees, and therefore the use of greater angles of tilt is unnecessary for obtaining an indication of the otolith function.
3. There is a constant fluctuation in counterrolling during sustained body tilt.
4. Counterrolling is not affected by the order (clockwise or counterclockwise) in which the measurements are made.
5. In labyrinthine-defective subjects, the counterrolling response was much lower than in the normal subjects. This strengthened the claim the OCR is a direct indication of otolith function.
6. In labyrinthine-defective subjects, reduced counterrolling will occur when tilted opposite the more defective side.
7. The angle of ocular counterrolling position does not decay during extended durations (8 hours) of body tilt.

The Department of Otolaryngology at St. Michael's Hospital in Toronto uses a similar chair and a similar protocol for their experiments [Kirienko et al., 1984]. Each subject underwent two tests:

1. Rotation from 0° to 45° in both directions at 15° increments.
2. Rotation from 0° to 45° in both directions at 5° increments.

Typical results for a subject who underwent two of each test are shown in Figure 2.3. The two major findings from these tests were:

1. Greater OCR values were found for right side down tilts than for left side down tilts. This was also found by Diamond et al. [1979].
2. Static OCR results were found to be very similar in magnitude and gain to the dynamic OCR results from Diamond and Markham.

Diamond and Markham also use a similar chair for their studies [Diamond et al., 1979; Diamond, Markham, 1983]; but their subjects are rotated at a constant angular velocity of $3^\circ/\text{sec}$, which is low enough to not induce semicircular canal response.

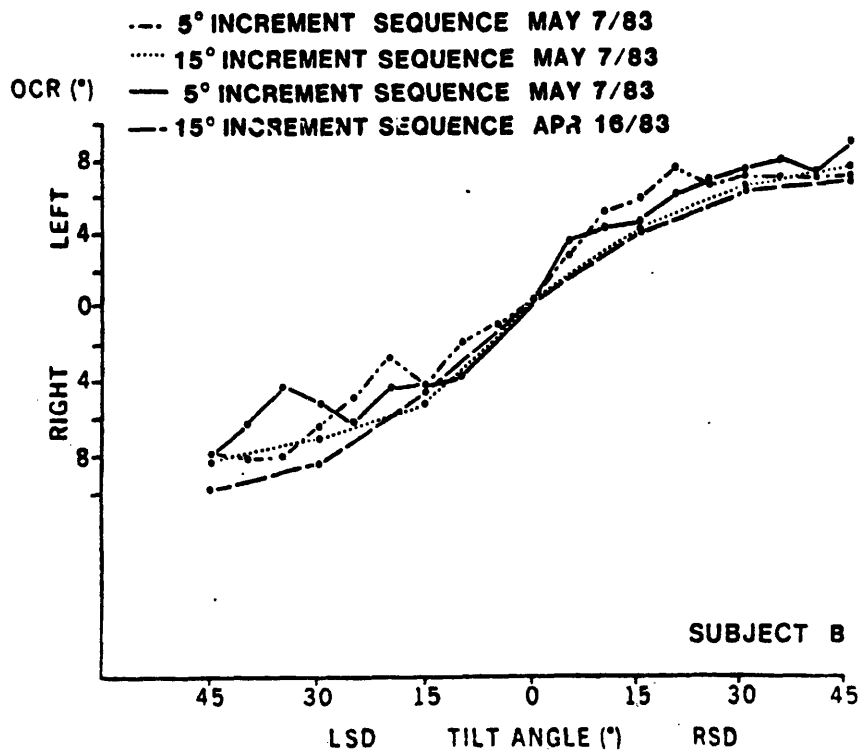


Figure 2.3 Counterrolling as a function of body tilt for one subject during four different testing sessions. From Kerienko, et al [1984].

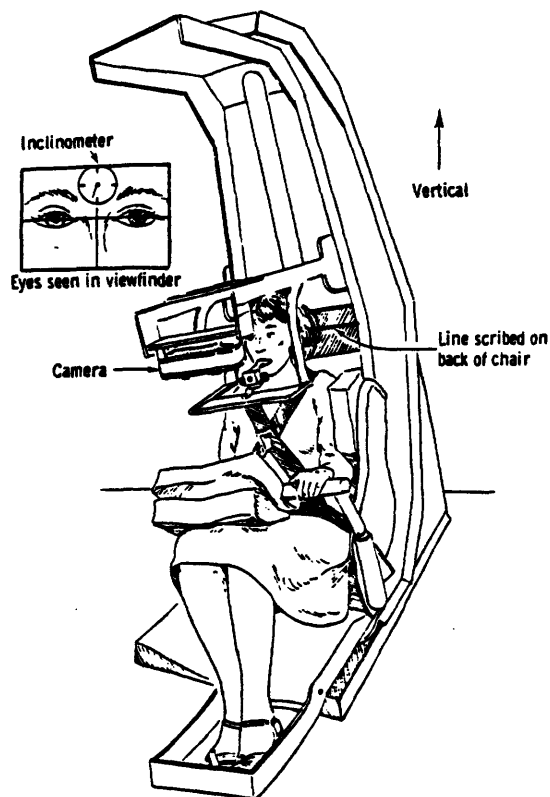


Figure 2.4 Slow rotating chair used by Diamond and Markham. The chair rotates through 360° at a rotation velocity of 3°/sec. From Diamond, et al [1979].

Diamond and Markham have reported that their subjects show enhanced ocular counterrolling while rotating dynamically as compared to static measurements. The chair, as shown in Figure 2.4, is motor driven to accelerate and decelerate during the first and last 20° of rotation at a rate of 0.21°/sec². Two different procedures were used for this study:

1. Subjects are rotated at a constant velocity from 0° to 360°. Photographs are taken at each 10° of rotation [Diamond et al., 1979].
2. Subjects are rotated at a constant velocity from 0° to 90° right ear down, held for 30 seconds, rotated at a constant velocity in the opposite direction to 90° left ear down, held for 30 seconds, and rotated back to 0°. Photographs are taken at each 10° of rotation and at each 10 seconds while at the 90° tilt position [Diamond, Markham, 1983].

Typical counterrolling results from these procedures are shown in Figure 2.5 and Figure

2.6. Significant results from these tests include:

1. More counterrolling was observed when subjects were tilted to right than left. This was also observed by Kompanajetz [1928] and Kirienko et al. [1984].
2. The downward eye shows more counterrolling than the upward eye.
3. The average OCR under static or dynamic tilt is approximately 12°, or ±6° each direction.
4. The amount of counterrolling was negatively correlated with age.
5. In subjects with unilateral labyrinthine dysfunction, reduced counterrolling will occur when tilted to the side opposite the defect. This result agrees with the results of the Miller experiments.
6. The angle of OCR position does not decay during 10 minutes of body tilt. This agrees with the findings of Miller and Graybiel [1972].
7. In a sustained tilted position, OCR is not constant and can vary randomly by as much as 4°.

Ocular counterrolling is induced by the rotation of the gravity vector around the roll axis in the above experiments. OCR can also be induced by the rotation of the gravito-inertial force (GIF) vector around the roll axis. This is achieved by accelerating and decelerating a subject in the horizontal plane, which results in dynamic ocular counterrolling. Many tests of this type have been conducted at MIT using the Man-Vehicle Lab linear accelerating sled [Lichtenberg, 1979; Young et al., 1981; Lichtenberg et al.,

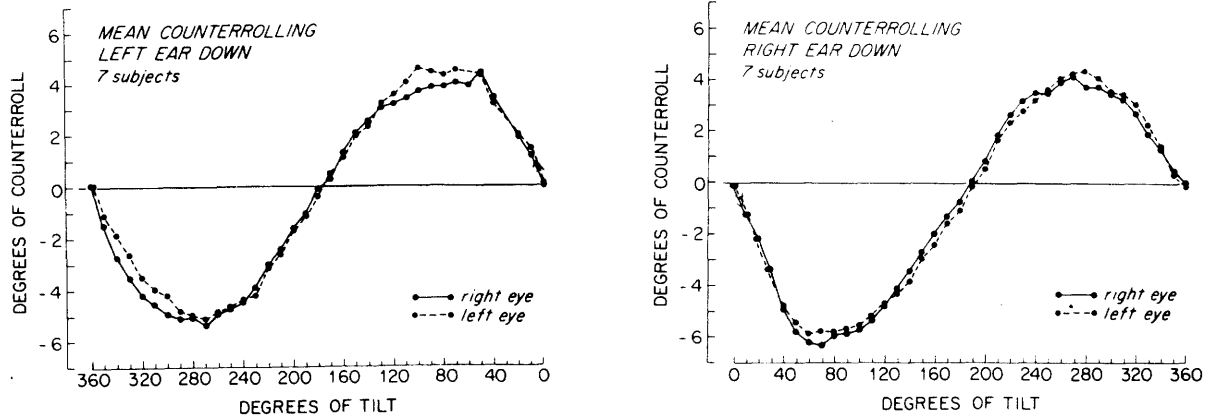


Figure 2.5 Average counterrolling as a function of body tilt for seven subjects during constant velocity rotation from 0° to 360° . The figure on the left is for rotations beginning with left ear down. The figure on the right is for rotations beginning with right ear down. Notice that in both plots, there is greater counterrolling for right ear down. Also notice that the downward eye shows more counterrolling than the upward eye. From Diamond, et al [1979].

DYNAMIC OCULAR COUNTERROLLING PROFILE

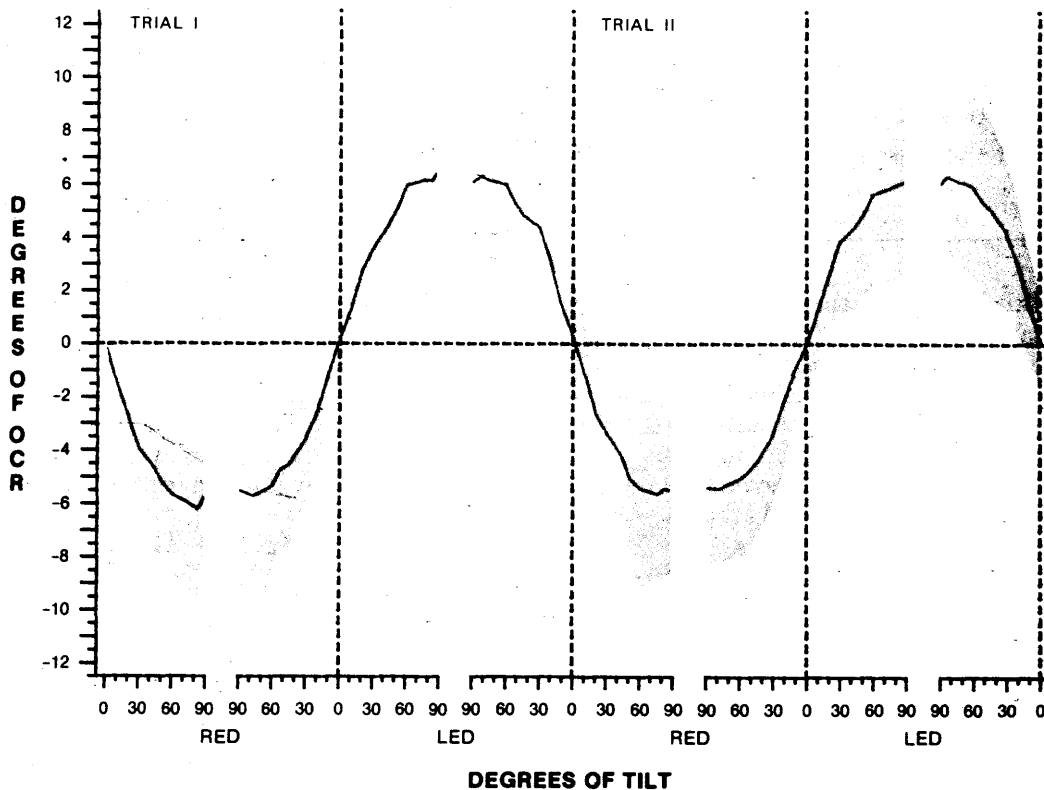


Figure 2.6 Counterrolling as a function of body tilt for sixteen subjects during rotations from 0° to 90° right ear down to 90° left ear down and back to 0° . The solid line shows the mean OCR and the gray band shows 1.5 standard deviations of the mean on each side. From Diamond, Markham [1983].

1982; Arrott 1982, 1985; Arrott, Young, 1986], which is fully described in Chapter 3.

Ocular counterrolling tests using the MIT sled include:

1. Lateral sinusoidal accelerations of 0.2 Hz, 0.4 Hz, and 1.0 Hz at 0.2-g [Lichtenberg, 1979].
2. Lateral step acceleration at 0.05-g, 0.1-g, 0.15-g, 0.2-g, and 0.3-g [Lichtenberg, 1979].
3. Lateral sinusoidal accelerations of 0.3 Hz at 0.1-g, 0.2-g, and 0.3-g [Lichtenberg, 1979].
4. Upright sinusoidal accelerations at a frequency of 0.4 Hz at amplitudes between 0.2-g and 0.8-g [Arrott, 1982, 1985].
5. Supine sinusoidal accelerations at a frequency of 0.4 Hz at 0.5-g or 0.8-g [Arrott, 1985].

Data from a typical subject is shown in Figure 2.7, and results of these tests included:

1. Resulting OCR for sinusoidal accelerations is sinusoidal.
2. Linear accelerations produce OCR similar to that produced by sinusoidal or static head tilt [Lichtenberg, 1979].
3. There is no habituation to repeated sled motions [Lichtenberg, 1979].
4. OCR response to linear accelerations is linear over a range of horizontal accelerations up to at least 0.3-g [Lichtenberg, 1979].
5. The phase lag of OCR increases with increasing sled frequency [Lichtenberg, 1979].
6. Linear accelerations produce an initial overshoot of OCR before it reaches steady-state [Lichtenberg, 1979].
7. The OCR response to linear accelerations is linear up to at least 0.8-g [Arrott, 1982].
8. Sensitivity of OCR in the upright position at 0.4 Hz was found to be about 3°/g (degree of OCR per g of head lateral GIF) [Arrott, 1982].
9. During linear accelerations at 0.4 Hz, the phase lag for both eyes is about 110° [Arrott, 1982].
10. Sensitivity of OCR in the supine position at 0.4 Hz was found to be about 1°/g [Arrott, 1985].
11. A change in the lateral component of GIF, without a rotation of the gravito-inertial vector, is an adequate stimulus for OCR [Arrott, 1985].

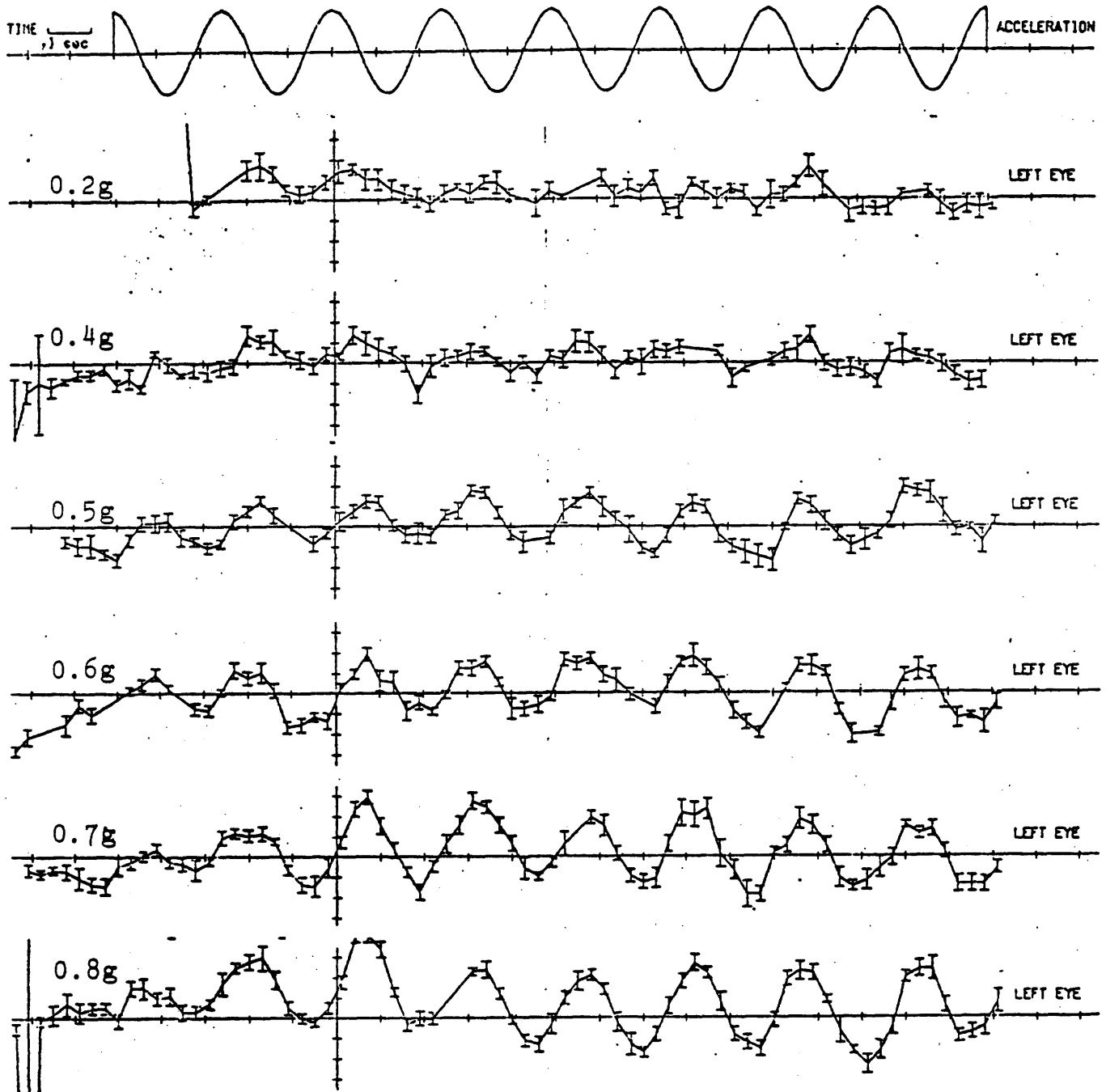


Figure 2.7 Counterrolling response of one subject to sinusoidal linear accelerations at six different acceleration levels. From Arrott [1982].

Ocular counterrolling can also be induced with the use of a centrifuge. With the subject facing toward or opposite the direction of motion, the rotation of the gravito-inertial vector in the centrifuge is similar to the rotation of the gravity vector when the subject is tilted in a tilt chair, as shown in Figure 2.8. Centrifuge experiments were conducted by Woellner and Graybiel [1959], which were later expanded by Miller and Graybiel [1971]. The subject was first tilted in the tilt chair to four tilt positions (15° , 30° , 43° , and 66° for Woellner and Graybiel; 25° , 50° , 58° , and 63° for Miller and Graybiel) and photographs were taken at each position. Then, the tilt chair, which was on the centrifuge, was spun up to a velocity that rotated the gravito-inertial vector to the same angles as in the tilt chair (15° , 30° , 43° , 66° ; or 25° , 50° , 58° , 63°). Significant results from the centrifuge experiments include:

1. For small angles of tilt, OCR for tilting and for centrifuge were similar; but for larger angles of tilt, the increased gravito-inertial force causes a greater increase in the centrifuge OCR (see Figure 2.9).
2. Subjects with labyrinthine defects revealed essentially no change in their counterrolling response with increased gravito-inertial force on the centrifuge (see Figure 2.9).
3. The counterrolling varied as a function of the magnitude of the lateral force even beyond the 1-g level (see Figure 2.10).
4. Beyond 1-g, counterrolling was found to increase as a direct and essentially linear function of the magnitude of the lateral force (see Figure 2.10).

From these results, it was hypothesized by Woellner and Graybiel [1959] and Miller and Graybiel [1971] that OCR is a result of the change in lateral GIF, rather than a rotation of the GIF vector. Results from Arrott [1982, 1985] agreed with this hypothesis.

Zero-g measurements of OCR have been taken during parabolic flights aboard special equipped aircraft as well as during space missions. The affect of space travel on ocular counterrolling was studied as early as Gemini flights V and VII [Graybiel et al., 1967]. Preflight and post flight measurements were taken using the Miller tilt chair on four astronauts and no change in ocular counterrolling was found, contrary to later studies. The Soviets also conducted similar preflight and postflight ocular counterrolling experiments on

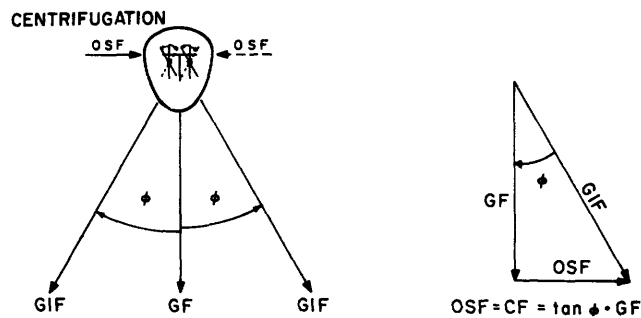
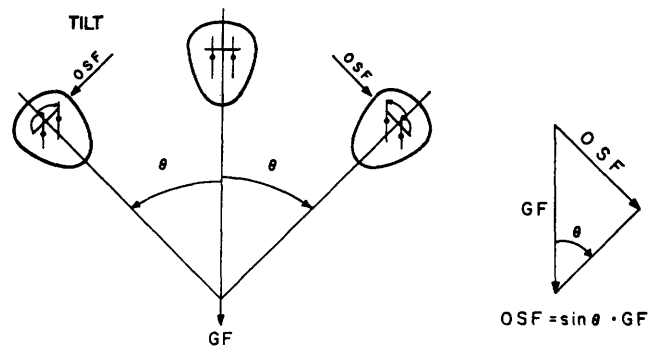


Figure 2.8 Comparison of the effects of body tilt and centrifugation on ocular counterrolling. Rotation produces a rotation of the gravity force (GF) while centrifugation produces the rotation of the gravito-inertial force (GIF). CF is centrifugal force and OSF is otolith shear force. From Miller, Graybiel [1971].

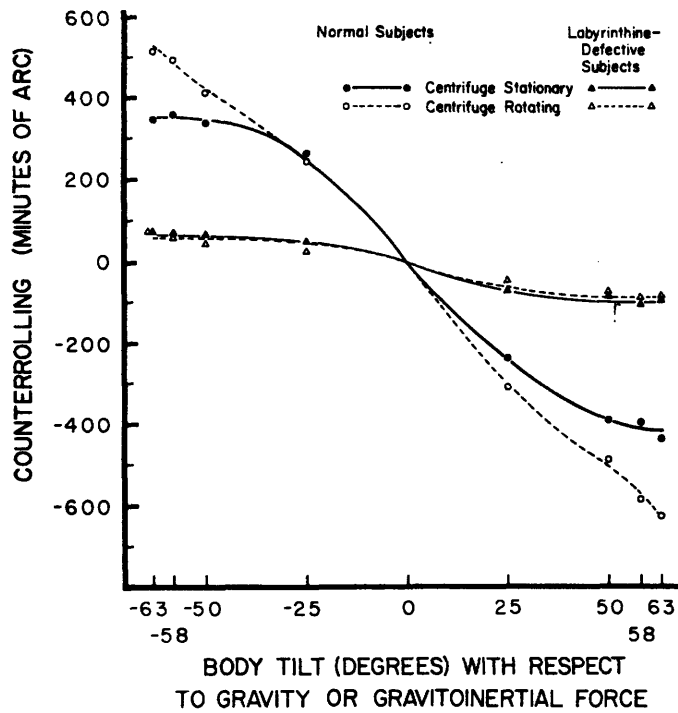


Figure 2.9 Counterrolling responses for tilting and for centrifugation of normal and labyrinthine-defective subjects. Notice that for small angles of tilt, OCR for tilting and for centrifuge were similar; but for larger angles of tilt, the OCR for centrifuge is greater. From Miller, Graybiel [1971].

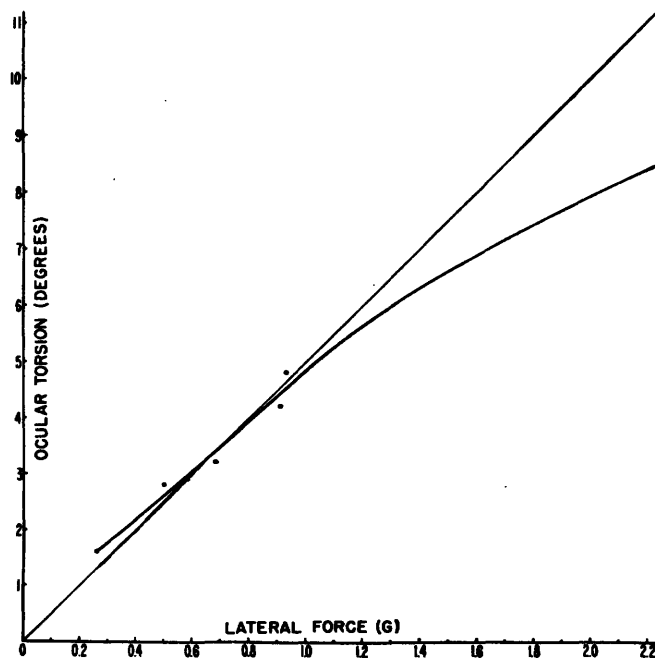


Figure 2.10 Counterrolling response as a function of the lateral force in tilt and centrifuge experiments. From Woellner, Graybiel [1959].

30 cosmonauts from the Soyuz and Salyut spacecrafts [Yakovleva et al., 1980, 1981, 1982]. The results from these studies showed an increase in ocular counterrolling, contrary to the later American studies which show a decrease in OCR. The method used by the Soviets is not clearly described, and therefore no speculations can be made concerning their results.

With the beginning of the shuttle era, more extensive studies of the affects of spaceflight on ocular counterrolling could be undertaken in the Spacelab module. Now, along with the preflight and post flight experiments, inflight experiments could be conducted as well. The first shuttle mission dedicated to the study of the vestibular system was the Spacelab-1 (SL-1) mission from November 29 to December 8, 1983. The experiments were conducted by three teams of investigators: one from MIT and Canada, one from Johnson Space Center and the University of Michigan, and one from the European Space Agency (ESA). The experiments were "aimed at assessing human vestibular and visual responses in space and are intended to clarify the presumed alteration in sensory and motor function in weightlessness" [Young et al., 1986a]. Instead of rotating the gravity vector or the gravitoinertial vector to induce rotation of the eyes, a different method was taken for the mission. Rotation of the visual field will also result in rotation of the eyes; in this case called ocular torsion instead of ocular counterrolling since there is no rotation of the gravity or gravitoinertial vector for the eyes to counterroll against. A rotating dome which filled the field of view was built at MIT to study this type of eye rotation as well as dynamic visual-vestibular interaction [Young et al., 1986b]. This rotating dome is shown in Figure 2.11. A video camera is located at the center of the dome to record the eye movements. Ocular torsion data from the dome was taken preflight, inflight, and postflight on four astronauts at rotations rates of 30, 45, and 60 deg/sec clockwise and counterclockwise. Dynamic ocular counterrolling data from the four astronauts was also taken preflight and postflight on the NASA linear accelerating sled, which was modeled after the MIT sled [Arrott, Young, 1986]. Subjects were sinusoidally

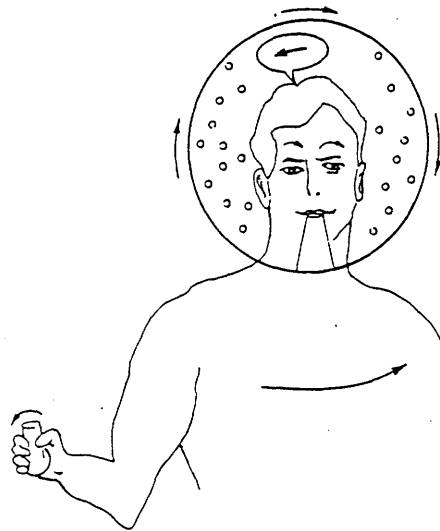
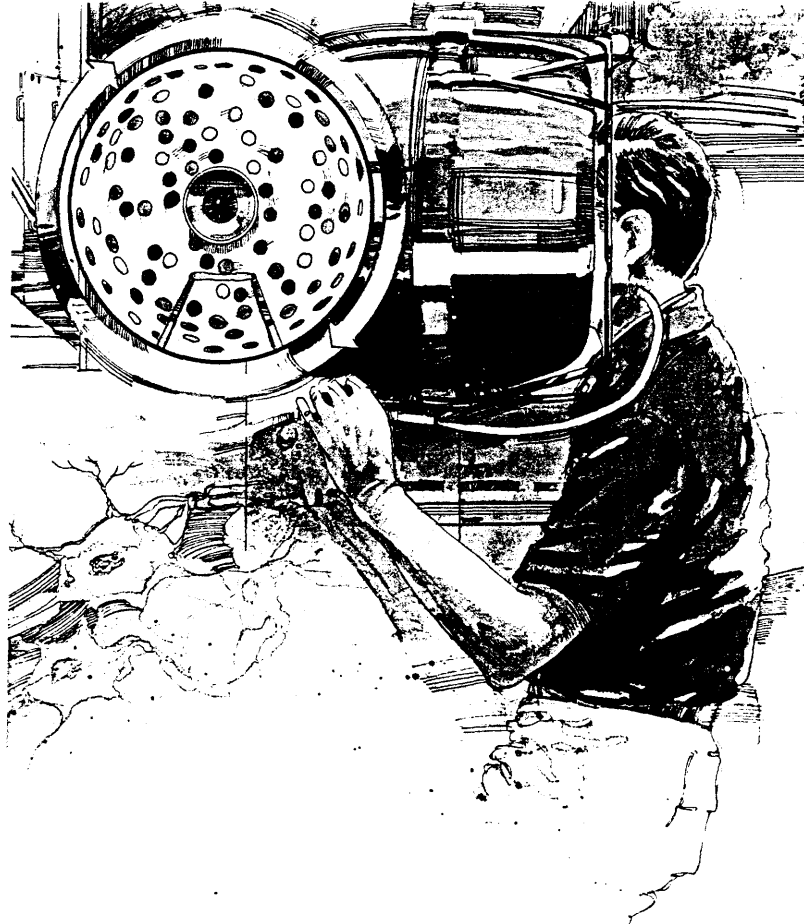


Figure 2.11 The MVL Rotating Dome. As the dome rotates clockwise, the subject's eyes also rotate clockwise with saccades counterclockwise. From Young, et al [1986].

accelerated at 0.61-g at frequencies of 0.42 Hz and 0.83 Hz for 12 and 25 seconds, respectively; and results from this experiment showed that OCR is decreased when measured on the day of landing and increases toward the preflight value during the week following weightlessness. The European investigators for the mission conducted preflight and postflight static ocular counterrolling measurements on a tilt chair similar to Miller's chair, with the main difference being that the European chair rotated around the subject's center of mass while Miller's chair rotated around the subject's line of sight [Vogel, Kass, 1986]. The subjects were rotated from 0° to 90° in both directions with measurements taken at each 15° increment. The results of the ESA experiments showed that:

1. The OCR-gain (OCR divided by tilt angle) is decreased after exposure to weightlessness. This is in agreement with the SL-1 sled experiments [Arrott, Young, 1986], but contrary to Soviet experiments [Yakovleva et al., 1980, 1981, 1982]
2. OCR-gain was higher when tilted to the left than to the right during preflight tests. This is opposite the results found by Kompanejetz [1928], Diamond, et al. [1979], and Kirienko et al. [1984].
3. OCR-gain is higher when tilted to the right than tilted to the left during the readaptation period after spaceflight.
4. OCR-gain for left tilt is decreased after spaceflight.
5. OCR-gain for right tilt remains unchanged after spaceflight.
6. There is an increased asymmetry between left and right tilts after spaceflight.

The second shuttle mission dedicated to the study of the vestibular system was the German D-1 mission from October 30 to November 7, 1985; and the MIT rotating dome and NASA linear accelerating sled were again used. Ocular torsion data from the dome was taken preflight, inflight, and postflight on five astronauts at 30, 45 and 60 deg/sec clockwise and counterclockwise. Preflight and postflight ocular counterrolling data was taken on the NASA sled during sinusoidal accelerations of 0.18 Hz and 0.81 Hz at 0.2-g and 0.30 Hz and 0.81 Hz at 0.7-g. Inflight data was also taken on the ESA Vestibular Sled during sinusoidal accelerations of 0.18 Hz and 0.81 Hz at 0.2-g. Significant results from the inflight sled tests were:

1. OCR induced by sinusoidal linear accelerations on the sled in microgravity exists despite the fact that the gravitoinertial vector reverses direction instead of rotating around the line of sight [Oman et al., 1988].
2. OCR induced by sinusoidal accelerations is reduced in weightlessness [Tse, 1990].

(The reason for the delay on the analysis of the SL-1 and D-1 ocular counterrolling data for the dome and the sled will be discussed in Section 2.2).

The third shuttle mission dedicated to the study of the vestibular system, the Spacelab Life Sciences 1 (SLS-1) mission, was scheduled to be launched in early 1986; but with delays in the shuttle launches, was finally launched in June 1991. Ocular torsion data was collected preflight and postflight by the author on the MIT rotating dome; and ocular counterrolling data was collected preflight and postflight by the author on the NASA linear sled during sinusoidal accelerations at 0.5-g at frequencies of 0.25 Hz, 0.42 Hz, 0.62 Hz, and 1.0 Hz and on the Miller tilt chair, which is on loan to MIT from the Navy, at 15° increments from 0° to 60° in both directions.

Keplerian parabolic flights aboard specially equipped aircraft have been used to simulate the zero-g environment of space. In the early parabolic tests, a C-131B was used [Miller, Graybiel, 1965; Miller et al., 1966]. Later, the more powerful KC-135 was used for the parabolic tests [Arrott, 1982, Lackner et al., 1987; Money et al. 1987; Diamond, Markham, 1988, 1991; Diamond et al. 1990]. Because it did not have enough power, the C-131B could only perform one parabola at a time, achieving zero-g for only five seconds, as shown in Figure 2.12. The more powerful KC-135 can perform a series of parabolas, each of which result in 25 seconds of weightlessness and 35 seconds of subjection to 1.8-g to 2-g, as shown in Figure 2.13. The tilting device used for the early C-131B experiments is shown in Figure 2.14. The two opposing chairs can be rotated to $\pm 50^\circ$ by a hand crank. The chair was rotated to one of five positions (0° , $\pm 25^\circ$, and $\pm 50^\circ$) and maintained for two parabolas. A photograph of the eye was taken at the end of the zero-g and the half-g periods. The same test under one-g conditions was conducted either during level flight or

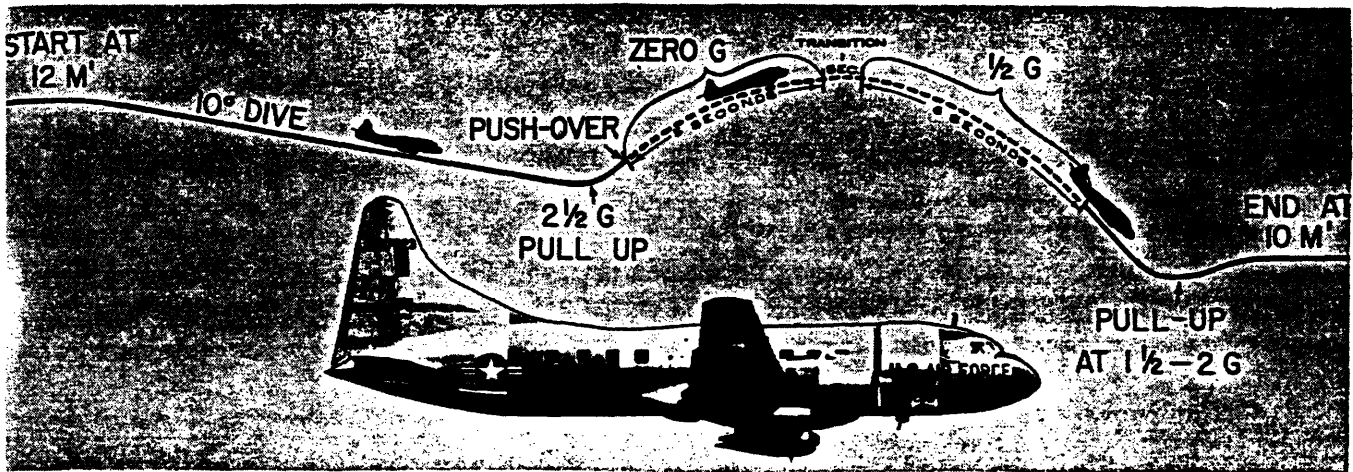


Figure 2.12 Parabolic flight path of the C131B. The C131B performed one parabola at a time, achieving zero g for only five seconds. From Miller, et al [1966].

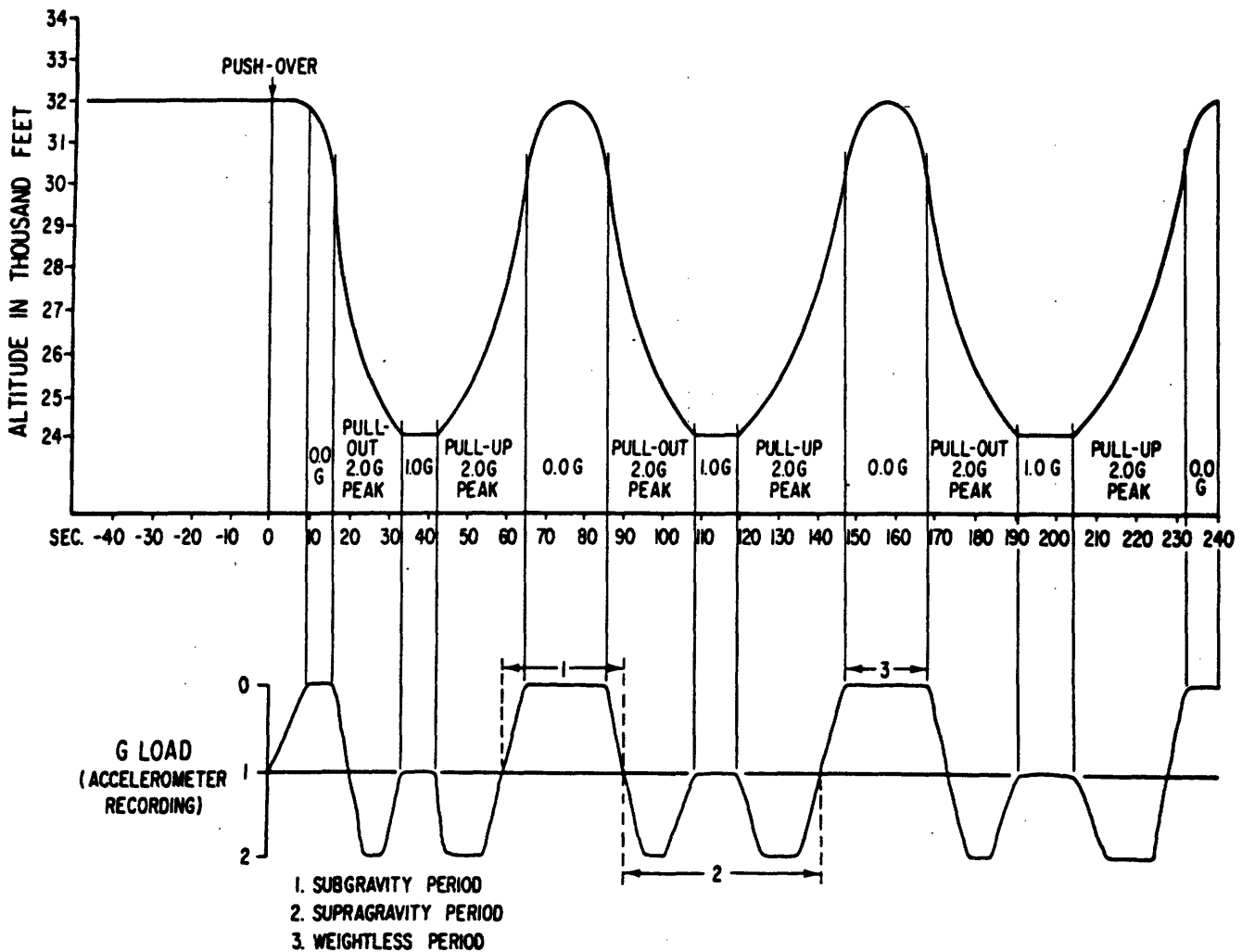


Figure 2.13 Parabolic flight path of the KC-135. The KC-135 can perform a series of parabolas, each of which result in 25 seconds of weightlessness and 35 seconds of subjection to 1.8-g to 2-g. From Lackner, et al [1987].

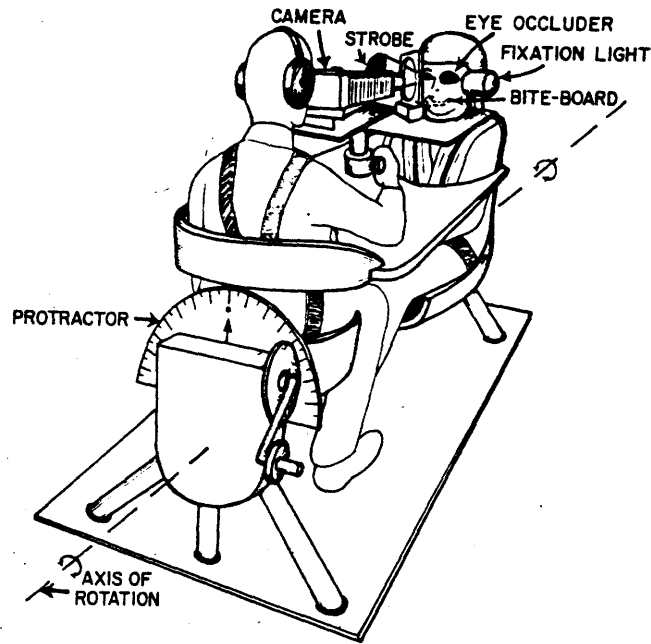


Figure 2.14 Tilting device used in the C131B parabolic flight experiments. Both the subject and the experimenter were rotated with the hand crank.. From Miller, et al [1966].

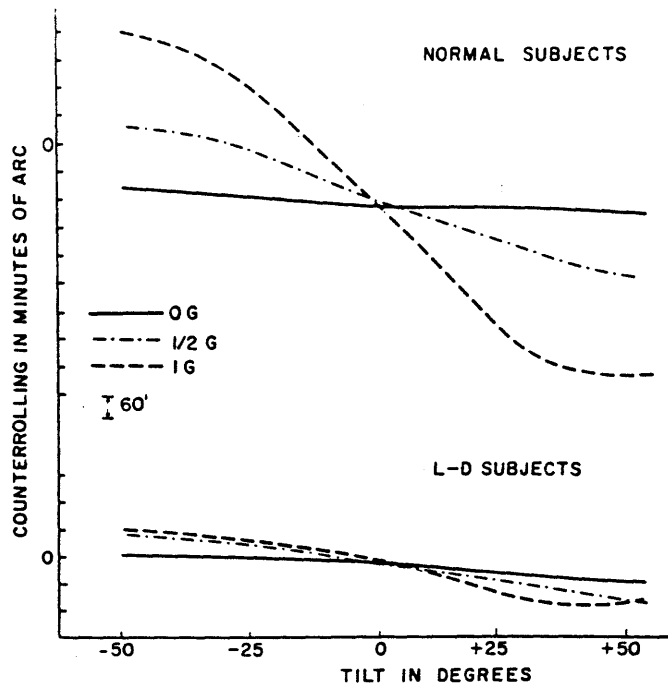


Figure 2.15 Counterrolling as a function of the magnitude of gravitational force and the angle of tilt for normal and labyrinthine-defective subjects. From Miller, et al [1966].

on the ground. The amount of counterrolling for the three conditions is shown in Figure 2.15, and the results showed:

1. The time period of OCR in response to the change in g-force occurs well within the short (5-6 seconds) periods of hypogravity.
2. No counterrolling occurred in zero-g when subjects were tilted rightward or leftward to 50°. Miller and Graybiel state that these results “provide the first quantitative evidence that the otolith organs in man are physiologically deafferentated when he is exposed to hypogravitational environments” [1965].
3. As the gravity force is reduced, counterrolling is reduced.
4. At half-g, the counterrolling is below the midpoint between one-g and zero-g, which suggests that there is a nonlinear relationship between OCR and g-force between zero-g and one-g.

In a followup study by Miller and Graybiel [1965], the parabolic trajectory was modified to produce the following subgravity levels: 0-g, 0.05-g, 0.10-g, 0.17-g, 0.20-g, 0.33-g, 0.50-g, 0.75-g, and 1-g. This test revealed the same results as the earlier test.

Experiments were conducted aboard the KC-135 to examine whether a change in the lateral component of the gravitoinertial vector is an adequate stimulus for OCR [Arrott, Young, 1981; Young et al., 1981; Arrott, 1982]. This was hypothesized by Woellner and Graybiel [1959] and Miller and Graybiel [1971] from the results of their centrifuge experiments, as discussed earlier. Subjects were positioned lying on their side so that the change in the gravitoinertial vector caused by the transition from 0-g to 2-g was lateral with respect to the head. The results from these experiments were:

1. Torsion was observed in the same direction as if the subject had been tilted to the 90° position from the upright.
2. There is a strong linear correlation between torsional eye position and lateral gravitoinertial force, as shown in Figure 2.16.
3. The sensitivity of the OCR response was about 4 deg/g. This is about the same as observed on earth.
4. The torsion response to gravitoinertial force in the range of 1-g to 2-g has the same sensitivity as the response in the range from 0-g to 1-g.
5. A change in the lateral component of the gravitoinertial vector, without a rotation of the gravitoinertial vector, is an adequate stimulus for OCR.

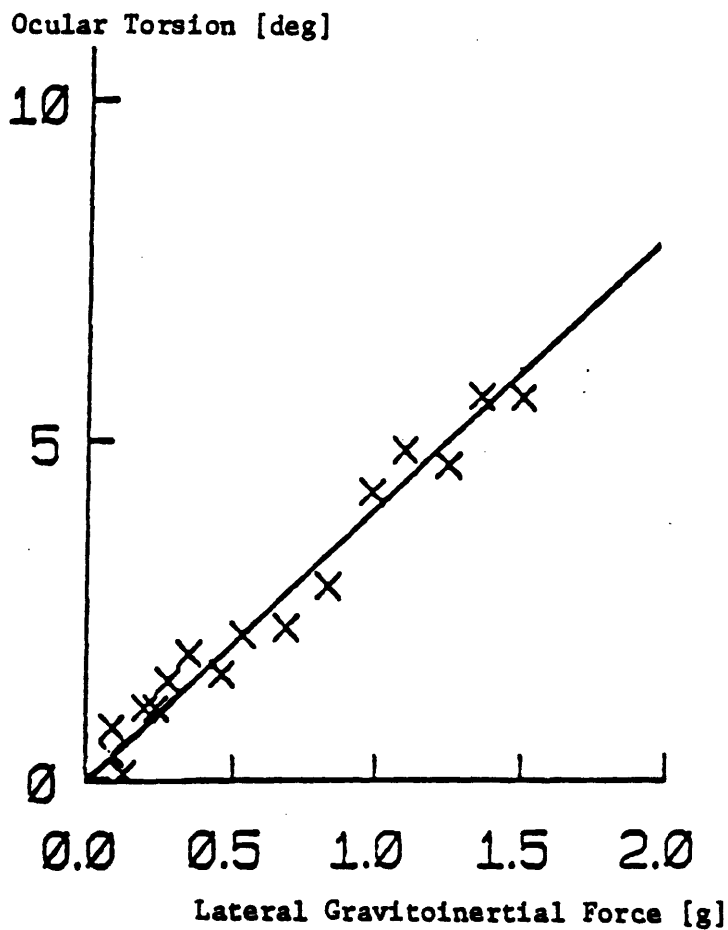


Figure 2.16 Counterrolling response versus lateral gravito inertial force in weightlessness. For this condition, there is no rotation of the gravito inertial force. From Arrott [1985].

Von Baumgarten and Thulmer [1978] have proposed that minor asymmetries between the left and right otolith, which can be compensated for on the ground, might be a possible cause of space motion sickness. They also state that after three or four days in weightlessness, which is the length of astronauts' space sickness symptoms, the otoliths adapt to the new environment. This theory has been tested aboard the KC-135 by Money et al. [1987], Lackner et al. [1987], and Diamond and Markham [Diamond, Markham, 1988, 1991; Diamond et al., 1990]. Money's experiment consisted of photographing of the subject's eye while upright at the zero-g position and the 1.8-g position during a series of parabolas. Lackner used the Miller tilt chair to position the subject to four tilt angles ($\pm 25^\circ$ and $\pm 50^\circ$), one during each series of parabolas. Diamond and Markham used their tilt chair and positioned the subject at 0° , 30° , and -30° , each for 5-10 parabolas. For their most recent study, nine former astronauts, whose histories of space motion sickness were revealed after the analysis, were used as subjects and seated in the upright position. The measure of OCR used in this study was disconjugate eye torsion, which is the mean right eye torsion minus the mean left eye torsion compared at 0-g and 1.8-g. Results of these KC-135 experiments include:

1. Torsional eye movements do occur in hypogravity and hypergravity.
2. In normal upright posture on the ground, the eyes are held in their torsional position by central mechanisms that have adapted to the 1-g inputs from the otoliths. In weightlessness, these mechanisms cause the eyes to torsionally displace from their normal positions [Money, et al., 1987].
3. Subjects with large asymmetries in counterrolling for leftward and rightward body tilts are more susceptible to motion sickness [Lackner et al., 1987].
4. During body tilts, the counterrolling at 1.8-g was greater than the ground tests at 1-g [Diamond, Markham, 1988]. This is consistent with the centrifuge tests conducted by Woellner and Graybiel [1959] and Miller and Graybiel [1971].
5. Astronauts who had been sick in space had higher disconjugate eye torsion between 0-g and 1.8-g [Diamond, Markham, 1991].
6. In 1-g, there were no differences in disconjugate eye torsion between the astronauts who had been sick and the ones who had not [Diamond, Markham, 1991].

All of these experiments and results support von Baumgarten and Thulmer's hypothesis that otolith asymmetries are compensated in the 1-g environment, and may suggest a possible predictive test for space motion sickness.

2.2 Data Acquisition and Analysis

The position of the eye can be measured with skin electrodes placed on either side of the eye. The cornea is 0.40 - 1.0 mV more positive than the retina. When the eyeball rotates in its socket, this electrostatic dipole also rotates; and the amount of rotation is related to the potential difference across the electrodes [Young, Sheena, 1975]. This method works very well for horizontal eye movements, but not as well for vertical eye movements because of the placement of the electrodes above and below the eye. The electrostatic dipole is offset approximately 15°, and counterrolling of the eye would result in counterrolling of the dipole. For measurement of ocular counterrolling, though, this misalignment is not of practical use; and therefore a different method of measuring OCR is needed. The method most used in the past as well as the present is to take still pictures of the eyeball and to compare the rotation of the eyeball from one picture to the next. This is done by locating natural landmarks in the iris and tracking the rotation compared to stable fiducial marks on a biteboard. Landmarks in the iris instead of landmarks or blood vessels in the conjunctiva are used because the conjunctiva is not connected to the eyeball, and therefore cannot be used as an indicator of OCR. Miller's procedure of analyzing the rotation angles involved enlarging the film image of the entire eye over 300 times the actual eye size by projection onto a distant screen. Each successive image was then projected onto an image of the subject's eye at the zero position, and the measurement of angular rotation could be made. This method, as stated by Miller, has an accuracy of 5 minutes of arc [Miller, 1961, 1966].

Diamond and Markham also use 35-mm still photography, but instead of taking photographs of one eye, photographs of both eyes are taken to study binocular

counterrolling. The analysis method is similar to Miller's in that each successive image was compared to an image in the upright position. Two projectors, as shown in Figure 2.17, superimpose the images, and the angle to which the image from the projector containing the photographs of the eye during rotation had to be rotated to coincide with the image in the upright position is the counterrolling angle. This method was stated to have an accuracy of 0.25° [Diamond, Markham, 1983], but also requires approximately 30 manhours to analyze the photographic data of one subject.

For the MIT sled experiments, a Hermes Senior film analyzer, which had previously been used by the Laboratory for Nuclear Science to analyze photographic records from bubble chamber experiments, was used to analyze the 35-mm photographs [Lichtenberg, 1979; Arrott, 1982; Arrott, 1985; Tse, 1990]. Strips of film were guided across a moveable stage, and each frame was projected onto a glass screen which had a cursor located at its center. The film was held in place on the moveable stage with suction from a vacuum pump, and a particular landmark was aligned with the cursor. The coordinates of this landmark were then read by a Digital Electronics Corporation PDP-8 minicomputer. For each frame, the coordinates for the two iral landmarks and the two fiducial marks were recorded. These coordinates were later used to calculate the rotation angle. This method was stated to have an accuracy of 0.5° [Lichtenberg, 1979], but the analysis process took an incredible amount of time.

In the European Spacelab study, a 35 mm camera was used to make color transparencies of the subject's eye at each tilt position. Ten to twelve iral landmarks on each transparency were used to compare each position to the 0° position. A graphic computer system measured the angles of rotation to an accuracy of ± 0.1 deg [Vogel, Kass, 1986].

All of the above methods track iral landmark rotation, which are very hard to locate and track from frame to frame. This problem of locating natural landmarks on the iris has been removed by some experimenters by using contact lenses. Deionized water is applied

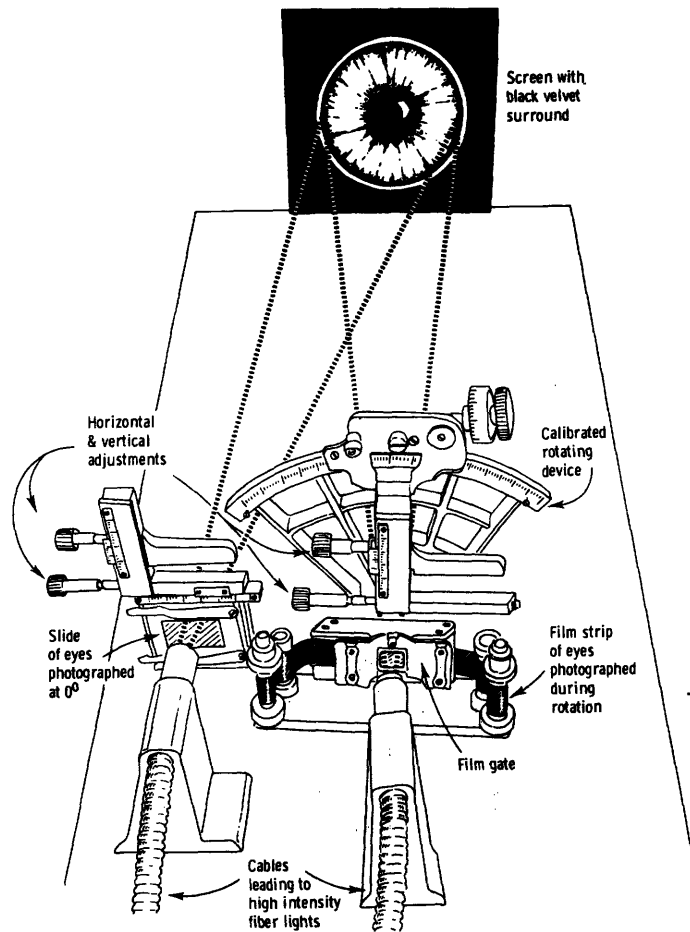


Figure 2.17 Projector system used by Diamond and Markham for analysis of ocular counterrolling. The projector at the left has a slide of the eye at 0° . Each frame in the film strip in the second projector is compared to the image from the first projector. From Diamond, et al [1979].

to the lens once in the eye, which causes it to adhere to the eye. An early attempt at better tracking of rotation was to sandwich a human hair between two soft contact lenses [Edelman et al., 1981]. Another attempt was to sandwich a polarized hard contact lens between two soft contact lenses and measure the phase difference between a rotating polarized light and the light reflected from the lens [Kenyon, Lichtenberg, 1981]. Both of these methods called for bulky lenses to be placed in the eye which were uncomfortable to the subject. Prior to the SL-1 Shuttle mission, the Man-Vehicle Lab decided to use contact lenses with line patterns on them. The lens pattern for the SL-1 and D-1 missions are shown in Figure 2.18a; the pattern for the SLS-1 mission is shown in Figure 2.18b. The marks on the contact lens are much easier to pinpoint and to track than the iral landmark method.

Even with the use of marked contact lenses, the still photography method had the following setbacks:

1. Analysis of the photographic data takes a considerable amount time.
2. For the dynamic movements (Markham/Diamond and Arrott), the data can not be taken continuously because of the slow shutter speed of the cameras.
3. Fast OCR movements, fluctuations, or nystagmus can not be measured.

The plan for analyzing the preflight and postflight sled data from SL-1 and the inflight sled data from D-1 was to use the still photograph method used by Arrott with the addition of the marked contact lenses. But, for the preflight, inflight, and postflight dome from both SL-1 and D-1 and the preflight and postflight sled from D-1, it was decided to videotape the subjects' eyes and to have a future graduate student write an image analysis program to track the contact lens landmarks. The only ocular counterrolling image analysis program that existed at the time was called EMIRAT [Vieville, Masse, 1987]. EMIRAT tracks the entire iris ring from frame to frame and the counterrolling angle is calculated in real time. The EMIRAT system was to be used on both SL-1 and D-1, but no results using

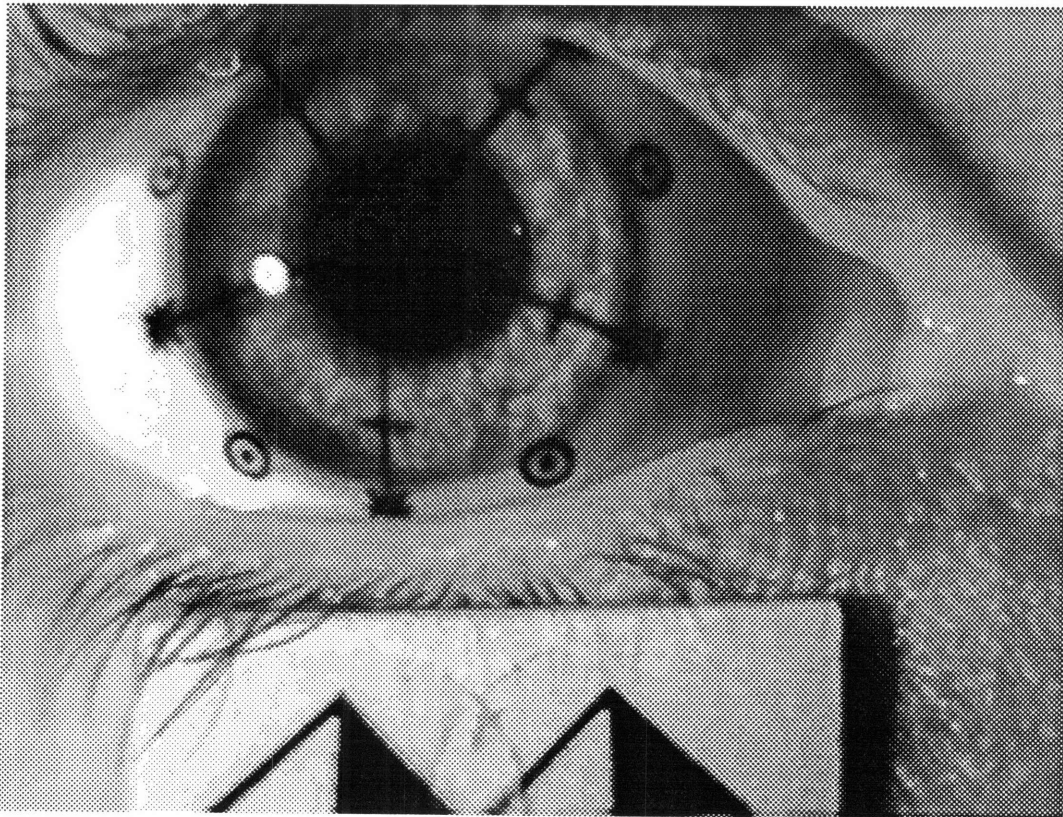
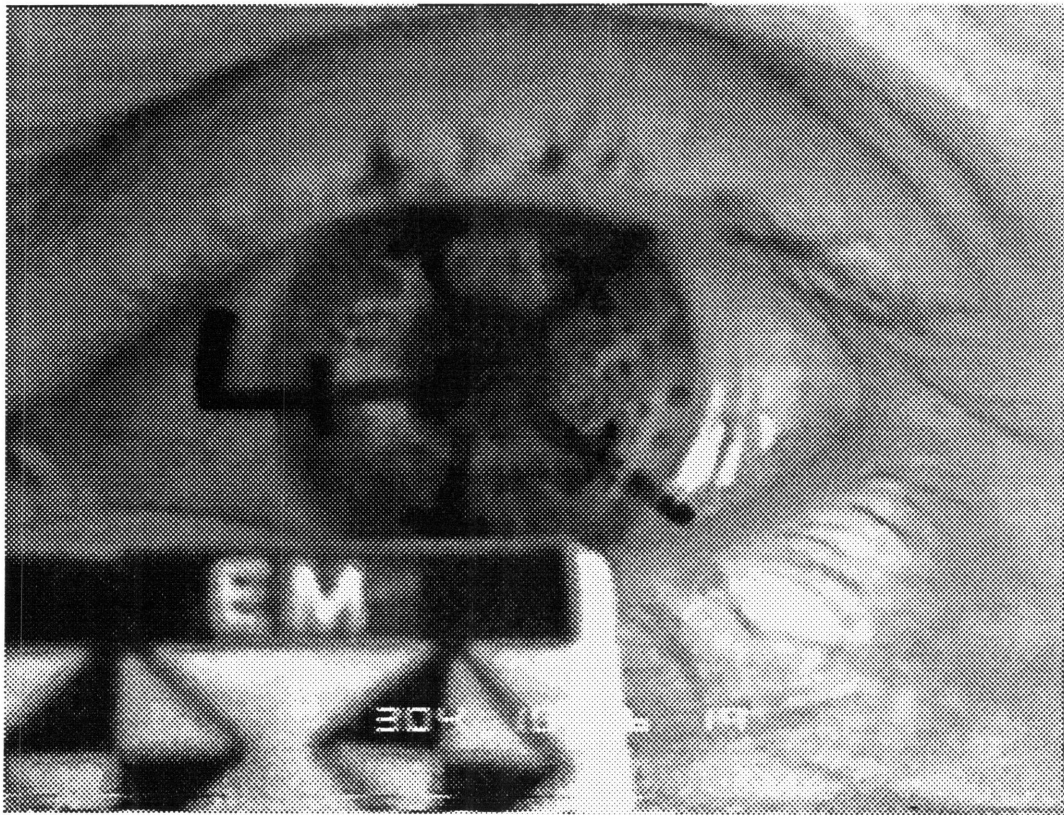


Figure 2.18 a. Contact Lens from D1 and SL1 Missions.
b. Contact Lens from SLS-1 Mission.

the system have yet been published. The reason for this could be the problems with the EMIRAT system which include:

1. The system had to locate the center of the pupil, which was not always precise.
2. If the eyelid covered part of the pupil or the subject blinked, the center of the pupil could not be located correctly.
3. Changes in the illumination of the eye cause errors in the calculation of the center of the pupil.
4. Measurements of counterrolling is only possible when the picture is of very good quality.
5. The system is sensitive to variations in iral features in subjects, and some subjects were found to have eyes that could not be analyzed.

It was decided to design a system that would track lens landmarks instead of the center of the iris, and the resulting system was TOMAS (Torsional Ocular Movement Analysis System) [Alston, 1989]. This system determines the translation of lens landmarks in rectilinear coordinates by crosscorrelation based on the "dumbbell" analysis method [Parker et al., 1985]. OCR data is recorded with a standard video camera and stored on Sony SuperBeta videotape for analysis. The operator of the system selects two of the landmarks on the contact lens, preferably close to 180° apart. Fiducial marks on a biteboard were also selected so as to subtract out head rotations. For each successive frame, the system searches a 128 x 128 region around the initial mark (instead of the whole screen) to locate its new position. The program uses the two dimensional Fast Fourier Transform to conduct rectilinear crosscorrelation of the chosen landmark and the 128 x 128 region. Before the run, the operator can choose preliminary filtering techniques, including Mexican hat filter, thresholding, inverted images, and binary images. When chosen correctly, these techniques provide better contrast between the lens landmarks and the eye. The program calculates the angle of the line containing the fiducial marks with respect to the horizontal defined by the camera and the angle of the line containing the iral landmarks with respect to the horizontal. The first angle is subtracted from the second angle, and this value is compared from frame to frame to produce OCR results. Once completed and tested, this

system was to be used to analyze the already existing SL-1 and D-1 data. One of the author's duties was to conduct this analysis. While using this program, many problems were found that inhibited the analysis of the data, including:

1. TOMAS works well when working with just the black landmarks and a white background (which is how the program was tested), but has problems with the contrasting greys in the area of the landmarks which are found for real subjects.
2. The code crashes quite often, and has never run more than 800 frames (27 seconds of data).
3. The running of TOMAS takes a considerable amount of time--20 seconds per frame.
4. Setting the parameters (e.g., thresholding, binary imaging, inverting, etc.) before the run takes a considerable amount of the operator's time.
5. The precision for the type of contact lenses used was found to be 0.45 degrees [Alston, 1989], which is higher than the 0.1 degrees precision of the still photograph methods.

The above reasons contributed to the fact that the SL-1 and D-1 OCR video data from the sled and the dome have not yet been analyzed. The upcoming SLS-1 mission will also involve video OCR data from the sled, dome, and Miller tilt chair that must be analyzed. Many large advancements in image analysis have occurred as of late, and better video image analysis systems for measuring ocular counterrolling are presently being worked on in the Man-Vehicle Lab and elsewhere [Okuda et al., 1989; Tsunekawa et al., 1989; Yamanobe et al., 1990; Clarke et al., 1990; Curthoys et al., 1991]. The video analysis method is theoretically better than the still photography method for two reasons:

1. Data is acquired at 30 Hz instead of the 3-5 Hz for the still photography method. This higher frequency can locate any fast eye movements that the still photography method may have missed.
2. The analysis should be faster since the computer is handling all the rotation calculations.

Once a properly working video system is produced, the efficiency of this method will reduce the analysis time considerably.

There are other methods besides still photography and video to analyze ocular counterrolling. One method involves placing a pointing device over two landmarks on the

iris, tilting the subject, repositioning the pointing device over the same two landmarks, and measuring the angle of rotation [Fluur, 1975]. This method may have also been used by Yakovleva in the Soviet Salyut experiments. This method's inaccuracies come from repositioning the pointing device onto the tiny iral landmarks. It is also ineffective for any dynamic ocular counterrolling tests since the pointing device must be repositioned between eye rotations.

Another method, called the after-image method, involves using a line flash to place an after-image on the subject's retina [Howard, Evans, 1963]. Once tilted to a set angle, the subject aligns a target line with the after-image. This method's errors come from the fact that the subject instead of the experimenter decides the OCR angle using his own visual perception.

The measurement method used at St. Michael's Hospital in Toronto involves using a goniometer to observe eye rotation directly [Kirienko et al., 1984]. A telescopic gunsight in front of the subject presents a magnified image of the subject's eye, and a straight line is placed through two iral landmarks. The rotation of this line compared to the line at the zero degree position is recorded, and the chair is rotated to its next position. This method removes the process of analyzing film data at a later time, and it is stated that the total time to collect and process the data is from 1.5 to 2.5 hours. This method, as in many of the above methods, has the problem of trying to track iral landmarks.

Some experimenters used a small transparent cap that would suction onto the eyeball of the subject. At the end of the cap would be an angle measuring device, such as a light bulb in the case of Petrov and Zenkin [1973]. In their experiments, the light bulb would be directed horizontally on a slit photokymograph, and the movement of the image would indicate ocular counterrolling. Obviously, this method was very uncomfortable for the subject.

The MVL experimented with fitting a conical ferromagnetic ring to the sclera to measure magnetic field variations due to OCR [Zeevi, Ish-Shalom, 1982]. The

ferromagnetic ring is embedded in a silicon rubber suction ring; and the variations in the magnetic field are measured with two symmetrical coils wound on two ferromagnetic C-shaped cores which are placed near the eye. This method was tested on cats and rabbits, but was never used on humans.

2.3 The Scleral Search Coil Method

The search coil method, which was first introduced by Robinson [1963], provides an alternative to the video and still photograph methods of analyzing ocular counterrolling. In this method, subjects wear a magnetic coil in their eye, and a magnetic field is generated around the subject's head. The voltage induced across the coil varies depending on the area of the coil perpendicular to the magnetic field, and can be converted to rotations in the horizontal, vertical, or torsional direction. For animal subjects, the coil has been surgically implanted in the eye [Baarsma, Collewijn, 1975, among others], but this is not appropriate for human subjects. In Robinson's method, the magnetic coil was embedded in a hard contact lens which was suctioned to the eye by evacuating the chamber between the lens and the cornea [Robinson, 1963]. This method of evacuation could cause corneal deformation, corneal abrasions, and serious increases in intra-ocular pressure. An improvement in this method was to have the magnetic coil embedded in a silicone rubber ring which was placed on the subject's eye [Collewijn et al., 1975; Collewijn et al., 1985]. The ring was suctioned on the scleral portion of the eye, and though it still increased the intra-ocular pressure, the increase was not as extreme. This method involved using anesthetic, and could still cause corneal abrasions. To remove these problems, the use of soft contact lenses has been proposed. One method was to sandwich the magnetic coil between two soft contact lenses and use distilled water to adhere it to the eye [Kenyon, 1985]. Another method had the coil glued to the outside of the contact lens and would protrude outward from the eye, as shown in Figure 2.19 [Malan, 1985]. The first method could not track torsional eye movements; the second method involved taping the subjects'

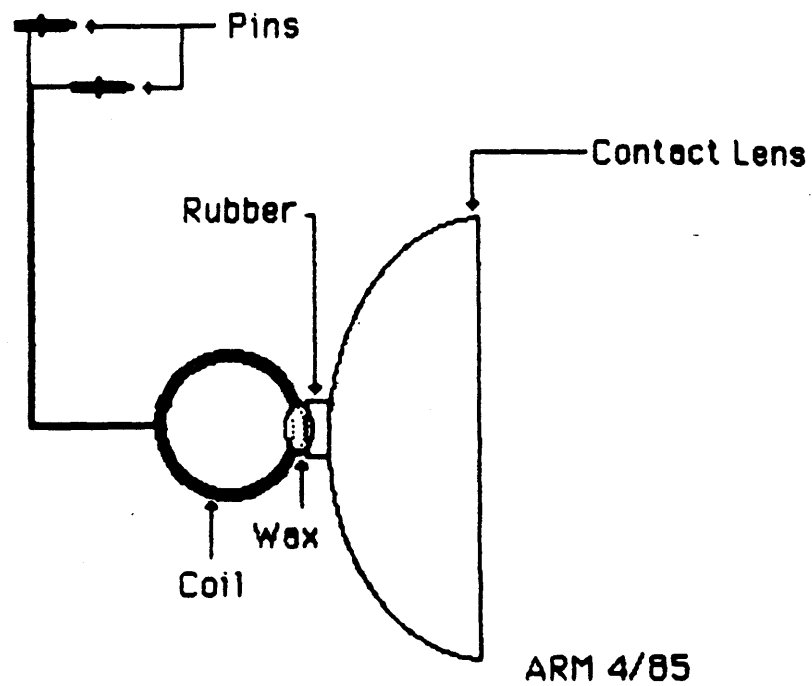


Figure 2.19 Torsion coil used by Malan. The coil is glued to the outside of a contact lens and protrudes outward from the eye. From Malan [1985].

eyes open so as not to upset the protruding coil, and both methods blocked vision in the eye with the lens. For these reasons and the fact that they are manufactured for experimental use by Skalar, Inc. in the Netherlands, the silicone rubber coils were chosen for use at MIT (The search coil method and equipment will be better described in Chapter 3). The scleral search coil method provides the following advantages over other OCR measurement methods:

1. Precise: Robinson [1963] reported a resolution better than 0.02° for horizontal and vertical movements.
2. Provide continuous information.
3. Can provide simultaneous measurement of horizontal, vertical, and torsional eye movements.
4. Blinking does not interfere with measurements.

But, the coils also have the following problems:

1. Uncomfortable to many subjects.
2. Coil can only be worn for thirty minutes.
3. Possibility of damage to cornea.
4. Can cause increases in intra-ocular pressure.
5. Fragile--the coil leads break very easily.
6. Expensive--each torsion coil costs \$210 and lasts about five trials.
7. Corneal anesthetics must be used.
8. No present method to calibrate torsion.

Though the search coil method has many setbacks, it produces excellent real-time results when used.

Chapter 3

Equipment

3.1 The MIT Sled

The MIT linear accelerating sled is shown in Figure 3.1. The sled consists of a cart which rides on two one-inch diameter circular hardened steel rails mounted on the top of a two-foot high cement block structure. The cart is constructed of aluminum angles and is guided along the rails by four pillow blocks with recirculating ball bushings. The two rails are five meters long and placed 1.7 meters apart on the cement blocks. The cart is aligned along the back rail which is mounted rigidly to its cement wall. The front rail is fixed loosely to its cement wall to provide alignment by the bushings as the cart travels along the back rail. The cart is driven along the length of the rails by a cable which is wound around a winch drum at one end and a pulley at the other. The winch drum is driven by a 3.5 horsepower DC permanent magnet torque motor (Inland TTB-5302-100c) which is controlled by a pulse-width modulated velocity controller (General Electric 3N2100FA301A1). In the past, the sled motion had been controlled by a Digital Electronics Corporation PDP 11/34 minicomputer and a Digital Lab Peripheral System using a FORTRAN program called CART, written by Arrott [1982]. Presently, this program is being upgraded; and for the present study, a function generator was used to generate sinusoidal profiles. The sled system provides safety stops at each end of the rails and two "panic buttons", one for the sled operator and one for the subject. If the sled slides over one of the safety stops, or a panic button is hit, the brakes are immediately applied. Shock cords are also mounted at the ends of the track to provide backup for the safety stops. An umbilical cord, providing input and output signals, runs from the back of

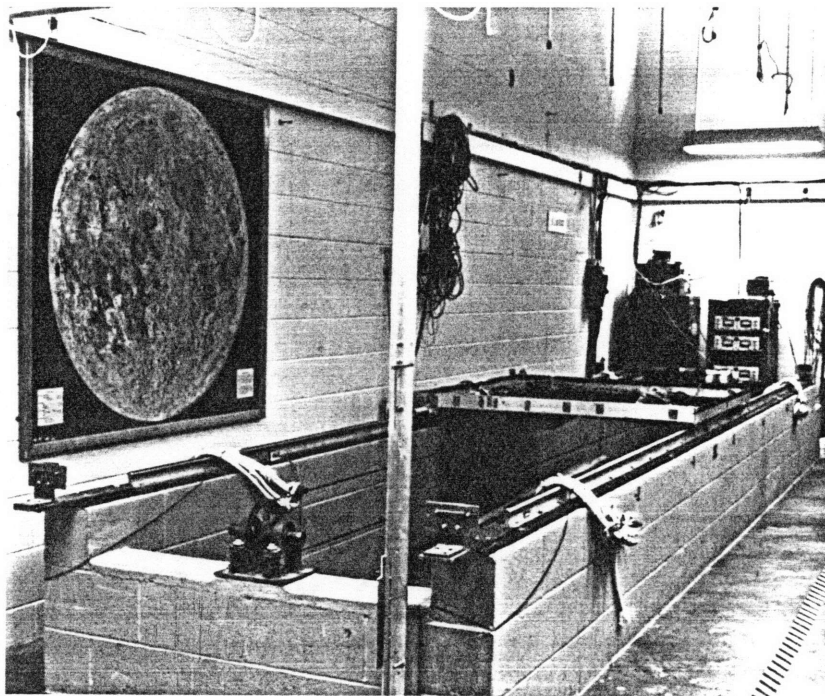
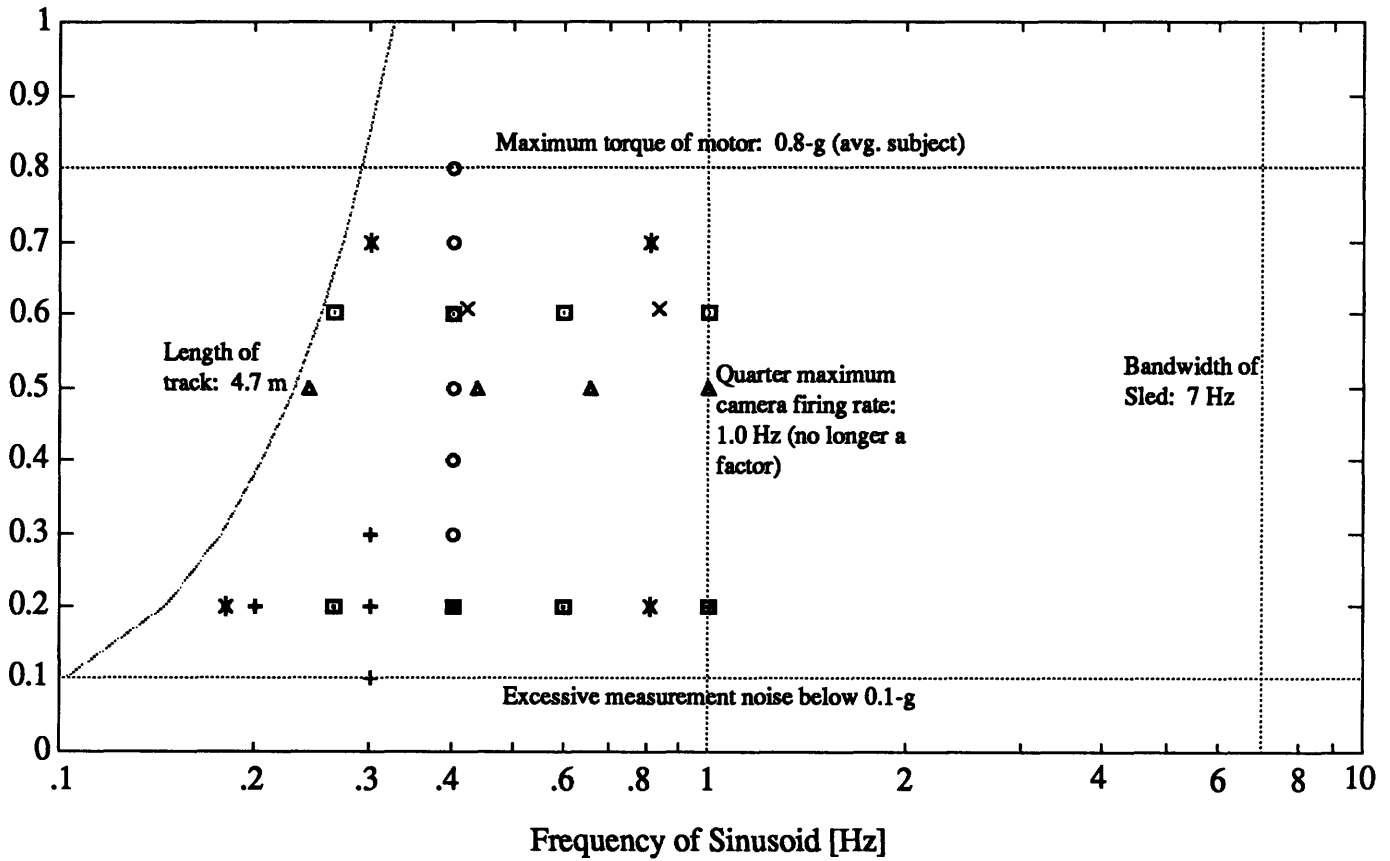


Figure 3.1 The MIT linear accelerating sled and cart. A new sled chair to sit atop the cart had to be designed and built to accommodate the coil system.

Amplitude of Sinusoid [g]



Key:

- + Lichtenberg
- o Arrott
- x SL-1
- * D-1
- ▲ SLS-1
- Present Study

Figure 3.2 MIT sled operating range. Also shown are the profiles from past ocular counterrolling studies. Adapted from Arrott [1985].

the cart, along the wall, to the control box at the operator's station. The umbilical is connected to the wall with a bungee cord, which stretches as the sled transverses the length of the rails. The limiting values for the sled profiles are shown in Figure 3.2. The values of frequency (f) and acceleration (A) of the sled are limited by the formula:

$$\frac{A}{4\pi^2 f^2} < \frac{L}{2} \quad (3.1)$$

where f is in Hz, A is in m/sec², and L is the length of usable track, which is 4.7 meters. The quarter maximum camera firing rate is no longer a limiting value; but based on the known characteristics of the sled operating range as well as the comfort levels of subjects, it is good practice to not use frequencies greater than 1.0 Hz. A more detailed description of the sled occurs elsewhere [Lichtenberg, 1979; Arrott, 1982; Arrott, 1985].

3.2 The Scleral Search Coils

The scleral coils used at MIT are purchased from Skalar, Inc. in the Netherlands, which manufactures the Collewijn-type coils for experimental use. Skalar produces two types of coils, as shown in Figure 3.3. The coil on the left, the standard coil, has only one winding of the wire and is used to measure horizontal and vertical eye movements. The coil on the right, the torsion coil, has two separate windings of the wire and is used to measure horizontal, vertical, and torsional eye movements. The coil consists of nine windings of 0.05 mm diameter insulated copper wire embedded in a silicone rubber ring. The torsion coil has a second wire wound perpendicular to the first wire which allows for measurements of torsional eye movements. The concave side of the ring is slightly more curved than the eye so that it can be suctioned to the subject's eye. The ring sits on the sclera of the subject's eye and does not disrupt vision. The leads of the coil exit the subject's eye at the nasal side, and the junction between the coil and the leads is strengthened with a silicone covering. The torsion coil, which was used in the present

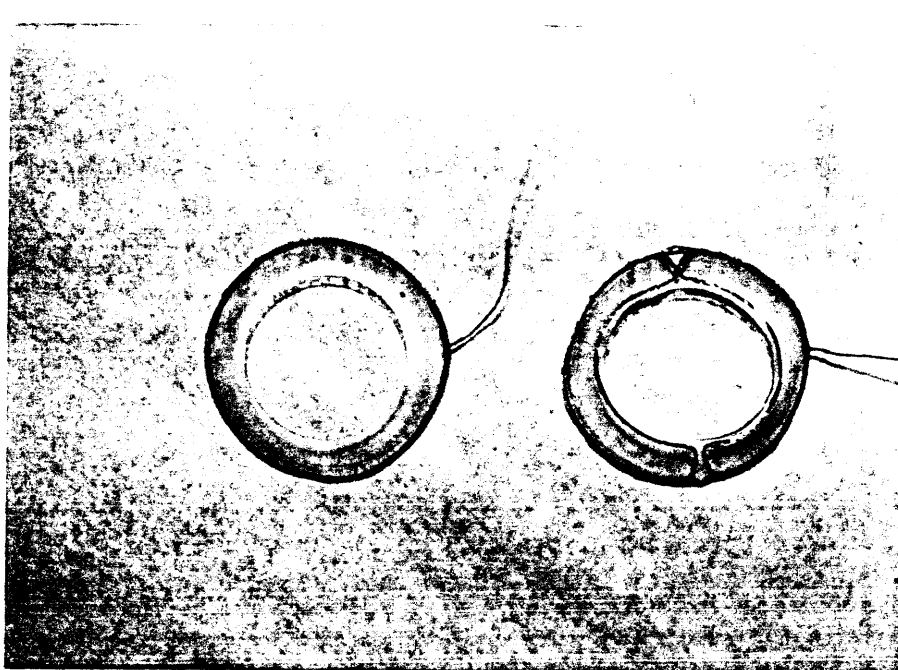


Figure 3.3 The two types of scleral search coils. The coil on the left has only one winding of wire and is used to measure horizontal and vertical eye movements. The coil on the right has two separate windings of wire and is used to measure horizontal, vertical, and torsional eye movements. The coil on the right was the one used in the present experiment.

study, has two output leads: one for horizontal and vertical eye movements and one for torsional eye movements. With the coil in the subject's eye and a magnetic field generated across the coil, an induced voltage will occur that varies depending on the area of the coil perpendicular to the magnetic field.

Before the coil can be inserted into the subject's eye, the eye must be anesthetized. Once anesthetized, the coil can remain in the subject's eye for a maximum of 30 minutes before a risk of corneal scratching arises. The subject's eye may need to be re-anesthetized during the 30 minutes, as requested by the subject. Appendix E describes the subject preparation, Appendix F describes coil insertion and removal, and Appendix G contains the COUHES human use application and the subject consent form.

3.3 The Magnetic Field Generating Coils

The MIT scleral search coil system was purchased from C-N-C Engineering, a division of Tekmate, in Seattle, Washington (see Appendix C for a copy of the C-N-C scleral coil system manual). The two-foot field coil has outside dimensions of 25" height x 31" width x 30" depth, with large openings provided on all six faces. The MIT coils are the Robinson style system as opposed to the Phase Angle style system. The Phase Angle system measures larger angles of movement, but is much more complex and expensive. Since the eye movements that will be measured at MIT are limited to small angles, the Phase Angle system was not needed. The Robinson system produces a signal that can represent horizontal and vertical eye movements within the range of $\pm 40^\circ$ and torsional eye movements within $\pm 20^\circ$. The coil system consists of two pairs of coils oriented at 90° to each other. Each coil is embedded in wooden frames for protection. The two coils operate at two different frequencies between 60 kHz and 135 kHz. The two-foot coils provide a two inch cube region at the center of the magnetic field which is the ideal position for the scleral coil, though tests have shown that accurate measurements can be taken well outside this region. The horizontal coil has a magnetic field strength of approximately 0.3 gauss at

the center and the vertical coil has a magnetic field strength of approximately 0.4 gauss at the center. For comparison, the strength of the earth's magnetic field is approximately 0.3 gauss at the equator, approximately 0.6 gauss at the poles, and approximately 0.55 gauss in Boston, MA. Typical noise for the coils was reported as 0.5 minutes of arc peak to peak when measuring saccades at a 500 Hz frequency limit.

The instrument panel for the coil system consists of three modules. The bottom module is the Power Oscillator Drivers which drive the two pairs of coils at two frequencies. On the front panel is a resonant frequency control which, for this particular coil system, is set to 5.17 Hz for the coils to be at resonance. At this setting, the horizontal coil has a frequency of approximately 122 kHz and the vertical coil has a frequency of approximately 83 kHz. The top two modules are the Dual Phase Detectors which recover the voltage output from a search coil placed within the electromagnetic fields and separate this voltage into horizontal, vertical, and torsional rotations. The Phase Detector controls are used for calibration purposes and include:

1. Offset Control: adjusts for zero degree eye position.
2. Gain Control: adjusts output voltage to match eye rotation angle.
3. Meter Sensitivity Switch: adjusts eye position meter to either $\pm 5^\circ$ or $\pm 50^\circ$ full range.
4. $0^\circ/180^\circ$ Switch: changes output phasing by 180° so that output dial corresponds to the direction of gaze.

One of the Dual Phase Detectors provides one channel for horizontal eye movements and one channel for vertical eye movements. The other Dual Phase Detector provides two channels for torsion. The additional torsion channel can be used to subtract out head rotations by attaching a second scleral coil to the subject's head. The horizontal/vertical output wire from the scleral coil is connected to a 147 ohm preamplifier, and the torsion output wire is connected to one of the two 357 ohm preamplifier. The three preamplifiers are located at the back of the sled chair, and output wires run along the umbilical cord to the coil instrument panel and connect to the horizontal, vertical, and two torsion output dials.

The output from the search coil is also fed into an IBM PC 386 computer. The program LabTech Notebook is used to collect and store the data on the 386 computer.

3.4 The Sled Chair

The coil system requires that a minimal amount of metal be within the coils, to insure uniformity of the magnetic field. Irregularities in the magnetic field caused mainly by metallic objects could adversely affect the data quality. For this reason, the existing metal sled chair had to be replaced, and a new chair constructed of non-metallic materials had to be designed and built. The chair was designed to fully replace the previously existing chair. For those experiments that do not involve the coil system, only the coil system needs to be removed, which is a very simple procedure. The chair is divided into three major parts:

1. The base, which serves as the connector between the chair and the sled.
2. The seat, which holds the subject in place.
3. The coil frame, which supports the coil system.

The base and the seat are constructed of aluminum while the coil frame is constructed of fiberglass. The aluminum from the base remains below the coils at all times to minimize interference with the magnetic field.

The base is constructed of four inch and three inch aluminum angles, with six 1.5 inch aluminum square tubing struts on which the seat is connected either in the upright or supine position. At each of the four corners of the base is located a shock support which connects directly to the sled. Small 1/8 inch thick angle shims are connected to each strut to provide a better fit inside the legs of the seat.

The seat is constructed of pieces of two inch aluminum square tubing which are welded together. When positioned on the struts of the base, the seat is held in place with eight 3/8 inch bolts, two in each leg. Two pieces of 3/4 inch plywood are fastened to the seat to form the backboard and bottomboard of the seat. A standard desk chair cushion is

attached to the bottomboard, and another cushion is velcroed to the backboard. The velcro allows for raising or lowering of the cushion to provide better back support for the subject. A five point parachute harness is connected to the plywood pieces to provide restraint and protection of the subject. The metal fasteners on the shoulder straps of the harness have been replaced with plastic pieces so as not to interfere with the magnetic field. To the bottom of the seat is connected a foot restraint system, which is constructed of aluminum angles and fastening belts. On the back side of the seat are mounted the pre-amplifiers for the coil outputs. An EOG amplifier box is connected to the left arm of the seat to provide for EOG output if needed. An accelerometer for recording the sled accelerations is mounted on the chair frame in the proper direction for the chair's orientation.

The coil frame is constructed of 1.5 inch square fiberglass tubing which is connected together with a two-part fiberglass epoxy. A pre-fabrication stress analysis study verified that this structure would hold up to 5-g with a weight of 100 lbs (which is much heavier than the coils) connected to it. The four legs of this frame slide into the legs of the seat, and each leg has eleven 3/8 inch holes 3/4 inch apart to provide for the raising and lowering of the coils for different subject heights. Each leg also has four pieces of teflon connected to each side with epoxy. The teflon first had to be treated with Chemgrip, a chemical that changes the chemical composition of the teflon so that it can be bonded to the fiberglass, on one side to prepare it for the epoxy. The teflon provides for a tight fit of the frame into the seat. Eight pull-pins, two for each leg, hold the frame in position and provide for easy raising and lowering of the coils. Once the coil frame was built, the coils themselves were mounted onto it. Fiberglass angles were connected to the frame using 3/8 inch fiberglass rods and fiberglass nuts, and the coils and the coil instrument box were connected to these angles. The bottom coil is hinged at the back to provide easy access into the chair, and two locking mechanisms on the front secure it during sled runs. The coil input and output wires run off the back of the sled along the umbilical which was discussed

earlier, and run around a ledge along the back wall to the coil oscillators and detectors and the data collection computer, which are situated at the foot of the sled track.

For the head restraint, a standard Ridell VSR1 professional football helmet was purchased. The helmet contains an inflatable air bladder, which, when inflated, restrains head movement within the helmet while not causing discomfort to the subject. Four different size jaw pads were also purchased. With the proper jaw pad in the helmet, lower head support is also provided. The helmet is placed within a layer of foam supported by three pieces of 2x8 wood. A fiberglass bolt connects the helmet to the wood; and four fiberglass bolts, which are epoxied into the wood, connect the wood pieces together. Four more fiberglass bolts, also epoxied into the wood, connect the head restraint to the backboard. The backboard contains four slots, which allow for adjusting of the head restraint to different subject heights.

A fixation light is needed for ocular counterrolling studies to eliminate horizontal and vertical eye movements of the subject. The fixation light mount is a piece of plywood with a center hold for the fixation light. At the top and bottom of the mount are brackets that fit around the top and bottom coils by tightening down fiberglass nuts until secure. Once in place, the fixation light is approximately sixteen inches from the eyes of the subject. The fixation light itself is a very dim red LED which is powered from a 15 volt DC power supply at the foot of the sled rails. The cable from the power supply runs along the wall, up the umbilical, and to the LED. The cable and light source were found to not interfere with the output of the coil system.

Past studies have shown that ocular counterrolling is much greater in the dark [Petrov, Zenkin, 1973; Collewijn, 1985; among others], and therefore a shroud is needed during the experiment. The shroud is made of black fabric that allows very little light through. The shroud encloses three of the four sides of the coil system and sled chair, and is held in place with velcro. The back side of the coil system and sled chair is not covered to allow for air to circulate within the shroud. The experiment is also run with the room

lights turned off. Enclosed in the shroud and with the room lights off, the subject is in complete darkness, except for the fixation light.

Before a subject is run, the coil system must be calibrated. The coil calibration device clamps onto two fiberglass struts on each side of the coil frame, which positions the protractor fixture at the left or right eye position (one inch to the left or right of the center of the magnetic field). A scleral coil is attached to the protractor fixture during calibration. The coil can then be rotated at one degree increments to calibrate the coil system (Appendix D describes the coil calibration procedure).

Figure 3.4 shows the chair in its lateral upright position, as used in the present experiments. The base can be rotated at the shocks supports to allow for a fore-aft upright position. The chair can also be rotated and positioned on the back struts of the base to allow for either lateral supine or z-axis supine. For the supine positions, two small blocks of wood are slid into the two unused struts to provide support for the coil frame. Appendix A describes the procedure for reconfiguring the sled into these four positions.

3.5 Controlling the Sled

With the new sled control program not yet completed, the sled had to be controlled using a function generator. The function generator has a triggered gate option, which is triggered using the IBM PC 386. The program LabTech Notebook on the 386 is used for data collection, data storage, and the triggering of the function generator. A program called Autorun, written by Merfeld [1990], is initiated to run LabTech Notebook and to change the file names between runs. The program asks the user for the name of a previously stored Notebook set-up file. In the present study, the set-up file is called Coils, and contains the parameters for the input channels from the coils and accelerometer, the plotting channels, and the sled triggering channel. The data is collected at 200 Hz in binary format using a Metrabyte data acquisition board installed in the 386. Once LabTech Notebook is running, it sends a series of one volt signals to the function generator, which causes the

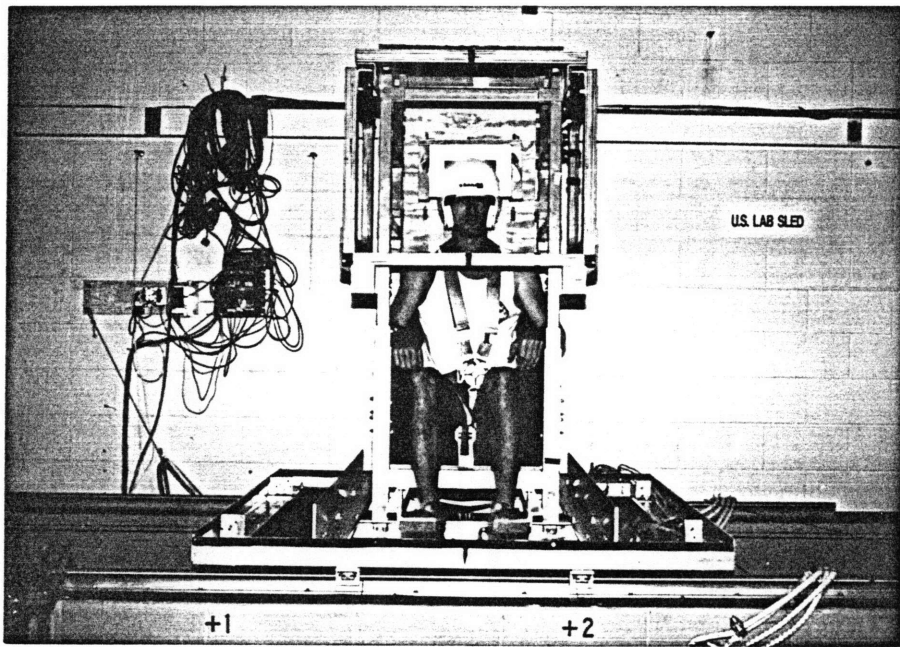


Figure 3.4 Coil system in lateral upright position, as used in the present experiment.

trigger gate to open and the sled to perform sine wave motions. The gate closes when it stops receiving the one volt signals. The frequency and amplitude of the signal being sent to the sled is adjusted on the function generator. A drift box, which is basically a ten turn potentiometer, is connected to the function generator to adjust the drift that exists in the system. The output voltage from the function generator is first filtered at 30 Hz and then sent to the sled through the Sled Control Panel. The output of the function generator is also sent to an oscilloscope so that the operator can monitor the function generator voltage. The output from the coil system is received by the AT through an interface box, which is connected to the ± 10 volt acquisition board in the computer. The accelerometer output is also received through the interface box, once it has been filtered to remove the noise in the signal caused by the coil system. The coil and accelerometer outputs are also channeled to a strip chart recorder to provide real time observations of the experiment data. Appendix B lists the cable setup and Appendix H lists the procedures for running the sled using the function generator.

Chapter 4

The Experiment

4.1 Experiment Design

The present experiment was modeled closely after those of Lichtenberg and Arrott. The subjects are seated upright in the linear accelerating sled, which performs sinusoidal horizontal lateral accelerations. Gravitational force remains constant along the subject's body axis while the acceleration force increases and decreases laterally. This motion produces a rotation of the gravito-inertial vector without rotating the subject, which produces a rotation of the gravity vector. The effect of linear acceleration is similar to rotating the subject, as shown in Figure 4.1. The differences between the two types of motion are shown in Figure 4.2. With the head restraint system, there is no movement of the subject's head, and therefore the semicircular canals are not stimulated. Two foam pads are inserted between the subject's shoulders and the fiberglass frame and two more foam pads are inserted between the subject's knees and the aluminum frame to restrict body movement. The subject is told to fixate on the fixation light during the entire forty seconds of each run to inhibit horizontal and vertical eye movements. Horizontal and vertical eye movements are monitored and stored to allow for cross-checking during questionable output. Once the subject is in the sled chair, the shroud is put over the coil system and the lights in the room are turned off to provide complete darkness except for the fixation light.

Past studies of ocular counterrolling during linear accelerations were done using a still photograph method. This method provided data acquisition at 3 Hz or less. This low frequency cannot account for any fast movements of the eye, and therefore cannot provide an accurate real-time study of the resulting ocular counterrolling. Video, which can provide

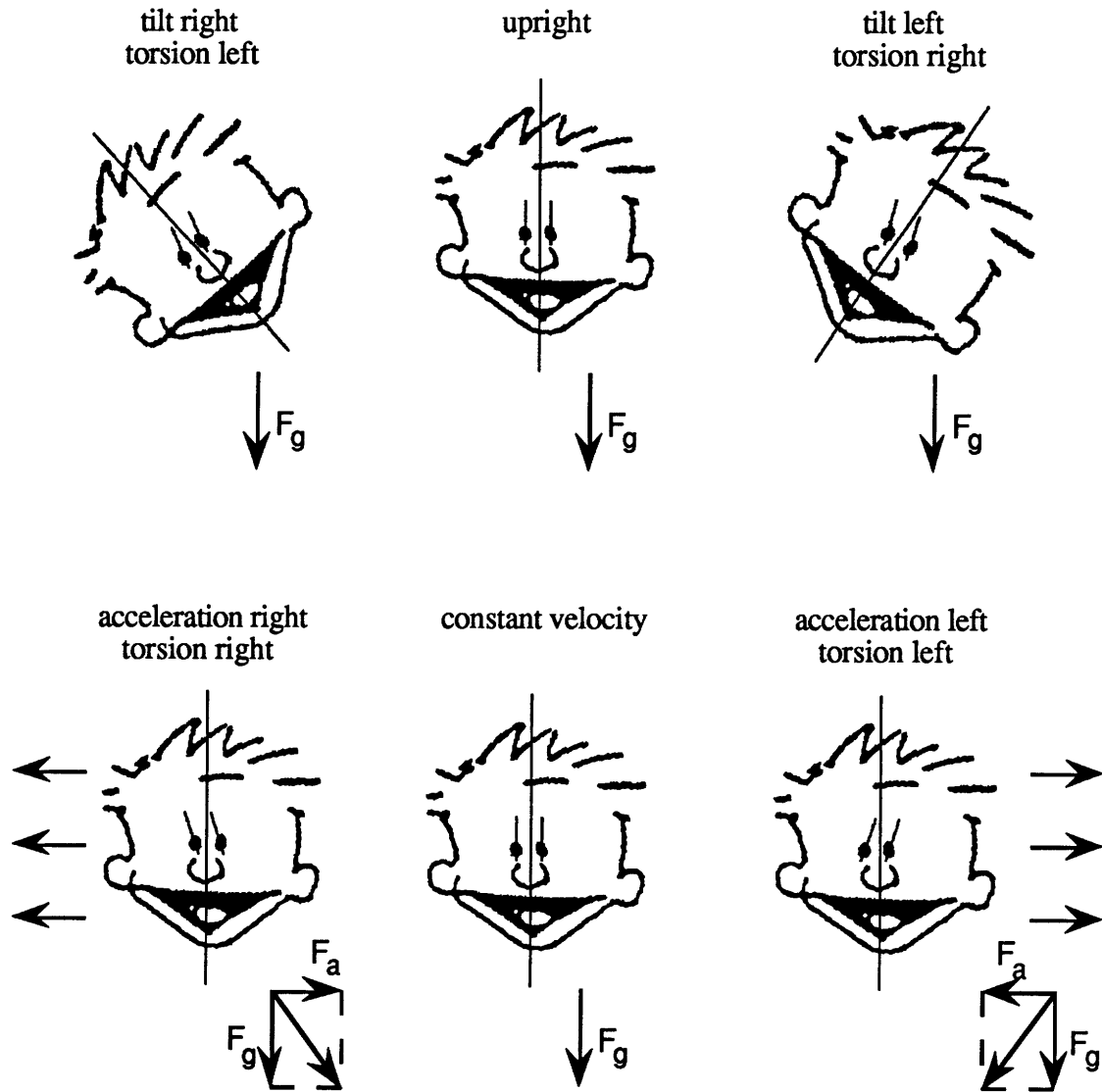
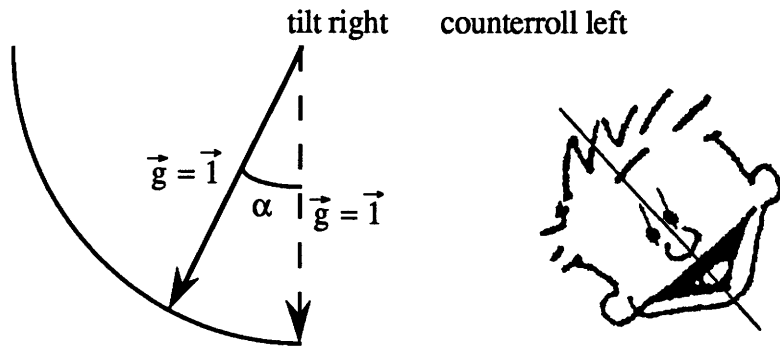
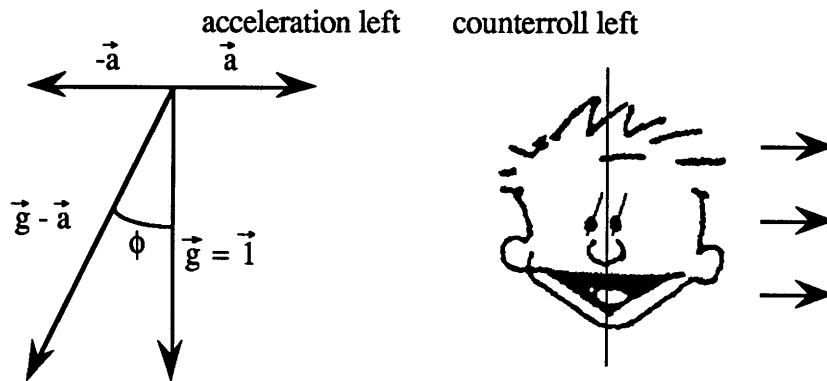


Figure 4.1 Ocular counterrolling produced by the rotation of the force vector. Head tilt produces a rotation of the gravity vector around the line of sight, which causes counterrolling in the opposite direction. Lateral acceleration produces a rotation of the gravitoinertial vector around the line of sight, which causes counterrolling in the direction of motion. Adapted from Arrott [1985].



α = rotation angle of gravity



ϕ = angle between gravity vector and gravitoinertial vector
 $= \text{Tan}^{-1}(a/g)$

$|\vec{g} - \vec{a}|$ = magnitude of the gravitoinertial vector
 $= \sqrt{g^2 + a^2} = \sqrt{1 + a^2}$

a (g)	ϕ (rad)	ϕ (deg)	$ \vec{g} - \vec{a} $ (g)
0.0	0.000	0.000	1.000
0.2	0.197	11.310	1.020
0.6	0.540	30.963	1.166

Figure 4.2 Comparison of the effects of rotation and linear acceleration on ocular counterrolling. Rotation produces the rotation of the gravity vector. Linear acceleration produces the rotation of the gravitoinertial vector. In rotation, the magnitude of the rotating gravity vector is constant; while in linear acceleration, the magnitude of the rotating gravitoinertial vector varies with the magnitude of the acceleration. Adapted from Arrott [1985].

data acquisition at 30 Hz, has recently been used; but without an adequate image analysis system, the data cannot be accurately analyzed. Though it is slightly invasive to the subject, the search coil method provides excellent real-time data of ocular counterrolling and can provide for data acquisition up to 500 Hz. For the present study, a data acquisition rate of 200 Hz was used.

Analysis of the data is mainly focused on the location of any torsional saccades during the sled motion as well as documenting trends of gains and phases of the eye movements for different sled frequencies and accelerations.

4.2 Protocol

As stated earlier, the limiting factor for the protocol for this experiment is the thirty minute time limit that the coils can be in the subject's eye. It was decided to run each subject at one low acceleration and one high acceleration with four frequencies at each. Each run would last 25 seconds to allow for the transients to die out and still provide enough steady-state results. Data would also be taken for five seconds before and ten seconds after the sled motion to allow for examination of non-acceleration eye movements.

The coil was put into the subject's eye as late as possible into the subject preparation time and removed immediately after the last sled run to optimize the time for the sled runs (see Appendix E for subject preparation and Appendix F for coil insertion). The right eye was used for this study, since most of the past ocular counterrolling studies also used the right eye. For all sled runs for the present study, the coil was in the subject's eye less than 30 minutes.

Figure 3.2 shows the MIT sled constraints as well as the profiles for past ocular counterrolling studies. The acceleration values of 0.2 g and 0.6 g were chosen since many of the studies had used these values. Choosing these values allows for comparison of results. For the choice of the four frequencies to use, the following factors were taken into account:

1. The choices of frequencies and accelerations are limited by the length of the rails as shown in the formula

$$\frac{A}{4\pi^2 f^2} < \frac{L}{2} \quad (3.1)$$

For 0.6-g, the minimum frequency would be 0.2519 Hz. Therefore 0.26 Hz was chosen as the lowest frequency.

2. Both Lichtenberg and Arrott have conducted tests at 0.2-g, 0.4 Hz; and Arrott has conducted tests at 0.6-g, 0.4 Hz. For this reason, 0.4 Hz was chosen as one of the frequencies so as to compare results.
3. The maximum frequency of 1.0 Hz was chosen based on the known characteristics of the sled operating range as well as the comfort levels of subjects. This also matches one of Lichtenberg's tests at 0.2-g, 1.0 Hz.
4. Halfway between 0.4 Hz and 1.0 Hz on a logarithmic scale is 0.6325 Hz. From this value comes the final frequency of 0.6 Hz, which is approximately the halfway point.

The order of the runs was chosen randomly to have the 0.2-g accelerations performed first, with the frequency order to be 0.6 Hz, 1.0 Hz, 0.4 Hz, and 0.26 Hz. The only constraint on the order was that it was ideal to have the 0.6 g, 0.26 Hz profile conducted last, since it was the most likely profile to hit an end stop. If this happened (which it did four times), the profile could be rerun without resetting the parameters and still remain within the 30 minute time limit. A horizontal and vertical calibration was also conducted as the first run and last run (time permitting), with the sled stationary. The calibrations were included to verify that the coils were working properly before and after the actual experiment. For the 0.26 Hz profile, the sled completed seven cycles, which took 26.9 seconds as compared to 25 seconds for the other three frequencies. The entire run was still 40 seconds long, and therefore there was less post-sled movement data taken for the 0.26 frequency runs. The order of runs was then:

- | | | | |
|----|-------------|---------|-----------|
| 1. | Calibration | | |
| 2. | 0.2 g | 0.6 Hz | 15 cycles |
| 3. | 0.2 g | 1.0 Hz | 25 cycles |
| 4. | 0.2 g | 0.4 Hz | 10 cycles |
| 5. | 0.2 g | 0.26 Hz | 7 cycles |
| 6. | 0.6 g | 0.6 Hz | 15 cycles |
| 7. | 0.6 g | 1.0 Hz | 25 cycles |

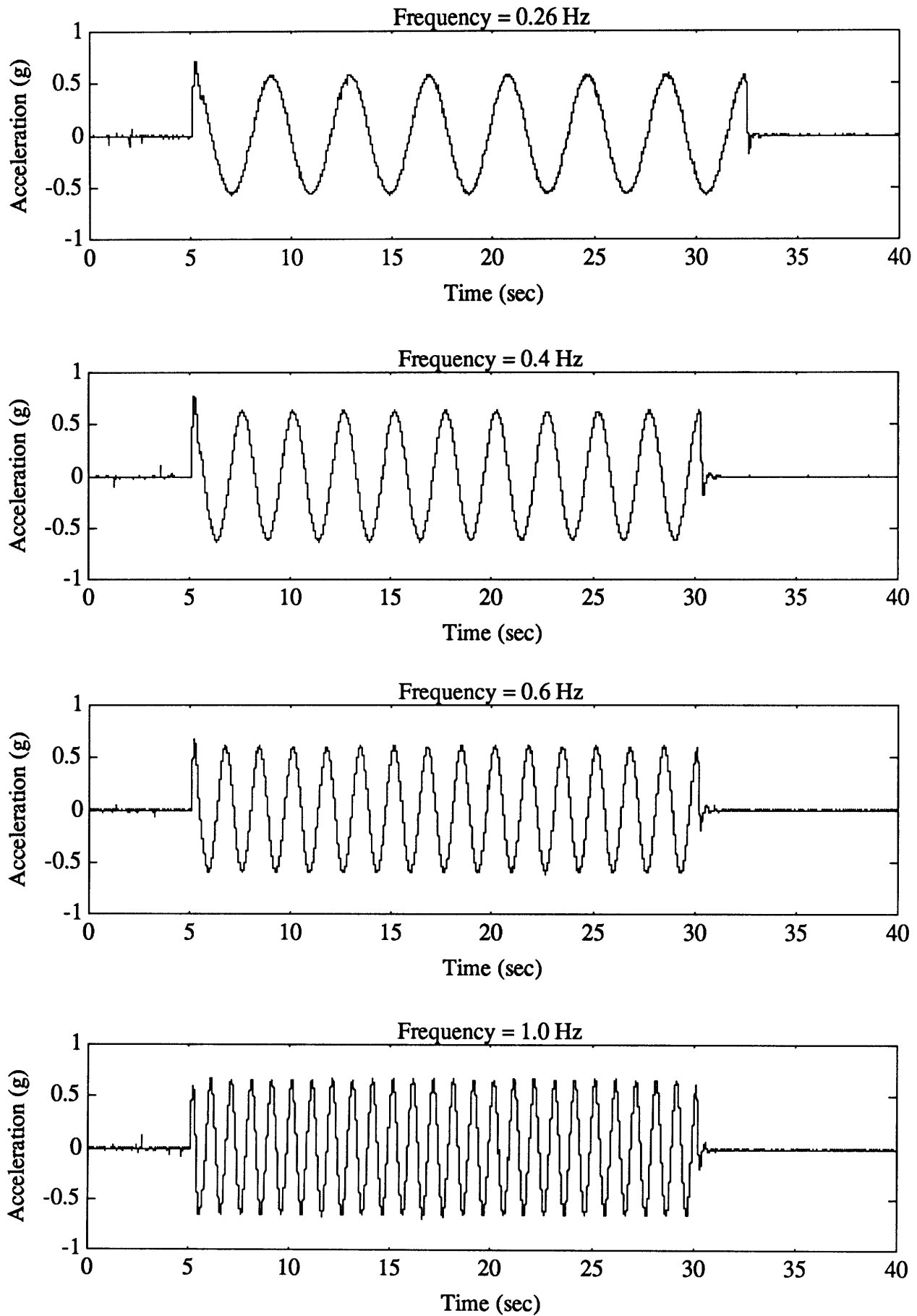


Figure 4.3 The four frequencies of sled motion for the present experiment. The sled motion was smooth. The noise is a result of plotting the data.

- 8. 0.6 g 0.4 Hz 10 cycles
- 9. 0.6 g 0.26 Hz 7 cycles
- 10. Calibration (time permitting)

The sled motion for the four frequencies is shown in Figure 4.3. It was found that twelve runs could be conducted within the 30 minute time limit, which provided for re-runs of two profiles if needed. One subject (subject B, first session) had a slight variation in the order of runs: the 0.2 g, 0.26 Hz profile was performed second, the 0.2 g, 1.0 Hz profile was performed third, and the 0.2 g, 0.4 Hz profile performed fourth; with all other profiles in the above order. Subject E was mistakenly run at 0.2 g, 0.9 Hz instead of 0.2 g, 1.0 Hz for the third profile during the second session.

4.3 Subjects

Six subjects were used for the present study. Three subjects were female and three subjects were male, and their ages ranged from 18 to 30. Subject descriptions are listed in Table 4.1. Each subject was run through the entire protocol twice. All twelve sled sessions were conducted between April 9 and April 15, 1991. Time between the two runs for the subjects varied from one day to six days. Subject A served as a test of the protocol and data taking methods and was run three times, the first time on March 9, 1991. The data from that session was not complete, and was not used for the present study.

Subject	Sex	Age	Time between runs
A	M	21	1 day
B	F	23	6 days
C	M	25	2 days
D	M	30	1 day
E	F	18	1 day
F	F	18	1 day

Table 4.1 Subject Profiles

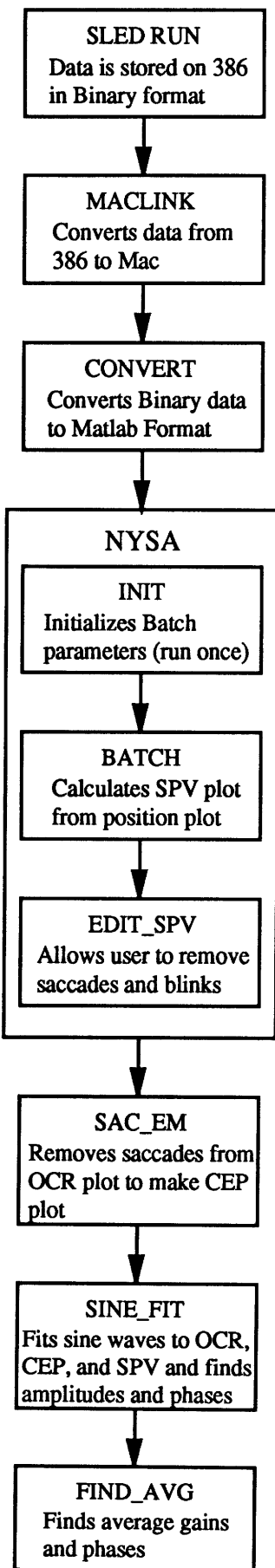
4.4 Data Analysis

The analysis process of the experimental data is shown as a flow chart in Figure 4.4. This process is done on each of the 96 OCR files (eight runs per subject, six subjects, two sessions). Once the sled run is complete, the data has to be transferred from IBM format to Apple Macintosh format. This is done using MacLink Plus, written by DataViz Inc. Once transferred to Macintosh format onto a SyQuest 44 megabyte cartridge, the program Convert, which is listed in Appendix I, is run to convert the data from binary format into Matlab Format. All analysis from this point on is conducted using Matlab scripts. The MVL nystagmus analysis program, called NysA, is run to find the OCR velocity from the OCR position plots and to remove saccades and blinks from the data. The NysA programs are described in the MVL NysA Manual. The program Init initializes the parameters to be used for the program Batch, and only needs to be run once. Batch is then run to calculate the slow phase velocity (SPV) plot from the position plot. Batch, as the name implies, is a batch program, and therefore the user only has to enter the file names and let the program calculate all the slow phase velocities.

Once Batch has calculated the slow phase velocities for all the files, the program Edit_spv is called up to conduct the removal of the blinks and saccades. NysA does offer a high pass filter to remove large eye saccades, but with torsional movements, the saccades are so small that the filter cannot catch them. Therefore, each saccade had to be located and removed by the author using the Edit_spv program. Each file took approximately 30 minutes to edit. This resulted in 48 hours of editing time, which took five days to finish. Once finished, a relatively smooth slow phase velocity plot for each file was stored.

All following analysis programs are listed in Appendix I, with full descriptions of their use. Since NysA removes the saccades from only the velocity plot, a program called Sac_em is run to remove the saccades from the position plot. This program locates each saccade from the SPV plot and adjusts the remaining data points to the pre-saccade value. This results in a Cumulative Eye Position (CEP) plot. The program Sine_fit is used to fit

For each data set, the following are performed



Once the gains and phases of all runs are found, the following are performed

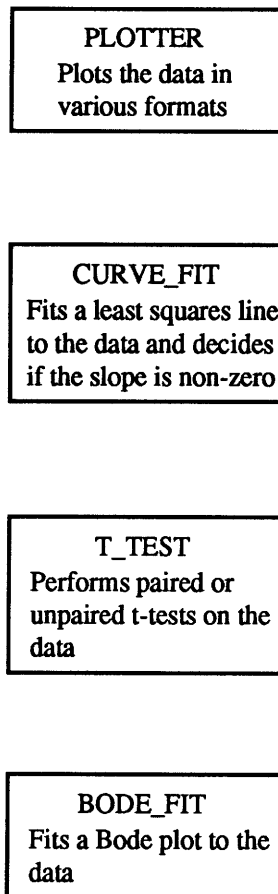


Figure 4.4 Diagram of the steps involved in analysis of data.

sine waves to the ocular counterrolling plots, the cumulative eye position plots, and the slow phase velocity plots. The program also finds the amplitudes and phases of both the signal and the acceleration for each cycle of the sled run. The program Find_Avg is used to convert these amplitudes and phases into gains and phases for each cycle as well as into average gains and phases for each run. Upon examination, and based upon the procedure of Lichtenberg and Arrott, it was decided that the first five seconds of each sled run would not be used in the analysis. This allowed for the transients to die out and analysis of the steady-state response. This resulted in the removal of the first two cycles of the 0.26 Hz frequency runs, the first two cycles of the 0.4 Hz runs, the first three cycles of the 0.6 Hz runs, and the first five cycles of the 1.0 Hz runs. The average gain and phase are calculated with these cycles removed.

Once the gains and phases of each sled run are found, the data can then be plotted and analyzed. Three programs are used from this point on. The program Plotter was used to plot the data in the user's choice of the following formats:

1. Signal plots (OCR, horizontal, vertical, acceleration, SPV, CEP).
2. Gains and Phases plots (gains or phases versus frequency, Bode plots).
3. Phase versus time plot.
4. One cycle plots.

The program Curve_fit is used to fit a least squares line to OCR gain, OCR phase, SPV gain, SPV phase, CEP gain, or CEP phase versus frequency. Using a 95% confidence interval, the program then decides if the slope is statistically different from zero, thus showing the trends of the parameter with respect to frequency. The program T-test was used to perform paired and unpaired t-tests on the sled runs. The program is a batch program and compares all files which are comparable and stores a 0 if they're not significantly different and a 1 if they are significantly different. Examples of the comparisons that this program makes are:

1. Gain (or phase) of OCR (or SPV or CEP) at different frequencies, same

acceleration.

- 2. Gain (or phase) of OCR (or SPV or CEP) at different accelerations, same frequency.**
- 3. Gain (or phase) of OCR (or SPV or CEP) for different runs, at same acceleration, same frequency.**

Chapter 5

Results

All six subjects show similar ocular counterrolling responses to the sinusoidal accelerations. The responses have the same frequency as the sled motion, with a slight phase lag from the acceleration of the sled. The response usually begins with an overshoot of OCR and then a settling down to steady state. During the sled runs, four channels are stored: ocular counterrolling, horizontal eye position, vertical eye position, and acceleration. Figure 5.1 shows these output channels for a representative sled run. For all the plots presented in this paper, the following method is used: positive OCR represents clockwise eye rotation as viewed by looking at the subject; positive horizontal eye movement represents right movement as viewed by looking at the subject (left subject eye movement); positive vertical eye movement represents upward eye movements; positive acceleration represents acceleration to the subject's left. Figure 5.2 shows a sample of the OCR responses to the four different frequencies at 0.2 g acceleration. Figure 5.3 shows a sample of the OCR responses to the four different frequencies at 0.6 g acceleration. Notice that the response to 0.6 g is approximately three times greater than the response to 0.2 g. For all subjects, the OCR response for the high acceleration runs were significantly greater than the response for the low acceleration runs at the same frequency.

As seen in Figure 5.2 and Figure 5.3, the ocular counterrolling response to the sinusoidal linear accelerations is a smooth sinusoidal motion interrupted by small saccades, some in the direction of eye roll and some against the direction of eye roll, which resemble horizontal and vertical compensatory eye movements. These saccades occurred at a rate of 0.2 to 2.8 per second in all subjects during the sinusoidal motion. Past studies had very

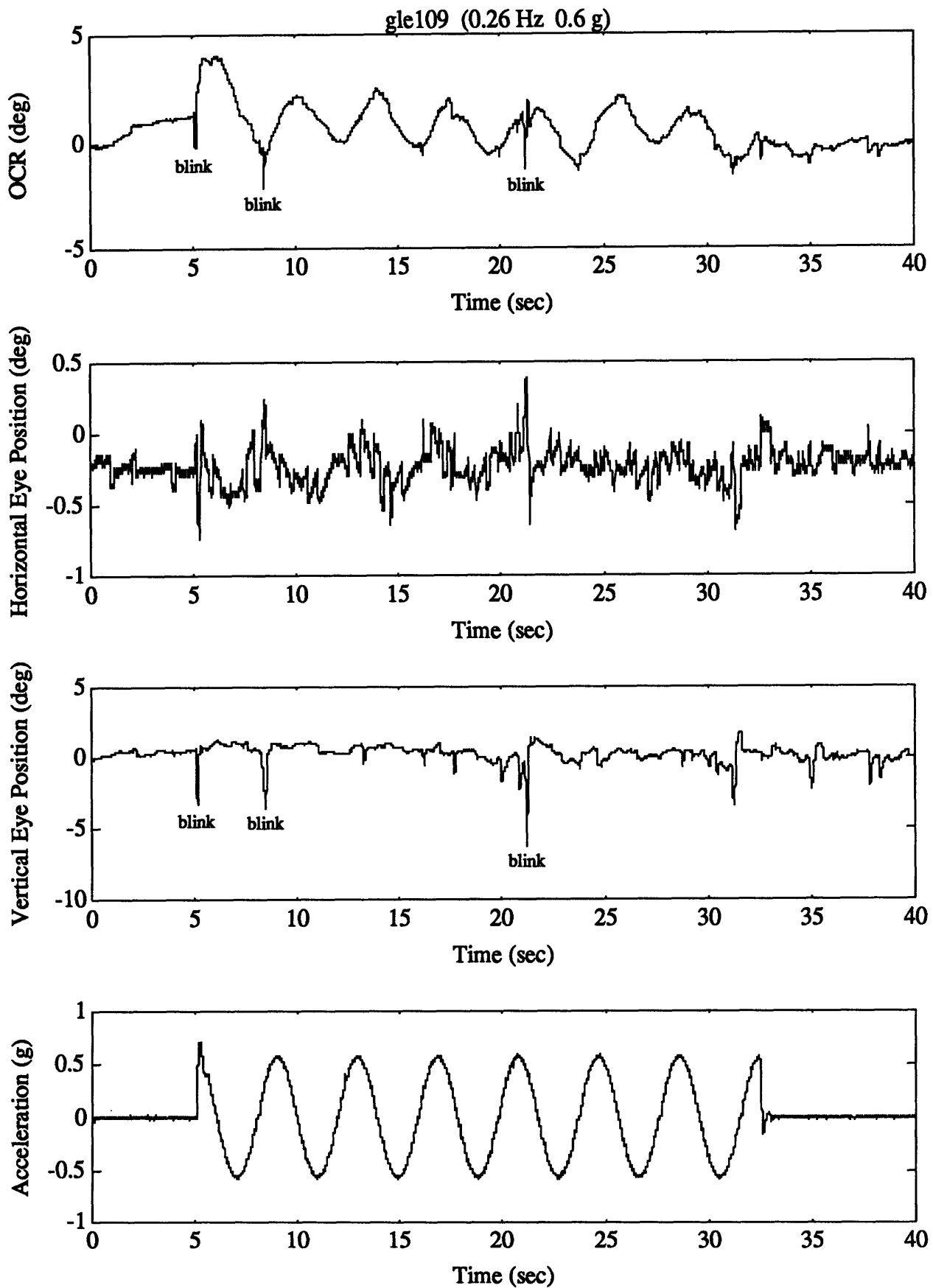


Figure 5.1 The four channels that are monitored during the experiment. The above are for Subject E. Notice the blinks on the OCR and Vertical channels.

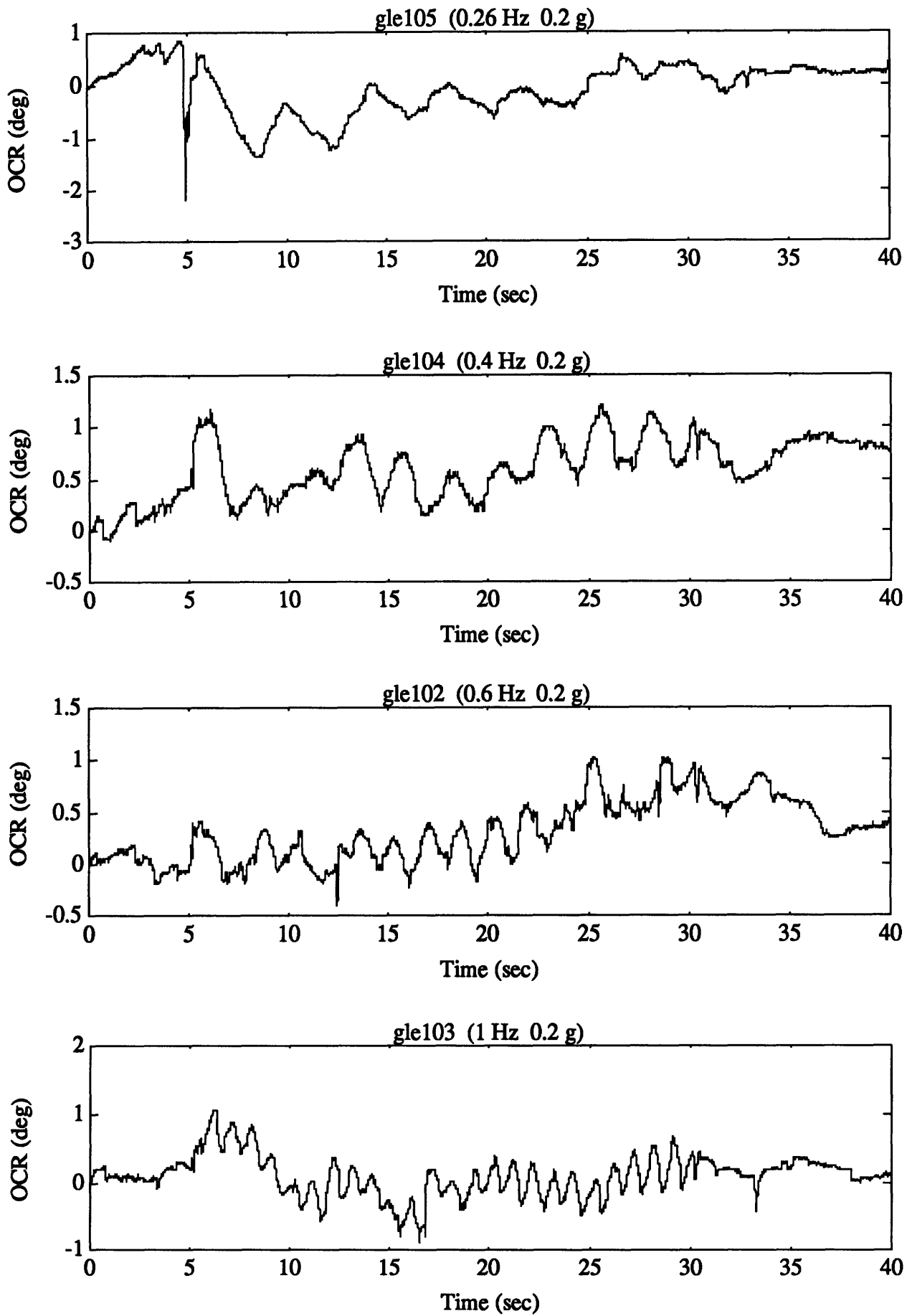


Figure 5.2 Ocular Counterrolling response of Subject E during four frequencies at 0.2 g.

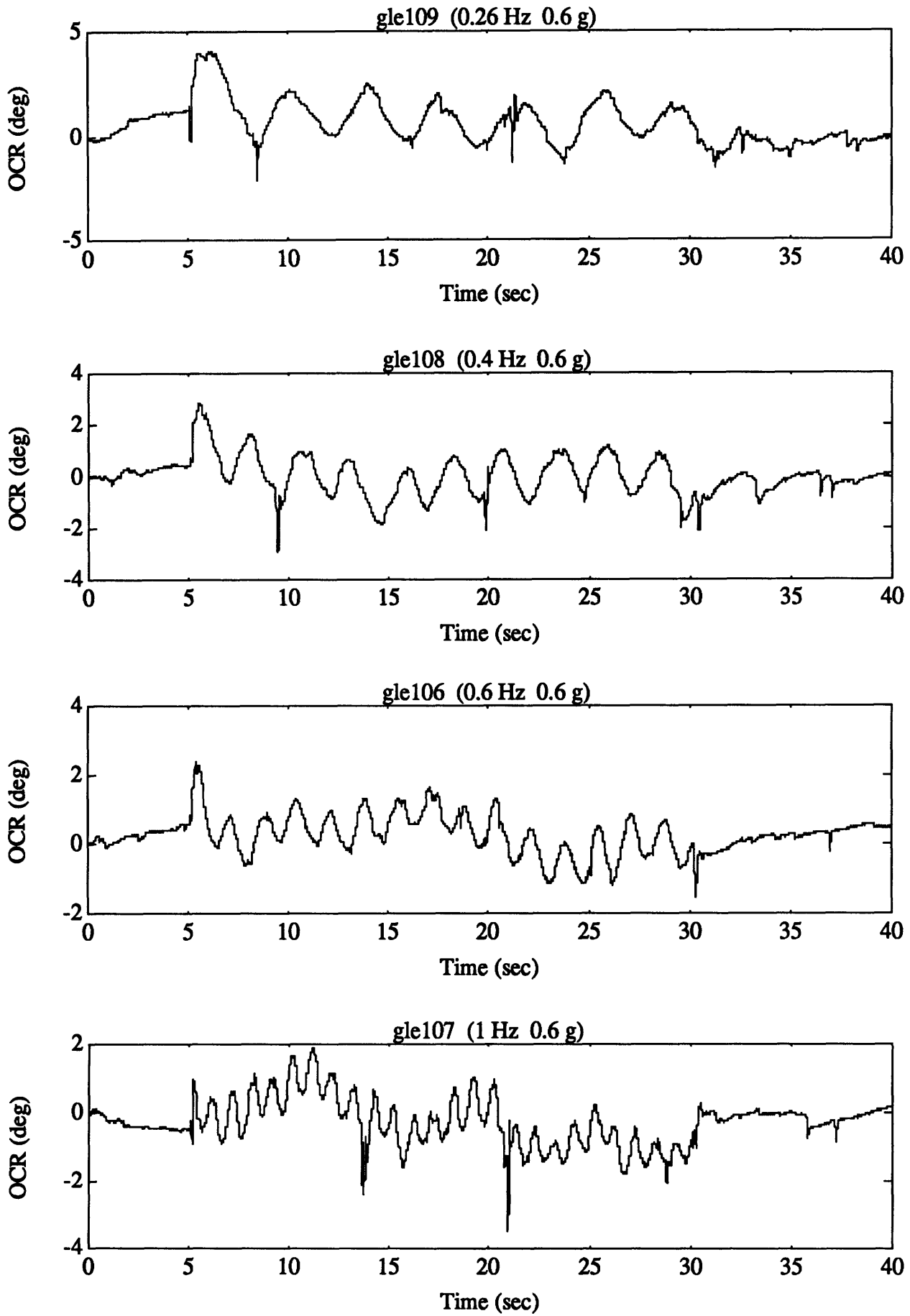


Figure 5.3 Ocular Counterrolling response of Subject E during four frequencies at 0.6 g.

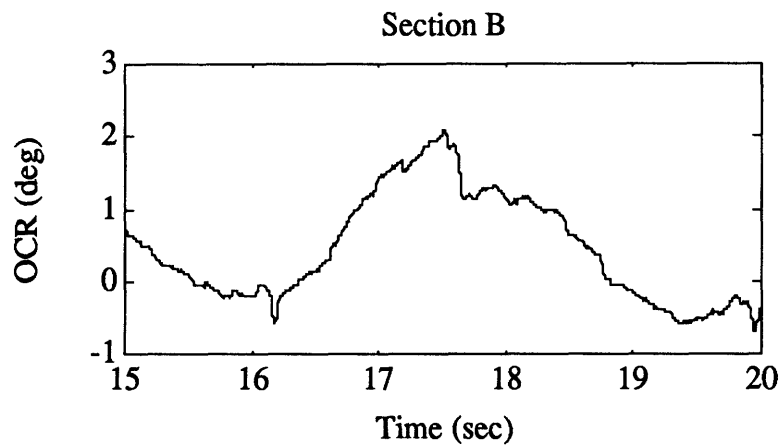
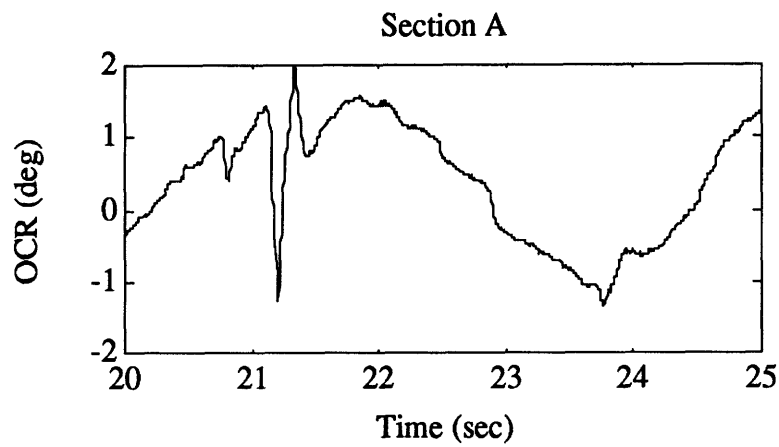
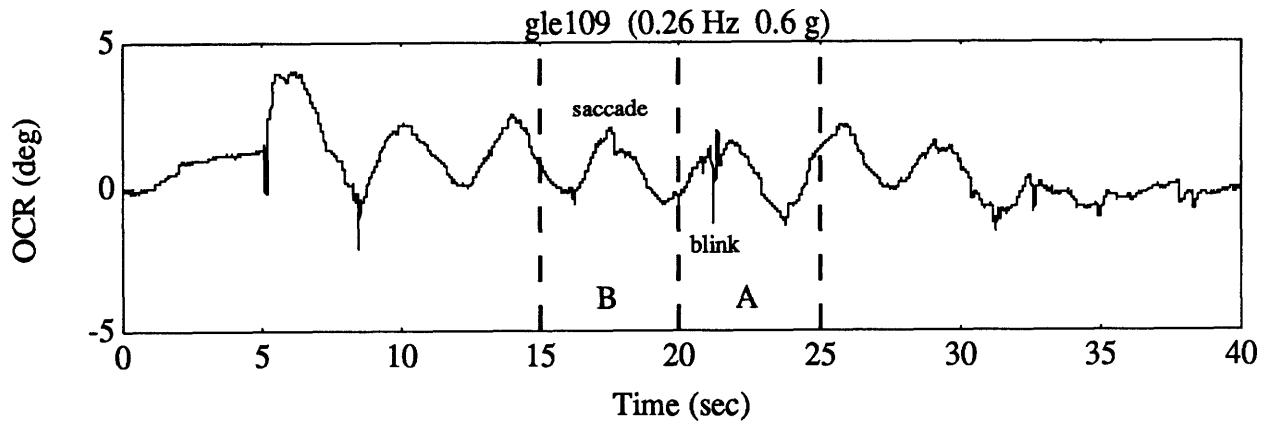


Figure 5.4 Blinks and saccades. The middle plot shows a blow up of the blink that occurs at 21 seconds. The bottom plot shows a blow up of the saccade that occurs at 17.5 seconds. Both of these eye movements must be removed from all of the OCR data.

slow data acquisition rates, and were not able to locate the saccades and separate them from the smooth eye motion. As can be seen in the ocular counterrolling channel and the vertical channel from Figure 5.1, blinks and saccades cause discontinuities in the OCR data.

Figure 5.4 shows just the ocular counterrolling channel as well as close ups of a blink and a saccade. The blinks can be removed quite easily from the position trace since the eye returns to its pre-blink position quite rapidly, but the saccades cause jumps in the OCR position which makes fitting a sine curve to the data impossible.

For this reason, the program NysA, described earlier, is used to calculate the velocity of the OCR motion and manually remove the saccades, resulting in a smooth sinusoidal slow phase velocity (SPV) profile. Table 5.1 lists the number of saccades during each run for each subject. The table also shows that the number of saccades per second tends to be larger during the run than during no motion. Notice that the number of saccades per second tends to increase with increasing acceleration and with increasing frequency. Once the SPV is found, the program Sac_em is used to remove the saccades from the position plot, forming the Cumulative Eye Position (CEP) plot as shown in Figure 5.5 for Subject A. The saccades are no longer present, and a sine curve can be fitted to the CEP plot. Using both SPV and CEP to describe eye movements is redundant since, in essence, CEP is just the integral of SPV. For the following analysis, it was decided to use Cumulative Eye Position, since all previous papers have used position as a reference.

Using the program Sine_fit, discussed in Chapter 4, both the OCR and the CEP are fitted to sinusoidal curves, as shown in Figure 5.6 for Subject A. Notice that the CEP curve fit is much smoother than the OCR curve fit because of the removal of the discontinuities caused by the saccades. The amplitudes of each cycle in the CEP curve fit are also much less variable than that of the OCR. Using the program Find_avg, the gains and phases for the OCR and CEP of each sled run are found by averaging over the cycles of the run.

Subject	Profile	Saccades/sec (during motion)	Saccades/sec (before motion)
A (Day 1)	0.2 g 0.26 Hz	0.52	0.2
	0.2 g 0.4 Hz	0.92	0.0
	0.2 g 0.6 Hz	0.92	0.0
	0.2 g 1.0 Hz	1.16	0.0
	0.6 g 0.26 Hz	0.88	0.2
	0.6 g 0.4 Hz	1.12	0.6
	0.6 g 0.6 Hz	1.28	1.0
	0.6 g 1.0 Hz	2.12	0.4
A (Day 2)	0.2 g 0.26 Hz	0.74	0.8
	0.2 g 0.4 Hz	0.88	0.8
	0.2 g 0.6 Hz	0.68	0.2
	0.2 g 1.0 Hz	1.08	0.6
	0.6 g 0.26 Hz	1.11	1.0
	0.6 g 0.4 Hz	1.60	1.4
	0.6 g 0.6 Hz	1.20	0.2
	0.6 g 1.0 Hz	1.92	0.6
B (Day 1)	0.2 g 0.26 Hz	0.74	0.0
	0.2 g 0.4 Hz	0.84	0.2
	0.2 g 0.6 Hz	0.64	0.2
	0.2 g 1.0 Hz	1.24	0.2
	0.6 g 0.26 Hz	1.60	0.0
	0.6 g 0.4 Hz	1.64	0.6
	0.6 g 0.6 Hz	1.36	0.0
	0.6 g 1.0 Hz	1.96	0.0
B (Day 2)	0.2 g 0.26 Hz	0.89	0.4
	0.2 g 0.4 Hz	1.36	0.4
	0.2 g 0.6 Hz	1.72	0.0
	0.2 g 1.0 Hz	1.68	0.0
	0.6 g 0.26 Hz	1.52	0.0
	0.6 g 0.4 Hz	1.64	1.0
	0.6 g 0.6 Hz	2.16	0.2
	0.6 g 1.0 Hz	2.84	0.4

Table 5.1 Number of saccades per second before and during the sled motion for each subject.

Subject	Profile	Saccades/sec (during motion)	Saccades/sec (before motion)
C (Day 1)	0.2 g 0.26 Hz	1.86	1.4
	0.2 g 0.4 Hz	1.20	0.6
	0.2 g 0.6 Hz	1.36	0.8
	0.2 g 1.0 Hz	1.40	0.8
	0.6 g 0.26 Hz	1.37	0.0
	0.6 g 0.4 Hz	1.40	1.6
	0.6 g 0.6 Hz	1.64	1.0
	0.6 g 1.0 Hz	1.12	0.8
C (Day 2)	0.2 g 0.26 Hz	1.00	1.0
	0.2 g 0.4 Hz	1.24	1.4
	0.2 g 0.6 Hz	1.04	0.6
	0.2 g 1.0 Hz	1.52	0.8
	0.6 g 0.26 Hz	1.45	0.8
	0.6 g 0.4 Hz	1.28	0.6
	0.6 g 0.6 Hz	1.52	1.2
	0.6 g 1.0 Hz	1.60	0.8
D (Day 1)	0.2 g 0.26 Hz	0.45	0.4
	0.2 g 0.4 Hz	0.56	0.2
	0.2 g 0.6 Hz	0.60	0.6
	0.2 g 1.0 Hz	0.68	0.4
	0.6 g 0.26 Hz	0.85	0.4
	0.6 g 0.4 Hz	1.20	0.6
	0.6 g 0.6 Hz	1.12	0.6
	0.6 g 1.0 Hz	1.52	0.4
D (Day 2)	0.2 g 0.26 Hz	0.22	0.4
	0.2 g 0.4 Hz	0.32	0.6
	0.2 g 0.6 Hz	0.72	0.4
	0.2 g 1.0 Hz	0.60	0.6
	0.6 g 0.26 Hz	1.04	0.0
	0.6 g 0.4 Hz	0.68	0.2
	0.6 g 0.6 Hz	0.92	0.6
	0.6 g 1.0 Hz	1.08	0.4

Table 5.1 Number of saccades per second before and during the sled motion for each subject (continued from previous page).

Subject	Profile	Saccades/sec (during motion)	Saccades/sec (before motion)
E (Day 1)	0.2 g 0.26 Hz	1.00	1.0
	0.2 g 0.4 Hz	0.96	1.2
	0.2 g 0.6 Hz	1.16	0.4
	0.2 g 0.9 Hz	1.39	0.4
	0.6 g 0.26 Hz	1.34	0.8
	0.6 g 0.4 Hz	1.32	0.6
	0.6 g 0.6 Hz	1.88	1.0
	0.6 g 1.0 Hz	1.32	1.0
E (Day 2)	0.2 g 0.26 Hz	1.08	0.8
	0.2 g 0.4 Hz	1.12	0.8
	0.2 g 0.6 Hz	1.60	1.4
	0.2 g 1.0 Hz	1.52	1.0
	0.6 g 0.26 Hz	1.41	0.6
	0.6 g 0.4 Hz	1.44	0.4
	0.6 g 0.6 Hz	1.28	0.8
	0.6 g 1.0 Hz	1.48	0.2
F (Day 1)	0.2 g 0.26 Hz	0.63	0.4
	0.2 g 0.4 Hz	0.76	0.4
	0.2 g 0.6 Hz	1.32	0.0
	0.2 g 1.0 Hz	1.08	0.6
	0.6 g 0.26 Hz	0.89	0.0
	0.6 g 0.4 Hz	1.24	0.4
	0.6 g 0.6 Hz	0.96	0.4
	0.6 g 1.0 Hz	1.08	0.4
F (Day 2)	0.2 g 0.26 Hz	0.67	0.4
	0.2 g 0.4 Hz	0.64	0.4
	0.2 g 0.6 Hz	0.36	0.0
	0.2 g 1.0 Hz	0.92	0.6
	0.6 g 0.26 Hz	0.59	0.8
	0.6 g 0.4 Hz	0.96	0.2
	0.6 g 0.6 Hz	0.92	0.2
	0.6 g 1.0 Hz	1.52	0.8

Table 5.1 Number of saccades per second before and during the sled motion for each subject (continued from previous page).

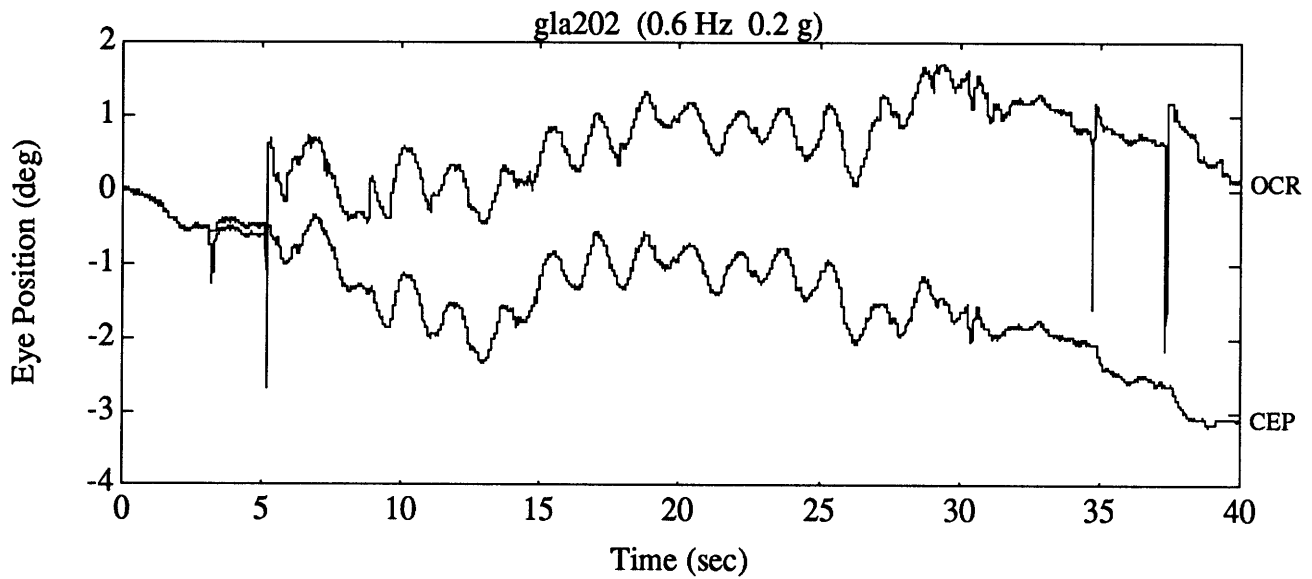


Figure 5.5 Cumulative eye position and OCR position. Notice that there is approximately 3° difference between the final values of CEP and OCR resulting from the removal of the saccades.

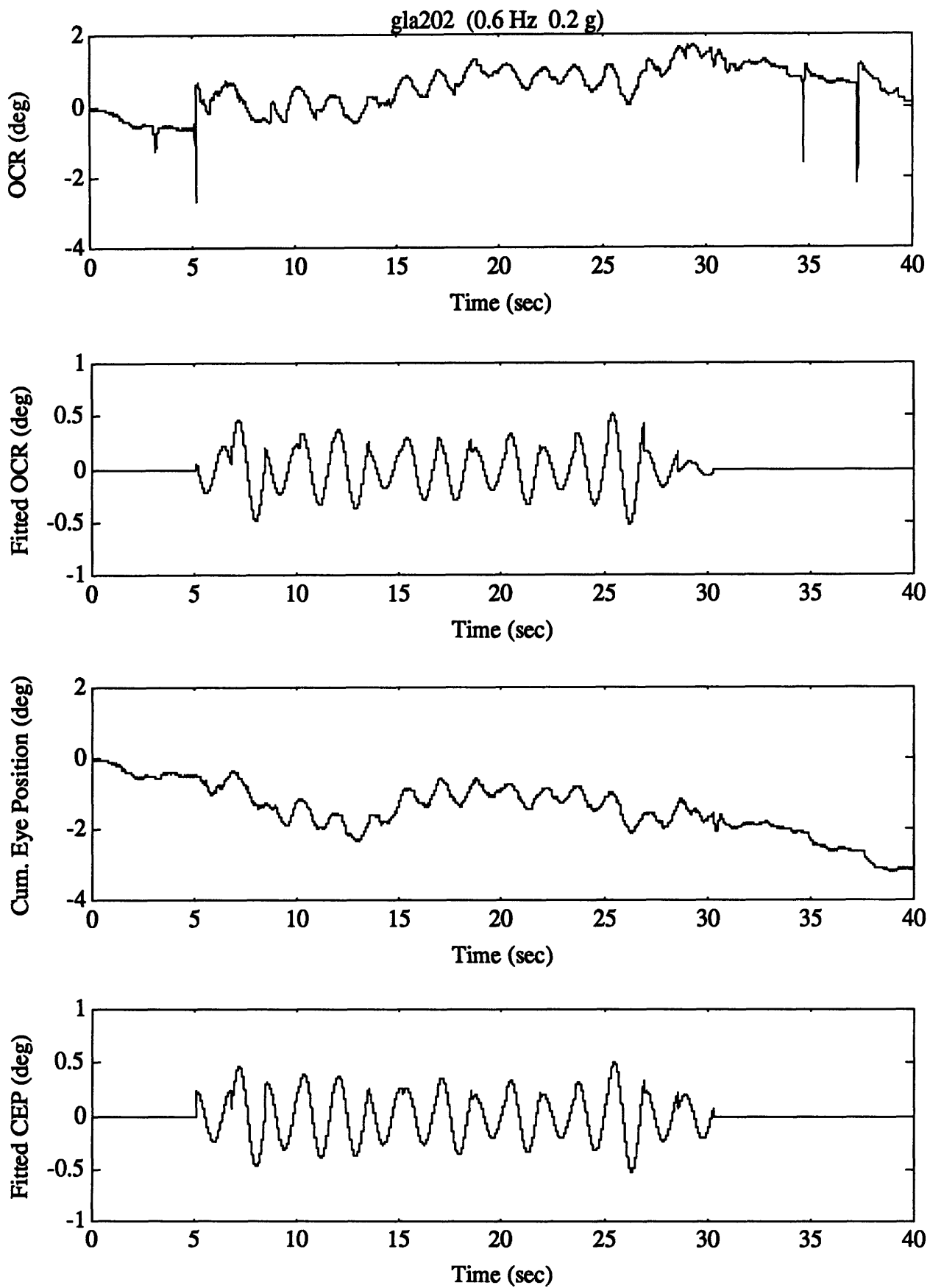


Figure 5.6 Curve fits for OCR and CEP. Notice that the CEP has a much smoother curve fit as well as less variability in amplitudes.

Figure 5.7 shows the Cumulative Eye Position gains and phases for all runs for Subject A. In the figure, the gain decreases with increasing frequency and flattens out at higher frequencies. The figure also shows a decrease in phase lag with increasing frequency. These trends suggest a position response in the form of the first order equation:

$$\frac{K(s + \omega_c)}{s} \quad (5.1)$$

The constant, K, and the cutoff frequency, ω_c , can be found from the gains and phases from each sled run. Putting the above formula into the form:

$$X + Yj \quad (5.2)$$

the result is

$$K - K \frac{\omega_c j}{\omega} \quad (5.3)$$

Since $X = G \cos \phi$ and $Y = G \sin \phi$, the following formulas for the gain and phase in terms of K and ω_c can be derived:

$$G = K \sqrt{\left(\frac{\omega_c}{\omega}\right)^2 + 1} \quad (5.4)$$

$$\tan \phi = - \frac{\omega_c}{\omega} \quad (5.5)$$

The program Bode_fit, listed in Appendix I, optimizes Equation 5.4 for the constant and the cutoff frequency and finds the best fit Bode plot. The program also optimizes Equation 5.5 for the cutoff frequency. The difference between the two calculated cutoff frequencies is then found. For the Bode fit based on phase, the K value from Equation 5.4 is used.

The ocular counterrolling responses of the linear accelerations for each subject was found to have statistically significant differences in gain and phase values. Therefore, the subjects could not be grouped together. An attempt was made to group the two test sessions for each subject together as well as to group the low acceleration and high acceleration runs for each subject together. Ideally, the data from the two different days should be exactly the same. Lichtenberg [1979] and Arrott [1982] had stated that the OCR

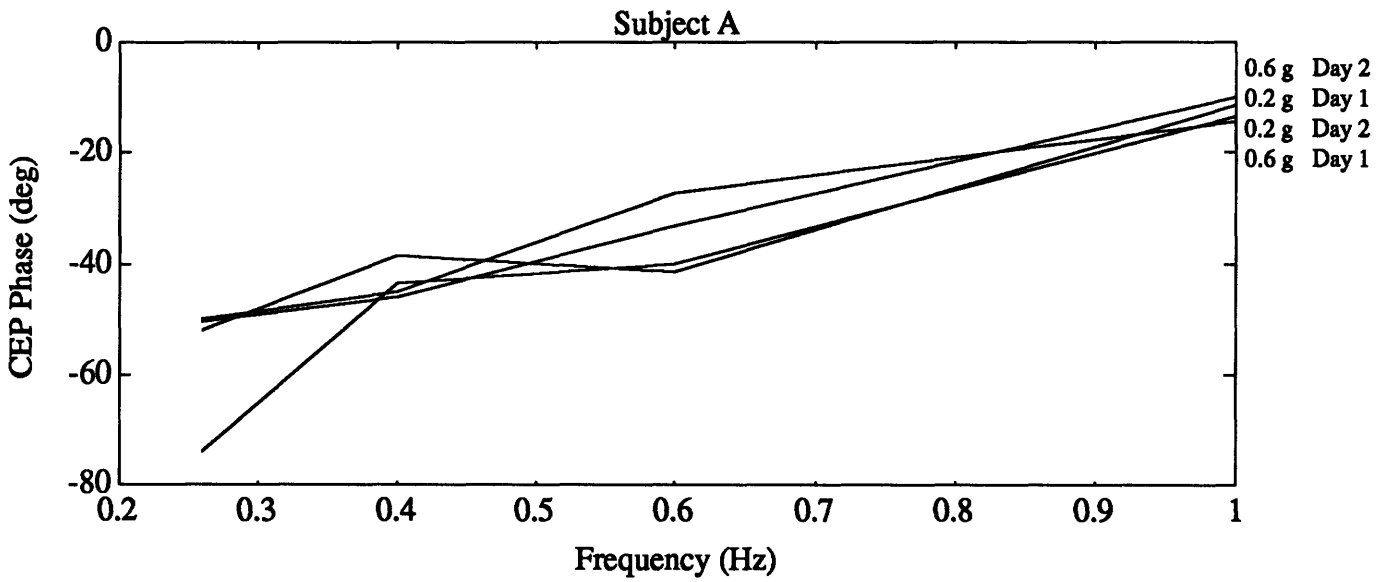
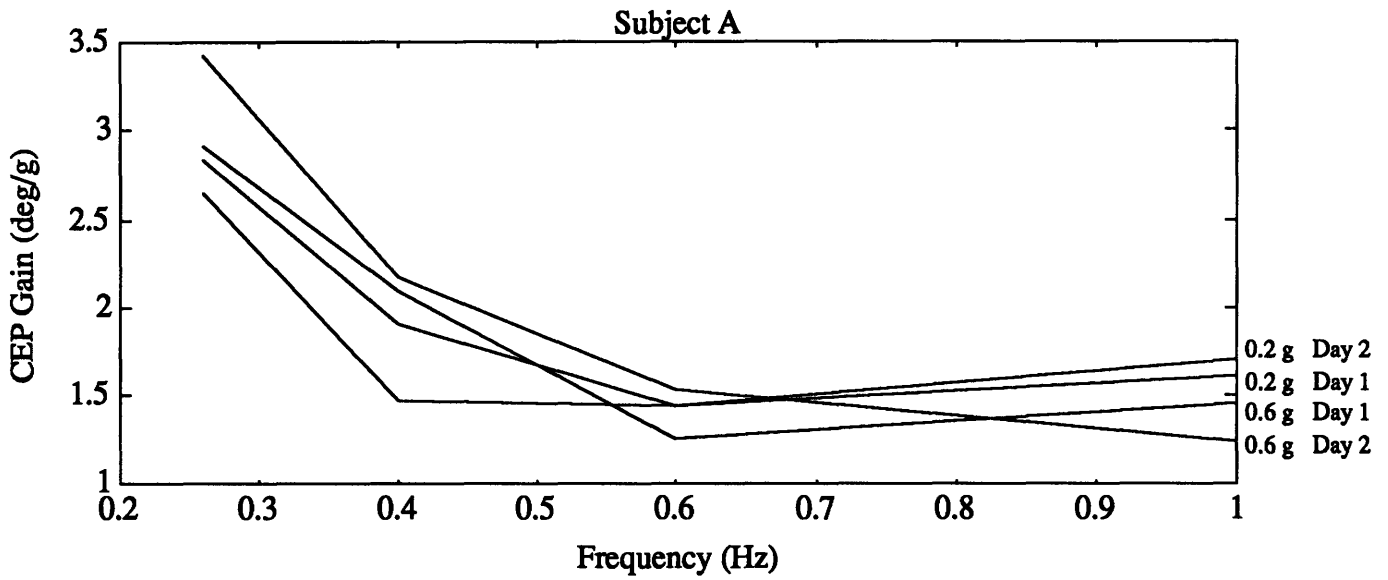


Figure 5.7 Average cumulative eye position gains and phases for all runs for subject A. Each line represents one set of runs at a constant acceleration on one session day.

response during linear accelerations is linear with respect to the acceleration. If this were true, then the CEP gain values would be constant for all acceleration values, and the low acceleration and high acceleration runs could be grouped together. With all four sets of data then grouped, each subject's data could be fitted to Equation 5.1. To attempt to group the two days and the two acceleration levels, a t-test was performed on the CEP gain values for each subject. Gain instead of phase is used for the t-test comparisons because small fluctuations in the data will cause large changes in the phases. Of the six subjects, subjects A, C, and D had statistically similar results for both days and during both acceleration levels; and therefore, all four sets of data could be grouped. Subject F had statistically different results for both days, but had statistically similar results during both acceleration levels; and therefore, the two acceleration levels could be grouped. Subjects B and E had statistically different results from both the two days and the two acceleration levels; and therefore none of the data sets could be grouped.

Bode_fit was run on all subjects' data to fit the CEP values to Equation 5.1. For subjects A, C, and D, one Bode plot was fitted to all data for each subject. For subject F, one Bode plot was fitted for each day. For subjects B and E, four Bode plots were fitted for each subject; one for each day at each acceleration level. Figure 5.8 through Figure 5.13 show these Bode plots. For the gain plots in the figures, the values for the constant, K , and the cutoff frequency, ω_c , were calculated from Equation 5.4. For the phase plots, the value for the cutoff frequency, ω_c , was calculated from Equation 5.5. The difference between the two cutoff frequencies is also shown in the figures. For the second testing day of subject F, the cutoff frequency was found never to converge, and therefore be at infinity; and therefore this Bode plot is not shown. Subject B had poor OCR responses, and at times had no response, during the low-g runs. Because of this fact, the curve fitting process for the low-g condition for subject B was difficult, as reflected in the phase plots in Figure 5.9. For both low-g runs of subject E, the break frequency was found to be at zero.

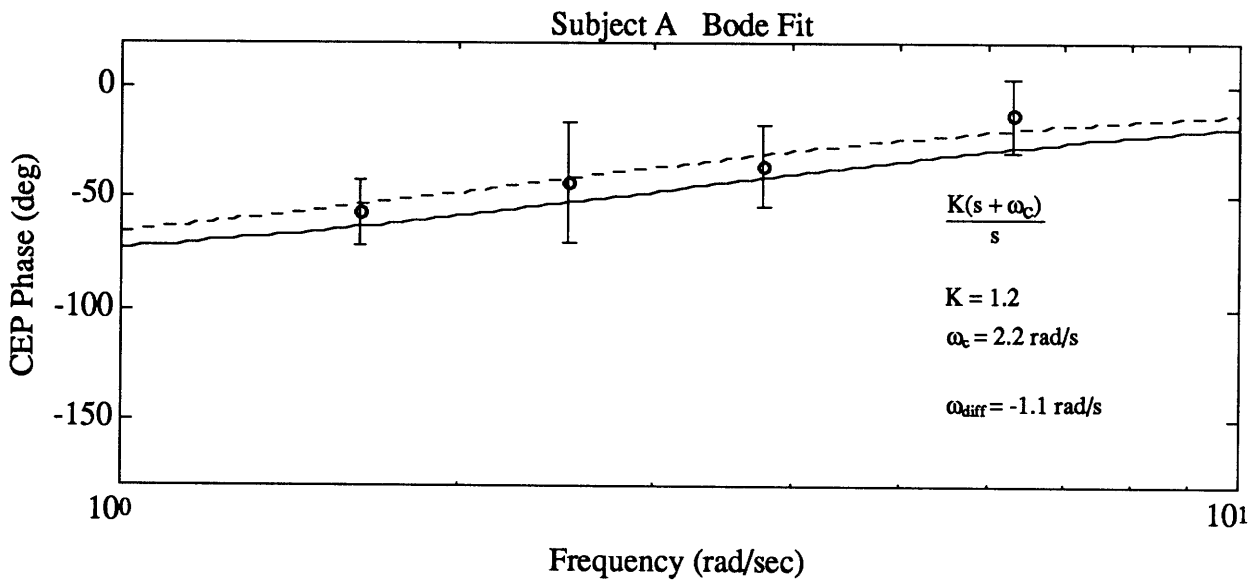
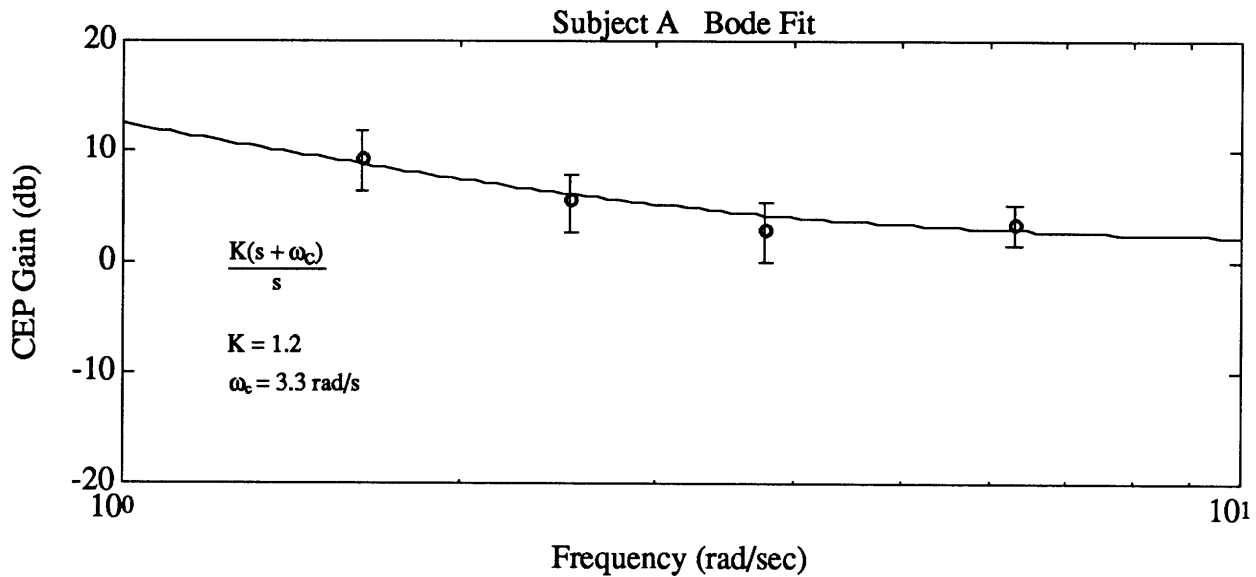


Figure 5.8 Bode plot for all runs from Subject A. The solid lines in both plots are based on the values of K and ω_c as calculated from the gains (Equation 5.4). The dashed line in the phase plot is based on the value of ω_c as calculated from the phases (Equation 5.5). The difference between these two cutoff frequency values is shown as ω_{diff} in the phase plot.

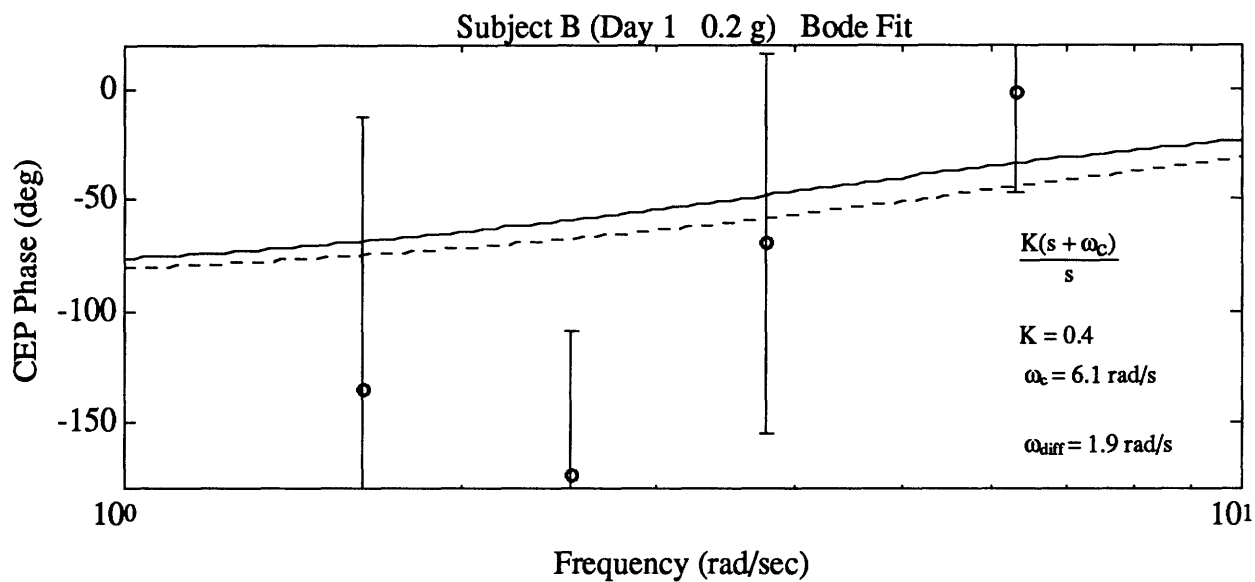
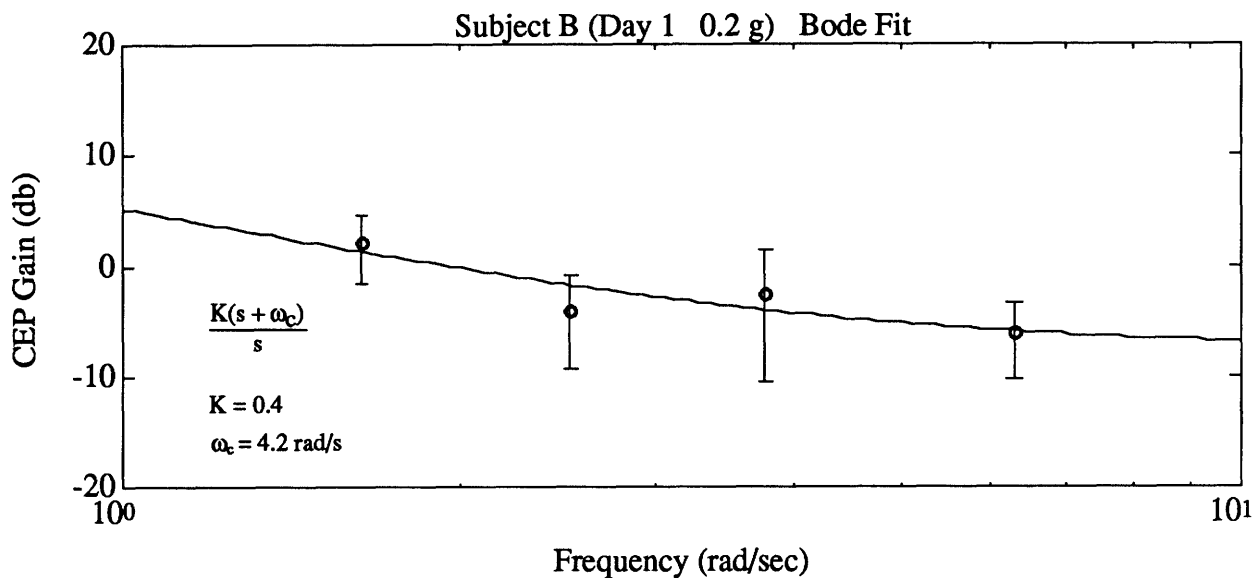


Figure 5.9a Bode plot for Subject B (Day 1, 0.2 g). The solid lines in both plots are based on the values of K and ω_c as calculated from the gains (Equation 5.4). The dashed line in the phase plot is based on the value of ω_c as calculated from the phases (Equation 5.5). The difference between these two cutoff frequency values is shown as ω_{diff} in the phase plot.

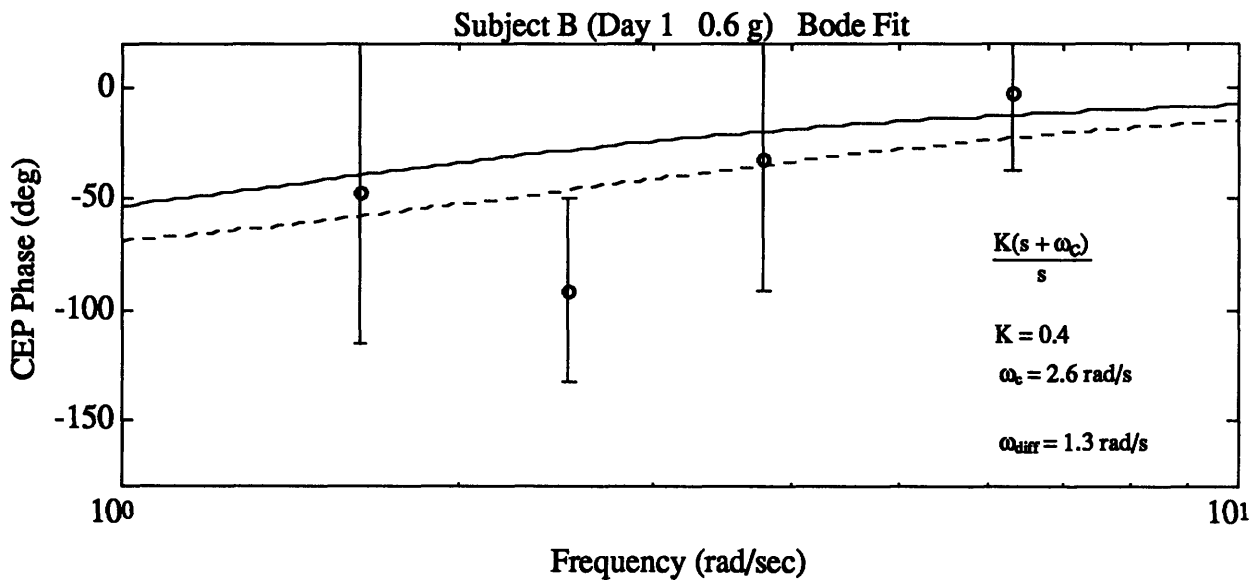
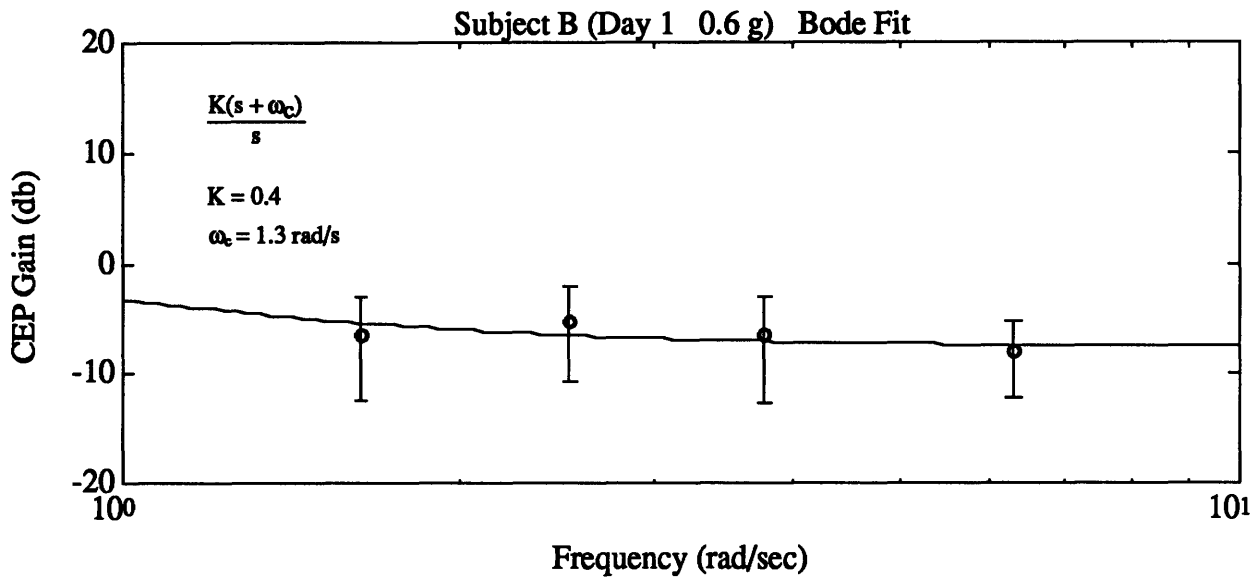


Figure 5.9b Bode plot for Subject B (Day 1, 0.6 g). The solid lines in both plots are based on the values of K and ω_c as calculated from the gains (Equation 5.4). The dashed line in the phase plot is based on the value of ω_c as calculated from the phases (Equation 5.5). The difference between these two cutoff frequency values is shown as ω_{diff} in the phase plot.

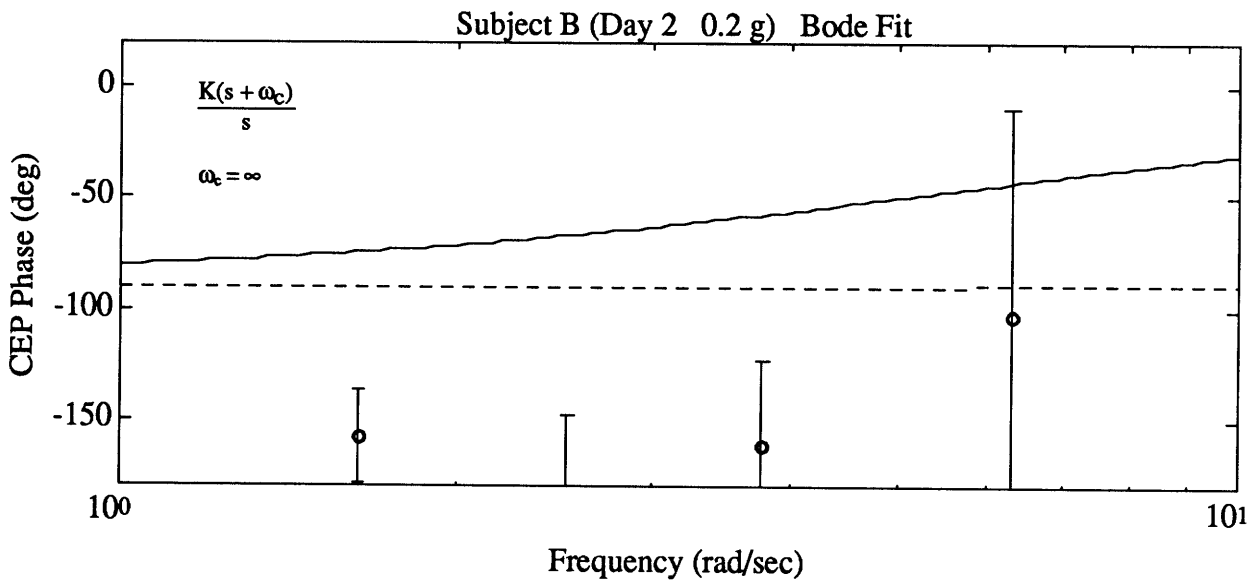
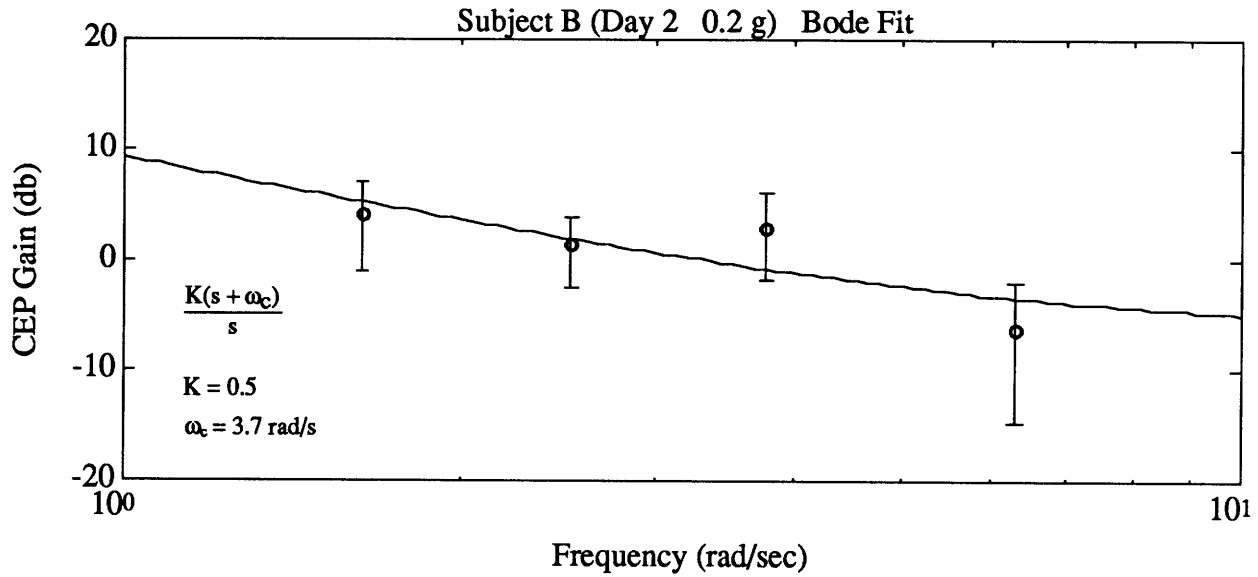


Figure 5.9c Bode plot for Subject B (Day 2, 0.2 g). The solid lines in both plots are based on the values of K and ω_c as calculated from the gains (Equation 5.4). The dashed line in the phase plot is based on the value of ω_c as calculated from the phases (Equation 5.5). The difference between these two cutoff frequency values is shown as ω_{diff} in the phase plot.

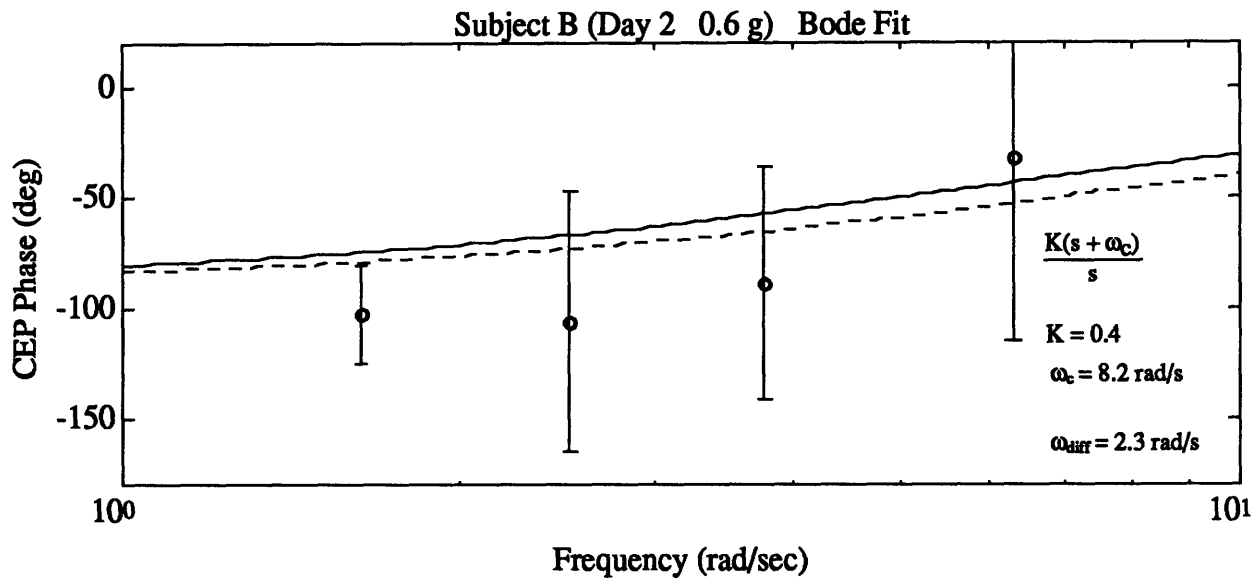
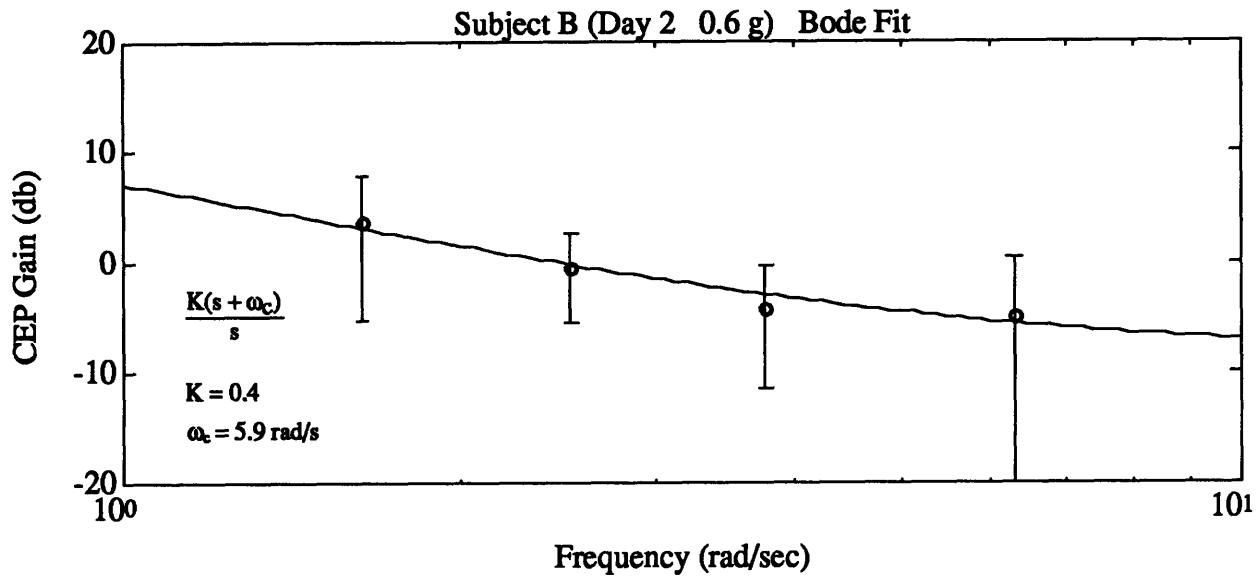


Figure 5.9d Bode plot for Subject B (Day 2, 0.6 g). The solid lines in both plots are based on the values of K and ω_c as calculated from the gains (Equation 5.4). The dashed line in the phase plot is based on the value of ω_c as calculated from the phases (Equation 5.5). The difference between these two cutoff frequency values is shown as ω_{diff} in the phase plot.

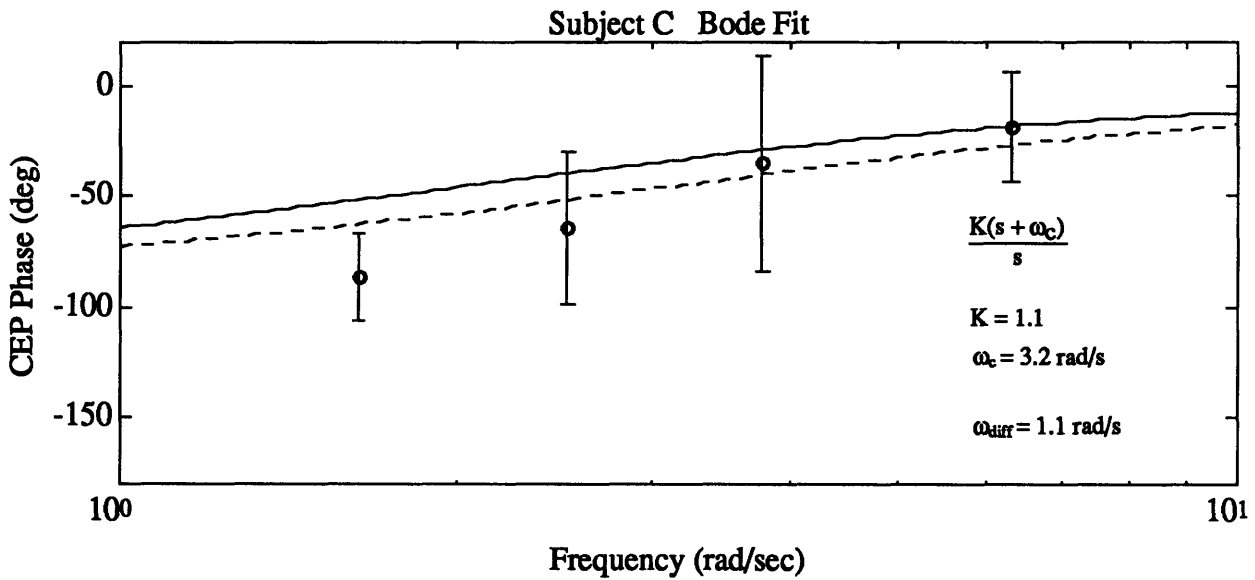
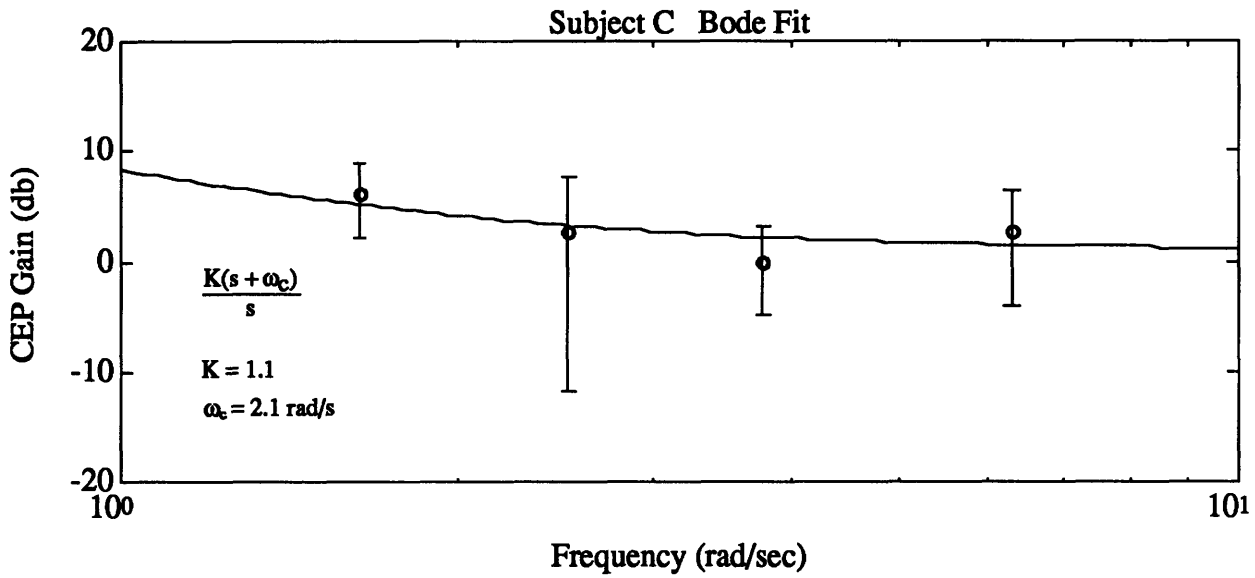


Figure 5.10 Bode plot for all runs from Subject C. The solid lines in both plots are based on the values of K and ω_c as calculated from the gains (Equation 5.4). The dashed line in the phase plot is based on the value of ω_c as calculated from the phases (Equation 5.5). The difference between these two cutoff frequency values is shown as ω_{diff} in the phase plot.

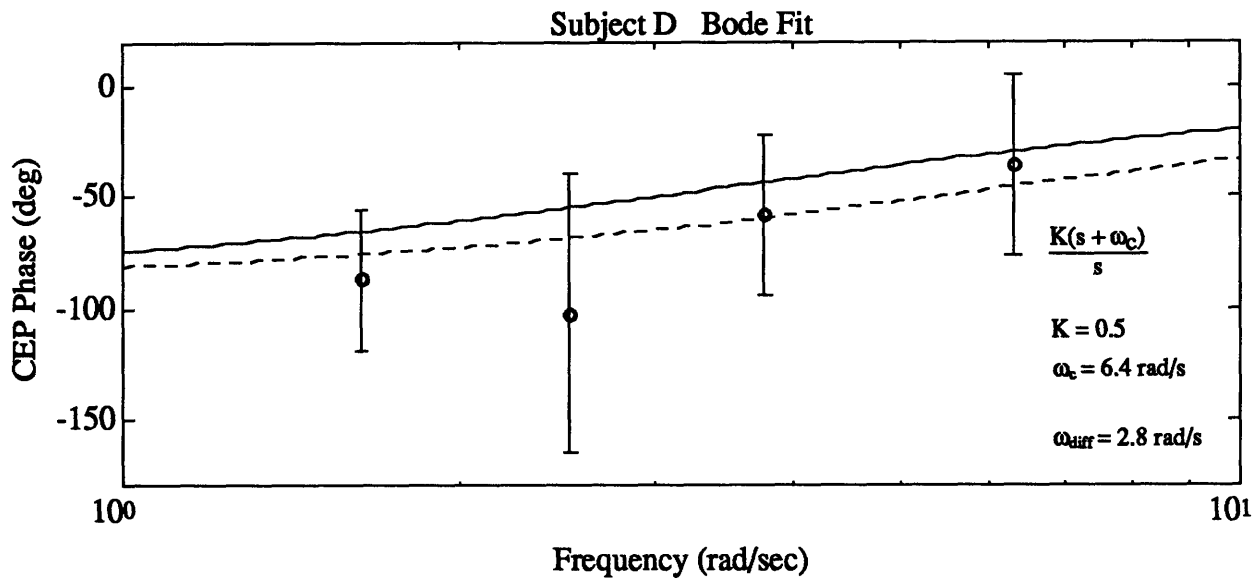
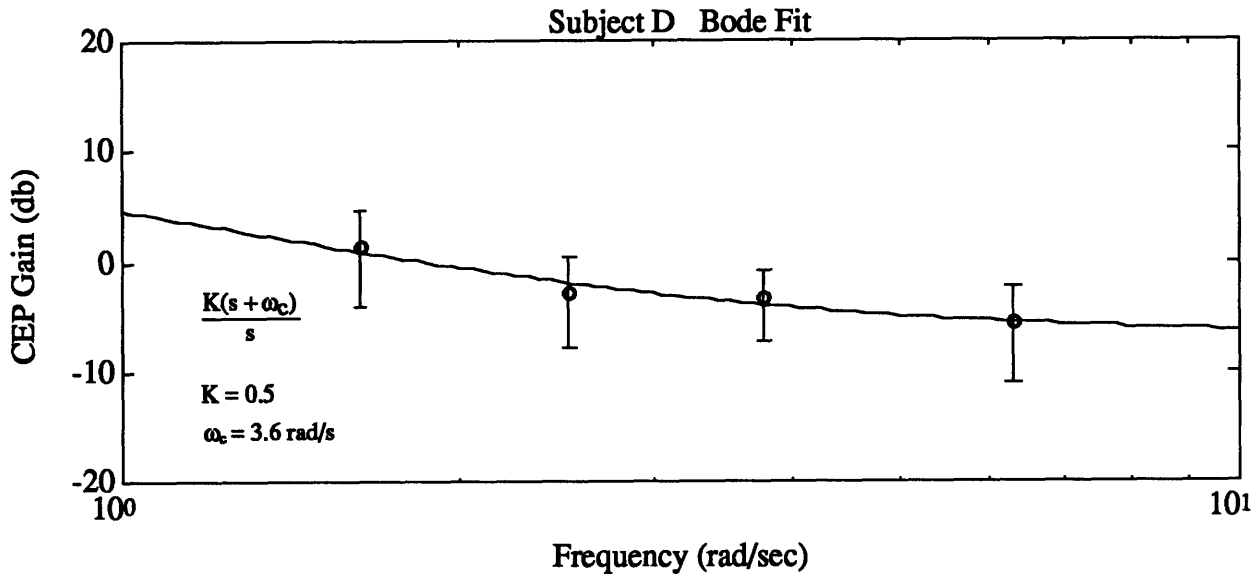


Figure 5.11 Bode plot for all runs from Subject D. The solid lines in both plots are based on the values of K and ω_c as calculated from the gains (Equation 5.4). The dashed line in the phase plot is based on the value of ω_c as calculated from the phases (Equation 5.5). The difference between these two cutoff frequency values is shown as ω_{diff} in the phase plot.

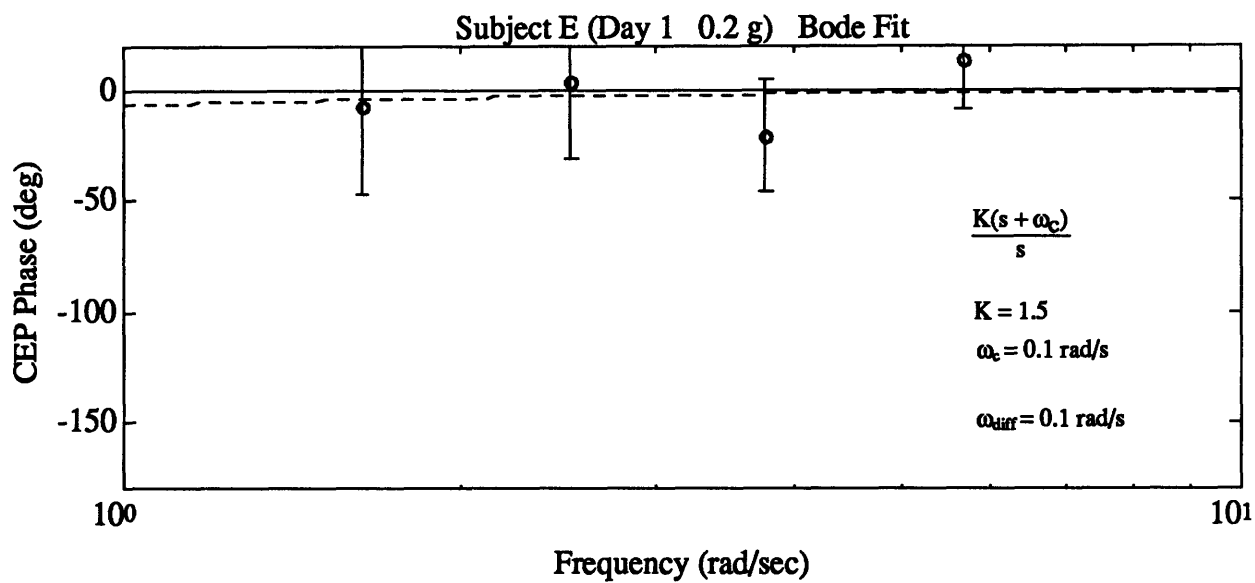
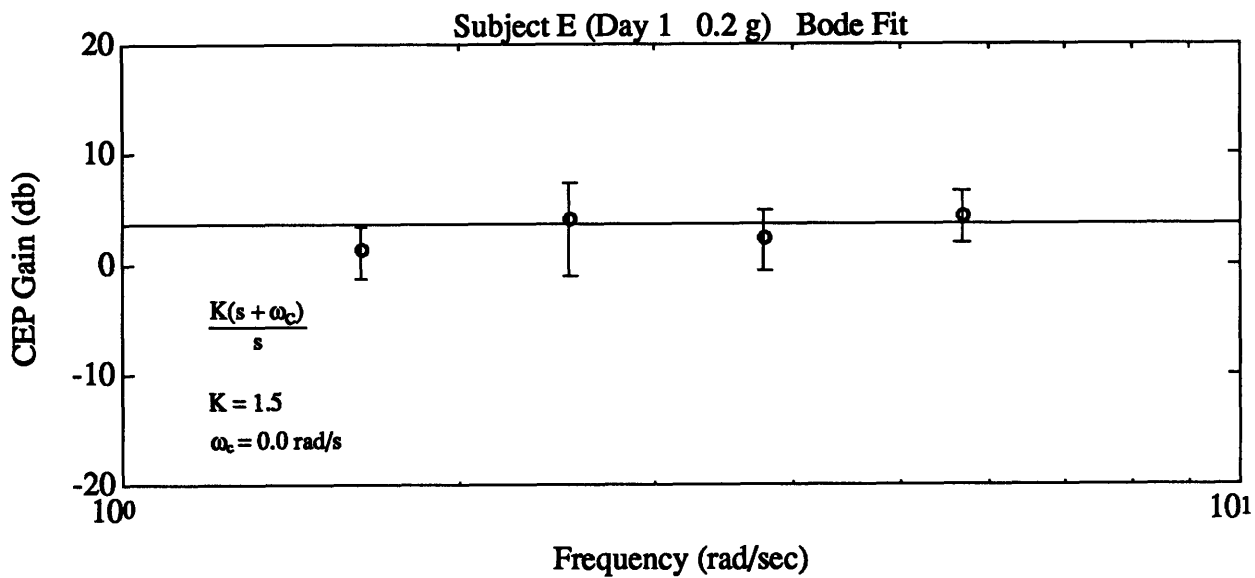


Figure 5.12a Bode plot for Subject E (Day 1, 0.2 g). The solid lines in both plots are based on the values of K and ω_c as calculated from the gains (Equation 5.4). The dashed line in the phase plot is based on the value of ω_c as calculated from the phases (Equation 5.5). The difference between these two cutoff frequency values is shown as ω_{diff} in the phase plot.

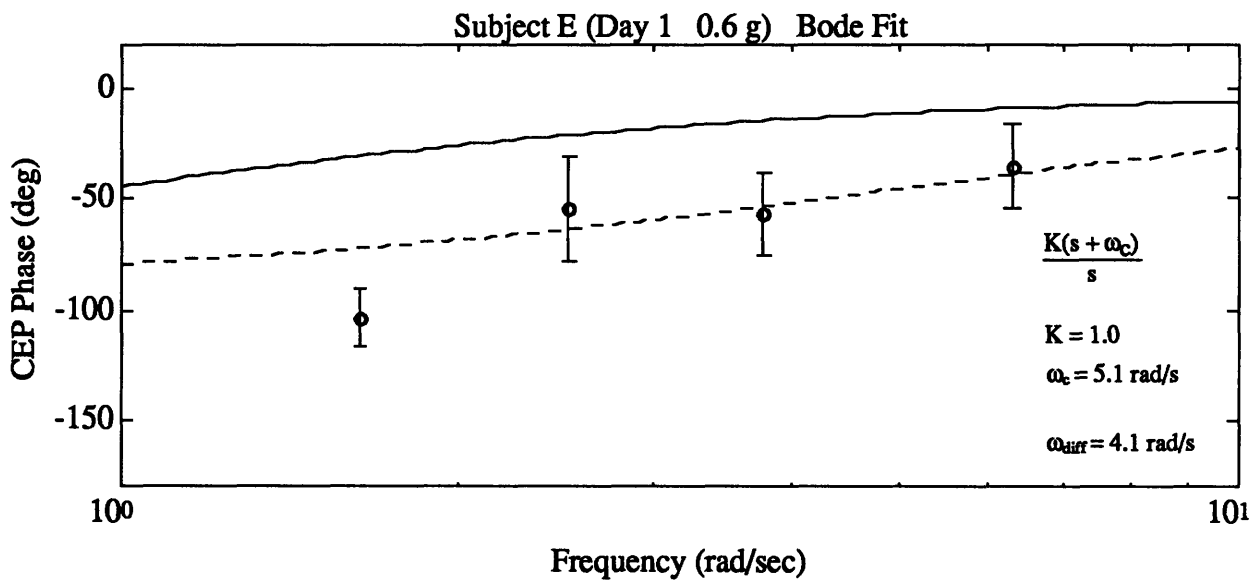
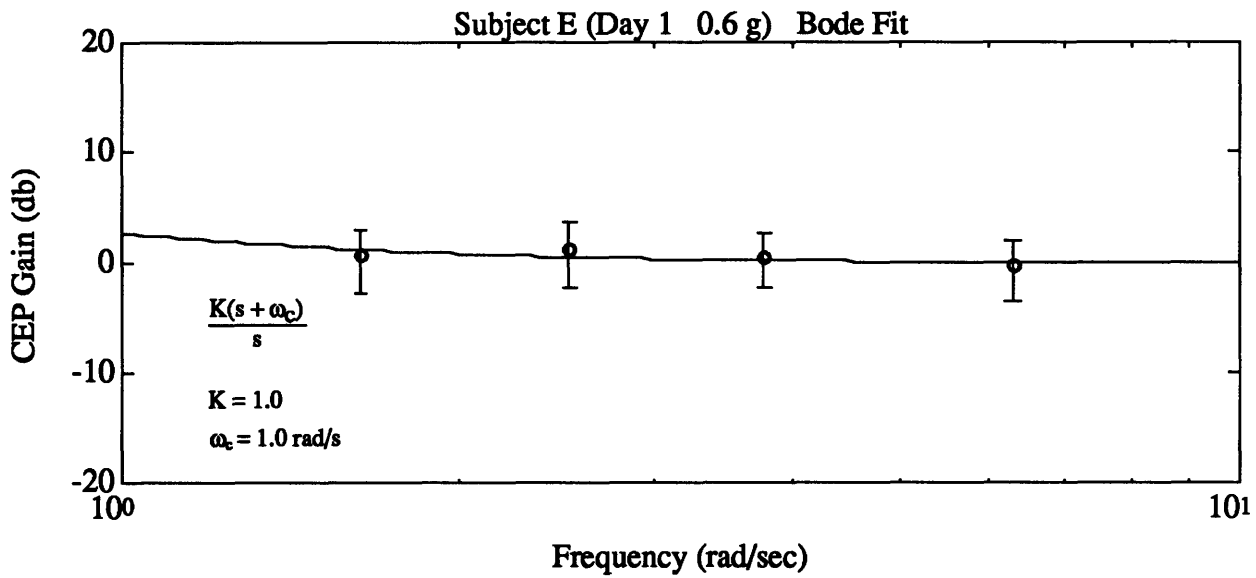


Figure 5.12b Bode plot for Subject E (Day 1, 0.6 g). The solid lines in both plots are based on the values of K and ω_c as calculated from the gains (Equation 5.4). The dashed line in the phase plot is based on the value of ω_c as calculated from the phases (Equation 5.5). The difference between these two cutoff frequency values is shown as ω_{diff} in the phase plot.

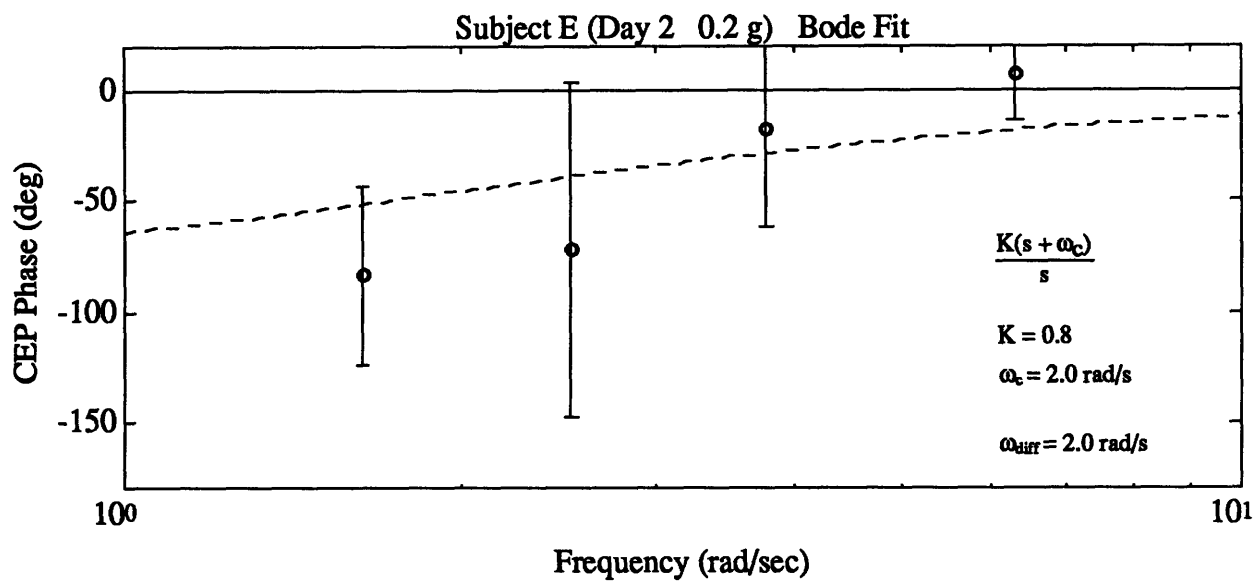
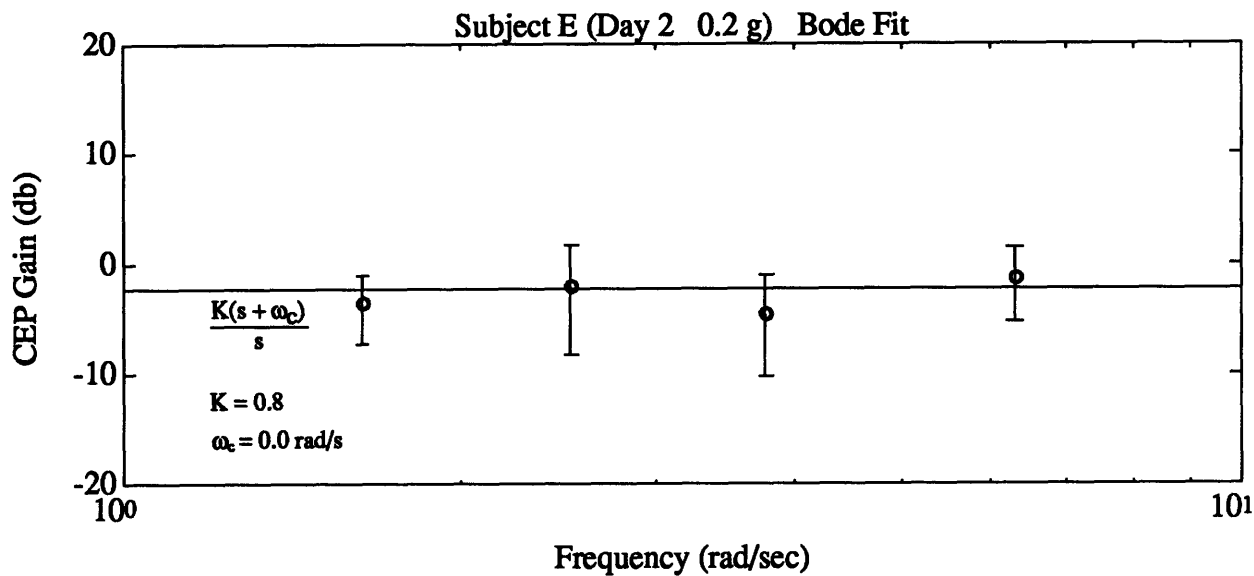


Figure 5.12c Bode plot for Subject E (Day 2, 0.2 g). The solid lines in both plots are based on the values of K and ω_c as calculated from the gains (Equation 5.4). The dashed line in the phase plot is based on the value of ω_c as calculated from the phases (Equation 5.5). The difference between these two cutoff frequency values is shown as ω_{diff} in the phase plot.

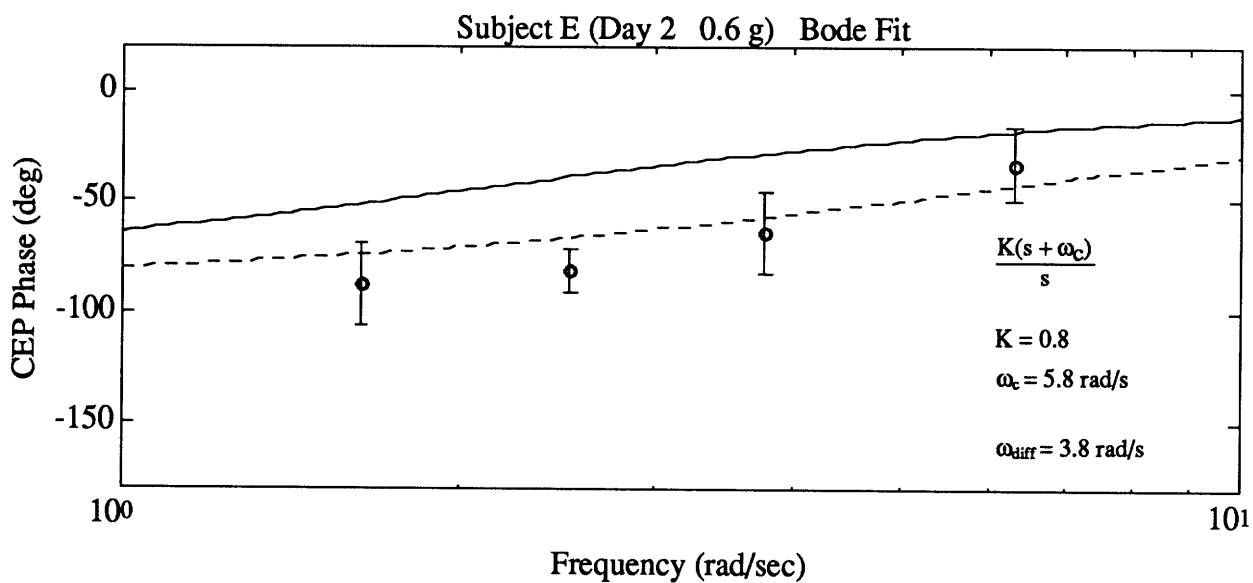
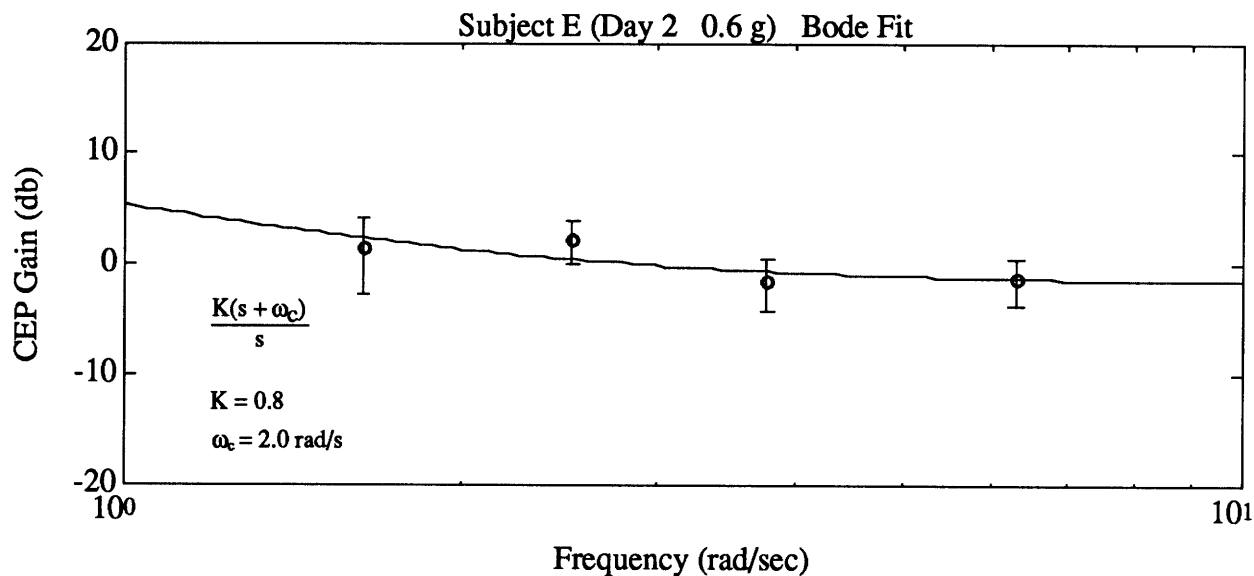


Figure 5.12d Bode plot for Subject E (Day 2, 0.6 g). The solid lines in both plots are based on the values of K and ω_c as calculated from the gains (Equation 5.4). The dashed line in the phase plot is based on the value of ω_c as calculated from the phases (Equation 5.5). The difference between these two cutoff frequency values is shown as ω_{diff} in the phase plot.

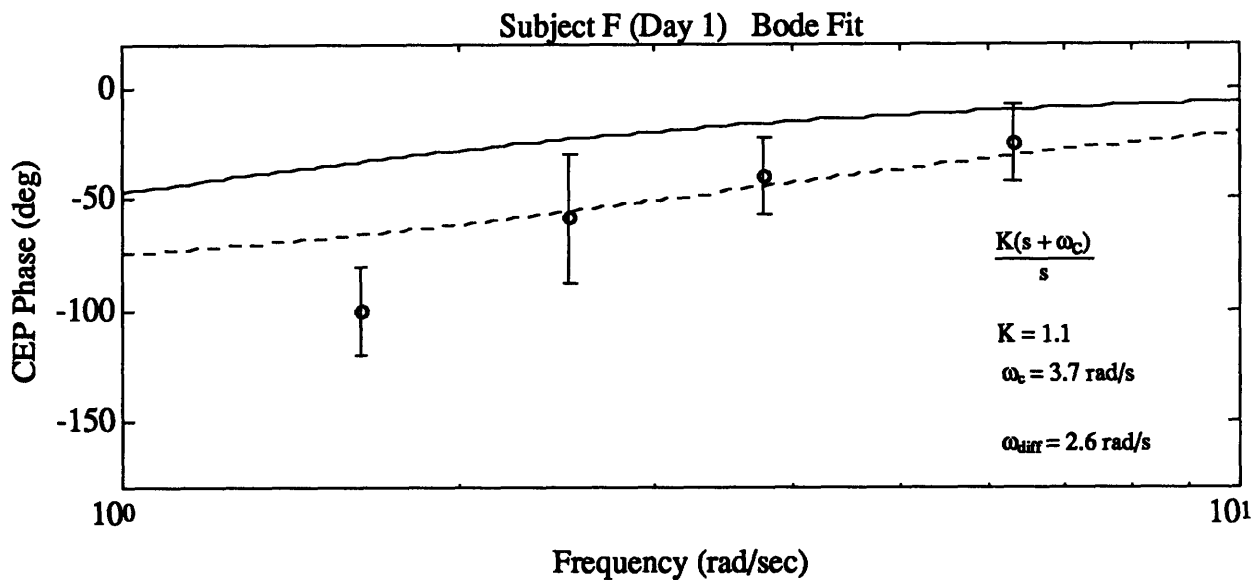
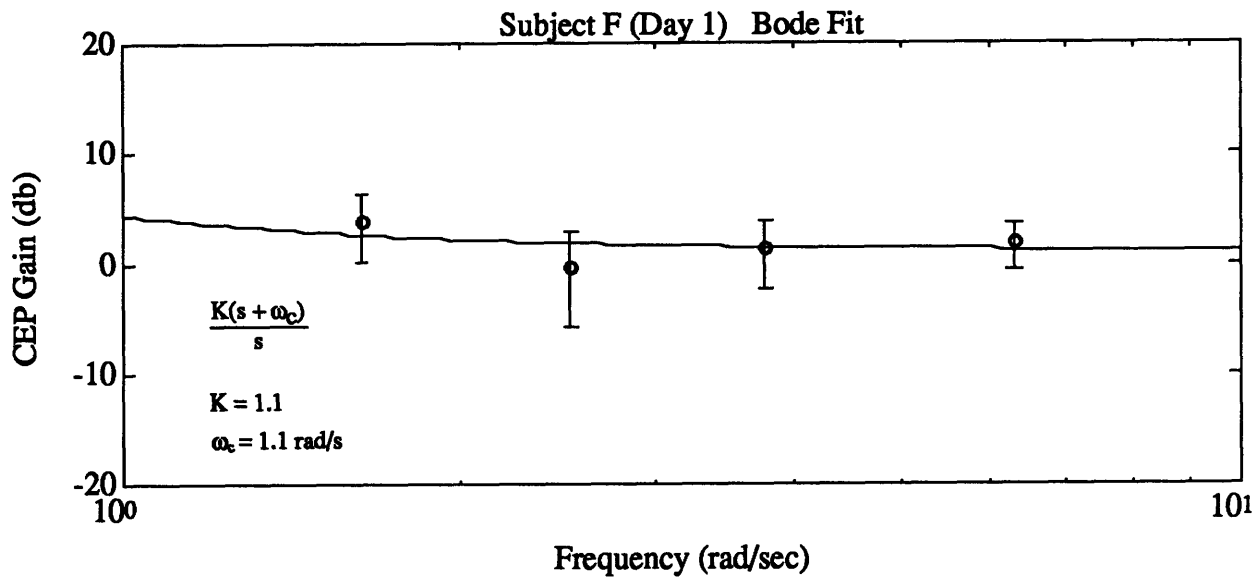


Figure 5.13 Bode plot for Subject F (Day 1). The solid lines in both plots are based on the values of K and ω_c as calculated from the gains (Equation 5.4). The dashed line in the phase plot is based on the value of ω_c as calculated from the phases (Equation 5.5). The difference between these two cutoff frequency values is shown as ω_{diff} in the phase plot.

The gain constant, based on Equation 5.4, was found to be between 0.4 and 1.2. The cutoff frequency, based on Equation 5.4, was found to be between 1.0 rad/sec and 5.9 rad/sec (0.2 Hz and 0.9 Hz). The cutoff frequency, based on Equation 5.5, was found to be between 2.2 rad/sec and 8.2 rad/sec (0.4 Hz and 1.3 Hz). The difference between the two cutoff frequencies was between 1.1 rad/sec and 4.1 rad/sec (0.2 Hz and 0.9 Hz). The above values do not include the runs in which the break frequency was at infinity or zero.

It was also found that the first order equation of Equation 5.1 fits the OCR position data as well, since the OCR position plots also show the trends of decreasing gain and decreasing phase lag with frequency. The fact that both the CEP plot and the OCR position plot fit Equation 5.1 means that the saccades are at a much higher frequency than the sled motion, and therefore do not affect the curve fitting process. Though it also fits Equation 5.1, the OCR position plots are much more variable than the CEP plots, and therefore not as accurate an indicator for the eye movements encountered during linear accelerations.

Theoretically, the OCR response should have a phase lag from the sled acceleration, and this can be modeled by adding an e^{-st} term to the first order equation of Equation 5.1:

$$\frac{K(s + \omega_c)}{s} e^{-st} \quad (5.6)$$

The phase lag can be calculated from the difference of the cutoff frequency based on phase, found from Equation 5.5, and the cutoff frequency based on gain, found from Equation 5.4. But, it was found that six of the twenty-four CEP data sets resulted in a negative phase lag, which is unrealistic. Therefore, the data could not be fitted to Equation 5.6.

5.1 Comparison to Previous Experiments

Comparison of the dynamic ocular counterrolling induced by the linear sled to static ocular counterrolling is difficult because in the sled motion, the ocular counterrolling may not have yet reached a steady state when the sled reverses direction. For this reason, it is assumed that the steady state ocular counterrolling position is achieved during the 0.26 Hz

sled motions, and these values are compared with the static OCR values from previous experiments.

Table 5.2 lists the average magnitudes of the OCR response for all subjects during each of the 0.26 Hz sled runs. OCR position instead of cumulative eye position is used for static comparisons because the magnitude of the position, and not the method of arrival to that position, is important.

From Figure 4.2, the angle between the gravity vector and the gravitoinertial vector was found to be:

$$\phi = \text{Tan}^{-1}(a/g) \quad (5.7)$$

and this value for 0.2 g and 0.6 g was found to be 11.310° and 30.963°, respectively. For comparison, the 0.2 g OCR values will be compared to the 10° values from previous experiments and the 0.6 g OCR values will be compared to the 30° values. Table 5.3 lists the approximate values of static ocular counterrolling from Miller [1969] (interpolated from Figure 2.2), Diamond et al. [1979] (interpolated from Figure 2.5), and Kirienko et al. [1984] (interpolated from Figure 2.3). The values for the present study are slightly lower than the values from the three studies.

In the parabolic flight ocular counterrolling experiments of Arrott [1982], the OCR response versus lateral gravitoinertial force was shown in Figure 2.16. For values of 0.2 g and 0.6 g, Arrott found values of approximately 0.8° and 2.4° respectively. Again, these values are slightly larger than the present study.

For the sled runs, Arrott [1982] had two runs of subject 3 that correspond to runs in the present study. The first run was a 0.2 g 0.4 Hz profile in which the gains were 2.725 deg/g for right eye and 1.805 deg/g for left eye, and the phases were 124.8° for right eye and 131.4° for left eye. The second run was a 0.6 g 0.4 Hz profile in which the gains were 2.089 deg/g for right eye and 2.120 deg/g for left eye, and the phases were 100.3° for right eye and 115.1° for left eye. These values are slightly higher than the values of the present study. The gains for the rest of Arrott's profiles [Arrott 1982, 1985] ranged

Subject	Profile (0.26 Hz)			
	0.2 g Day 1	0.2 g Day 2	0.6 g Day 1	0.6 g Day 2
A	0.491°	0.552°	1.586°	2.049°
B	0.299°	0.310°	0.487°	0.770°
C	0.273°	0.240°	1.003°	1.024°
D	0.287°	0.412°	0.614°	0.710°
E	0.378°	0.308°	1.519°	1.280°
F	0.220°	0.333°	1.106°	1.618°

Table 5.2 Counterrolling for each subject for each run at 0.26 Hz.

Experiment	10° OCR	30° OCR
Miller 1969	1.75°	4.50°
Diamond, et al 1979	1.25°	3.00°
Kerienko, et al 1984	2.50°	6.00°

Table 5.3 Counterrolling values from three static OCR studies.

between 0.65 deg/g and 4.980 deg/g, with one subject having quite high gains and two subject having relatively lower gains. The phase lags for the rest of the runs, for the most part, were above 90°; which disagrees with the first order OCR response of Equation 5.1 found in the present study.

As stated above, the OCR values for the present study were slightly lower than the previous studies compared. One explanation for these differences as well as the differences among the previous studies, is the fact that there is a great variability of OCR response between subjects, as seen in the present study. The OCR responses of Subject A in the present study were much higher than the other subjects. Also, the responses of Subject D were lower than the other subjects. The data in Figure 2.3 from Kirienko, from which the OCR approximations were taken, is for one subject who seemed to have high OCR response. Arrott also had one subject who had twice the gain of the other subjects. The fact that the OCR response is highly variable between subjects makes these types of comparisons difficult.

Hannen et al. [1966] presented a model for the ocular counterrolling response in the form:

$$\frac{0.02e^{-as}}{(s + 3.14)} \quad (5.8)$$

where a is a time constant ranging from zero to 400 msec. Young and Meiry [1968] also presented a model for the ocular counterrolling response with the form:

$$\frac{1.5(s + 0.076)}{s(s + 0.19)(s + 1.5)} \quad (5.9)$$

This model was later fitted to the MVL linear accelerating sled ocular counterrolling data [Lichtenberg et al., 1982]. The response from the two models, as well as the results from all of the MVL linear accelerating sled ocular counterrolling experiments, is shown in Figure 5.14. Both the models and the previous data predict that the gain will decrease with increasing frequency, which was found in the present study. This study also finds a

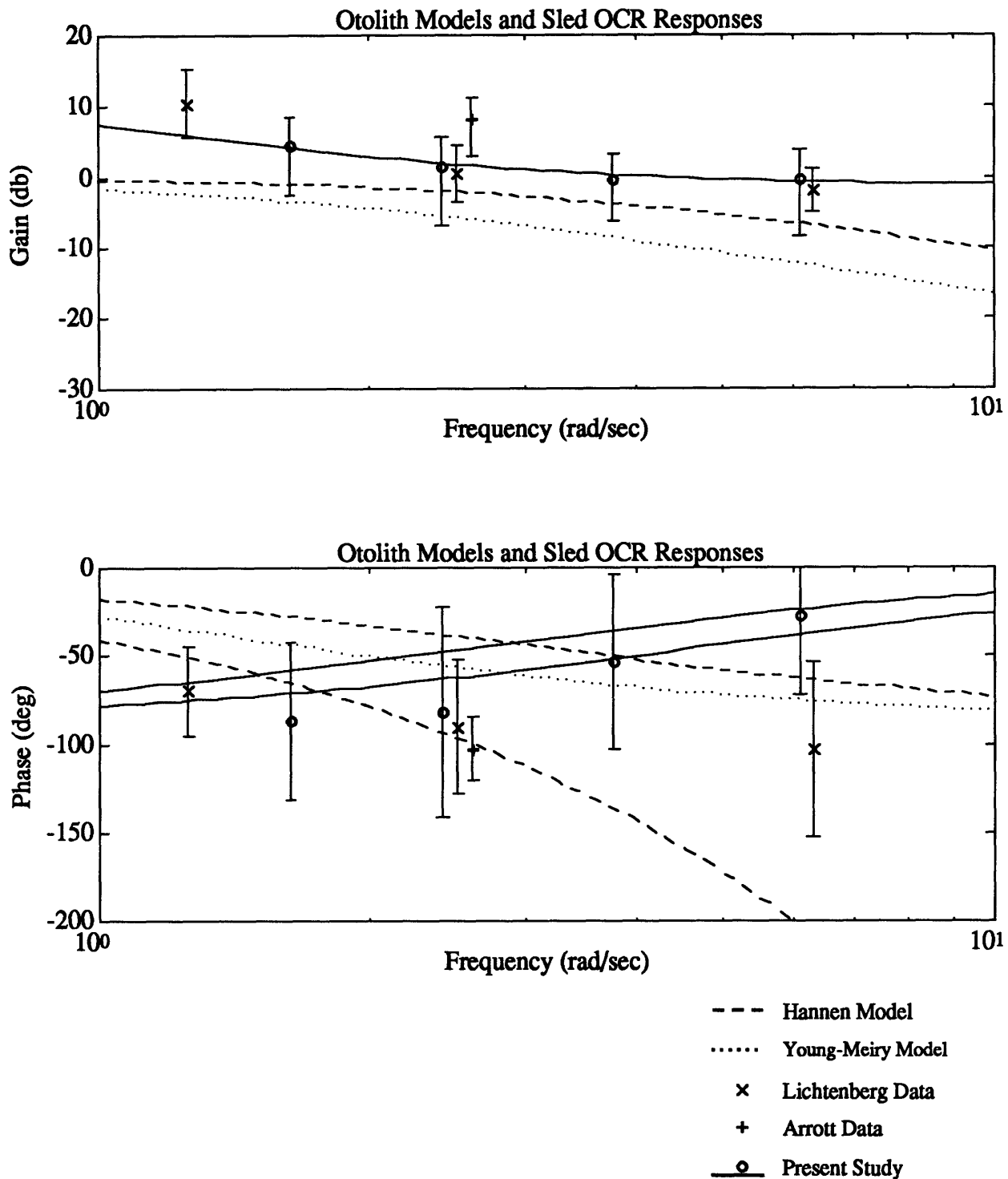


Figure 5.14 Bode plot of otolith models and OCR data. Shown are the Hannen model, the Young-Meiry model, and the data from Lichtenberg, Arrott, and the present study. The vertical lines are ± 1 standard deviation. On the phase plot, the Hannen model is shown with both a zero time delay and a 400 msec time delay. The solid lines represent the curve fit of all subjects for the present study. In the phase plot, the top solid line is based on the gains and the bottom solid line is based on the phases. Notice that the decreasing gains found in the present study agree with the models and the previous data, but the flattening out of the gains and the decreasing phase lags in the present study disagree with the models and the previous data. Adapted from Lichtenberg [1979].

flattening of the gain at higher frequencies, which does not agree with the models. The models also predict that the phase lag will increase with increasing frequency. This does not agree with the present study. Since the data taken in this study was real time, as opposed to using a photographic technique, the question arises as to whether the ocular counterrolling response during linear accelerations fits the the Hannen model or the Young and Meiry model.

Chapter 6

Conclusions

The Man-Vehicle Lab's linear accelerating sled was modified to accommodate a scleral search coil system. An experiment was then devised that would collect real-time ocular counterrolling data during linear sinusoidal accelerations. Six subjects were accelerated at four frequencies and two acceleration levels. Data was collected at 200 Hz.

Upon examination of the data, it was found that counterrolling saccades existed in the motion of the eye in all subjects. Because of the presence of these saccades, ocular counterrolling position can not be used as an indicator of the eye motion. The program NysA was used to find the slow phase velocity (SPV) of the eye motion. The cumulative eye position (CEP), which is the position of the eye without the saccades, was then found from the slow phase velocity. Gains and phases for OCR position and cumulative eye position were found. The experimental data showed that, for both the OCR position and the cumulative eye position, the gain decreased and the phase lag decreased with increasing frequency.

The cumulative eye position data was fit by a first order equation of the form:

$$\frac{K(s + \omega_c)}{s} \quad (5.1)$$

The gain constant, K , for the experimental data was between 0.4 and 1.2; and the cutoff frequency, ω_c , was between 1.0 rad/sec and 5.9 rad/sec (0.2 Hz and 0.9 Hz). With a decreasing phase lag and a flattening out of the gain at higher frequencies, Equation 5.1 disagrees with past models of OCR, such as those presented by Hannen et al. [1966] and by Young and Meiry [1968], and with results from Lichtenberg [1979] and Arrott [1982, 1985]. This fact brings into question and may change the models now in use.

6.1 Suggestions for Further Research

With the addition of the coil system to the MVL linear accelerating sled, countless experiments can now be performed to gather real-time eye movements. At the present time, two experiments are being conducted on the sled using the coil system: analysis of vertical optokinetic nystagmus, and analysis of horizontal optokinetic nystagmus. Also, another experiment is being conducted with the coil system on the MVL rotating dome to study eye movements induced by a rotating visual field. Ideas to implement the coil system to other experiments, including the Miller tilt chair and the MVL rotating chair, have also been suggested and may be followed through in the future.

For further research of ocular counterrolling on the MVL sled, many possibilities arise from this thesis. Since the data from this thesis does not agree with the present models, explanations for the differences could be studied, as well as a new model proposed. With the variability among and between subjects found in this thesis, a more thorough study with many more subjects could be performed. Also, running one subject many times could verify whether or not subjects have a steady state ocular counterrolling response. Longer runs could be performed to provide more values of gain and phase to average. A check of Lichtenberg's hypothesis that OCR response is linear with respect to acceleration [Lichtenberg, 1979] could be performed by running subjects at varying accelerations and constant frequency. A coil could also be put into both eyes of the subject at the same time to study otolith asymmetries during linear accelerations. If otolith asymmetries are the cause of space motion sickness, as Baumgarten and Thulmer [1978] have suggested and Diamond and Markham [1991] have been testing, results of this type of experiment could be used as a predictor of space motion sickness.

APPENDICES

APPENDIX A

Reconfiguring the Coil System on the Sled

The coil system can be configured into four different orientations: lateral upright, fore-aft upright, lateral supine and z-axis supine. Switching the coils to the different configurations is relatively easy, though the weight of the coil system complicates the process somewhat. For the lateral upright and the lateral supine orientations, the base should be positioned in the front and back holes. For fore-aft upright and z-axis supine, the base should be positioned in the right and left holes, with the front of the base directed away from the motor controller. Before making any changes to the configuration of the coil system, the pre-amplifiers must be removed from the back of the chair and the coil power cable must be disconnected from the coils. The accelerometer should also be removed. All three should be left on the sled cart while configuration changes are made. To switch the base from one position to the other, the four nuts under the cart which are connected to the four shocks must be removed. The base can then be rotated to the other position, and the shafts on the shocks are slid into the holes. The nuts are then tightened onto the shock shafts under the cart. For switching from lateral upright to fore-aft upright or from lateral supine to z-axis supine (or the reverse of each), the chair and coil system do not have to be removed from the base. For switching from upright to supine orientations (or the reverse), it is suggested that the chair be taken off the base before rotation of the base, since it would have to be removed later anyway.

For switching from upright to supine (or the reverse), the eight bolts holding the chair to the base must first be removed. The chair and coil system must then be rotated 180° and tipped backward (or upward). It is suggested that the chair and coil system be removed completely and in one piece from the sled cart and placed on the video cart, which is essentially a table with wheels. Once on the video cart, the chair and coils can be rotated to the proper orientation without having to balance precariously on the sled cart. For the

supine position, the two wooden support blocks must be slid into the two front struts of the base. The chair is then slid onto the proper struts on the base, which may have been rotated while the chair was off, as described above. For upright positions, the chair is slid over the middle four struts; for supine positions, the chair is slid over the rear four struts. The eight bolts are then inserted into the legs of the chair and tightened into the nuts. It is advised that the bolts be tightened only to the point where the lock washers are flat, otherwise the aluminum square tubing of the chair will be crushed. Once the chair is mounted in position, the foot restraint is moved to the proper position on its support struts: for upright, the front two holes are used and for supine, the back two holes are used. The pre-amplifiers can be remounted and the coil power cable plugged in. The accelerometer should then be taped to the chair in the proper direction for the configuration of the chair.

A sample step-by-step procedure, in this case for changing from lateral upright to z-axis supine, is listed below.

1. Remove pre-amplifiers from back of chair and set them on sled cart (7/16" nut).
2. Disconnect coil power cable from coils and set it on sled cart.
3. Remove the accelerometer from the chair and set it on sled cart.
4. Remove the eight bolts connecting chair to base (9/16" nut).
5. Position video cart directly in front of sled cart.
6. Move chair and coils onto video cart.
7. Unscrew the four shock nuts from under sled cart (9/16" nut).
8. Rotate base so that its front is directed away from the motor controller.
9. Slide shock shafts into the holes and screw the four nuts onto the shafts under the sled cart.
10. Rotate the video cart 90° so that the head of the chair is directed away from the motor controller.
11. While still on the video cart, tip the chair and coils into the supine position.
12. Slide the two wooden support blocks into the front two struts of the base.
13. Move the chair and coils back onto the sled cart, sliding the chair over the back

four base struts.

- 14. Insert the eight bolts into the legs of the chair.**
- 15. Tighten the nuts onto the bolts only to the point that the lock washers are flat.**
- 16. Move foot restraint to back two holes on support struts and screw into place (3/8" nut).**
- 17. Remount pre-amplifiers.**
- 18. Plug in coil power cable.**
- 19. Tape accelerometer to the chair in proper orientation.**

The procedure for all other orientation changes is very similar to the above procedure.

APPENDIX B

Setup for Control of Sled with Function Generator

To use the function generator to control the sled, the following equipment is needed:

1. Techtronix FG501A 2 MHz Function Generator.
2. A standard Oscilloscope.
3. A 15 volt power supply.
4. The sled filter.
5. The Krohn-Hite filter.
6. The Drift Box.
7. The 386 Interface Box.

The oscilloscope is used to monitor the function generator and adjust the acceleration voltage values for the sled. The power supply powers the sled filter and the drift box. The sled filter is used to filter the voltage input from the function generator to the sled. The Krohn-Hite filter is used to filter the acceleration output from the sled, and should be set to 100 Hz, 0dB gain, Low Pass Max Flat. The drift box is a ten-turn potentiometer used to correct the drift of the sled. The interface box transfers the outputs from the coil system and the accelerometer to the 386 computer for data collection.

The above components are connected together in the following way:

1. Function Generator OUTPUT to DC Offset "+" INPUT.
2. DC Offset OUTPUT to Sled Filter IN.
3. Sled Filter OUT to C13 Cable from Control Panel.
4. Sled Filter OUT to CH1 on Oscilloscope.
5. [CH1 on Oscilloscope to CHØ in Interface Box--only for test runs]
6. Acceleration on Control Panel to Krohn-Hite filter INPUT.
7. Krohn-Hite filter OUTPUT to CH2 on Oscilloscope.

8. Krohn-Hite filter OUTPUT to CH4 on Interface Box.
9. Drift Box to DC Offset "-" INPUT. (Plug Drift Box into Power Source).
10. OPØ on Interface Box to TRIG/GATE IN on Function Generator.

APPENDIX C

Scleral Search Coil System Manual

This appendix contains a copy of the manual for the scleral search coil system as provided by C-N-C Engineering, a division of Tekmate. The address for C-N-C Engineering is:

CNC Engineering
2414 N.E. 123rd
P.O. Box 75567
Seattle, Washington 98125
(206) 362-8264

C-N-C Engineering

A Division of Tekmate, Inc.

Scleral Eye Coil System General Information

The Scleral Search Coil systems manufactured by C-N-C Engineering offer superior measurement accuracy and lower noise than other techniques currently available. The standard coil system (with custom adaptation available) covers a wide range of applications including VOR, fixation, OKN, OKAN, and "dizzy patient" studies.

Systems have evolved in performance and flexibility to meet the requirements of the researchers at the National Institutes of Health Eye Institute. Our specialized design of the electronics and coil apparatus yield a superior signal to noise ratio. Typical noise level for the 15" diameter coil is 0.5 minutes of arc peak to peak when measuring saccades at a 500 Hz frequency limit. The low noise level of the system allows analog differentiation of the eye position signal to provide a velocity output in real time.

All systems operate at high carrier frequencies to allow eye movement monitoring with simultaneous single cell recording in research animals. With either technique, unlike the system described by Dr. Han Collewyn, large square openings are provided on all six faces of the coil frame allowing visual stimulation from outside the framework. The presentation stimulus can be in the form of a rear projection tangential screen or light arrays. Large open areas of the coil framework provide easy access to the research subject.

For unrestrained head movements over a limited range, an additional phase detector furnishes head movement data. Head angular position could then be subtracted from the eye signal to determine eye movements relative to the head without physically restraining the subject's head.

C-N-C Engineering manufactures two styles of coil systems which use innovative electromagnetic field generating and detection principles to yield horizontal and vertical angular eye movements:

- 1.) The Robinson systems use an amplitude detection technique with phase detectors operating as synchronous demodulators (please see enclosed reprint for explanation). This technique is the one typically used for all systems except where oscillating human subject chairs or measurements of large angles is required. Only two magnetic field axis are necessary, reducing system complexity and cost, to produce a signal which can discriminate horizontal and vertical eye movement within the range of ± 40 degrees from a frontal plane. Larger eye movement angles are possible with the use of linearity corrections.

Coil General Description contd.

2.) Phase Angle systems measure the difference in the phase angle between the eye coil horizontal field and that of the reference coil. This method produces a linear, instead of $\sin H$ times $\cos V$, output for the horizontal eye movement. This technique is most advantageous where large angles are to be measured or when the subject platform must be rotated greater than 30 degrees and the small Robinson style coil would be impractical (i.e., must have minimal weight, unrestricted peripheral vision, unrestrained head movements, or use with human subjects).

The vertical eye movement, for a Phase Angle System, is derived from a Robinson technique which produces an output proportional to the sine of the angle. This provides a vertical signal which has a usable range of ± 40 degrees of elevation or depression. The sine of the angle is linear for 20 degrees of vertical movement and has a few percent error at 30 degrees.

Linear output voltage for horizontal angles throughout 360 degree rotation of the subject is a feature of the Phase Angle style system. The horizontal output is referenced to a coil mounted on the subject platform to discriminate eye movements of ± 180 degrees relative to the reference coil position. Therefore, to obtain the absolute position for the horizontal angle of eye or head position the signal must be analog summed with the chair position feedback potentiometer signal.

The Phase Angle technique allows the magnetic field generating coils to remain stationary while the subject is oscillated horizontally within the central portion of the field. In addition to the lower moment of inertia, allowing higher oscillating frequencies of the chair, the stationary coils do not require high power slip rings to connect power to field generating coils.

Robinson 3' and 6' diameter systems can be upgraded to the Phase Angle technique if future research dictates the need for the additional features.

Purchase of on-site installation, with operator instruction, is recommended. Detailed discussions of the operating principles, solutions to complex mechanical or highly conductive structures near the fields, and optimal equipment placement within the lab result from on-site installation. Experience obtained from previous installations enhances prompt answers to initial start-up questions allowing immediate application of our system. Six foot diameter systems are only sold with on-site installation due to their size and interactions with their surroundings.

C-N-C Engineering

A Division of Tekmate, Inc.

Scleral Search Coil System Magnetic Field Descriptions

Standard Coil Frames Available

15" Frame Size

The 15" field coil is used primarily for animal VOR, OKN, or other studies requiring small mass and moment of inertia. The external frame size is 20" along an edge, excluding the resonating capacitor box. The open interior volume is a cube 16" on an edge. With the coil frame fabricated from Plexiglas and shipped as an assembled unit, the structure withstands the accelerations which a servo-controlled platform generates. This size is manufactured only as a Robinson style system.

3' Frame Size

The three-foot field coil is suitable for use with animal and human subjects. An overall exterior of 42"H X 42"W X 40"D, with an interior open volume of approximately 38" along an edge, allows ease of subject access. The coil frame allows small nystagmus drums with a stripe width of 1/4 inch per degree to be placed within the coil field. This coil size is manufactured in both the Robinson and Phase Angle system styles with a Formica surface finish.

6' Frame Size

The six-foot diameter square coil permits easy full field visual presentation with large nystagmus drums, tangential screens, or hemispheres placed within the fields. Exterior dimension of 79" X 80" X 80" with an interior open volume of 74" X 75" X 77" allow easy access for human subjects. The opening in the top coil allows a 5 1/2 foot diameter nystagmus drum to be within the coil field. With large openings on all faces of the frame, human subject testing is easily accomplished. The coil frame is fabricated from oak and finished with a Watco Danish Finish which is alcohol and water resistant. This coil size is manufactured in both the Robinson and Phase Angle system styles.

C-N-C Engineering

A Division of Tekmate, Inc.

Scleral Search Coil System Robinson Style System Description

Robinson Power Drivers

The Power Oscillator drives the two pairs of coils at two frequencies which are locked to an internal temperature-compensated oscillator.

The magnetic field orientation of each axis is sensed from an additional feedback winding on the driven coils. The current drive amount is controlled within the power driver to provide a constant flux density. Current sample BNC outputs provide a convenient method of checking coil current with a sensitivity of 1 Volt/AMP.

A front panel frequency control allows adjustment of the resonant frequency by viewing the front panel LED display and adjusting for a green display. The LED display presents a visual resonance point monitor of the output voltage to the series resonant coils.

Robinson Phase Detectors

The Phase Detectors recover amplitude modulated information from the electromagnetic fields. A coil of wire attached to a contact lens, or implanted for research animals, generates a voltage proportional to the area of the coil perpendicular to the magnetic field vector. Voltage output from the Vertical axis is proportional to the sine of the angle. The output of the Horizontal axis is proportional to the sine of the Horizontal angle times the cosine of the Vertical angle. This is due to the geometry of the coil movement in space as described in Dr. David A. Robinson's 1963 article (A method of measuring eye movement using a scleral coil in a magnetic field. IEEE Transactions on Biomedical Electronics BME-10, 137-145).

The following is a list of Phase Detector controls and their usage:

1. **OFFSET CONTROL** - allows the adjustment of a zero degree eye position out of the detectors.
2. **GAIN CONTROL** - adjusts the output voltage to provide a nominal output of 1 volt for 10 degrees of rotation. An internal output sensitivity pot allows for adjusting the output to be from 0.2V/10 degrees to 2V/10 degrees.

Robinson Description continued

3. METER SENSITIVITY SWITCH - adjusts the eye position meter calibration for either +/- 5 degrees or +/- 50 degrees full scale.
4. PHASE CONTROL - adjusts the detector to reject implant or contact placement skew, axis rotation, or metals within the magnetic fields. To adjust the control use the calibration coil, or have the subject track a Horizontal or Vertical target, while setting the opposite channel's phase control. The object is to adjust the phase control to eliminate cross coupling of the axis. For example, if the subject is tracking a Horizontal movement, adjust the Vertical phase for a no output change. The isolation of Horizontal and Vertical channels should be greater than 50db. NOTE: For Vertical movements, the phase control can only be adjusted for a Horizontal position near zero degrees due to the area interactions.
5. TIME CONSTANT SWITCHES - thumbwheel and multiplier switch, in conjunction, establish a single pole filter which is selectable from 0.1 to 9 milliseconds (1.6 KHz to 18 Hz bandwidth). This filter is followed by a fixed 3 KHz bandwidth 5 pole Bessel low-pass filter yielding at least an 80db rejection of the carrier signal.
6. $0^{\circ}/180^{\circ}$ SWITCH - changes analog output phasing by 180 degrees. This allows the output monitor oscilloscope to display a spot which is in the same quadrant as the subject is looking.

Coil Pairs

The coil framework is composed of four electromagnetic generating coils. Each pair of two coils (similar to Helmholtz generators but at a spacing of a coil diameter) are physically oriented at 90 degrees. These coils produce an electromagnetic field which will induce a voltage in a small multi-turn coil of wire attached to the subject's eye. The output voltage is proportional to the area of the coil perpendicular to the magnetic field. The subject coil produces a voltage which is separated into Horizontal and Vertical components by the Phase Detector.

The coil pairs are an electrically series resonant tuned circuit which has a minimum real impedance at resonance. All coils are electrostatically connected to ground. This shielding also reduces the radiated electric field to allow removal of the coil frequency from any unit electrode stage. In addition, the shielding reduces the electric field which might interact with other research or clinical measuring equipment. The coil system operates at two frequencies which are ratios of 3/2 chosen among a frequency range from 60 to 120 KHz.

Scleral Search Coil System

Specifications for Robinson Style Systems

System

When connected as a system, the output of the Phase Detectors will yield at least ± 0.5 degree accuracy within ± 30 degrees for a Robinson system assuming a straight line fit was calibrated at ± 20 degree points. System noise at the 0.3 millisecond time-constant setting (530 Hz bandwidth) is less than 1 minute of arc peak to peak when measured with the test fixture. Typical noise levels for a 15 inch square coil is 0.25 minutes with 1 minute of arc pp noise for the 3 foot or 6 foot coil. At lower bandwidths, the noise will be reduced below the typical figures. Front panel time constant settings allow eye position bandwidth selection from 18 Hz to 1.6 KHz.

Power Driver

Output Voltage Compliance: ± 60 volts @ 2 amps rms load each channel.

Frequency Adjustment Range: $\pm 10\%$ of resonant frequency range of 60 KHz to 135 KHz depending on coil diameter.

Output Current Stability: $\pm 0.1\%$ after temperature stabilization.

Preamplifier

Differential Gain: 40 to 60db (depending on coil diameter).

Common Mode Rejection Ratio: Greater than 80db @ 120KHz.

Gain Stability: 50ppm/ $^{\circ}$ C or better.

Frequency Response: 1 KHz to 1 MHz frequency bandwidth @ -3db points.

Input Impedance: 30 K-ohms differential and 10pf capacitance to ground.

Phase Detector

Gain: Continuously adjustable from -10db to +10db.

Time Constant: Adjustable from 1×10^{-4} to 9×10^{-3} seconds.

Zero Drift: $\pm 0.01\%$ / degree Centigrade plus $\pm 0.01\%$ for a 10% change in line voltage.

Linear Output: ± 12 volts

C-N-C Engineering

A Division of Tekmate, Inc.

Scleral Search Coil System Phase Angle Style System Description

Phase Angle Power Drivers

The Power Oscillators drive the three pairs of coils at two frequencies which are locked to an internal crystal oscillator. The two coil pair which generate the rotating horizontal phasor have a control circuit which constantly adjusts the phase of the two fields. The magnetic fields are dynamically controlled to be at 90 degrees in phase at the central portion of the field.

For the vertical field the magnetic field orientation of each axis is sensed from an additional feedback winding on the driven coils. The vertical field current drive amount is controlled within the power driver to provide a constant flux density. The orientation and flux density for the horizontal axis are controlled by measuring the field strength and orientation with two control coil loops near the subject. Front panel current sample BNC outputs provide a convenient method of checking coil current with a sensitivity of 1 Volt/AMP.

Front panel controls allows adjustment of the phase angle (quadrature) of the horizontal fields. A LED display presents a visual resonance monitor for each of the three series resonant coil pairs.

Phase Angle Phase Detectors

The Vertical Phase Detector recovers amplitude modulated information from the electromagnetic fields. A coil of wire attached to a contact lens, or implanted for research animals, generates a voltage proportional to the area of the coil perpendicular to the magnetic field vector. Voltage output from the Horizontal axis is proportional to the phase angle difference between the subject reference and the eye coil signal.

The following is a list of Phase Detector controls and their usage:

1. OFFSET CONTROL - allows the adjustment of a zero degree eye position out of the detectors.
2. GAIN CONTROL - adjusts the output voltage to provide a nominal output of 1 volt for 10 degrees of rotation. An internal output sensitivity pot allows for adjusting the output to be from 0.2V/10 degrees to 2V/10 degrees.

Phase Angle Description continued

3. METER SENSITIVITY SWITCH - adjusts the eye position meter calibration for either +/- 5 degrees or +/- 50 degrees full scale.
4. PHASE CONTROL - adjusts the detector to reject implant or contact placement skew, axis rotation, or metals within the magnetic fields. To adjust the control use the calibration coil, or have the subject track a Horizontal or Vertical target, while setting the opposite channel's phase control. The object is to adjust the phase control to eliminate cross coupling of the axis. For example, if the subject is tracking a Horizontal movement, adjust the Vertical phase for a no output change. The isolation of Horizontal and Vertical channels should be greater than 50db.
5. TIME CONSTANT SWITCHES - thumbwheel and multiplier switch, in conjunction, establish a single pole filter which is selectable from 0.1 to 9 milliseconds (1.6 KHz to 18 Hz bandwidth). This filter is followed by a fixed 3 KHz bandwidth 5 pole Bessel low-pass filter yielding at least an 80db rejection of the carrier signal.
6. $0^{\circ}/180^{\circ}$ SWITCH - changes analog output phasing by 180 degrees. This allows the output monitor oscilloscope to display a spot which is in the same quadrant as the subject is looking.

Coil Pairs

The coil framework is composed of six electromagnetic generating coils. Each pair of two coils (similar to Helmholtz generators but at a spacing of a coil diameter) are mutually oriented at 90 degrees. These coils produce an electromagnetic field which will induce a voltage in a small multi-turn coil of wire attached to the subject's eye. The output voltage is proportional to the area of the coil perpendicular to the magnetic field for the vertical channel. The horizontal channel is measuring the phase difference between the placement of the reference coil and the horizontal component of the eye coil output. The subject coil signal is separated into Horizontal and Vertical components by the Phase Detector.

The coil pairs are an electrically series resonant tuned circuit which has a minimum real impedance at resonance. All coils are electrostatically connected to ground. This shielding also reduces the radiated electric field to allow removal of the coil frequency from any unit electrode stage. In addition, the shielding reduces the electric field which might interact with other research or clinical measuring equipment.

Scleral Search Coil System

Specifications for Phase Angle Systems

System

When connected as a system, the output of the Phase Detectors will yield at least ± 0.5 degree accuracy within ± 30 degrees for the vertical channel assuming a straight line fit was calibrated at ± 20 degree points. The horizontal axis output will be within ± 0.5 degree accuracy within a range of ± 170 degrees of the reference coil placement. System noise at the 0.3 millisecond time-constant setting (530 Hz bandwidth) is less than 3 minutes of arc peak to peak when measured with the test fixture. Typical noise levels are 2 minutes of arc pp noise for the 3 foot or 6 foot coil. At lower bandwidths, the noise will be reduced below the typical figures. Front panel time constant settings allow eye position bandwidth selection from 18 Hz to 1.6 KHz.

Power Driver

Output Voltage Compliance: ± 60 volts @ 2 amps rms load each channel.

Frequency : crystal controlled at 60 KHz and 120 KHz.

Output Current Stability: $\pm 0.1\%$ after temperature stabilization.

Preamplifier

Differential Gain: 40 to 60db (depending on coil diameter).

Common Mode Rejection Ratio: Greater than 80db @ 120KHz.

Gain Stability: 50ppm/ $^{\circ}$ C or better.

Frequency Response: 1 KHz to 1 MHz frequency bandwidth @ -3db points.

Input Impedance: 30 K-ohms differential and 10pf capacitance to ground.

Phase Detector

Gain: Continuously adjustable from -10db to +10db.

Time Constant: Adjustable from 1×10^{-4} to 9×10^{-3} seconds.

Zero Drift: $\pm 0.01\%$ / degree Centigrade plus $\pm 0.01\%$ for a 10% change in line voltage.

Linear Output: ± 12 volts

Synchronous demodulation explained

Modulation imposes an information-bearing signal on a carrier signal in a predictable way. In instrumentation and measurement systems where transducer signals have fundamental frequency components at or near dc, modulation can be used to great advantage. It can place the signal information on a high-frequency carrier wave well above common low-frequency disturbances such as 1/f noise and power-line interference. Signal information can thus be amplified and extracted from a region of minimum noise after modulation.

A synchronous demodulator (or phase-sensitive detector) extracts the information in the best of ways: only those signals in synchronization with the carrier frequency are detected—which means that all random or nonsynchronous interfering signals are rejected.

As shown in (a), a mixer performs the actual signal demodulation. After filtering, a dc signal is left that contains the magnitude and phase information (relative to the carrier) produced by the transducer. Demodulation is theoretically equivalent to passing the modulated transducer signal through a gating switch that toggles in phase with the carrier reference signal. Input signals synchronized with the carrier reference signal are half-wave-rectified—for a 0° phase shift, positive-wave rectification occurs, whereas for a 180° phase shift, the negative peaks are rectified. The trick is to use two gating switches and to

sum alternate input signal cycles with positive and negative gain in order to obtain a full-wave-rectified result, as illustrated in (b).

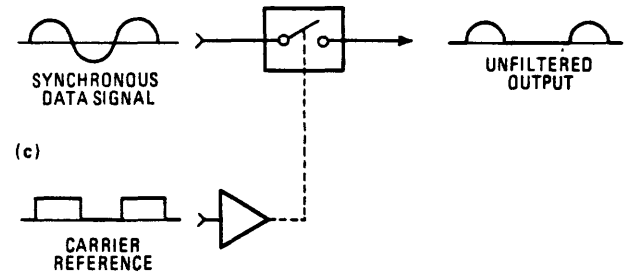
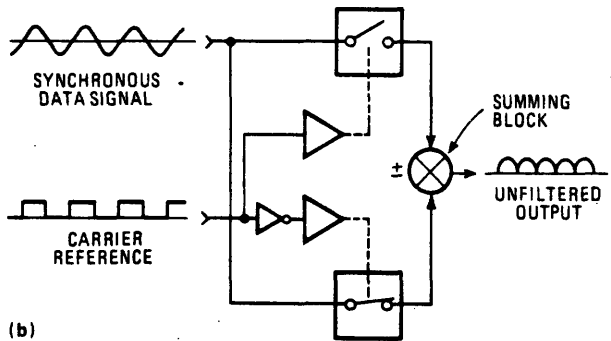
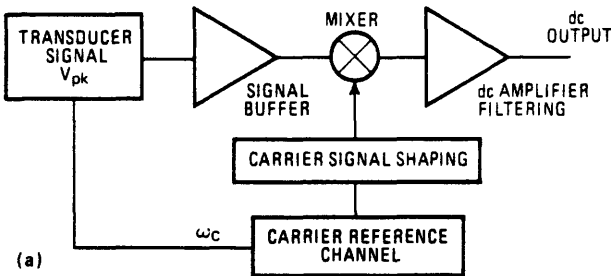
Since the full-wave demodulator's lowest frequency component is twice the carrier frequency, much greater bandwidth is possible than with half-wave demodulation. Also, the amount of filtering needed to extract the dc signal that is proportional to the transducer signal is far less than with half-wave demodulation (c).

Full-wave synchronous demodulation is readily described mathematically. Consider a sinusoidal input signal in phase with a carrier signal. Let the carrier signal equal $V_c \cos \omega_c t$ and the modulated input signal equal $V_{pk} \cos \omega_c t$, where V_{pk} is the information-carrying signal. Since the full-wave synchronous demodulator multiplies the input signal by +1 when the carrier signal exceeds zero and by -1 when it is less than zero, a full-wave, positively rectified signal results. The output can be represented by a Fourier series:

$$V_o = V_{pk} \left[\frac{2}{\pi} - \frac{4}{\pi} \left(\frac{1}{4} \cos 2\omega_c t - \frac{1}{3.5} \cos 4\omega_c t \dots \right) \right]$$

After passing through a low-pass filter, the signal will have all its ac terms eliminated from it or reduced. The low-pass filter output will equal the Fourier series average value and thus be proportional to input signal $V_o = 2V_{pk}/\pi$. The synchronous demodulator also performs a full-wave rectification if the input signal and carrier signal are 180° out of phase. The demodulator output is, however, negatively full-wave-rectified. Being below ground, it has an average value of $V_o = -2V_{pk}/\pi$. As before, the first ac ripple term is at twice the carrier frequency. A high carrier frequency ensures that the ac frequency components will be attenuated by relatively simple low-pass filtering circuits.

Nonideal transducer behavior will often produce quadrature signals, which are 90° out of phase with respect to the carrier. As shown in (d), a synchronous demodulator's full-wave rectification averages quadrature signals to zero after low-pass filtering.



C-N-C ENGINEERING WARRANTY STATEMENT

C-N-C ENGINEERING, a division of Tekmate Inc., warrants to its customers that the products that it manufactures and sells will be free from defects in materials and workmanship for a period of ninety (90) days after installation; or from the date of shipment for those systems purchased without installation. If any product fails to operate properly during the warranty period, as a result of a defect in materials or workmanship, C-N-C ENGINEERING, at its option, either will repair the defective product and restore it to normal operation without charge for parts and labor or will provide a replacement in exchange for the defective product.

In order to obtain service under this warranty, the customer must notify C-N-C ENGINEERING of any defects before the expiration of the warranty period and make suitable arrangements for the prepaid return of the equipment. Upon prior agreement, C-N-C ENGINEERING may provide on-site service subject to the payment of all travel expenses by the customer. The customer shall be responsible for the packaging and shipping of the defective product to C-N-C ENGINEERING in Seattle, Washington, with the shipping charges prepaid. C-N-C ENGINEERING shall pay for the return of the product to the customer if the shipment is to a location within the Continental United States. The customer shall be responsible for paying all shipping charges, duties and taxes if the product is returned to any other location.

This warranty shall not apply to any defect, failure or damage caused by misuse or improper or inadequate maintenance and care. C-N-C ENGINEERING shall not be obligated to furnish service under this warranty:

- a) to repair damage resulting from attempts by personnel (other than C-N-C ENGINEERING representatives) to install, repair or service the product;
- b) to repair damage resulting from improper use or connection to incompatible equipment; or
- c) to service a product that has been modified or integrated with other products when the effect of such modification or integration increases the time or difficulty of servicing the product.

THIS WARRANTY IS THE ONLY WARRANTY GIVEN BY C-N-C ENGINEERING AND IS GIVEN IN LIEU OF ANY OTHER WARRANTY EXPRESSED OR IMPLIED. C-N-C ENGINEERING DISCLAIMS ANY IMPLIED WARRANTIES OR MERCHANTABILITY OR FITNESS FOR A PARTICULAR PURPOSE. C-N-C ENGINEERING'S RESPONSIBILITY TO REPAIR OR REPLACE DEFECTIVE PRODUCTS IS THE SOLE AND EXCLUSIVE REMEDY FOR BREACH OF THIS WARRANTY. C-N-C ENGINEERING WILL NOT BE LIABLE FOR ANY INDIRECT, SPECIAL, INCIDENTAL OR CONSEQUENTIAL DAMAGES.

An extended warranty period can be purchased which extends the warranty to a total of twelve (12) months. This Warranty Extension is available to installed systems only and will be charged at a rate of nine per cent (9%) of the amount of the current selling price of the equipment covered under the Warranty Extension. The Warranty Extension must be purchased prior to the expiration of the initial ninety (90) day warranty and will include on-site servicing of the equipment within the Continental United States only.

For information and further details regarding C-N-C ENGINEERING warranties and service policies, please consult CHARLES E. CHASE, President, C-N-C ENGINEERING, in Seattle, Washington, (206) 362-8264.

SETUP PROCEDURES FOR ROBINSON SCLERAL SEARCH COIL EYE POSITION MONITOR

INITIAL SETUP

Connect all cables, including eye coil, to the system electronics and check for correct connections - BEFORE - turning on power to the electronics. Turn on POWER DRIVER switch and allow 30 minutes for the electronics to temperature stabilize.

POWER DRIVER ADJUSTMENT

After stabilization, adjust the 10 turn FREQUENCY potentiometer until both HORIZONTAL and VERTICAL LEDS are green. As long as the GREEN LEDS or the two YELLOW LEDS are displayed, the system is dynamically controlling the system gain. In normal operation, the GREEN LEDS will not change unless the introduction of metal near the coil changes the inductance of the coils. The frequency is not normally readjusted for each usage.

PHASE DETECTOR ADJUSTMENTS

- 1.) Set the TIME CONSTANT thumbwheel and MULTIPLIER switch to select a position bandwidth necessary for the application. The smaller the time constant is, the larger the position bandwidth. (See attached listing for various time constant/frequency conversions.) A setting of 3 X 0.1 msec. translates to approximately a 530 Hz signal bandwidth. Horizontal and vertical time constants do not have to be identical.
- 2.) Set the PHASE switch to either the 0 or 180 position to define the same display quadrant as the subject's viewed quadrant.
- 3.) Have the subject view a zero position spot. Monitor the output on an oscilloscope or switch the meters to 5 DEGREE FULL SCALE position. Now adjust the OFFSET and POLARITY controls for an electrical "0" voltage output for both HORIZONTAL and VERTICAL. ***CAUTION*** The 5 DEGREE switch position is ONLY to be used for adjusting a fine zero. Return the switch to the 50 degree position IMMEDIATELY after adjusting the zero.

- 4.) Have the subject view a calibrated position along the HORIZONTAL and alternately the VERTICAL axis while monitoring the display on an oscilloscope or by using the meters. DO NOT calibrate at an oblique angle due to SINE times COSINE output from the horizontal axis. Adjust the 10 turn GAIN control to provide an electrical output calibrated to the eye position. Calibration points at 30 degree angles are convenient for typical studies.
- 5.) While monitoring the output on an oscilloscope (after zeroing the position of the scope beam in the center of the screen), repeat steps 3 and 4 until calibration is correct. NOTE - Check the amount of offset added to the system by switching the polarity switch to OFF. If the equivalent offset added to the system is greater than 5 degrees (as measured by the electrical output voltage or meter position), a non-uniform left/right or up/down gain will exist. This is caused by an "extraneous eye coil loop" at the head junction connector or other connections. ** THIS IS NOT AN ELECTRONICS PROBLEM. ** Contact C-N-C ENGINEERING for suggestions on eliminating implanted extra loops or coil connection problems.
- 6.) Now have the subject perform saccadic or smooth pursuit movements in alternately the Horizontal and Vertical directions along the zero-zero axis while monitoring the display on a X-Y oscilloscope. Adjust the phase control of the Horizontal and alternately the Vertical channel to remove the "skew" of the pick-up coil due to placement of the coil in a non-frontal plane. Zero skew represents a value of 5 on the 10 turn dial. NOTE - the line displayed on the oscilloscope will tilt, as the adjustment is made, while the patient is tracking the movement and will go through a reversal of slope at the zero skew value.
- 7.) Repeat steps 3, 4 and 6.
- 8.) Record the values of the 10 turn dials in a log to allow fast setup of the dials when the subject is tested again. This is normally most beneficial for animal research where the implanted coil does not change orientation from day to day.
- 9.) Run the subject.

QUICK SETUP FOR ROBINSON SCLERAL SEARCH COIL EYE MONITOR

- 1.) Set TIME CONSTANT SWITCHES.
- 2.) Set PHASE switch for correct quadrant of view.
- 3.) Adjust OFFSET zero.
- 4.) Adjust GAIN for correct sensitivity.
- 5.) Repeat steps 3 and 4.
- 6.) Adjust PHASE pot. to remove placement skew.
- 7.) Repeat 3, 4 and 6.
- 8.) Record readings.
- 9.) Run subject.

DIAL SETTINGS FOR TIME CONSTANT SWITCHES ON PHASE DETECTOR

Thumbwheel Dial		Multiplier switch setting
Setting Number	X10 ⁻⁴ Sec. (0.1 msec)	X10 ⁻³ Sec. (1 msec)
1	1.6 KHz	160 Hz
2	800 Hz	80 Hz
3	530 Hz	53 Hz
4	400 Hz	40 Hz
5	320 Hz	32 Hz
6	270 Hz	27 Hz
7	230 Hz	23 Hz
8	200 Hz	20 Hz
9	180 Hz	18 Hz

NOTE: Horizontal and Vertical time constant thumbwheel setting is a single digit number and may be set to unequal values for each channel.

APPENDIX D

Coil Calibration

To calibrate the coils before a run, the calibration device should be mounted on the fiberglass structure. The device is mounted by unscrewing the right fiberglass nut and then sliding the left brace over the left fiberglass beam. The right brace is then slid over the right beam. For the supine position, a wooden stand is placed into the middle holes of the backboard to support the calibration device, and is held in place with a fiberglass nut. The calibration device is positioned to the point where the braces are aligned with the back of the tape, and the nut on the right brace is tightened.

The protractor device is then placed in the center of the calibration device and aligned with the zero marks. For torsion and vertical calibration, either the 0° or the 180° mark on the protractor should be aligned with the zero mark. For horizontal calibration, either the 90° or the 270 mark is aligned. For torsion calibration, a torsion coil must be taped to the center of the protractor; for horizontal and vertical calibrations, the coil in the protractor can be used. The output leads are then connected to the Eye 1 pre-amplifier for the horizontal/vertical leads and to the Tor 1 (or Tor 2) pre-amplifier for the torsion leads.

The protractor can then be rotated at one degree increments to calibrate the coil system. The following procedure will calibrate all three channels:

1. Align the 0° mark on the protractor with the zero mark and tape the protractor to the calibration device.
2. Turn the gains of the torsion, horizontal, and vertical channels to full maximum.
3. Adjust the offsets of all three channels so that each needle points to zero (if any of the channels cannot be zeroed, either the coil should be removed from the protractor and repositioned or the leads should be switched).
4. Switch the degrees full scale switch to 5 and again zero each channel.
5. Switch the degrees full scale switch back to 50.
6. Turn the gains of the three channels all the way down.

7. Rotate the protractor torsionally to 10° clockwise. If no movement of the needle is observed, check the leads on the coil.
8. Increase the gain on the torsion channel to show a 10° rotation clockwise. (Clockwise for these experiments was to the right on the dials. If the needle goes to the left, flick the phase switch to correct it and re-zero.)
9. Rotate the protractor torsionally to 10° counterclockwise.
10. Check to see that the dial shows -10° . If not, then try either re-zeroing the channel or readjusting the gain.
11. Rotate the protractor back to 0° .
12. The coils are calibrated in the same manner in the vertical direction, with right movements of the needle indicating up.
13. For horizontal calibration, the protractor must be rotated so that the 90° mark is aligned with the zero mark.
14. The horizontal calibration is then performed in the same manner as the torsion and vertical calibration.

The calibration device can then be removed from the coil system.

Once the coil is in the subject's eye, the horizontal and vertical channels can again be calibrated. This allows for minor gain changes encountered when the coil was suctioned to the subject's eye. The coil forms to the subject's eye, and therefore a change in the area of the coil perpendicular to the magnetic field may be encountered. To conduct this calibration, the fixation light mount must be mounted to the front of the coil system and the cross piece attached to the fixation light mount. The fixation light mount has the fixation light at its center and two marks which are positioned at an eye rotation angle of 10° above and below the fixation light for vertical calibration. When centered on the fixation light, the cross piece has two marks positioned 10° right and left of the fixation light for horizontal calibration. The subject is first asked to look at the fixation light. The channels can then be zeroed (without changing the gains this time). The subject is then asked to look at the top and bottom marks in succession, and the vertical gain can be adjusted. The horizontal gain can be adjusted using the right and left marks. The torsional gains cannot be adjusted in this manner, since most subjects cannot willfully torsion their eyes to a certain angle. It has

been found in tests conducted in the MVL, that the gain for the protractor closely resembles the gain of the human eye, and therefore is sufficient for the calibration.

APPENDIX E

Subject Preparation

The major constraint in the subject preparation is that the search coil can only be worn for 30 minutes. Therefore, it is ideal to insert the coil in the subject's eye as close to the start of the run as possible. If there were no 30 minute constraint, then the easiest way would be to insert the coil in the subject's eye first and then have the subject get into the coil system. But, to maximize the time for the sled runs, the subject is partially strapped into the coil system and the coil is then inserted into the subject's eye. Also, it is recommended that the coil leads be connected before inserting the coil into the subject's eye since the leads are very fragile. If they do break, it is easier to replace the coil with a backup coil if it is not already in the subject's eye. Following is the recommended procedure for subject preparation:

1. Brief subject on experiment.
2. Have subject sign consent form.
3. Have subject test jaw pad sizes and insert chosen one in helmet.
4. Have subject remove all jewelry and items from pockets.
5. Have subject get onto sled using foot stool.
6. Close and lock bottom coil.
7. Raise coil to proper subject height.
8. Mount fixation light onto coil system.
9. Have subject buckle lower straps of harness.
10. Strap subject's feet into foot restraint.
11. Have subject put helmet on.
12. Put shoulder pads and leg pads in place.
13. Have subject tilt head upward and insert coil in the subject's right eye (see Appendix F for coil insertion).

14. **Tape coil lead to forehead of subject.**
15. **Tape coil lead to helmet.**
16. **Tighten helmet onto backboard.**
17. **Buckle shoulder harness straps and tighten all straps.**
18. **Pump up the helmet to subject's comfort.**
19. **Put calibration cross piece on light source and calibrate (see Appendix D for subject calibration). Remove cross piece after calibration.**
20. **Give panic button to subject.**
21. **Put shroud around coil system.**

The subject is now ready for the experiment to run. Once the experiment is finished, the coil should be removed from the subject's eye as soon as possible (see Appendix F for coil removal) to reduce the chance of irritation.

APPENDIX F

Scleral Coil Insertion and Removal

The following is a step by step description of the method used to insert and remove the scleral coil for all Man Vehicle Lab coil experiments. Dr. Janice Cotter at the Massachusetts Eye and Ear Infirmary instructed the use of this method, and all experimenters using the coil system are required to learn this method from her or another accredited doctor of optometry. For the present study, the coil was inserted into the subject's right eye.

I Coil Insertion

1. Soak coil in hydrogen peroxide for one and a half hours before insertion.
2. Wash hands thoroughly.
3. Wash coils with saline solution--Don't hold lenses by wires!
4. Put coils in saline solution.
5. Perform retinal scan.
6. Instruct subject to look up and put one drop of anesthetic in lower part of eye.
7. Put one more drop of anesthetic in subject's eye, wiping with tissue if needed.
8. Allow one to two minutes for anesthetic to take affect.
9. Hold coil between thumb and forefinger of right hand with wires toward subject's nose.
10. Instruct subject to look down.
11. Open upper lid with left thumb (wide).
12. Instruct subject to look up.
13. Open lower lid with right middle finger.
14. Instruct subject to look straight ahead.
15. Put lens into eye, top first.
16. Rotate lens to have wires come out nasal side of eye.

17. Instruct subject to close eye and press on eyelid to suction coil to eye.

II Coil Removal

1. Instruct subject to look down.
2. Open upper lid with left thumb.
3. Instruct subject to look up.
4. Open lower lid with right middle finger.
5. Push down on lower lid.
6. Instruct subject to look down slowly. The lower lid will pry the lens out of the eye.
7. Perform retinal scan.
8. Soak lenses in hydrogen peroxide overnight.

APPENDIX G

Human Use Application and Consent Form

The following pages present a copy of the COUHES human use application, as well as a copy of the consent form which each of the subjects signed before participating in the experiment.

Application Number _____

MASSACHUSETTS INSTITUTE OF TECHNOLOGY
Committee on the Use of Humans as Experimental Subjects

APPLICATION FOR APPROVAL TO USE HUMANS AS EXPERIMENTAL SUBJECTS

PART I.

TITLE OF STUDY: Visual Vestibular Interaction

PRINCIPAL INVESTIGATOR: C.M. Oman, L.R. Young Dept. A&A
Room 37-211
Telephone 3-7508

ASSOCIATED INVESTIGATORS: Conrad Wall, Ph.D., Mass Eye and Ear Infirmary

Collaborating Institution(s), if applicable: Mass Eye and Ear Institute
(Please attach copies of approval documents or correspondence from
collaborating institution(s) where applicable.)

FINANCIAL SUPPORT: (Research grant title, agency and award number, if any.

If not applicable, please indicate how project will be financed.)

NASA Ames Research Center NAG2-445

PURPOSE OF STUDY: (Please provide a concise statement of the background,
nature and reasons for the proposed study.)

Human visual-vestibular interaction will be investigated by studying eye movements and perception of self-motion. The experiments will emphasize vertical eye movements and ocular torsion in conjunction with vertical linearvection. Motions which stimulate the utricular or saccular otolith organs will be combined with corresponding wide field motion displays capable of producing optokinetic nystagmus and self-motion illusions. The experiments utilize our linear acceleration sled.

This research concerns human visual vestibular interaction with emphasis on stimulation in the vertical and longitudinal axes. The measurements will be psychophysical estimates of vection and objective measurements of ocular torsion and vertical eye movements. We will utilize our linear "sled" to produce horizontal longitudinal linear acceleration for comparison with horizontal lateral acceleration. Measurements of vertical

eye movements for z-axis acceleration, in comparison with lateral eye movements for y-axis acceleration, with and without confirming and conflicting visual wide field stimuli, will be made in conjunction with subjective estimations of self-motion. This set of experiments will permit us to delineate between linear acceleration effects on eye movements and affects on motion perception when the stimulus is primarily along the presumed axis of sensitivity of the saccular otolith organ.

Part II.

EXPERIMENTAL PROTOCOL: Please provide an outline of the actual experiments to be performed, including, where applicable, detailed information as to exact dosages of drugs and chemicals to be used, total quantity of blood samples to be drawn, nature of any special diets, physical or emotional stress, and the appropriate protective measures you are planning to take.

For applications in the social sciences, please provide a detailed description of your proposed study, and include a copy of any questionnaire you plan to incorporate into your project. If your study involves interviews, please submit an outline indicating the types of questions you will include.

If convenient, you may attach photocopies of material from previously-submitted proposals, etc.; however, please try to avoid submitting extraneous material, such as grant applications in their entirety.

The ultimate goals of these experiments are to quantitatively describe the transfer functions of both the utricular and saccular otolithic and optokinetic torsion systems and to understand their interactions when suppressive and conflicting visual/motion conditions are produced.

Torsion eye movements will be measured using the magnetic search coil method described below. The coils used to generate the external magnetic field will be mounted on the sled. He will wear either a commercial Skalar lenses or the coil lenses described below. The subject will be secured in the sled by shoulder and lap seatbelts and his head will be held in position by a bite-bar and wood/foam head restraint. Sinusoidal and step profiles will be the motion stimuli.

The proposed experiments on linear visual-vestibular interaction emphasize the differences between Z-axis optokinetic and vestibular responses and the corresponding Y-axis responses. For all of the experiments in the series two kinds of measurements are taken: eye movements along the axis of stimulation and subjective magnitude estimation of body velocity. The experiments will begin with simple tests of pure optokinetic and pure inertial stimuli, in Z and Y axes, followed by interactive experiments with confirming and conflicting visual and vestibular stimuli.

The principal motion stimulus will be provided by the MIT Sled, a rail mounted linear acceleration cart designed by Lichtenberg (1979) and modified by Loo (1980) and by Arrott (1982). In the most closely related work, using measurements of motion perception and of eye movements, it was employed for the normative studies supporting our Spacelab-1 pre and post flight vestibular assessments, and in the lateral visual-vestibular interaction perception experiments (Huang, 1983). The seat can be positioned to allow X, Y or Z axis motion of the subject along the horizontal rails. The cart is controlled by a pre-tensioned cable wound around a pulley at one end and a winch at the other. Power is supplied through a 3.5 hp DC permanent magnet torque motor controlled by a pulse-width modulated velocity control. Sled motion as well as data logging is under the control of a PDP 11/34 microcomputer and Lab Peripheral System. An interactive FORTRAN program provides real time control of cart motion profiles and provides supervisory control and one level of safety devices (Arrott, 1985). A dedicated microcomputer (PC type) will be programmed to take over this function. This should further increase the reliability of the system. Current motion profiles provide for single sinusoids, sum of sines, constant accelerations, subthreshold positioning, frequency sweep, and subject control of cart velocity. The envelope of sled motion is determined by its length (4.7 m), maximum acceleration (0.8 g) and bandwidth (7 Hz).

Visual stimulus for our visual-vestibular interaction experiments has, in the past, been provided through a point-light source, moving film strip system which reflected from a long mirror to a rear projection screen attached to the sled cart (Huang, 1983). In order to provide a flexible moving field linear display which could be mounted to the cart for z-axis (subject supine) as well as y-axis acceleration, we recently developed a new mechanical stimulator. This "window shade" device (Vargas, 1985) provides computer controlled linear acceleration of a 47.5 x 47.5 cm screen placed 47.5 cm from the subject, and will be our primary source for optokinetic and linear VVI experiments in conjunction with the sled. A drawing of the windowshade attachment is enclosed.

Eye movements will be measured both by means of the coil system and standard electro-oculography, using our own dc-coupled, high input impedance amplifiers and pregelled infant EOG electrodes. We record EOG binocularly for horizontal eye movements and have determined that, for normal subjects, vergence eye movements and lack of conjugate gaze is not a problem. By using pre-experiment time for dark adaptation and electrode stabilization, we can achieve stable recordings requiring only pre and post-test calibration. Three distinct types of lateral or vertical eye movements are encountered during linear body acceleration in the dark, as opposed to the simple OKN seen for field motion. The eye movement pattern may be nystagmoid, a smooth pendular response, or highly irregular. In all cases the EOG records are inspected and then "desaccaded" by computer (Massoumnia, 1983) to produce the cumulative slow phase eye position and slow phase velocity (SPV).

The scleral search coil method of measuring eye movements uses two sets of coils. One or more pairs of transmitter coils surrounds the subject's head and transmit an electromagnetic field that is designed to be uniform in the area of the subject's eye. Another set of receiving coils is temporarily attached to the subject's eye via a silastic rubber annulus and move with the eye. Eye movements are detected and measured by electrically comparing the received signals to the transmitted signals. Properly selected combinations of coils allow for measurement of horizontal, vertical, and torsional eye movement components. The scleral search coil method will be the primary means to measure ocular torsion and will also be useful in assessing vertical eye movements. The C&C search coil system will be specifically designed for use with our sled. Phase detector sensors will be provided to measure horizontal, vertical and torsional eye movements simultaneously. The Skalar medical torsion coil annulus may be used. The procedures recommended by Skalar Medical for safe use and installation of the coil annulus will be followed. Care will be taken to limit the time that the annulus is worn by the subject to a maximum of 30 minutes. Since the coils are relatively expensive and can be re-used, they will be disinfected and stored in accordance with the Skalar Medical procedure. This procedure has been approved by the National Institutes of Health and the Center for Disease Control. Subject calibration for this system will be provided by a calibration fixture which comes with the C&C search coil system.

The sequence of visual-vestibular interaction experiments begins with pure visual (optokinetic) stimuli, comparing vertical eye movements and linear-vection to lateral (horizontal) responses for subjects supine and erect. The next step will be pure vestibular experiments on the sled, in darkness, comparing z-axis to y-axis horizontal acceleration conditions. Finally, visual and vestibular conditions will be combined by putting the linear "window shade" on the sled.

For each condition there will be three basic stimulus profiles: steps of constant velocity, sines of constant peak velocity covering the range of frequencies, and pseudorandom sums of 25 sinusoids. Both the eye movement and the subjective velocity measurements will be analyzed using linear systems analysis techniques to extract the gain and phase of the response velocity relative to the stimulus velocity. For the case of vertical motions, particular attention will be paid to up-down asymmetries, which will necessitate separate consideration of upward and downward phases of eye and self-motion velocity indications. For the sines and pseudo-random signals, we use FFT analysis of self velocity and cumulative slow phase velocity to calculate the frequency response, harmonics, and remnant.

For these linear visual-vestibular interaction experiments, we plan to use the same four combinations of stimuli which have proven effective in the development of models for VVI about the angular axes. The first is the counter-motion (CON) condition, in which the visual field moves opposite to the sled, at the same speed, so that it represents the fixed laboratory environment and the optokinetic and vestibular drives are consistent. The second condition is the fixed (FIX) visual field, which provides for

visual suppression of vestibular nystagmus and inhibition ofvection, but which also promotes the oculogravic illusion. The third condition is constant velocity (CV) field motion, independent of the sled motion. The last condition is the dual random input stimulus in which independent pseudorandom inputs of different frequency content are presented to the sled motion drive and to the visual velocity drive to enable calculation of the subject's dual input describing function (DIDF). This technique has proven very valuable when used with closed loop velocity nulling by the subject in yaw (Zacharias and Young, 1981, Huang and Young 1985a), but has been difficult to implement for linear acceleration studies (Hiltner, 1983, Huang, 1983.)

For the static visual stimulation experiments, the subject's head will be fixed by the helmet we also use in the sled experiments or the subject will be provided with a personal biteboard. Following calibration with fixed 15 degree targets the subject will be instructed to stare ahead to generate "stare nystagmus" as opposed to tracking nystagmus. The vertical EOG calibration problem will be dealt with by a separate investigation of each subject in which voluntary fixation and vertical saccades will be monitored by EOG and the coil system and the extent of the correction noted. Pattern movements for constant velocity steps are anticipated to be of 20 second durations at five speeds in each direction, logarithmically spaced between 1 cm/sec and 1 m/sec. Sines will also be logarithmically spaced between 0.02 Hz and 2.0 Hz, with a peak velocity of 50 cm/sec. The pseudorandom signal will consist of 25 sines between 0.02 Hz and 1.25 Hz. The pure vestibular linear acceleration tests on the sled will follow a similar pattern, limited only by the performance envelope of the device. The sled has been safety rated up to 1.0 g's for subject erect (y-axis) and subject supine (z-axis). The combined visual and vestibular stimuli are conducted on the sled with the moving visual field device attached.

The total number of subjects to be used in each test series depends, of course, on the stability of the measurements and the inter-subject variability. Based upon our experience over the course of many years, we estimate that at least six subjects will be required for each of the subjective estimation tests, but that 10-15 subjects will be required to obtain reliable patterns of linear acceleration induced eye movements. Since so many of the tests involve comparison between conditions, subjects will be selected from within the Laboratory's population of students and staff, who will be willing to commit to a long duration study with numerous retests over the course of several years. Order effects will be taken into account in the experimental design for each comparison, such as y-axis vs. z-axis.

PART III. Please answer all questions and indicate NA where not applicable. Positive answers should be briefly explained, with detailed information included in Part II.

1. How will subjects be obtained? Word-of-mouth
Number of subjects needed? 20
Age(s) of subjects? > 18
2. Will subjects receive any payment or other compensation for participation? Yes
3. Will your subjects be studied outside MIT premises? No.
If so, please indicate location.
4. Will the facilities of the Clinical Research Center be used? No.
If so, the approval of the CRC Policy Committee is also required.

For proposed investigations in social sciences, management, and other non-biomedical areas, please continue with question 9.

5. Will drugs be used? No.
Any Investigational New Drugs (IND)?
6. Will radiation or radioactive materials be employed? No.
If so, your study must also be approved by the Committee on Radiation Exposure to Human Subjects. Application forms are available from Mr. Francis X. Masse, Radiation Protection Office, 20B-238, x3-2180 or 18-3212.
7. Will special diets be used? If so, please state proposed duration(s).
No.
8. Will subjects experience physical pain or stress? No.
9. Will a questionnaire be used? No.
If so, please attach a copy.
10. Are personal interviews involved? No.
If so, include an explanation in Part II and attach an outline.
11. Will subjects experience psychological stress? No.
12. Does this study involve planned deception of subjects? No.
13. Can information acquired through this investigation adversely affect a subject's relationship with other individuals (e.g. employee-supervisor, patient-physician, student-teacher, co-worker, family relationships)? No.
14. Please explain how subject's anonymity will be protected and/or confidentiality of data will be preserved.

Subjects will be referred to only by codes.

PART IV.

- A. Please summarize the risks to the individual subject, and the benefits, if any; include any possible risk of invasion of privacy, embarrassment or exposure of sensitive or confidential data, and explain how you propose to deal with these risks.

Risks associated with the use of the Skalar search coil system: The subject wears a very small coil that is completely imbedded in a silicon rubber annulus and which is shaped to adhere to the limbus of the eye. There is a 12.5 mm central hole in the annulus so that vision is not occluded. The manufacturer of the annulus has developed procedures for the safe insertion of the coil and also for cleaning, disinfecting and storing the coils. These procedures will be adhered to in the measurement protocol. Personnel who insert the coil will be approved in writing by a collaborating ophthalmologist or doctor of optometry. A 30 minute guideline for maximum wearing of the search coil will be adhered to as mentioned in the manufacturer's procedures.

Prior to insertion of the annulus, the eye will be briefly anesthetized by 1 or 2 drops of a topical ophthalmic anesthesia such as Novosine (oxybuprocane 0.4%). The annulus will be removed from the subject's eye in accordance with the recommended procedures. After use, the annulus will be cleaned by thorough rinsing in a stream of lukewarm water and subsequently disinfected by immersion in fresh 3% hydrogen peroxide for 10 minutes. This procedure is in agreement with a recent guideline based on studies at the National Institutes of Health and the Center for Disease Control. After the immersion, there will be a second thorough rinsing with water and the device will be air dried on tissue paper.

- B. Detection and reporting of harmful effects: If applicable here, please describe what follow up efforts will be made to detect harm to subjects, and how this committee will be kept informed.

The probability of even a minor irritation to the eye is very low. Investigators at other institutions (National Eye Institute, Johns Hopkins University, UCLA) have found it to be less than one percent. All subjects will be examined by an optometrist prior to participating in any experiments involving lenses or annular rings. In case of irritation, the subject's eye will be patched and treated with an ophthalmologic topical antibiotic and then re-examined the next day. The Committee will be informed in the event of any such occurrences. These procedures have been carried out on 50-60 insertions of the lenses with subjects from Dr. Wall's laboratory with only one case of minor irritation (see attached protocol from MEEI).

PART V.

INFORMED CONSENT MECHANISMS: The committee is mandated by the DHHS and Institute regulations to require documentation of informed consent. Under certain circumstances, the committee may waive documentation. The elements of such informed consent are:

1. An instruction that the person is free to withdraw his/her consent and to discontinue participation in the project or activity at any time without prejudice to the subject.
2. A fair explanation of the procedures to be followed and their purposes, including identification of any procedures which are experimental.
3. A description of any attendant discomforts and risks reasonably to be expected.
4. A description of any benefits reasonably to be expected.
5. A disclosure of any appropriate alternative procedures that might be advantageous for the subject.
6. An offer on the part of the investigator to answer any inquiries concerning the procedures.
7. There shall be no exculpatory language making the subject seem to waive any rights.
8. The following statement shall appear on all informed consent documents, except that in certain cases of experiments in the social sciences, management, or other non-biomedical disciplines, where it is clearly not applicable, it may be omitted. COUHES, however, reserves the right to request that this paragraph be included.

"In the unlikely event of physical injury resulting from participation in this research, I understand that medical treatment will be available from the MIT Medical Department, including first aid, emergency treatment and follow-up care as needed, and that my insurance carrier may be billed for the cost of such treatment. However, no compensation can be provided for medical care apart from the foregoing. I further understand that making such medical treatment available, or providing it, does not imply that such injury is the investigator's fault. I also understand that by my participation in this study I am not waiving any of my legal rights.

I understand that I may also contact the Chairman of the Committee on the Use of Humans as Experimental Subjects (MIT, 253-6787), if I feel I have been treated unfairly as a subject."

Consent forms in cooperating institutions must assure that the rights of the subjects are protected at least to the same degree.

These elements should be clearly stated in a document to be signed by the subject or a legally authorized representative in the case of minors or

incompetent individuals. The material presented in such as document must be in clear English, easily understandable to the least educated of subjects. Diagrams or pictures may make such an exposition simpler to comprehend. Where minors are involved as subjects, due consideration should be given to their capability to give consent. The Informed Consent document should be signed by both the subject and parent and guardian wherever possible.

In the case of Questionnaires or Interviews, the Committee may decide that a consent form is not required if the intent is merely to obtain the requested information. However, it must be clear to the subject that:

- Participation is voluntary.
- The subject may decline to answer any questions.
- The subject may decline further participation at any time without prejudice.
- Confidentiality and/or anonymity are assured.

In addition:

- No coercion to participate will be involved. For example, handing out or collecting questionnaires personally may be so interpreted.
- The data collected will be reported in such a way that the identity of individuals is protected.
- Proper measures will be taken to safeguard the data.

Other examples of situations in which informed consent documentation is not required include use of discarded blood, certain psychological studies involving intentional deception or use of stored data. In a case of any deception, debriefing mechanisms must be acceptable before the approval of an application may be completed. The committee expects that the investigators will notify the committee if any hazards develop in excess of those anticipated.

Principal Investigator _____ Date _____

Department Head _____ Date _____

Please return this application with 3 photocopies to COUHES Chairman, E23-389, 253-6787

INFORMED CONSENT STATEMENT

You have been asked to participate in an experiment aimed at better understanding the workings of the inner ear and the eyes. Your participation is purely voluntary and you are free to withdraw at any time. In the experiment, you will be seated and strapped into a linear acceleration device (sled) either in the upright or supine position and asked to look straight ahead. The sled may or may not move. You may be asked to look at a moving display and you may be asked to indicate your perception of movement. At the end of the experiment, you may be asked to discuss how you perceived various stages of the experiment.

Please feel free to ask any questions you care to about the experiment. When the sled is moving, you can stop it at any time by pushing the "panic button". If at any time, you experience any discomfort or have any misgivings about continuing the experiment, we ask that you tell us - we will stop the test at any time you like.

Your eye movements will be measured using soft contact lens search coils, the most accurate method available today. The cornea of your eye will be anaesthetised using eye drops. The anesthetic used is Ophthetic (0.5%). If you have any allergies to this anesthetic, you should withdraw from participation in this experiment. The lens, in which a tiny search coil is embedded, will be applied to your eye. This will be worn for no longer than thirty minutes. Before application and after removal, your eyes will be examined by an optometrist to rule out any possible corneal abrasion. There is a less than one percent chance that the wearing of the soft contact lens may cause a slight corneal abrasion. If this does occur, a prophylactic antibiotic and covering will be applied overnight. Finally, we may also video your eye movements, using a small video camera with a low level light source.

"In the unlikely event of injury resulting from participation in this research, I understand that medical treatment will be available from the MIT Medical Department, including first aid, emergency treatment and follow-up care as needed, and that my insurance carrier may be billed for the cost of such treatment. However, no compensation can be provided for medical care apart from the foregoing. I further understand that making such medical treatment available, or providing it, does not imply that such injury is the investigator's fault. I also understand that by my participation in this study I am not waiving any of my legal rights (for more information, call the Institute's Insurance and Legal Affairs Office at 253-2822). I understand that I may also contact the Chairman of the Committee on the Use of Humans as Experimental Subjects, Dr. H. Walter Jones (MIT E23-389, 253-6787), if I feel I have been treated unfairly as a subject."

I have been informed as to the procedures and purpose of this experiment and agree to participate.

Signed: _____

Date: _____

Witness: _____

APPENDIX H

Procedure for Conducting a Sled Run

To conduct a sled run, all the components must be coordinated correctly between runs. Before any runs can be performed, though, all the components must be zeroed. It is recommended that the function generator, the 15 volt power source, the two filters, and the oscilloscope be turned on and given time to stabilize before beginning the zeroing process. It is also recommended that the zeroes be checked occasionally between sled runs. The zeroing process is listed below:

1. Set Drift Box to 5.0.
2. Press GND on DC Offset "+".
3. Zero line on Oscilloscope using STEP GAIN DC BAL on Function Generator.
4. Press GND again.
5. Switch CH1 on Oscilloscope to GND.
6. Zero line using POSITION dial.
7. Switch CH1 to DC.
8. Turn Trigger Source to CH2
9. Zero line using POSITION dial (do not ground first because Krohn-Hite filter has a small offset).

Once the equipment is zeroed, a sled run can be performed. The LabTech Notebook program must first be run on the 386 computer and all questions should be answered except "Continue with same set-up parameters?" At that point, the input parameters are entered. The following is the list of steps that must be performed to change the input parameters before each sled run:

1. Press STOP on Sled Control Panel.
2. Disable sled on Sled Control Panel.
3. Press FREE run on Function Generator.

4. Set the frequency value (from Table H.1 below) on the Frequency Dial on Function Generator. The frequency on the Function Generator is off by 0.05 Hz; this is compensated for in column three of the table.
5. Set Drift Box to 5.0.
6. Turn the OFFSET AMPL dial on Function Generator until Oscilloscope shows proper voltage (from Table H.1).
7. Set Drift Box to proper setting (from Table H.1). This is not necessary for all runs, as 5.0 is satisfactory for most profiles.
8. Press GATE on Function Generator.
9. Turn CH1 to 50 mV per division.
10. Zero line on Oscilloscope using VARØ dial on Function Generator.
11. Turn CH1 back to 1 Volt per division.
12. Wait until data storage from last run is completed to continue.
13. Press START on Sled Control Panel.
14. Enable Sled.
15. Zero any drift or position sled using VARØ dial on Function Generator.
16. Type "y" on computer. The Computer will take approximately 45 seconds to set up its parameters, and will then begin the run.

The above steps sound complicated and time-consuming, but they can all be completed during the time that the Notebook program on the 286 computer is transferring the temporary data files to permanent files.

Acceleration (g's)	Frequency (Hz)	Frequency (on Fn Gen)	Input Voltage (V) (based on g)	Drift	Order
.2	.26	.31	1.4	5.0	4
	.4	.45	.9	5.0	3
	.6	.65	.6	4.0	1
	1.0	1.05	.35	5.0	2
.6	.26	.31	3.9	8.0	8
	.4	.45	2.7	6.5	7
	.6	.65	1.7	5.0	5
	1.0	1.05	1.0	5.0	6

Table H.1 Function Generator Input Parameters

The input voltage values in the above table were found using the following method:

1. Set frequency dial on Function Generator to desired frequency +0.05 Hz.
2. Set input voltage to an approximate value using OFFSET AMPL dial on Function Generator.
3. Run Sled.
4. Monitor CH2 on Oscilloscope.
5. Increase or decrease input voltage until correct acceleration value is read on CH2 (1 Volt = 1 g).
6. Record the input voltage value.
7. At successive runs, this value is set to achieve the proper acceleration.

APPENDIX I

Program Listings

This appendix lists the programs used in data conversion and analysis for this experiment.

The program `Convert` was written by Dave Balkwill and modified to be used for the data for this thesis. `Convert` is used to convert the data from binary format to Matlab format. The program converts all four channels of each run, and only the first six letters (e.g.: `gl103`) of the file need be entered. The program adds Matlab flags to each channel: `tor` for channel 1, `hor` for channel 2, `ver` for channel 3, and `acc` for channel 4. This allows for all files to be called up by Matlab scripts simply by using the same flag.

The program `Sac_em` was written by Keoki Jackson and is run to remove the saccades from the position plot. This program locates each saccade from the SPV plot and adjusts the remaining data points to the pre-saccade value. This results in a Cumulative Eye Position (CEP) plot which is saved into a file called `xxxxxx.cum`, where `xxxxxx` is the individual run codes for each sled run.

The program `Sine_fit` was initially written by Jock Christie and highly modified by the author, and is used to fit sine waves to the ocular counterrolling plots, the cumulative eye position plots, and the slow phase velocity plots. The ocular counterrolling, cumulative eye position, and the slow phase velocity are save into files called `xxxxxx.fittedt`, `xxxxxx.fittedc`, and `xxxxxx.fittedv`, respectively. The program also finds the amplitudes and phases of both the signal and the acceleration for each cycle of the sled run, and saves them into files called `xxxxxx.gnpt`, `xxxxxx.gnpc`, and `xxxxxx.gnpv`, respectively.

The program `Find_Avg` is used to convert these amplitudes and phases into gains and phases for each cycle, which are saved into a file called `xxxxxx.cycgnp`, and to

calculate average gains and phases for each run, which are saved into a file called values.all.

The program Plotter was used to plot the data in the user's choice of the following formats:

1. Signal plots (OCR, horizontal, vertical, acceleration, SPV, CEP).
2. Gains and Phases plots (gains or phases versus frequency, Bode plots).
3. Phase versus time plot.
4. One cycle plots.

The program Curve_fit is used to fit a least squares line to OCR gain, OCR phase, SPV gain, SPV phase, CEP gain, or CEP phase versus frequency. Using a 95% confidence interval, the program then decides if the slope is statistically different from zero, thus showing the trends of the parameter with respect to frequency.

The program T-test was used to perform paired and unpaired t-tests on the sled runs. The program is a batch program and compares all files which are comparable and stores a 0 if they're not significantly different and a 1 if they are significantly different.

Examples of the comparisons that this program makes are:

1. Gain (or phase) of OCR (or SPV or CEP) at different frequencies, same acceleration.
2. Gain (or phase) of OCR (or SPV or CEP) at different accelerations, same frequency.
3. Gain (or phase) of OCR (or SPV or CEP) for different runs, at same acceleration, same frequency.

The program Bode_fit optimizes the formula

$$G = K \sqrt{\left(\frac{\omega_c}{\omega}\right)^2 + 1} \quad (5.4)$$

for the constant K and the cutoff frequency ω_c and finds the best fit Bode plot. The program also optimizes the formula

$$\text{Tan } \phi = - \frac{\omega_c}{\omega} \quad (5.5)$$

for the cutoff frequency. The optimization procedures in Bode_fit call up the M-files Fun1, Fun2, Funp1, and Funp2. The difference between the two calculated cutoff frequencies is then found. For the Bode fit based on phase, the K value from Equation 5.4 is used.

```
/*Program Convert*/
```

```
#include <stdio.h>
#include <stdlib.h>
#include <fcntl.h>
#include <unix.h>
```

```
#define FALSE 0
#define TRUE 1
```

```
#define MAX_LINE_LENGTH 81
```

```
#define BLOCK_SIZE 16384
```

```
#define MATLAB_NAME "info"
```

```
#define BAD_TYPE 0
#define DOUBLE_TYPE 1
#define FLOAT_TYPE 2
#define LONG_TYPE 3
#define SHORT_TYPE 4
```

```
#define MATLAB_DOUBLE 1000
#define MATLAB_FLOAT 1010
#define MATLAB_LONG 1020
#define MATLAB_SHORT 1030
```

```
#define TORSIONAL_VAR "tor" /* channel 1 */
#define HORIZONTAL_VAR "hor" /* channel 2 */
#define VERTICAL_VAR "ver" /* channel 3 */
#define ACCELERATION_VAR "acc" /* channel 4 */
```

```
char *matvar_names[] = {
    TORSIONAL_VAR, HORIZONTAL_VAR, VERTICAL_VAR,
    ACCELERATION_VAR
};
```

```
char run_code[MAX_LINE_LENGTH];
```

```
char in_filename[MAX_LINE_LENGTH];
int in_handle;
FILE *in_fptr;
char *in_buffer;
int in_bytes;
```

```
char out_filename[MAX_LINE_LENGTH];
int out_handle;
FILE *out_fptr;
char *out_buffer;
int out_bytes;
```

```
char inter_filename[MAX_LINE_LENGTH];
```

```

int inter_handle;
FILE *inter_fptr;

typedef struct {
    long type;
    long mrows;
    long ncols;
    long imagf;
    long namlen;
} Fmatrix;

Fmatrix F_out;
long mrows = 0L;
long ncols = 0L;

int sample_size[5] = { 0, 10, 4, 4, 2 };
int in_size, out_size;
int in_type, out_type;
int num_channels;
long total_bytes;

int save_intermediate = FALSE;

#define ALLOCATE_BUFFER(BUF) \
{ \
(BUF) = malloc(BLOCK_SIZE); \
if (!(BUF)) { \
printf("Out of memory on buffer allocation.\n"); \
goto done; \
} \
}

#define READ_BUFFER() \
in_bytes = read(in_handle,in_buffer,BLOCK_SIZE);

#define WRITE_BUFFER(NUM) \
write(out_handle,out_buffer,NUM);

#define WRITE_INTER(NUM) \
write(inter_handle,out_buffer,NUM);

char in_line[MAX_LINE_LENGTH];
char matlab_name[MAX_LINE_LENGTH];

main()
{
    int open_input_file(), create_output_file(), create_inter_file(), get_file_parameters();
    int specify_run();
    long calculate_num_samples();
    void write_matlab_header(), transfer_data();
    int i;

    ALLOCATE_BUFFER(in_buffer)
    ALLOCATE_BUFFER(out_buffer)

```

```

while (specify_run()) {
for (i = 1; i <= 4; i++) {
    in_filename[7] = '0' + i;
    if (open_input_file()) {
        if (create_output_file()) {
            if (get_file_parameters(i)) {
/*
printf("input file = %s\n",in_filename);
printf("output file = %s\n",out_filename);
printf("input type = %d\n",in_type);
printf("ouput type = %d\n",out_type);
printf("number of channels = %d\n",ncols);
printf("matlab name = %s\n",matlab_name);
*/
/*
                if (save_intermediate) {
                    if (create_inter_file()) {
                        mrows = calculate_num_samples();
                        write_matlab_header();
                        transfer_data();
                    }
                }
                else {
*/
                    mrows = calculate_num_samples();
                    write_matlab_header();
                    transfer_data();
/*
                }
*/
            }
        }
    }
    save_intermediate = FALSE;
}
}
done:
close(in_handle);
close(out_handle);
close(inter_handle);
}

```

```

int specify_run()
{
    int i,l;
    int retval = TRUE;

    printf("Enter input file name (6 character run code):");
    gets(run_code);
    l = strlen(run_code);
    while (l != 6) {

        if (l == 0) {
            retval = FALSE;
            break;
        }

        printf("\nInvalid file name -- enter only first six characters.\n");
        printf("Enter input file name (6 character run code):");
        gets(run_code);
        l = strlen(run_code);
    }

    strcpy(in_filename,run_code);
    for (i = 0; i < 3; i++) {
        if ((in_filename[i] >= 'a') && (in_filename[i] <= 'z'))
            in_filename[i] += 'A' - 'a';
    }
    strcat(in_filename,"C1.DAT");

    return(retval);
}

int open_input_file()
{
    int l;
    int retval = TRUE;

    in_handle = open(in_filename,O_BINARY|O_RDONLY);
    if (in_handle <= 0) {
        printf("Input file %s is missing.\n",in_filename);
        retval = FALSE;
    }
    return(retval);
}

int create_output_file()
{
    int l;
    int retval = TRUE;

    l = strlen(in_filename);
    strcpy( (char *)out_filename, (char *)in_filename );
    if (strncmp(".DAT",(char *)&out_filename[l-4],4))
        strcat(out_filename,".matlab");
}

```



```

else
    out_filename[1-3] = 'M';
out_fptr = fopen(out_filename,"rt");
if (out_fptr) {
    printf("Output file %s already exists. Overwrite (y/n) ?", out_filename);
    gets(in_line);
    if ((in_line[0] == 'y') || (in_line[0] == 'Y')) {
        printf("Overwriting %s.\n",out_filename);
        fclose(out_fptr);
        out_fptr = fopen(out_filename,"wt");
    }
    else {
        printf("Aborting for this file.\n");
        fclose(out_fptr);
        retval = FALSE;
    }
}
else {
    printf("Creating new output file %s.\n",out_filename);
    out_fptr = fopen(out_filename,"wt");
}
return(retval);
}

```

```

int create_inter_file()
{
    int l;
    int retval = TRUE;

    l = strlen(in_filename);
    strcpy( (char *)inter_filename, (char *)in_filename );
    if (strncmp(".DAT",(char *)&inter_filename[l-4]),4)
        strcat(inter_filename, ".nysa");
    else {
        inter_filename[1-3] = 'N';
        inter_filename[1-2] = 'Y';
        inter_filename[1-1] = 'S';
    }
    inter_fptr = fopen(inter_filename,"rt");
    if (inter_fptr) {
        printf("NysA file %s already exists. Overwrite (y/n) ?", inter_filename);
        gets(in_line);
        if ((in_line[0] == 'y') || (in_line[0] == 'Y')) {
            printf("Overwriting %s.\n",inter_filename);
            fclose(inter_fptr);
            inter_handle = open(inter_filename,O_BINARY|O_RDWR);
        }
        else {
            printf("Aborting for this file.\n");
            fclose(inter_fptr);
            retval = FALSE;
        }
    }
}
else {

```

```

        printf("Creating new NysA file %s.\n",inter_filename);
        inter_handle = open(inter_filename,O_BINARY|O_RDWR|O_CREAT);
    }
    return(retval);
}

int get_file_parameters(index)
int index;
{
    int get_buffer_type();
    int retval = TRUE;
    int i, j;

    in_type = get_buffer_type("input");
    if (in_type == BAD_TYPE) {
        retval = FALSE;
    }
    else {
        in_size = sample_size[in_type];
        out_type = get_buffer_type("output");
        if (out_type == BAD_TYPE) {
            retval = FALSE;
        }
        else {
            out_size = sample_size[out_type];
        }
    }

    /* modified for Jock's special use -- assumes only one column of data per file */
    /*
        printf("Enter number of data channels:");
        gets(in_line);
        sscanf(in_line,"%d",&num_channels);
    */

    num_channels = 1;
    if (num_channels <= 0)
        retval = FALSE;
    else {
        ncols = num_channels;
        strcpy(matlab_name,matvar_names[index-1]);

        /*
            save_intermediate = (index > 2);
            printf("Enter MatLab variable name:");
            gets(in_line);
            if (strlen(in_line) == 0)
                retval = FALSE;
            else {
                for (i = 0; in_line[i] <= ' '; i++);
                for (j = i; in_line[j] > ' '; j++)
                    matlab_name[j-i] = in_line[j];
                matlab_name[j-i] = '\0';
                if (strcmp(matlab_name,HEOG_VAR) == 0)
                    save_intermediate = TRUE;
                else if (strcmp(matlab_name,VEOG_VAR) == 0)
                    save_intermediate = TRUE;
            }
        */
    }
}

```

```

*/
    }
    }
    }
    return(retval);
}

int get_buffer_type(io)
char *io;
{
    int type;

/*
    printf("Enter %s file type.\n",io);
    printf(" 1: double\n");
    printf(" 2: float\n");
    printf(" 3: long\n");
    printf(" 4: short\n");
    gets(in_line);
    sscanf(in_line,"%d",&type);
    if ((type < 1) || (type > 4)) {
        type = BAD_TYPE;
        printf("Invalid %s file type. Aborting this file.\n",io);
    }
*/
/* modified for Jock's special use -- assumes I/O types are short two-byte integer */
    type = 4;

    return(type);
}

long calculate_num_samples()
{
    long num = 0L;

    do {
        READ_BUFFER()
        num += in_bytes;
    }
    while (in_bytes == BLOCK_SIZE);
    total_bytes = num;
    num /= (ncols * in_size);
    close(in_handle);
    printf("Converting %ld samples.\n",num);
    return(num);
}

void write_matlab_header()
{
    switch (out_type) {
        case DOUBLE_TYPE:
            F_out.type = MATLAB_DOUBLE;
            break;

```

```

case FLOAT_TYPE:
    F_out.type = MATLAB_FLOAT;
    break;
case LONG_TYPE:
    F_out.type = MATLAB_LONG;
    break;
case SHORT_TYPE:
    F_out.type = MATLAB_SHORT;
    break;
}
F_out.mrows = mrows;
F_out.ncols = ncols;
F_out.imagf = FALSE;
/* F_out.namlen = strlen(MATLAB_NAME) + 1;*/
/* allow user-specified matlab variable name */
F_out.namlen = strlen(matlab_name) + 1;
fwrite( &F_out, sizeof(Fmatrix), 1, out_fptr );
/* fwrite( MATLAB_NAME, sizeof(char), (int)F_out.namlen, out_fptr);*/
/* allow user-specified matlab variable name */
fwrite( matlab_name, sizeof(char), (int)F_out.namlen, out_fptr);
fclose(out_fptr);
}

void transfer_data()
{
    void double_to_float(), double_to_long(), double_to_short();
    void float_to_double(), float_to_long(), float_to_short();
    void long_to_double(), long_to_float(), long_to_short();
    void short_to_double(), short_to_float(), short_to_long();
    void short_reverse(), long_reverse();

    in_handle = open(in_filename,O_BINARY|O_RDONLY);
    out_handle = open(out_filename,O_BINARY|O_RDWR|O_APPEND);
    if (in_type == out_type) {
        do {
            READ_BUFFER()
/* reverse order of bytes in a word for data ported from VAX -- mod. for JC */
            if (in_type == SHORT_TYPE)
                short_reverse();
            else if (in_type == LONG_TYPE)
                long_reverse();
            WRITE_BUFFER(in_bytes)
            if (save_intermediate)
                WRITE_INTER(in_bytes)
        }
        while (in_bytes == BLOCK_SIZE);
    }
    else {
        switch (in_type) {
            case DOUBLE_TYPE:
                switch (out_type) {
                    case FLOAT_TYPE:
                        double_to_float();

```

```

        break;
    case LONG_TYPE:
        double_to_long();
        break;
    case SHORT_TYPE:
        double_to_short();
        break;
    }
    case FLOAT_TYPE:
        switch (out_type) {
            case DOUBLE_TYPE:
                float_to_double();
                break;
            case LONG_TYPE:
                float_to_long();
                break;
            case SHORT_TYPE:
                float_to_short();
                break;
        }
    case LONG_TYPE:
        switch (out_type) {
            case DOUBLE_TYPE:
                long_to_double();
                break;
            case FLOAT_TYPE:
                long_to_float();
                break;
            case SHORT_TYPE:
                long_to_short();
                break;
        }
    case SHORT_TYPE:
        switch (out_type) {
            case DOUBLE_TYPE:
                short_to_double();
                break;
            case FLOAT_TYPE:
                short_to_float();
                break;
            case LONG_TYPE:
                short_to_long();
                break;
        }
    }
}
close(in_handle);
close(out_handle);
}

```

```

void short_reverse()
{
    int i;

```

```

for (i = 0; i < in_bytes; i += 2) {
    out_buffer[i] = in_buffer[i+1];
    out_buffer[i+1] = in_buffer[i];
}

}

void long_reverse()
{
    int i;

    for (i = 0; i < in_bytes; i += 4) {
        out_buffer[i] = in_buffer[i+3];
        out_buffer[i+1] = in_buffer[i+2];
        out_buffer[i+2] = in_buffer[i+1];
        out_buffer[i+3] = in_buffer[i];
    }
}

void double_to_float()
{
    int i,j,k;
    int ratio;
    double *in;
    float *out;
    int in_samples, out_samples;
    long remaining;

    in = (double *)in_buffer;
    out = (float *)out_buffer;
    ratio = in_size / out_size;
    in_samples = BLOCK_SIZE / in_size;
    out_samples = BLOCK_SIZE / out_size;
    remaining = mrows * ncols;
    READ_BUFFER()
    j = 0;
    k = 0;
    while (remaining) {
        out[k] = in[j];
        j++;
        k++;
        remaining--;
        if (j == in_samples) {
            READ_BUFFER()
            j = 0;
        }
        if (k == out_samples) {
            WRITE_BUFFER(BLOCK_SIZE)
            k = 0;
        }
    }
    if (k > 0)

```

```

        WRITE_BUFFER(k * out_size)
    }

void double_to_long()
{
    int i,j,k;
    int ratio;
    double *in;
    long *out;
    int in_samples, out_samples;
    long remaining;

    in = (double *)in_buffer;
    out = (long *)out_buffer;
    ratio = in_size / out_size;
    in_samples = BLOCK_SIZE / in_size;
    out_samples = BLOCK_SIZE / out_size;
    remaining = mrows * ncols;
    READ_BUFFER()
    j = 0;
    k = 0;
    while (remaining) {
        out[k] = in[j];
        j++;
        k++;
        remaining--;
        if (j == in_samples) {
            READ_BUFFER()
            j = 0;
        }
        if (k == out_samples) {
            WRITE_BUFFER(BLOCK_SIZE)
            k = 0;
        }
    }
    if (k > 0)
        WRITE_BUFFER(k * out_size)
}

```

```

void double_to_short()
{
    int i,j,k;
    int ratio;
    double *in;
    short *out;
    int in_samples, out_samples;
    long remaining;

    in = (double *)in_buffer;
    out = (short *)out_buffer;
    ratio = in_size / out_size;
    in_samples = BLOCK_SIZE / in_size;

```

```

out_samples = BLOCK_SIZE / out_size;
remaining = mrows * ncols;
    READ_BUFFER()
    j = 0;
    k = 0;
    while (remaining) {
        out[k] = in[j];
        j++;
        k++;
        remaining--;
        if (j == in_samples) {
            READ_BUFFER()
            j = 0;
        }
        if (k == out_samples) {
            WRITE_BUFFER(BLOCK_SIZE)
            k = 0;
        }
    }
    if (k > 0)
        WRITE_BUFFER(k * out_size)
}

```

```

void float_to_long()
{
    int i,j,k;
    int ratio;
    float *in;
    long *out;
    int in_samples, out_samples;
    long remaining;

    in = (float *)in_buffer;
    out = (long *)out_buffer;
    ratio = in_size / out_size;
    in_samples = BLOCK_SIZE / in_size;
    out_samples = BLOCK_SIZE / out_size;
    remaining = mrows * ncols;
    READ_BUFFER()
    j = 0;
    k = 0;
    while (remaining) {
        out[k] = in[j];
        j++;
        k++;
        remaining--;
        if (j == in_samples) {
            READ_BUFFER()
            j = 0;
        }
        if (k == out_samples) {
            WRITE_BUFFER(BLOCK_SIZE)
            k = 0;
        }
    }
}

```



```

    }
    }
    if (k > 0)
        WRITE_BUFFER(k * out_size)
}

void float_to_short()
{
    int i,j,k;
    int ratio;
    float *in;
    short *out;
    int in_samples, out_samples;
    long remaining;

    in = (float *)in_buffer;
    out = (short *)out_buffer;
    ratio = in_size / out_size;
    in_samples = BLOCK_SIZE / in_size;
    out_samples = BLOCK_SIZE / out_size;
    remaining = mrows * ncols;
    READ_BUFFER()
    j = 0;
    k = 0;
    while (remaining) {
        out[k] = in[j];
        j++;
        k++;
        remaining--;
        if (j == in_samples) {
            READ_BUFFER()
            j = 0;
        }
        if (k == out_samples) {
            WRITE_BUFFER(BLOCK_SIZE)
            k = 0;
        }
    }
    if (k > 0)
        WRITE_BUFFER(k * out_size)
}

void long_to_short()
{
    int i,j,k;
    int ratio;
    long *in;
    short *out;
    int in_samples, out_samples;
    long remaining;

    in = (long *)in_buffer;

```

```

out = (short *)out_buffer;
ratio = in_size / out_size;
in_samples = BLOCK_SIZE / in_size;
out_samples = BLOCK_SIZE / out_size;
remaining = mrows * ncols;
    READ_BUFFER()
    j = 0;
    k = 0;
    while (remaining) {
        out[k] = in[j];
        j++;
        k++;
        remaining--;
        if (j == in_samples) {
            READ_BUFFER()
            j = 0;
        }
        if (k == out_samples) {
            WRITE_BUFFER(BLOCK_SIZE)
            k = 0;
        }
    }
    if (k > 0)
        WRITE_BUFFER(k * out_size)
}

```

```

void float_to_double()
{
    int i,j,k;
    int ratio;
    float *in;
    double *out;
    int in_samples, out_samples;
    long remaining;

    in = (float *)in_buffer;
    out = (double *)out_buffer;
    ratio = out_size / in_size;
    in_samples = BLOCK_SIZE / in_size;
    out_samples = BLOCK_SIZE / out_size;
    remaining = mrows * ncols;
    READ_BUFFER()
    j = 0;
    k = 0;
    while (remaining) {
        out[k] = in[j];
        j++;
        k++;
        remaining--;
        if (j == in_samples) {
            READ_BUFFER()
            j = 0;
        }
    }
}

```

```

        if (k == out_samples) {
            WRITE_BUFFER(BLOCK_SIZE)
            k = 0;
        }
    }
    if (k > 0)
        WRITE_BUFFER(k * out_size)
}

```

```

void long_to_double()
{
    int i,j,k;
    int ratio;
    long *in;
    double *out;
    int in_samples, out_samples;
    long remaining;

    in = (long *)in_buffer;
    out = (double *)out_buffer;
    ratio = out_size / in_size;
    in_samples = BLOCK_SIZE / in_size;
    out_samples = BLOCK_SIZE / out_size;
    remaining = mrows * ncols;
    READ_BUFFER()
    j = 0;
    k = 0;
    while (remaining) {
        out[k] = in[j];
        j++;
        k++;
        remaining--;
        if (j == in_samples) {
            READ_BUFFER()
            j = 0;
        }
        if (k == out_samples) {
            WRITE_BUFFER(BLOCK_SIZE)
            k = 0;
        }
    }
    if (k > 0)
        WRITE_BUFFER(k * out_size)
}

```

```

void long_to_float()
{
    int i,j,k;
    int ratio;
    long *in;
    float *out;
    int in_samples, out_samples;

```

```

long remaining;

in = (long *)in_buffer;
out = (float *)out_buffer;
ratio = out_size / in_size;
in_samples = BLOCK_SIZE / in_size;
out_samples = BLOCK_SIZE / out_size;
remaining = mrows * ncols;
    READ_BUFFER()
    j = 0;
    k = 0;
    while (remaining) {
        out[k] = in[j];
        j++;
        k++;
        remaining--;
        if (j == in_samples) {
            READ_BUFFER()
            j = 0;
        }
        if (k == out_samples) {
            WRITE_BUFFER(BLOCK_SIZE)
            k = 0;
        }
    }
    if (k > 0)
        WRITE_BUFFER(k * out_size)
}

```

```

void short_to_double()
{
    int i,j,k;
    int ratio;
    short *in;
    double *out;
    int in_samples, out_samples;
    long remaining;

    in = (short *)in_buffer;
    out = (double *)out_buffer;
    ratio = out_size / in_size;
    in_samples = BLOCK_SIZE / in_size;
    out_samples = BLOCK_SIZE / out_size;
    remaining = mrows * ncols;
    READ_BUFFER()
    j = 0;
    k = 0;
    while (remaining) {
        out[k] = in[j];
        j++;
        k++;
        remaining--;
    }
}

```

```

        if (j == in_samples) {
            READ_BUFFER()
            j = 0;
        }
        if (k == out_samples) {
            WRITE_BUFFER(BLOCK_SIZE)
            k = 0;
        }
    }
    if (k > 0)
        WRITE_BUFFER(k * out_size)
}

```

```

void short_to_float()
{
    int i,j,k;
    int ratio;
    short *in;
    float *out;
    int in_samples, out_samples;
    long remaining;

    in = (short *)in_buffer;
    out = (float *)out_buffer;
    ratio = out_size / in_size;
    in_samples = BLOCK_SIZE / in_size;
    out_samples = BLOCK_SIZE / out_size;
    remaining = mrows * ncols;
    READ_BUFFER()
    j = 0;
    k = 0;
    while (remaining) {
        out[k] = in[j];
        j++;
        k++;
        remaining--;
        if (j == in_samples) {
            READ_BUFFER()
            j = 0;
        }
        if (k == out_samples) {
            WRITE_BUFFER(BLOCK_SIZE)
            k = 0;
        }
    }
    if (k > 0)
        WRITE_BUFFER(k * out_size)
}

```

```

void short_to_long()
{

```

```

int i,j,k;
int ratio;
short *in;
long *out;
int in_samples, out_samples;
long remaining;

in = (short *)in_buffer;
out = (long *)out_buffer;
ratio = out_size / in_size;
in_samples = BLOCK_SIZE / in_size;
out_samples = BLOCK_SIZE / out_size;
remaining = mrows * ncols;
    READ_BUFFER()
    j = 0;
    k = 0;
    while (remaining) {
        out[k] = in[j];
        j++;
        k++;
        remaining--;
        if (j == in_samples) {
            READ_BUFFER()
            j = 0;
        }
        if (k == out_samples) {
            WRITE_BUFFER(BLOCK_SIZE)
            k = 0;
        }
    }
    if (k > 0)
        WRITE_BUFFER(k * out_size)
}

```

```
%Sac_em
```

```
%find saccade frequency, size, max velocity  
%uses diff_list to find location of events  
%should probably use edit_spv to deselect non-saccade events  
% and separate multiple saccades
```

```
%Written by Keoki Jackson
```

```
file_specs;  
data_path3 = 'HugeGLAW3:CEP:';  
SPV1_Var = 'Edited1_Var';  
t=.005;  
bin_size = 4;  
run_code = input('Enter run code: ','s');  
cal = .02241406;  
%ans = input('Enter position file calibration: [def = .0224] ');  
%if (isempty(ans) == 0)  
%     cal = ans;  
%end
```

```
%Load tor, velt, SPV
```

```
in_file = file_name(Pos1_File, run_code);  
eval(['load ', data_path, in_file]);  
scale_other = 2048/50; % Convert from A/D units.  
tor = ((tor) - 2048)/scale_other;  
torcor = (tor - tor(1));  
pos = torcor;
```

```
in_file = file_name(Vel1_File, run_code);  
eval(['load ', data_path, in_file]);  
eval(['vel = ', Vel1_Var, ';']);  
if (length(Vel1_Var) ~= 3)  
    eval(['clear ', Vel1_Var]);  
elseif sum (Vel1_Var ~= 'vel')  
    eval(['clear ', Vel1_Var]);  
end
```

```
in_file = file_name(Edited1_File, run_code);  
eval(['load ', data_path, in_file]);  
eval(['spv = ', SPV1_Var, ';']);  
if (length(SPV1_Var) ~= 3)  
    eval(['clear ', SPV1_Var]);  
elseif sum (SPV1_Var ~= 'spv')  
    eval(['clear ', SPV1_Var]);  
end
```

```
l = length(pos);  
time = [0:t:t*(l-1)];
```

```
cum = pos;
```

```

events = diff_list(vel,spv);
n = size(events);
n = n(1,1);

%Remove saccades from position plot

for i=1:n
    x = events(i,1);
    y = events(i,2);
    if ((y-x)>1)
        cum((x+1):(y-1)) = cum(x)*ones((y-x-1),1);
    end
    if (y<l)
        cum(y:l) = cum(y:l) - (pos(y) - pos(x));
    end
end

end

time_sp ave_spv'];
eval(['save ',data_path3,run_code, '.cum cum;']);

%Plot torcor & cum

plot(time,torcor,time,cum,'b')
ylabel('OCR (deg)');
xlabel('Time (sec)');
title([run_code,' OCR response    red = OCR    blue = CEP']);

```



```

%Sine_fit

% This stupid program belongs to GLAW

% The following code was ruthlessly plagiarized from previous
% work done by Jock R. I. Christie and Lilac Muller.

hold off
clg

scale_accel = 2048/10; % Convert from A/D units.
scale_other = 2048/50;
srate = 200; % Sampling rate in Hz.

fprintf('\nThis program does curve fitting for GLAW.\n');
% Input data is called sled
%if (~exist('tor_new'))
    data_path1 = 'HugeGLAW3:data:.';
    data_path2 = 'HugeGLAW3:.';
    data_path3 = 'HugeGLAW3:CEP:.';
    fprintf('\nYou need to load the data bonehead.\n');
    cc = input('Enter name of data file (6 digits). ','s');
    data_path = [data_path2,cc(3),'.'];
    choose = MENU('Choose a signal','tor','SPV','CEP');
if (choose == 1)
    cc1 = [cc,'.tor'];
    eval(['load ',data_path1,cc1])
    tor = ((tor) - 2048)/scale_other;
    tor_new = tor - tor(1);
elseif (choose == 2)
    cc1 = [cc,'.editedt'];
    eval(['load ',data_path1,cc1])
    tor_new = Edited1_Var;
elseif (choose == 3)
    cc1 = [cc,'.cum'];
    eval(['load ',data_path3,cc1])
    tor_new = cum;
end
    cc2 = [cc,'C4.MAT'];
    eval(['load ',data_path,cc2])
    %load Untitled:matlab.glaw
    %load Untitled:acc

%Convert A/D to g's

if (cc ~= 'gla999')
    acc = ((acc) - mean(acc(1:1000)))/scale_accel;
end

    len = length(tor_new);

%Get Profile from file name.files

```

```

eval(['load ',data_path2,'name.files'])
for roundout = 1:96,
    if (files(roundout,:) == cc)
        latch_on = roundout;
    end
    if (cc == 'gla999')
        latch_on = 3;
    end
end
freq_in = freq(latch_on);
gforce = accel(latch_on);

% freq_in = input('Frequency = ? ');
% gforce = input('Acceleration = ? ');
cycs = 25 * freq_in;
if (freq_in == .26)
    cycs = 7;
end
if (freq_in == .9)
    cycs = 22;
end
%end
%stand = input('Is this a complete run (5 sec to ~30 sec) ? ','s');
stand = 1;
if (stand == 'y')|(stand == 'Y')|(stand == 1)

%Find start of run

check = 0;
for loop1 = 1:1500,
    if (check == 0) & (acc(loop1) > (.5*gforce))
        start = loop1;
        start_time = loop1/srate;
        fprintf('Sled starts at time = %1.5f\n',start_time);
        check = 1;
    end
end

%Find end of run

check = 0;
for loop1 = 8000:-1:5500,
    if (check == 0) & (acc(loop1) > (.5*gforce))
        last_pt = loop1;
        last_pt_time = loop1/srate;
        fprintf('Sled stops at time = %1.5f\n',last_pt_time);
        check = 1;
    end
end

%Find real frequency of run

sled_time = last_pt_time - start_time;

```

```

freq_stim = cycs/sled_time;
fprintf('Real Freq of Sled Motion = %1.5f\n',freq_stim);

else
freq_stim = freq_in;
click_here = input('Do you want to mark the start of the run ? ','s');
if (click_here == 'y')|(click_here == 'Y')
plot(tor_new,'g')
title('Differentiated Ocular Torsion during a sled Run. ');
fprintf('\nClick at the beginning and end of the run with the mouse.\n');
[xx,yy] = ginput(2);
last_pt = max(xx);
start = min(xx);
end
end

scale_gain = 2.0;
%freq_stim=[0.26]; % will need to change this to include 4 freq.
num_freq = length(freq_stim);
step = srates/freq_stim(1); % see below
num_steps = round((last_pt - start)/step);
sum_error = 0;
coeff_sled = zeros(num_steps*num_freq,6);
coeff_tor = zeros(num_steps*num_freq,6);
time = [1:step]/step;
s = sin(2*pi*time);
c = cos(2*pi*time);
k = ones(time);
MEAN = zeros(2,6);
MEAN(1:2,1) = [1 2]';
fake_sled = [zeros(round(start),1); 20*s; 20*s; 20*s; 20*s; 20*s; 20*s; 20*s];
sled = acc;

%Plot SPV, acc

%plot(tor_new,'g')
%hold on
%plot(sled)
%hold off

tor_fit = zeros(start,1);

%Calculate sin, cos, const, amp, and phase of each cycle
% for sled and torsion

for loop = 1:num_steps,
% fprintf('\nStarting Loop # %1.1f\n',loop);
temp_sled = ([s c k]\sled(start+1:start+step)); % formerly included time.
coeff_sled(loop,1) = loop;
coeff_sled(loop,2:4) = temp_sled;
coeff_sled(loop,5) = sqrt(temp_sled(1)^2+temp_sled(2)^2);
coeff_sled(loop,6) = (180/pi)*atan2(temp_sled(2),temp_sled(1));
temp_tor = ([s c k]\tor_new(start+1:start+step));
coeff_tor(loop,1) = loop;

```

```

coeff_tor(loop,2:4) = temp_tor;
coeff_tor(loop,5) = sqrt(temp_tor(1)^2+temp_tor(2)^2);
coeff_tor(loop,6) = (180/pi)*atan2(temp_tor(2),temp_tor(1));

%Correct for > 180 deg angles (not for tor though)

if (coeff_sled(loop,6) < 0)
    coeff_sled(loop,6) = 360 + coeff_sled(loop,6);
end
if (choose == 2) & (coeff_tor(loop,6) < 0)
    coeff_tor(loop,6) = 360 + coeff_tor(loop,6);
end

tor_fit = [tor_fit; coeff_tor(loop,5)*sin(2*pi*time+(coeff_tor(loop,6)*pi/180)];
start = start+step; % increment for next round
end

%Set up values to be saved into .gnpt, .gnpv, or .gnpc (done later)

sled_vals = coeff_sled(:,4:6);
tor_vals = coeff_tor(:,4:6);

%Save curve fit first

tor_fit = [tor_fit; zeros((len-length(tor_fit)),1)];
if (choose == 1)
    var = ['fittedt'];
    out_file = [cc,'fittedt'];
elseif (choose == 2)
    var = ['fittedv'];
    out_file = [cc,'fittedv'];
elseif (choose == 3)
    var = ['fittedc'];
    out_file = [cc,'fittedc'];
end
eval(['var, '= tor_fit;']);
if (choose == 3)
    eval(['save ',data_path3,out_file,' ',var]);
else
    eval(['save ',data_path1,out_file,' ',var]);
end

%Plot curve fit

plot((1:len)/srate,tor_fit,'b');
hold on
%plot((1:len)/srate,tor_new,'g');
%plot((1:len)/srate,tor_fit);
%plot((1:len)/srate,tor_fit,'b');
%plot((1:len)/srate,sled)
title('Curve Fit in Blue, Original Signal in Green. ');
xlabel('Time in seconds. ');
hold off

```

```

%Save constants, amplitudes, and phases for sled & torsion

if (choose == 1)
    out_file2 = [cc,'gnpt'];
elseif (choose == 2)
    out_file2 = [cc,'gnpv'];
elseif (choose == 3)
    out_file2 = [cc,'gnpc'];
end
eval(['save ',data_path1,out_file2,' sled_vals tor_vals;']);

%Print out curve fit info

fprintf('\nTor cycle #   sin   cos   const   amp   phase \n')
disp(coeff_tor)
fprintf('\nSled cycle #   sin   cos   const   amp   phase \n')
disp(coeff_sled)

%Calculate means: sled amp, tor amp, sled gain, tor gain

MEAN(1,3:4) = [mean(coeff_sled(1:num_steps,5)) std(coeff_sled(1:num_steps,5))];
MEAN(2,3:4) = [mean(coeff_tor(1:num_steps,5)) std(coeff_tor(1:num_steps,5))];
MEAN(1,5:6) = [mean(coeff_sled(1:num_steps,6)) std(coeff_sled(1:num_steps,6))];
MEAN(2,5:6) = [mean(coeff_tor(1:num_steps,6)) std(coeff_tor(1:num_steps,6))];

fprintf('\n
           st.dev      st.dev ')
fprintf('\n cycle#   rad/sec gain   gain   phase   phase ')

MEAN

fprintf('\nEstimated Gain = %3.3f \nEstimated Phase = %3.3f degrees.
\n\n',MEAN(2,3)/MEAN(1,3), MEAN(2,5)-MEAN(1,5))

fprintf(cc);
fprintf(' %1.0f\n',choose);
end

```

```
%Find_avg
```

```
%This program finds the averages and standard deviations of the  
%gains and phases for all runs and saves them into a file called  
%values.all
```

```
data_path1 = 'HugeGLAW3:';  
data_path2 = 'HugeGLAW3:data:';  
ccout = 'values.all';
```

```
%Find gains and phases for ALL files
```

```
q1 = input('Do you want to calculate gains and phases for all runs ? ','s');  
%q1 = 'n';  
if (q1 == 'Y')|(q1 == 'y')  
    cc1 = 'name.files';  
    eval(['load ',data_path1,cc1])  
    for loop = 1:96,  
        % for loop = 9:12,  
        %loop = 1;  
        cct = [files(loop,:),'.gnpt'];  
        ccv = [files(loop,:),'.gnpv'];  
        ccc = [files(loop,:),'.gnpc'];
```

```
%Gains and phases for torsion first
```

```
    eval(['load ',data_path2,cct])  
    if (freq(loop) == .26)  
        start = 3;  
        num_cyc = 7;  
    elseif (freq(loop) == .4)  
        start = 3;  
        num_cyc = 10;  
    elseif (freq(loop) == .6)  
        start = 4;  
        num_cyc = 15;  
    elseif (freq(loop) == 1.0)  
        start = 6;  
        num_cyc = 25;  
    elseif (freq(loop) == .9)  
        start = 5;  
        num_cyc = 22;  
    end  
    for loop1 = start:num_cyc,  
        gain(loop1) = (tor_vals(loop1,2))/(sled_vals(loop1,2));  
        phase(loop1) = (tor_vals(loop1,3)) - (sled_vals(loop1,3));  
        freq_each(loop1) = freq(loop);  
    end  
    gaintor = gain(start:num_cyc);  
    phasetor = phase(start:num_cyc);  
    freq_cyc = freq_each(start:num_cyc);  
    gain_t(loop) = mean(gain(start:num_cyc));
```

```

phase_t(loop) = mean(phase(start:num_cyc));
gain_t_std(loop) = std(gain(start:num_cyc));
phase_t_std(loop) = std(phase(start:num_cyc));

```

%Gains and phases for SPV now

```

eval(['load ',data_path2,ccv])
for loop1 = start:num_cyc,
    gain(loop1) = (tor_vals(loop1,2))/(sled_vals(loop1,2));
    phase(loop1) = (tor_vals(loop1,3)) - (sled_vals(loop1,3));
end
gainvel = gain(start:num_cyc);
phasevel = phase(start:num_cyc);
gain_v(loop) = mean(gain(start:num_cyc));
phase_v(loop) = mean(phase(start:num_cyc));
gain_v_std(loop) = std(gain(start:num_cyc));
phase_v_std(loop) = std(phase(start:num_cyc));

```

%Gains and phases for CEP last

```

eval(['load ',data_path2,ccc])
for loop1 = start:num_cyc,
    gain(loop1) = (tor_vals(loop1,2))/(sled_vals(loop1,2));
    phase(loop1) = (tor_vals(loop1,3)) - (sled_vals(loop1,3));
end
gaincep = gain(start:num_cyc);
phasecep = phase(start:num_cyc);
gain_c(loop) = mean(gain(start:num_cyc));
phase_c(loop) = mean(phase(start:num_cyc));
gain_c_std(loop) = std(gain(start:num_cyc));
phase_c_std(loop) = std(phase(start:num_cyc));

```

%Save the cycle gains and phases for each run

```

out_file2 = [files(loop,:),'.cycgnp'];
eval(['save ',data_path2,out_file2,' freq_cyc gaintor phasetor gainvel phasevel gaincep
phasecep;']);

```

end

%Save the averages of all runs into values.all

```

%save values.all files freq accel gain_t gain_t_std phase_t phase_t_std gain_v gain_v_std
phase_v phase_v_std gain_c gain_c_std phase_c phase_c_std;

```

%Recall gains and phases for all runs

else

```

q2 = input('Do you want to recall gains and phases for all runs ? ','s');
if (q2 == 'Y')|(q2 == 'y')
    eval(['load ',data_path1,ccout])
fprintf('\n          Position Position SPV   SPV');
fprintf('\nFile  Freq  Acc  gain  phase  gain  phase\n');
for r = 1:96,

```

```

    fprintf(files(r,:));
fprintf(' %1.2f %1.1f,freq(r),accel(r));
fprintf(' %3.3f %3.3f %3.3f,gain_t(r),phase_t(r),gain_v(r));
fprintf(' %3.3f\n',phase_v(r));

    end
fprintf('\nSTANDARD DEVIATIONS');
fprintf('\nFile          st.dev  st.dev  st.dev  st.dev\n');
    for r = 1:96,
        fprintf(files(r,:));
fprintf('          %3.3f %3.3f,gain_t_std(r),phase_t_std(r));
fprintf(' %3.3f %3.3f\n',gain_v_std(r),phase_v_std(r));
    end
end

%for CEP

    q3 = input('Do you want to recall gains and phases for CEP ? ','s');
    if (q3 == 'Y')|(q3 == 'y')
        eval(['load ',data_path1,ccout])
fprintf('\n          CEP      CEP      st.dev  st.dev');
fprintf('\nFile Freq Acc gain  phase gain  phase\n');
    for r = 1:96,
        fprintf(files(r,:));
fprintf(' %1.2f %1.1f,freq(r),accel(r));
fprintf(' %3.3f %3.3f %3.3f,gain_c(r),phase_c(r),gain_c_std(r));
fprintf(' %3.3f\n',phase_c_std(r));
    end
end

end

```



```

%Plotter

% Initially written by JC, for glaw
% Very much updated since then

%axis([1 2 3 4]);axis;
%subplot;
%hold off;

x = [];
ygt = [];
ypt = [];
ygv = [];
ypv = [];
ygc = [];
ygc = [];

N = 2048;
scale_accel = 2048/10; % Convert from A/D units.
scale_other = 2048/50; % Convert from A/D units.
srate = 200;
fmax = 100;
len = 2*N*fmax/srate;

if (fmax > (srate/2))
    fmax = srate/2;
end

%Load files

ccin = input('Enter name of data file (6 digits). ','s');
%geek = input('Do you want to load data ? ','s');
data_path1 = 'HugeGLAW3:';
data_path2 = 'HugeGLAW3:data:';
data_path3 = 'HugeGLAW3:CEP:';
%data_path1 = 'plus_hd:GLAW:';
%if (geek == 'Y')|(geek == 'y')
if (length(ccin) == 6)
if (ccin(1) == 'g') & (ccin(2) == 'l')
    cc = ccin;
    %cc = input('Enter name of data file (6 digits). ','s');
    data_path = [data_path1,cc(3),':'];

%Load tor and acc files (hor and ver loaded later)

cc1 = [cc, '.tor'];
eval(['load ',data_path2,cc1])
cc4 = [cc, 'C4.MAT'];
eval(['load ',data_path,cc4])

%Convert A/D to degrees or g's

```

```

tor = ((tor) - 2048)/scale_other;
%tor = ((tor) - mean(tor))/scale_other;
torcor = (tor - tor(1));
acc = ((acc) - mean(acc))/scale_accel;

%Get Profile from file values.all
%(These are used for the title of the plot and for choosep = 2)

eval(['load ',data_path1,'values.all'])
for round = 1:96,
    if (files(round,:) == cc)
        latch_on = round;
    end
end
freq_in = freq(latch_on);
gforce = accel(latch_on);

% freq = input('Frequency = ? ');
% gforce = input('Acceleration = ? ');

end
end

file_len = length(acc);
time = (1:file_len)/srate;

%Choose type of plot

choosep = MENU('Choose type of plot','Signal Plot','Gains/Phases Plot','Phase vs.
Time Plot','One Cycle Plot');

%choosep = 2;

%Gains/Phases plots (choice 2)

if (choosep == 2)
    choose2 = MENU('Which do you want plotted','OCR gain','OCR phase','SPV
gain','SPV phase','CEP gain','CEP phase','OCR Bode Plot','SPV Bode Plot');

%choose2 = 6;

%Get all 4 files with the same accel as chosen file

while freq(latch_on) ~= .6
    latch_on = latch_on - 1;
end

ccnow = files(latch_on,1:4);
latch_end = latch_on + 3;
for quad = latch_on:latch_end,
    cc5 = [files(quad,),'cycgnp'];
    eval(['load ',data_path2,cc5]);
    len_file = length(freq_cyc);
    len_y = length(ygt);

```

```

x(len_y+1:len_y+len_file) = freq_cyc;
ygt(len_y+1:len_y+len_file) = gaintor;
ypt(len_y+1:len_y+len_file) = phasetor;
ygv(len_y+1:len_y+len_file) = gainvel;
ypv(len_y+1:len_y+len_file) = phasevel;
ygc(len_y+1:len_y+len_file) = gaincep;
ypc(len_y+1:len_y+len_file) = phasecep;
if (freq(quad) == .26)
    rl_order = 1;
    num_cyc = 5;
elseif (freq(quad) == .4)
    rl_order = 2;
    num_cyc = 8;
elseif (freq(quad) == .6)
    rl_order = 3;
    num_cyc = 12;
elseif (freq(quad) == 1.0)|(freq(quad) == .9)
    rl_order = 4;
    if (freq(quad) == 1.0)
        num_cyc = 20;
    else
        num_cyc = 18;
    end
end
end
g_t(rl_order) = gain_t(quad);
p_t(rl_order) = phase_t(quad);
g_v(rl_order) = gain_v(quad);
p_v(rl_order) = phase_v(quad);
g_c(rl_order) = gain_c(quad);
p_c(rl_order) = phase_c(quad);
g_t_std(rl_order) = gain_t_std(quad);
p_t_std(rl_order) = phase_t_std(quad);
g_v_std(rl_order) = gain_v_std(quad);
p_v_std(rl_order) = phase_v_std(quad);
g_c_std(rl_order) = gain_c_std(quad);
p_c_std(rl_order) = phase_c_std(quad);
hz(rl_order) = freq(quad);
end

if (choose2 == 1)
    plot(x+.01,ygt,'ob')
    hold on
    plot(hz,g_t)
    plot(hz,g_t,'o')
    std_err = g_t_std/(sqrt(num_cyc));
    errorbar(hz,g_t,std_err);
%    errorbar2(hz,g_t,std_err);
    hold off
    ylabel('OCR Gain (deg/g)');
elseif (choose2 == 2)
    plot(x+.01,ypt,'ob')
    hold on
    plot(hz,p_t)
    plot(hz,p_t,'o')

```

```

    std_err = p_t_std/(sqrt(num_cyc));
    errorbar(hz,p_t,std_err);
%   errorbar2(hz,p_t,std_err);
    ylabel('OCR Phase (deg)');
elseif (choose2 == 3)
    plot(x+.01,ygv,'ob')
    hold on
    plot(hz,g_v)
    plot(hz,g_v,'o')
    std_err = g_v_std/(sqrt(num_cyc));
    errorbar(hz,g_v,std_err);
%   errorbar2(hz,g_v,std_err);
    ylabel('SPV Gain (deg/sec/g)');
elseif (choose2 == 4)
    plot(x+.01,ypv,'ob')
    hold on
    plot(hz,p_v)
    plot(hz,p_v,'o')
    std_err = p_v_std/(sqrt(num_cyc));
    errorbar(hz,p_v,std_err);
%   errorbar2(hz,p_v,std_err);
    ylabel('SPV Phase (deg)');
elseif (choose2 == 5)
%   lark = 0.03;
%   plot(x+.01,ygc,'ob')
%   hold on
    plot(hz,g_c)
%   plot(hz+lark,g_c,'o')
    std_err = g_c_std/(sqrt(num_cyc));
    errorbar(hz,g_c,std_err);
%   errorbar(hz+lark,g_c,std_err);
%   errorbar2(hz+lark,g_c,std_err);
%   ylabel('CEP Gain (deg/g)');
elseif (choose2 == 6)
%   plot(x+.01,ypc,'ob')
%   hold on
    plot(hz,p_c)
%   plot(hz+lark,p_c,'o')
    std_err = p_c_std/(sqrt(num_cyc));
    errorbar(hz,p_c,std_err);
%   errorbar2(hz+lark,p_c,std_err);
%   ylabel('CEP Phase (deg)');

```

%Bode Plot

```

elseif (choose2 == 7)|(choose2 == 8)
    ang_hz = hz * (pi/180);
    x_hz = x * (pi/180);
    if (choose2 == 7)
        var_g = g_t;
        pts_g = ygt;
        var_p = p_t;
        pts_p = ypt;
        type_plot = 'OCR';

```

```

else
    var_g = g_v;
    pts_g = ygv;
    var_p = p_v;
    pts_p = ypv;
    type_plot = 'SPV';
end
% axis([0,360,-1*val_top1,val_top1]);
subplot(211), loglog(x_hz,pts_g,'ob')
hold on
subplot(211), loglog(ang_hz,var_g)
hold off
ylabel('Gain');
title([ccnow,' (' ,num2str(gforce),' g) ',type_plot]);
% axis([0,360,-1*val_top2,val_top2]);
subplot(212), semilogx(x_hz,pts_p,'ob')
hold on
subplot(212), semilogx(ang_hz,var_p)
xlabel('Angular Frequency (rad/sec)');
ylabel('Phase');
hold off
% subplot

end

if (choose2 ~= 7)&(choose2 ~= 8)
% xlabel('Frequency (Hz)');
% title([ccnow,' (' ,num2str(gforce),' g)']);
end

%Phase vs Time Plot (choice 3)

elseif (choosep == 3)
    choose3 = MENU('Which do you want plotted','tor','SPV');
    if (choose3 == 1)
        cc2 = [cc,'.gnpt'];
    elseif (choose3 == 2)
        cc2 = [cc,'.gnpv'];
    end
    eval(['load ',data_path2,cc2])
    phase_now = tor_vals(:,3) - sled_vals(:,3);
    plot(phase_now)
    ylabel('Phase (deg)');
    xlabel('Cycles');
    title([cc,' (' ,num2str(freq_in),' Hz ',num2str(gforce),' g)']);

%One Cycle Plot (choice 4)

elseif (choosep == 4)
    phase_t_rad = phase_t(latch_on)*(pi/180);
    phase_v_rad = phase_v(latch_on)*(pi/180);
    time_one = 1.0/freq(latch_on);
    t_time = [0:time_one/100:time_one];
    wt = 360 * freq(latch_on) * t_time;

```

```

acc_one = accel(latch_on) * cos(wt*pi/180);
ocr_one = gain_t(latch_on) * cos(wt*pi/180 + phase_t_rad);
spv_one = gain_v(latch_on) * cos(wt*pi/180 + phase_v_rad);
val_max1 = max(accel(latch_on),gain_t(latch_on));
val_max2 = max(10*accel(latch_on),gain_v(latch_on));
val_top1 = val_max1 + .1 * val_max1;
val_top2 = val_max2 + .1 * val_max2;
axis([0,360,-1*val_top1,val_top1]);
subplot(211), plot(wt,ocr_one)
axis([0,360,-1*val_top2,val_top2]);
subplot(212), plot(wt,spv_one,'g')
hold on;
subplot(212), plot(wt,10*acc_one,'b')
xlabel('blue = acc      red = OCR      green = SPV');
ylabel('SPV');
axis([0,360,-1*val_top1,val_top1]);
subplot(211), plot(wt,acc_one,'b')
ylabel('OCR');
title(['cc,' (, num2str(freq_in), ' Hz ', num2str(gforce), ' g')]);
hold off
% subplot
fprintf('\nPHASES:  OCR: %1.4f deg',phase_t(latch_on));
fprintf('\n      SPV: %1.4f deg\n',phase_v(latch_on));

%Plot Signals (Choice 1)

elseif (choosep == 1)

choose = MENU('Choose a signal for plotting','tor','hor','ver','acc','Corrected
tor','SPV','Fitted tor','Fitted SPV','Cum. Eye Position','Fitted CEP');
ptype = input('Do you want to choose y-axis scale ? ','s');
if (ptype == 'Y')|(ptype == 'y')
    bord1(1) = 0;
    bord1(2) = 40;
    bord1(3) = input('Minimum Y = ? ');
    bord1(4) = input('Maximum Y = ? ');
    axis(bord1);
end
if (choose == 1)
    raw_dat1 = tor;
    plot(time, tor)
    ylabel('OCR (deg)');
elseif (choose == 2)
    cc2 = [cc,'C2.MAT'];
    eval(['load ',data_path,cc2])
    hor = ((hor) - 2048)/scale_other;
    raw_dat1 = hor;
    plot(time, hor)
    ylabel('Horizontal Eye Position (deg)');
elseif (choose == 3)
    cc3 = [cc,'C3.MAT'];
    eval(['load ',data_path,cc3])
    ver = ((ver) - 2048)/scale_other;
    raw_dat1 = ver;

```

```

    plot(time, ver)
    ylabel('Vertical Eye Position (deg)');
elseif (choose == 4)
    raw_dat1 = acc;
    plot(time, acc)
    ylabel('Acceleration (g)');
elseif (choose == 5)
    raw_dat1 = torcor;
    plot(time, torcor)
    ylabel('OCR (deg)');
elseif (choose == 6)
    cc2 = [cc, '.editedt'];
    eval(['load ', data_path2, cc2])
    raw_dat1 = Edited1_Var;
    plot(time, Edited1_Var)
    ylabel('Slow Phase Velocity (deg/sec)');
elseif (choose == 7)
    cc2 = [cc, '.fittedt'];
    eval(['load ', data_path2, cc2])
    raw_dat1 = fittedt;
    plot(time, fittedt)
    ylabel('Fitted OCR (deg)');
elseif (choose == 8)
    cc2 = [cc, '.fittedv'];
    eval(['load ', data_path2, cc2])
    raw_dat1 = fittedv;
    plot(time, fittedv)
    ylabel('Fitted SPV (deg/sec)');
elseif (choose == 9)
%   cc2 = [cc, '.editedt'];
%   eval(['load ', data_path2, cc2])
%   spp(1) = Edited1_Var(1) * (1/200);
%   for rub = 2:length(Edited1_Var),
%       spp(rub) = spp(rub-1) + (Edited1_Var(rub) * (1/200));
%   end
    cc2 = [cc, '.cum'];
    eval(['load ', data_path3, cc2])
    raw_dat1 = cum;
    plot(time, cum)
    ylabel('Cum. Eye Position (deg)');
elseif (choose == 10)
    cc2 = [cc, '.fittedc'];
    eval(['load ', data_path3, cc2])
    raw_dat1 = fittedc;
    plot(time, fittedc)
    ylabel('Fitted CEP (deg)');
end

xlabel('Time (sec)');
title([cc, ' (', num2str(freq_in), ' Hz ', num2str(gforce), ' g)']);
if (ptype == 'Y')|(ptype == 'y')
    axis;
end

```

```
%Plot acc also
```

```
duo = input('Do you want acc plotted ? ','s');  
if (duo == 'Y')|(duo == 'y')  
    scal = input('Scale Factor (default = 3) = ? ');  
    if (isempty(scal) == 1)  
        scal = 3;  
    end  
    acc2 = acc*scal;  
    hold on;  
    plot(time, acc2,':')  
    hold off;  
end
```

```
%Plot beginning and ending lines
```

```
quiz1 = input('Do you want start & finish lines ? ','s');  
if (quiz1 == 'Y')|(quiz1 == 'y')  
    line_it = linspace(-20,20);  
    %Find start of run  
    check = 0;  
    for loop1 = 1:1500,  
        if (check == 0) & (acc(loop1) > (.5*gforce))  
            start_time = loop1/srate;  
            check = 1;  
        end  
    end  
    %Find end of run  
    check = 0;  
    for loop1 = 8000:-1:5500,  
        if (check == 0) & (acc(loop1) > (.5*gforce))  
            last_pt_time = loop1/srate;  
            check = 1;  
        end  
    end  
    x_pos1 = start_time*ones(line_it);  
    x_pos2 = last_pt_time*ones(line_it);  
    % if (freq_in == 0.26)  
    % x_pos2 = (5+7/0.26)*ones(line_it);  
    % elseif (freq_in == 0.9)  
    % x_pos2 = (5+22/0.9)*ones(line_it);  
    % end  
    hold on;  
    plot(x_pos1,line_it,'--')  
    plot(x_pos2,line_it,'--')  
    hold off;  
end
```

```
%Plot offset lines (only for tor and torcor)
```

```
if (choose == 1)|(choose == 5)  
    quiz2 = input('Do you want offset line ? ','s');  
    if (quiz2 == 'Y')|(quiz2 == 'y')  
        line_it = linspace(-5,45);
```



```

    cc2 = [cc,'.gnpt'];
    eval(['load ',data_path2,cc2])
    offset1 = tor_vals(:,1);
    if (choose == 1)
        offset1 = offset1 + tor(1);
    end
    offset_avg = mean(offset1);
    y_pos = offset_avg*ones(line_it);
    hold on;
    plot(line_it,y_pos,'--')
    hold off;
end
end

%Frequency Response (Y/N)

yorn = input('Do you want to plot frequency response ? ','s');
if (yorn == 'Y')|(yorn == 'y')

%RMS Noise

geeky = input('Do you want to find RMS noise ? ','s');
if (geeky == 'Y')|(geeky == 'y')
    rem = sqrt(sum((raw_dat1.*raw_dat1))/length(raw_dat1));
    fprintf('\n\nThe noise has an rms amplitude of %4.4f \n',rem);
end

%Plot Frequency Response

g1 = fft(raw_dat1,2*N);
mag = abs(g1(1:N));
freak = (srate*(0:N-1)/(2*N));
plot(freak(1:len),mag(1:len)); % FFT response
title('FFT response of coils, sampled at 200 Hertz. ');
xlabel('Frequency (Hz)');

%Zoom Plot

jric = input('Do you want a zoom plot ? ','s');
if (jric == 'Y')|(jric == 'y')
    bord2(1) = 0;
    %bord2(2) = 1;
    bord2(2) = input('Maximum X = ? ');
    bord2(3) = 0;
    bord2(4) = input('Maximum Y = ? ');
    axis(bord2);
    plot(freak(1:len),mag(1:len)); % FFT response
    title('FFT response of coils, sampled at 200 Hertz. ');
    xlabel('Frequency (Hz)');
    axis;
end
end

end %ends choose2 loop

```

```

%Curve_fit

%fits least squares line to OCR, SPV, or CEP data

data_path1 = 'HugeGLAW3:';
data_path2 = 'HugeGLAW3:data:';

x = [];
ygt = [];
ypt = [];
ygv = [];
ypv = [];
ygc = [];
ygc = [];

%hold off
%clg

num_times=input('How many files -- 1 or 2? ');

eval(['load ',data_path1,'values.all'])

for loopy = 1:num_times,

ccin = input('Enter name of data file (6 digits). ','s');
if (length(ccin) == 6)
if (ccin(1) == 'g') & (ccin(2) == 'l')
    cc(loopy,:) = ccin;

%Get Profile from file values.all (loaded earlier)

    for roundout = 1:96,
        if (files(roundout,:) == cc(loopy,:))
            latch_on = roundout;
        end
    end
    gforce(loopy) = accel(latch_on);

%Get all 4 files with the same accel as chosen file

    while freq(latch_on) ~= .6
        latch_on = latch_on - 1;
    end
    latch_end = latch_on + 3;
    for quad = latch_on:latch_end,
        cc1 = [files(quad,),'cycgnp'];
        eval(['load ',data_path2,cc1]);
        len_file = length(freq_cyc);
        len_y = length(ygt);
        x(len_y+1:len_y+len_file) = freq_cyc;
        ygt(len_y+1:len_y+len_file) = gaintor;
        ypt(len_y+1:len_y+len_file) = phasetor;
    end
end

```

```

    ygv(len_y+1:len_y+len_file) = gainvel;
    ypv(len_y+1:len_y+len_file) = phasevel;
    ygc(len_y+1:len_y+len_file) = gaincep;
    ypc(len_y+1:len_y+len_file) = phasecep;
end
end
end

if (loopy == 1)

choose = MENU('Which do you want to work with?','OCR gain','OCR phase','SPV
gain','SPV phase','CEP gain','CEP phase');

end

if (choose == 1)
    y = ygt;
    y_ax = 'OCR Gain (deg/g)';
elseif (choose == 2)
    y = ypt;
    y_ax = 'OCR Phase (deg)';
elseif (choose == 3)
    qqin = input('Do you want rotation velocity divided out? ','s');
    if (qqin == 'y')|(qqin == 'Y')
        y = ygv./(360*x);
        y_ax = 'Corrected SPV Gain';
    else
        y = ygv;
        y_ax = 'SPV Gain (deg/s/g)';
    end
elseif (choose == 4)
    y = ypv;
    y_ax = 'SPV Phase (deg)';
elseif (choose == 5)
    y = ygc;
    y_ax = 'CEP Gain (deg/g)';
elseif (choose == 6)
    y = ypc;
    y_ax = 'CEP Phase (deg)';
end

%Find and plot least squares fit line

% hold off
% clg
    A=[x' ones(y)'];
    coef=A\y';
    b=coef(1);
slope(loopy) = b;
    a=coef(2);
interc(loopy) = a;
xplot=[-100 100];
    yplot=a + b*xplot;
ymax = max(y);

```

```

ymax_plot = ymax + .1 * ymax;
% axis([0,1.2,0,20]);
if (loopy == 1)
    plot(x,y,'+');
    hold on
    plot(xplot,yplot)
    xlabel('Frequency');
    ylabel(y_ax);
    string=sprintf('slope1 = %1.3f   intercept1 = %1.3f\n',b,a);
    text(.11,.8,string,'sc');
elseif (loopy == 2)
    plot(x-.01,y,'ob');
    hold on
    plot(xplot,yplot,'b')
    title([cc(1,:),' (red pluses) vs. ',cc(2,:),' (blue circles)']);
    string=sprintf('slope2 = %1.3f   intercept2 = %1.3f\n',b,a);
    text(.11,.75,string,'sc');
end
if (num_times == 1)
% title([cc(1,1:4),' (',num2str(gforce(1)), ' g)']);
end
%prtsc

%Perform t-test on lines
%This assumes that data is normally distributed

%t-values
t(41) = 2.020;
t(43) = 2.018;

    y_cap=a + b*x;
    x_ave=mean(x);
    len=length(y);
    y_sum=0;
    x_sum=0;
    for j=1:len
        y_sum=y_sum + (y(j)-y_cap(j))^2;
        x_sum=x_sum + (x(j)-x_ave)^2;
    end
% variance=y_sum/len;
c_interval=sqrt(y_sum/((len-2)*x_sum));
% sd_slope(loopy) = c_interval*sqrt(len);
se_int = sqrt((y_sum/(len-2))*(1/len+((x_ave^2)/x_sum)));
% sd_int(loopy) = se_int*sqrt(len);
lambda=sqrt(len-2)*b*sqrt(x_sum)/sqrt(y_sum);
arg = len - 2;
if (arg ~= 43)&(arg ~= 41)
    t(arg)=input('enter t(.025) value ');
end
if (lambda > t(arg))|(lambda < (-1.0 * t(arg)))
    fprintf('\nSlope is Significant\n\n');
else
    fprintf('\nSlope is Not Significant\n\n');
end

```

```

a_minus(loopy) = a - t(arg)*se_int;
a_plus(loopy) = a + t(arg)*se_int;
b_minus(loopy) = b - t(arg)*c_interval;
b_plus(loopy) = b + t(arg)*c_interval;
if (loopy == 1)
    string=sprintf('CI1 = %1.3f to %1.3f\n',b_minus(loopy),b_plus(loopy));
    text(.11,.65,string,'sc');
elseif (loopy == 2)
    string=sprintf('CI2 = %1.3f to %1.3f\n',b_minus(loopy),b_plus(loopy));
    text(.11,.6,string,'sc');
end

ygt = [];

end                %ends loopy

%See if the two lines are comparable

if (num_times == 2)

    if ((slope(1)>b_minus(2))&(slope(1)<b_plus(2)))
        if ((interc(1)>a_minus(2))&(interc(1)<a_plus(2)))
            fprintf('\nLines are comparable\n\n');
        else
            fprintf('\nIntercepts are not comparable\n\n');
        end
    elseif ((slope(2)>b_minus(1))&(slope(2)<b_plus(1)))
        if ((interc(2)>a_minus(1))&(interc(2)<a_plus(1)))
            fprintf('\nLines are comparable\n\n');
        else
            fprintf('\nIntercepts are not comparable\n\n');
        end
    else
        fprintf('\nLines are not comparable\n\n');
    end

end

hold off

```

%T-test

%Performs a t-test on the inputed data

```
data_path1 = 'HugeGLAW3:';  
eval(['load ',data_path1,'values.all'])
```

%F and t values

```
F(4,4) = 9.6;  
F(4,7) = 5.52;  
F(4,11) = 4.28;  
F(4,17) = 3.66;  
F(4,19) = 3.56;  
F(7,4) = 9.07;  
F(7,7) = 4.99;  
F(7,11) = 3.76;  
F(7,17) = 3.16;  
F(7,19) = 3.05;  
F(11,11) = 3.48;  
F(11,17) = 2.87;  
F(11,19) = 2.77;  
F(19,17) = 2.63;  
F(19,19) = 2.53;
```

```
t(1) = 12.706;  
t(2) = 4.303;  
t(3) = 3.182;  
t(4) = 2.776;  
t(5) = 2.571;  
t(6) = 2.447;  
t(7) = 2.365;  
t(8) = 2.306;  
t(9) = 2.262;  
t(10) = 2.228;  
t(11) = 2.201;  
t(12) = 2.179;  
t(13) = 2.160;  
t(14) = 2.145;  
t(15) = 2.131;  
t(16) = 2.120;  
t(17) = 2.110;  
t(18) = 2.101;  
t(19) = 2.093;  
t(20) = 2.086;  
t(21) = 2.080;  
t(22) = 2.074;  
t(23) = 2.069;  
t(24) = 2.064;  
t(25) = 2.060;  
t(26) = 2.056;  
t(27) = 2.052;
```

```

t(28) = 2.048;
t(29) = 2.045;
t(30) = 2.042;
t(31) = 2.040;
t(32) = 2.038;
t(33) = 2.036;
t(34) = 2.034;
t(35) = 2.032;
t(36) = 2.029;
t(37) = 2.027;
t(38) = 2.025;
t(39) = 2.023;
t(40) = 2.021;
t(41) = 2.020;
t(42) = 2.019;
t(43) = 2.018;
t(44) = 2.017;
t(45) = 2.016;
t(46) = 2.015;
t(47) = 2.014;
t(48) = 2.013;
t(49) = 2.012;
t(50) = 2.011;
t(51) = 2.009;
t(52) = 2.008;
t(53) = 2.007;
t(54) = 2.006;
t(55) = 2.005;
t(56) = 2.004;
t(57) = 2.003;
t(58) = 2.002;
t(59) = 2.001;
t(60) = 2.0;

```

```

quiz1 = input('Do you want t-test results? ','s');
if (quiz1 == 'y')|(quiz1 == 'Y')
    out_file = 'stat.sig';
    eval(['load ',data_path1,out_file]);
    for r = 1:288,
        fprintf(file1(r,:));
        fprintf(' ');
        fprintf(file2(r,:));
        % fprintf(' %1.0f %1.0f ',signif(r,1),signif(r,2));
        % fprintf('%1.0f %1.0f',signif(r,3),signif(r,4));
        fprintf(' %1.0f %1.0f\n',signif(r,5),signif(r,6));
    end

```

```
end
```

```

choose = MENU('Which do you want to perform?','t-test on 2 files','t-test on all files');
if (choose == 1)

```

```

    cc1 = input('Enter name of 1st data file (6 digits). ','s');
    cc2 = input('Enter name of 2nd data file (6 digits). ','s');

```

%Get Profile from file values.all

```
for round = 1:96,  
    if (files(round,:) == cc1)  
        flag1 = round;  
    end  
    if (files(round,:) == cc2)  
        flag2 = round;  
    end  
end
```

**%Find number of samples (cycles - 5 sec) in each file
%(Change to 7 and 22 for no removal of first 5 seconds)
%(and remove 5 from (25 - 5))**

```
n1 = (25 - 5) * freq(flag1);  
if (freq(flag1) == .26)  
    n1 = 5;  
end  
if (freq(flag1) == .9)  
    n1 = 18;  
end  
n2 = (25 - 5) * freq(flag2);  
if (freq(flag2) == .26)  
    n2 = 5;  
end  
if (freq(flag2) == .9)  
    n2 = 18;  
end
```

choose = MENU('Which do you want to work with?','OCR gain','OCR phase','SPV gain','SPV phase','CEP gain','CEP phase');

```
if (choose == 1)  
    x1 = gain_t(flag1);  
    s1 = gain_t_std(flag1);  
    x2 = gain_t(flag2);  
    s2 = gain_t_std(flag2);  
elseif (choose == 2)  
    x1 = phase_t(flag1);  
    s1 = phase_t_std(flag1);  
    x2 = phase_t(flag2);  
    s2 = phase_t_std(flag2);  
elseif (choose == 3)  
    x1 = gain_v(flag1);  
    s1 = gain_v_std(flag1);  
    x2 = gain_v(flag2);  
    s2 = gain_v_std(flag2);  
elseif (choose == 4)  
    x1 = phase_v(flag1);  
    s1 = phase_v_std(flag1);  
    x2 = phase_v(flag2);  
    s2 = phase_v_std(flag2);  
elseif (choose == 5)
```



```

x1 = gain_c(flag1);
s1 = gain_c_std(flag1);
x2 = gain_c(flag2);
s2 = gain_c_std(flag2);
elseif (choose == 6)
x1 = phase_c(flag1);
s1 = phase_c_std(flag1);
x2 = phase_c(flag2);
s2 = phase_c_std(flag2);
end

%Test for equality of two variances

if (s1 > s2)
lambda = (s1*s1)/(s2*s2);
else
lambda = (s2*s2)/(s1*s1);
end
fprintf('F(%1.0f,%1.0f)    lambda = %1.4f\n',n1-1,n2-1,lambda);
if (lambda <= F(arg1,arg2))

%For equal variances

s = sqrt(((n1-1)*s1*s1 + (n2-1)*s2*s2)/(n1+n2-2));
lambda1 = (abs(x1 - x2))/(s*sqrt(1/n1 + 1/n2));
fprintf('t(%1.0f)    lambda = %1.4f\n',n1+n2-2,lambda1);
arg3 = n(flag1) + n(flag2) - 2;
if (lambda1 > t(arg3))
fprintf('Significant\n');
else
fprintf('Not Significant\n');
end

%For different variances

else
lambda2 = (abs(x1 - x2))/(sqrt(s1*s1/n1 + s2*s2/n2));
dtop = (s1*s1/n1 + s2*s2/n2)^2;
dbottom = ((s1*s1/n1)^2)/(n1-1) + ((s2*s2/n2)^2)/(n2-1);
d = dtop/dbottom;
arg4 = fix(d);
fprintf('t(%1.4f)    lambda = %1.4f\n',dfix,lambda2);
if (lambda2 > t(arg4))
fprintf('Significant\n');
else
fprintf('Not Significant\n');
end
end

%t-test for all files

elseif (choose == 2)
signif = 0;

```

```
%Fix the 1 out of place file (glb003)
```

```
dummy_file = files(18,:);  
dummy_freq = freq(18);  
dummy_acc = accel(18);  
dummy_gt = gain_t(18);  
dummy_pt = phase_t(18);  
dummy_gv = gain_v(18);  
dummy_pv = phase_v(18);  
dummy_gt_st = gain_t_std(18);  
dummy_pt_st = phase_t_std(18);  
dummy_gv_st = gain_v_std(18);  
dummy_pv_st = phase_v_std(18);
```

```
for dumb = 18:19,  
files(dumb,:) = files(dumb+1,:);  
freq(dumb) = freq(dumb+1);  
accel(dumb) = accel(dumb+1);  
gain_t(dumb) = gain_t(dumb+1);  
phase_t(dumb) = phase_t(dumb+1);  
gain_v(dumb) = gain_v(dumb+1);  
phase_v(dumb) = phase_v(dumb+1);  
gain_t_std(dumb) = gain_t_std(dumb+1);  
phase_t_std(dumb) = phase_t_std(dumb+1);  
gain_v_std(dumb) = gain_v_std(dumb+1);  
phase_v_std(dumb) = phase_v_std(dumb+1);  
end  
files(20,:) = dummy_file;  
freq(20) = dummy_freq;  
accel(20) = dummy_acc;  
gain_t(20) = dummy_gt;  
phase_t(20) = dummy_pt;  
gain_v(20) = dummy_gv;  
phase_v(20) = dummy_pv;  
gain_t_std(20) = dummy_gt_st;  
phase_t_std(20) = dummy_pt_st;  
gain_v_std(20) = dummy_gv_st;  
phase_v_std(20) = dummy_pv_st;
```

```
%Find number of samples (cycles - 5 sec) in each file  
%(Change to 7 and 22 for no removal of first 5 seconds)  
%(and remove 5 from (25 - 5))
```

```
for round = 1:96;  
n(round) = (25 - 5) * freq(round);  
if (freq(round) == .26)  
n(round) = 5;  
end  
if (freq(round) == .9)  
n(round) = 18;  
end  
end
```

```
%Choose files to compare
```

```

%If frequencies are the same, do a paired t-test (since there
%are the same number of samples in each run)
%Otherwise, do unpaired t-test

```

```

count_it = 0;
for loop1 = 1:16:96,
    for loop2 = loop1:loop1+14,
        for loop3 = loop2+1:loop1+15,
            do_it = 0;

```

```

%Unpaired t-test

```

```

    if (loop3 <= loop1+3)
        do_it = 1;
    elseif (loop2 > loop1+3) & (loop3 <= loop1+7)
        do_it = 1;
    elseif (loop2 > loop1+7) & (loop3 <= loop1+11)
        do_it = 1;
    elseif (loop2 > loop1+11) & (loop3 <= loop1+15)
        do_it = 1;

```

```

%Paired t-test

```

```

        elseif (loop3 == loop2+4)
            do_it = 2;
        elseif (loop3 == loop2+8)
            do_it = 2;
        elseif (loop3 == loop2+12)
            do_it = 2;
        end

```

```

    if (do_it == 1)|(do_it == 2)

```

```

        count_it = count_it + 1;
        flag1 = loop2;
        flag2 = loop3;

```

```

        change = 0;

```

```

%Independent t-test

```

```

if (do_it == 1)

```

```

%Want 7, 4 first and 7, 4, 11, 19, 17 last
%(This is for removal of the first five seconds of data)

```

```

    if (n(loop2) == 18)
        change = 1;
    elseif (n(loop2) == 20)
        if (n(loop3) == 18)
            change = 1;
        end
    elseif (n(loop2) == 12)

```

```

        if (n(loop3) ~= 20) & (n(loop3) ~= 18)
            change = 1;
        end
    end
    if (change == 1)
        flag1 = loop3;
        flag2 = loop2;
    end

end

    file1(count_it,:) = files(loop2,:);
    file2(count_it,:) = files(loop3,:);
%    file1(count_it,:) = files(flag1,:);
%    file2(count_it,:) = files(flag2,:);

%Do OCR gain, OCR phase, SPV gain, SPV phase

for choose1 = 1:6,
    if (choose1 == 1)
        x1 = gain_t(flag1);
        s1 = gain_t_std(flag1);
        x2 = gain_t(flag2);
        s2 = gain_t_std(flag2);
    elseif (choose1 == 2)
        x1 = phase_t(flag1);
        s1 = phase_t_std(flag1);
        x2 = phase_t(flag2);
        s2 = phase_t_std(flag2);
    elseif (choose1 == 3)
        x1 = gain_v(flag1);
        s1 = gain_v_std(flag1);
        x2 = gain_v(flag2);
        s2 = gain_v_std(flag2);
    elseif (choose1 == 4)
        x1 = phase_v(flag1);
        s1 = phase_v_std(flag1);
        x2 = phase_v(flag2);
        s2 = phase_v_std(flag2);
    elseif (choose1 == 5)
        x1 = gain_c(flag1);
        s1 = gain_c_std(flag1);
        x2 = gain_c(flag2);
        s2 = gain_c_std(flag2);
    elseif (choose1 == 6)
        x1 = phase_c(flag1);
        s1 = phase_c_std(flag1);
        x2 = phase_c(flag2);
        s2 = phase_c_std(flag2);
    end

%Test for equality of two variances

if (s1 > s2)

```

```

    lambda = (s1*s1)/(s2*s2);
else
    lambda = (s2*s2)/(s1*s1);
end
arg1 = n(flag1) - 1;
arg2 = n(flag2) - 1;
if (lambda <= F(arg1,arg2))
%fprintf('%1.2fn',F(arg1,arg2));

%For equal variances

s = sqrt(((n(flag1)-1)*s1*s1 + (n(flag2)-1)*s2*s2)/(n(flag1)+n(flag2)-2));
lambda1 = (abs(x1 - x2))/(s*sqrt(1/n(flag1) + 1/n(flag2)));
arg3 = n(flag1) + n(flag2) - 2;
if (arg3 > 60)
    signif(count_it,choose1) = arg3;
elseif (lambda1 > t(arg3))
    signif(count_it,choose1) = 1;
end

%For different variances

else
    lambda2 = (abs(x1 - x2))/(sqrt(s1*s1/n(flag1) + s2*s2/n(flag2)));
    dtop = (s1*s1/n(flag1) + s2*s2/n(flag2))^2;
    dbottom = ((s1*s1/n(flag1))^2)/(n(flag1)-1) + ((s2*s2/n(flag2))^2)/(n(flag2)-1);
    d = dtop/dbottom;
    arg4 = fix(d);
    if (arg4 > 60)
        signif(count_it,choose1) = arg4;
    elseif (lambda2 > t(arg4))
        signif(count_it,choose1) = 1;
    end
end

    end        %ends--for choose1 = 1:6,

%Paired t-test

elseif (do_it == 2)

file1(count_it,:) = files(loop2,:);
file2(count_it,:) = files(loop3,:);
in_file1 = [files(loop2,:),'.cycgnp'];
eval(['load ',data_path1,in_file1])
    gaint1 = gaintor;
    phaset1 = phasetor;
    gainv1 = gainvel;
    phasev1 = phasevel;
    gaint1 = gaintor;
    phasec1 = phasecep;
in_file1 = [files(loop3,:),'.cycgnp'];
eval(['load ',data_path1,in_file1])
    gaint2 = gaintor;

```

```

    phaset2 = phasetor;
    gainv2 = gainvel;
    phasev2 = phasevel;
    gainc2 = gaincep;
    phasec2 = phasecep;
    diff(1) = gaint1 - gaint2
    diff(2) = phaset1 - phaset2
    diff(3) = gainv1 - gainv2
    diff(4) = phasev1 - phasev2
    diff(5) = gainc1 - gainc2
    diff(6) = phasec1 - phasec2
    for p_loop1 = 1:6,
        sum1 = 0;
        sum2 = 0;
        for p_loop2 = 1:n(loop2),
            sum1 = sum1 + (diff(p_loop1))^2;
            sum2 = sum2 + diff(p_loop1);
        end
        s_d = sqrt((sum1 - ((sum2^2)/n(loop2)))/(n(loop2)-1));
        lambda = (sum2/n(loop2))/(s_d/sqrt(n(loop2)));
        arg = n(loop2) - 1;
        if (arg > 60)
            signif(count_it,p_loop1) = arg;
        elseif (lambda > t(arg))|(lambda < (-1.0*t(arg)))
            signif(count_it,p_loop1) = 1;
        end
    end

end
end

    end          %ends--if (do_it == 1)
end
end          %ends loop1, loop2, loop3
end

%Save data to file stat.sig

out_file = 'stat.sig';
eval(['save ',data_path1,out_file,' file1 file2 signif;']);

end          %ends choose

```

```
%Bode Fit
```

```
%This program fits a bode plot to the data
```

```
global Data;  
global Data2;
```

```
data_path1 = 'HugeGLAW3:';  
data_path2 = 'HugeGLAW3:data:';
```

```
%Get all Profiles from file values.all
```

```
eval(['load ',data_path1,'values.all'])
```

```
x = [];  
ygt = [];  
ypt = [];  
ygv = [];  
ypv = [];  
ygc = [];  
ypc = [];  
Data = [];
```

```
ygc_26 = [];  
ypc_26 = [];  
ygc_4 = [];  
ypc_4 = [];  
ygc_6 = [];  
ypc_6 = [];  
ygc_1 = [];  
ypc_1 = [];
```

```
all_p1 = 0;  
ques = input('How many sets in the group? ');  
if (ques > 23)
```

```
    ques = 1;  
    all_p1 = 1;
```

```
end
```

```
for quesloop = 1:ques,
```

```
    ccin = input('Enter name of data file (6 digits). ','s');  
    if (length(ccin) == 6)  
        if (ccin(1) == 'g') & (ccin(2) == 'l')  
            cc = ccin;  
        end  
    end  
end
```

```
%Get Profile from file values.all
```

```
for roundout = 1:96,  
    if (files(roundout,:) == cc)  
        latch_on = roundout;
```

```

    end
end

%Get all 4 files with the same accel as chosen file
%(Put the files into frequency order--0.26, 0.4, 0.6, 1.0)

while freq(latch_on) ~= .6
    latch_on = latch_on - 1;
end
latch_end = latch_on + 3;
latch_num = 0;
for quad = latch_on:latch_end,
    if (freq(quad) == 0.26)
        open_it(1,:) = files(quad,:);
    elseif (freq(quad) == 0.4)
        open_it(2,:) = files(quad,:);
    elseif (freq(quad) == 0.6)
        open_it(3,:) = files(quad,:);
    else
        open_it(4,:) = files(quad,:);
    end
end
end

%Bode plot (can also do plot for ALL points)

all_p = 'n';
if (all_p1 == 1)
    all_p = input('Do you want to bode fit all points ? (y/n) ','s');
end
if (all_p == 'Y')|(all_p == 'y')
    loop_fin = 96;
else
    loop_fin = 4;
end

for loopy = 1:loop_fin,
    if (loop_fin == 96)
        cc1 = [files(loopy,:),'.cycgnp'];
    else
        latch_num = latch_num + 1;
        cc1 = [open_it(loopy,:),'.cycgnp'];
    end
    eval(['load ',data_path2,cc1]);
    len_file = length(freq_cyc);
    len_y = length(ygt);
    x(len_y+1:len_y+len_file) = freq_cyc;
    ygt(len_y+1:len_y+len_file) = gaintor;
    ypt(len_y+1:len_y+len_file) = phasetor;
    ygv(len_y+1:len_y+len_file) = gainvel;
    ypv(len_y+1:len_y+len_file) = phasevel;
    ygc(len_y+1:len_y+len_file) = gaincep;
    ypc(len_y+1:len_y+len_file) = phasecep;

%Get mean and Sd for plotting (only for CEP)

```



```

    x_val = [0.26,0.4,0.6,1.0];
    x_val = x_val*(2*pi);

    if (loopy == 1)
        len_y1 = length(ygc_26);
        ygc_26(len_y1+1:len_y1+len_file) = gaincep;
        ypc_26(len_y1+1:len_y1+len_file) = phasecep;
    elseif (loopy == 2)
        len_y1 = length(ygc_4);
        ygc_4(len_y1+1:len_y1+len_file) = gaincep;
        ypc_4(len_y1+1:len_y1+len_file) = phasecep;
    elseif (loopy == 3)
        len_y1 = length(ygc_6);
        ygc_6(len_y1+1:len_y1+len_file) = gaincep;
        ypc_6(len_y1+1:len_y1+len_file) = phasecep;
    else
        len_y1 = length(ygc_1);
        if (freq_cyc(1) == 0.9)
            x_val(4) = 0.9*(2*pi);
        end
        ygc_1(len_y1+1:len_y1+len_file) = gaincep;
        ypc_1(len_y1+1:len_y1+len_file) = phasecep;
    end
end

end          %ends quesloop

%Find avg and Sd of gain and phase for all freq

avg_gc = [mean(ygc_26),mean(ygc_4),mean(ygc_6),mean(ygc_1)];
avg_pc = [mean(ypc_26),mean(ypc_4),mean(ypc_6),mean(ypc_1)];
std_gc = [std(ygc_26),std(ygc_4),std(ygc_6),std(ygc_1)];
std_pc = [std(ypc_26),std(ypc_4),std(ypc_6),std(ypc_1)];

% ypt = ypt*(pi/180);
% ypv = ypv*(pi/180);
x = x*(2*pi);

choose = MENU('Which do you want to work with?','OCR','SPV','CEP');

if (choose == 1)
    y = ygt;
    y_ax = 'OCR Gain (deg/g)';
elseif (choose == 2)
    y = ygv;
    y_ax = 'SPV Gain (deg/s/g)';
elseif (choose == 3)
    y = ygc;
    % y_ax = 'CEP Gain (deg/g)';
    y_ax = 'CEP Gain (db)';
end

Data(:,1) = x';

```

```

Data(:,2) = y';

loglog(x,y,'o')

if (choose == 1)|(choose == 3)
    k = [2; 3];
% k = [.01337; 190]; %for glf106 (comment next line)
    k = fmins('fun1',k,.005)
elseif (choose == 2)
    k = [2; 3];
% k = [.01337; 190]; %for gld102 & glf106 (comment next line)
    k = fmins('fun2',k,.005)
end

for j = 1:length(x),
    A(j,1) = k(1) * sqrt(k(2)^2 + x(j)^2);
end

%Generate Bode Plot for Gain

blowup = input('Do you want to see full bode fit ? ','s');
if (blowup == 'Y')|(blowup == 'y')
    num1 = k(1);
    num2 = k(1) * k(2);
    num = [num1 num2];
    if (choose == 1)|(choose == 3)
        den = [1 0];
    elseif (choose == 2)
        den = 1;
    end
    l = logspace(0,1,100);
% l = logspace(-1,2,100);
% l = logspace(-5,2,200);
    [mag,phase] = bode(num,den,l);
    magdb = 20*log10(mag);
    axis([0,1,-20,20]);
    semilogx(l,magdb)
% loglog(l,mag)
    hold on
    if (choose == 3)
        g_avgdb = 20*log10(avg_gc);
        g_low = avg_gc - std_gc;
        g_lowdb = 20*log10(g_low);
        g_hi = avg_gc + std_gc;
        g_hidb = 20*log10(g_hi);
        lhs = [0.015,0.03,0.05,0.085];
        rhs = [0.02,0.045,0.06,0.11];
        semilogx(x_val,g_avgdb,'o')
% loglog(x_val,avg_gc,'o')

    for i = 1:4,
        blinel = [g_lowdb(i),g_hidb(i)];
        xspot1 = [x_val(i),x_val(i)];
        xtb1 = [x_val(i)-lhs(i),x_val(i)+rhs(i)];

```

```

        ytop1 = [g_hidb(i),g_hidb(i)];
        ybottom1 = [g_lowdb(i),g_lowdb(i)];
        semilogx(xspot1,bline1)
        semilogx(xtb1,ytop1)
        semilogx(xtb1,ybottom1)
    end

    end
%   loglog(x,y,'o')
    xlabel('Frequency (rad/sec)');
    ylabel(y_ax);
%   title([cc,' Bode Fit']);
%   title('Subject A (0.6 g Day 1)');
%   title('Subject E (Day 2 0.6 g Bode Fit)');
%   title('Subject F (Day 1) Bode Fit');
%   title('Subject D Bode Fit');
    title('Bode Fit for all Subjects');
    hold off
end

%Fit phase

q1 = input('Do you want to fit the phase plot ? ','s');
if (q1 == 'Y')|(q1 == 'y')
    if (choose == 1)
        y = ypt;
        y_ax = 'OCR Phase (deg)';
    elseif (choose == 2)
        y = ypv;
        y_ax = 'SPV Phase (deg)';
    elseif (choose == 3)
        y = ypc;
        y_ax = 'CEP Phase (deg)';
    end

    Data(:,2) = y';

    semilogx(x,y,'o')

    if (choose == 1)|(choose == 3)
        p = fmin('funp1',290,1000)
    %   p = fmin('funp1',-1,10)
    elseif (choose == 2)
        p = fmin('funp2',-1,10)
    end

%Find frequency difference between gain calculation and phase calc.

    freq_diff = k(2) - p;
    fprintf('Frequency difference = %1.4f \n',freq_diff);

%Generate Bode Plot for Phase

    blowup = input('Do you want to see full bode fit ? ','s');

```

```

if (blowup == 'Y')|(blowup == 'y')
    num2 = k(1) * p;
    num = [num1 num2];
    [mag2,phase2] = bode(num,den,1);
    axis([0,1,-180,20]);
%    semilogx(1,phase2,'b')
    semilogx(1,phase2,'--')
    hold on
    if (choose == 3)
        semilogx(x_val,avg_pc,'o')
        for i = 1:4,
            bline1 = [avg_pc(i)+std_pc(i),avg_pc(i)-std_pc(i)];
            xspot1 = [x_val(i),x_val(i)];
            xtb1 = [x_val(i)-lhs(i),x_val(i)+rhs(i)];
            ytop1 = [avg_pc(i)+std_pc(i),avg_pc(i)+std_pc(i)];
            ybottom1 = [avg_pc(i)-std_pc(i),avg_pc(i)-std_pc(i)];
            semilogx(xspot1,bline1)
            semilogx(xtb1,ytop1)
            semilogx(xtb1,ybottom1)
        end
    end
%    semilogx(x,y,'o')
    semilogx(1,phase)
    xlabel('Frequency (rad/sec)');
    ylabel(y_ax);
%    title([cc,' Bode Fit']);
%    title('Subject E (Day 2 0.6 g) Bode Fit');
%    title('Subject F (Day 1) Bode Fit');
%    title('Subject D Bode Fit');
    title('Bode Fit for all Subjects');
end

```

```

function f = fun1(k)

%fits the gain function:  $g = k \cdot \sqrt{(wc/w)^2 + 1}$ 
%for OCR & CEP

x = Data(:,1);
y = Data(:,2);

for j = 1:length(x),
    A(j,1) = k(1) * sqrt((k(2)/x(j))^2 + 1);
end

% f is kind of like a standard deviation for all points

f = norm(A-y)/sqrt(length(x));

fprintf('std dev = %1.4f \n',f);

% Statements to plot progress of fitting:

%clg
%loglog(x,A,x,y,'o')
%text(.11,.75,['k = ' num2str(k(1)) ' w = ' num2str(k(2))], 'sc')
%text(.11,.7,['std dev = ' num2str(f)], 'sc')

```

```

function f = fun2(k)

%fits the gain function:  $g = k \cdot \sqrt{wc^2 + w^2}$ 
%for SPV

x = Data(:,1);
y = Data(:,2);

for j = 1:length(x),
    A(j,1) = k(1) * sqrt(k(2)^2 + x(j)^2);
end

% f is kind of like a standard deviation for all points

f = norm(A-y)/sqrt(length(x));

fprintf('std dev = %1.4f \n',f);

% Statements to plot progress of fitting:

%clg
%loglog(x,A,x,y,'o')
%text(.11,.75,['k = ' num2str(k(1)) ' w = ' num2str(k(2))], 'sc')
%text(.11,.7,['std dev = ' num2str(f)], 'sc')

```

```

function f = funp1(p)

%fits the phase function: phase = atan[-(wc/w)]
%for OCR & CEP

x = Data(:,1);
y = Data(:,2);

for j = 1:length(x),
    A(j,1) = (180/pi)*atan(-1*(p/x(j)));
end

% f is kind of like a standard deviation for all points

f = norm(A-y)/sqrt(length(x));

fprintf('std dev = %1.4f \n',f);

% Statements to plot progress of fitting:

%clg
%loglog(x,A,x,y,'o')
%text(.11,.75,['k = ' num2str(k(1)) ' w = ' num2str(k(2))], 'sc')
%text(.11,.7,['std dev = ' num2str(f)], 'sc')

```

```

function f = funp2(p)

%fits the phase function: p = atan(w/wc)
%for SPV

x = Data(:,1);
y = Data(:,2);

for j = 1:length(x),
    A(j,1) = (180/pi)*atan(x(j)/p);
end

% f is kind of like a standard deviation for all points

f = norm(A-y)/sqrt(length(x));

fprintf('std dev = %1.4f \n',f);

% Statements to plot progress of fitting:

%clg
%loglog(x,A,x,y,'o')
%text(.11,.75,['k = ' num2str(k(1)) ' w = ' num2str(k(2))], 'sc')
%text(.11,.7,['std dev = ' num2str(f)], 'sc')

```

References

- Alston, A. E. (1989): An integrated system for tracking of landmarks on video data: TOMAS, the torsional ocular movement analysis system. S. M. Thesis, MIT, Cambridge.
- Arrott, A. P. (1982): Torsional eye movements in man during linear accelerations. S. M. Thesis, MIT, Cambridge.
- Arrott, A. P. (1985): Ocular torsion and gravito-inertial force. PhD Thesis, MIT, Cambridge.
- Arrott, A. P., Young, L. R. (1981): Torsional eye movements in man during linear accelerations upon emerging from weightlessness (abstract).
- Arrott, A. P., Young, L. R. (1986): MIT/Canadian vestibular experiments on the Spacelab-1 mission: 6. Vestibular reactions to lateral acceleration following ten days of weightlessness. Experimental Brain Research 64:347-357.
- Baarsma, E. A., Collewijn, H. (1975): Eye movements due to linear accelerations in the rabbit. Journal of Physiology 245:227-247.
- von Baumgarten, R. J., Thulmer, R. (1978): A model for vestibular function in altered gravitational states. In: Holmquist, R. (Ed.), COSPAR Life Sciences Space Research, Vol XVII. Oxford, NY. Pergamon Press. 161-170.
- von Baumgarten, R. J. (1986): European vestibular experiments on the Spacelab-1 mission: 1. Overview. Experimental Brain Research 64:239-246.
- Clarke, A. H., Teiwes, W., Scherer, H. (1990): Video-oculography - an alternative method for measurement of three-dimensional eye movements. Proceedings of the 5th European Conference on Eye Movements (in press).
- Cohen, L. A. (1961): Role of eye and neck proprioceptive mechanisms in body orientation and motor coordination. Journal of Neurophysiology 24:1-11.
- Collewijn, H., van der Mark, F., Jansen, T. C. (1975): Precise recording of human eye movement. Vision Research 15:447-450.
- Collewijn, H., van der Steen, J., Ferman, L., Jansen, T. C. (1985): Human ocular counterroll: Assessment of static and dynamic properties from electromagnetic scleral coil recordings. Experimental Brain Research 59:185-196.
- Curthoys, I. S., Moore, S. T., Diamond, S. G., Markham, C. H., Wade, S., Halmagyi, G. M. (1991): A direct comparison of video and photographic methods of measuring ocular torsion. Vision Research (in press).
- Diamond, S. G., Markham, C. H., Simpson, N. E., Curthoys, I. S. (1979): Binocular counterrolling in humans during dynamic rotation. Acta Otolaryngol 87:490-498.
- Diamond, S. G., Markham, C. H. (1983): Ocular counterrolling as an indicator of vestibular otolith function. Neurology 33:1460-1469.

- Diamond, S. G., Markham, C. H. (1988): Ocular torsion in upright and tilted positions during hypo- and hypergravity of parabolic flight. Aviation, Space, and Environmental Medicine 59:1158-1162.
- Diamond, S. G., Markham, C. H., Money, K. E. (1990): Instability of ocular torsion in zero gravity: possible implications for space motion sickness. Aviation, Space, and Environmental Medicine 61:899-905.
- Diamond, S. G., Markham, C. H. (1990): Prediction of space motion sickness susceptibility by disconjugate eye torsion in parabolic flight. Aviation, Space, and Environmental Medicine 62:201-205.
- Edelman, E. R., Oman, C. M., Cavallerano, A. A., Schluter, P. S. (1981): Video measurements of torsional eye movement using a soft contact lens technique. "OMS-81", Conference on the Oculomotor System, Caltech, January.
- Fluur, E. (1975): A comparison between subjective and objective recording of ocular counterrolling as a result of tilting. Acta Otolaryngol 79:111-114.
- Galoyan, V. R., Zenkin, G. M., Petrov, A. P. (1976): Investigation of the torsional movements of the human eyes. I. Some special aspects of the torsional movements of tilting the head towards the shoulder. Biofizika 21:570-577.
- Graybiel, A., Miller, E. F. II, Billingham J., Waite, R., Berry, C. A., Dietlein, L. F. (1967): Vestibular experiments in Gemini flights V and VII. Aerospace Medicine 38:360-370.
- Hannen, R. A., Kabrisky, M., Replogle, C. R., Hartzler, V. L., Roccaforte, P. A. (1966): Experimental determination of a portion of the human vestibular response through measurement of eyeball counterroll. IEEE Transactions on Biomedical Engineering Vol. BME-13:65-70.
- Howard, I. P., Evans, J. A. (1963): The measurement of eye torsion. Vision Research 3:447-455.
- Hunter, J. (1786): Observations on Certain Parts of the Animal Economy, London.
- Kenyon, R. V., Lichtenberg, B. K. (1981): Measurement of ocular counterrolling (OCR) by polarized light. Proceedings of SPIE (International Society for Optical Engineering), Trapani, G. B., ed., San Diego, August, 1981.
- Kenyon, R. V. (1985): A soft contact lens search coil for measuring eye movements. Vision Research 25:1629-1633.
- Kirienko, N. M., Money, K. E., Landolt, J. P., Graybiel, A., Johnson, W. H. (1984): Clinical testing of the otoliths: a critical assessment of ocular counterrolling. The Journal of Otolaryngology 13(5):281-288.
- Kompanajetz, S. (1928): Investigations on the counterrolling of the eyes in optimum head-positions. Acta Otolaryngologica 12:332-350.
- Lackner, J. R., Graybiel, A., Johnson, W. H., Money, K. E. (1987): Asymmetric otolith function and increased susceptibility to motion sickness during exposure to variations in

gravitoinertial acceleration level. Aviation, Space, and Environmental Medicine 58:652-657.

Lichtenberg, B. K. (1979): Ocular counterrolling induced in humans by horizontal accelerations. Sc.D. Thesis, MIT, Cambridge.

Lichtenberg, B. K., Young, L. R., Arrott, A. P. (1982): Human ocular counterrolling induced by varying linear accelerations. Experimental Brain Research 48:127-136.

Malan, A. R. (1985): Characteristics of optokinetic torsion in upright and supine orientations. S. M. Thesis, MIT, Cambridge.

Merfeld, D. M. (1990): Spatial orientation in the squirrel monkey: an experimental and theoretical investigation. PhD Thesis, MIT, Cambridge.

Miller, E. F. II (1961): Counterrolling of the human eyes produced by head tilt with respect to gravity. Acta Otolaryngol (Stockh) 54:479-501.

Miller, E. F. II, Fregly, A. R., van den Brink, G., Graybiel, A. (1965): Visual localization of the horizontal as a function of body tilt up to +90° from gravitational vertical. USN School of Aviation Medicine Report 942, Pensacola, Florida. 1-23.

Miller, E. F. II, Graybiel, A. (1965): Otolith function as measured by ocular counterrolling. In: The Role of the Vestibular Organs in the Exploration of Space. NASA SP-77. Washington D. C. 121-131.

Miller, E. F. II (1966): Ocular counterrolling. In: Wolfson, R. J. (Ed.), The Vestibular System and Its Diseases. Philadelphia, Pa. University of Pennsylvania Press. 229-241.

Miller, E. F. II, Graybiel, A., Kellogg, R. S. (1966): Otolith organ activity within Earth standard, one-half standard and zero gravity environments. Aerospace Medicine 37:399-403.

Miller, E. F. II, Fregly, A. R., Graybiel, A. (1968): Visual horizontal perception in relation to otolith function. American Journal of Psychology 81:488-496.

Miller, E. F. II (1969): Evaluation of otolith organ function by means of ocular counterrolling measurements. Naval Aerospace Medical Institute Report 1063, Pensacola, Florida. 1-14.

Miller, E. F. II, Graybiel, A. (1971): Effect of gravitational force upon ocular counterrolling. Journal of Applied Physiology 31:697-700.

Miller, E. F. II, Graybiel, A. (1972): Ocular counterrolling measured during eight hours of sustained body tilt. Naval Aerospace Medical Research Laboratory Report 1154, Pensacola, Florida. 1-10.

Money, K. E., Kirienko, N. M., Watt, D. G. D., Johnson, W. H., Markham, C. H., Diamond, S. G. (1987): Ocular torsion in response to hypogravity. Symposium on Vestibular Organs and Altered Force Environment, Oct. 1987.

Okuda, N., Tsunekawa, F., Awaya, S., Watanabe, S. (1989): Analysis of motor response with respect to the time course in cyclofusion. Acta Soc. Ophthalmol. Jpn. 93(2):218-226.

- Oman, C. M. (1987): Spacelab experiments on space motion sickness. Acta Astronautica 15(1):55-66.
- Oman, C. M., Young, L. R., Watt, D. G. D., Money, K. E., Lichtenberg, B. K., Kenyon, R. V., Arrott, A. P. (1988): MIT/Canadian spacelab experiments on vestibular adaptation and space motion sickness. In: Hwang, J. C., Daunton, N. G., Wilson, V. J. (Eds.), Basic and Applied Aspects of Vestibular Function. Hong Kong. Hong Kong University Press. 183-192.
- Parker, J. A., Kenyon, R. V., Young, L. R. (1985): Measurement of torsion from multitemporal image of the eye using digital signal processing techniques. IEEE Transactions on Biomedical Engineering Vol. BME-32, No. 1:28-36.
- Petrov, A. P., Zenkin, G. M. (1973): Torsional eye movements and constancy of the visual field. Vision Research 13:2465-2476.
- Robinson, D. A. (1963): A method of measuring eye movement using a scleral search coil in a magnetic field. IEEE Transactions on Bio-Medical Electronics 10:137-145.
- Tse, M. I. (1990): Ocular torsion during linear acceleration in space. B. S. Thesis, MIT, Cambridge.
- Tsunekawa, F., Okuda, N., Awaya, S., Watanabe, S. (1989): Study of dynamic counterrolling of the eye--Quantitative analysis of effects by visual and vestibular systems. Acta Soc. Ophthalmol. Jpn. 93(2):227-233.
- Vieville, T., Masse, D. (1987): Ocular counter-rolling during active head tilting in humans. Acta Otolaryngol (Stockh) 130:280-290.
- Vogel, H., Kass, J. R. (1986): European vestibular experiments on the Spacelab-1 mission: 7. Ocular counterrolling measurements pre- and post-flight. Experimental Brain Research 64:284-290.
- Walton, W. G. (1948): Compensatory cyclo-torsion accompanying head tilt. American Journal of Optometry 25:525-534.
- Wapner, S., Werner, H., Chandler, K. A. (1951): Experiments of sensory-tonic field theory of perception: 1. Effect of extraneous stimulation on visual perception of verticality. Journal of Experimental Psychology 42:341-345.
- Woellner, R. C., Graybiel, A. (1959): Counterrolling of the eyes and its dependence on the magnitude of gravitational or inertial force acting laterally on the body. Journal of Applied Physiology 14:632-634.
- Yakovleva, I. Y., Kornilova, L. N., Syrykh, G. D., Tarasov, I. K., Alekseyev, V. N. (1980): Results of studies of vestibular function and spatial perception in the crews of the first and second expeditions aboard Salyut-6 station. Kosm Biologiya 1:19-23.
- Yakovleva, I. Y., Kornilova, L. N., Tarasov, I. K., Alekseyev, V. N. (1981): Results of the study of the vestibular apparatus and the functions of the perception of space in cosmonauts (pre- and post-flight observations). NASA Technical Memorandum, NASA TM-76485, Washington D.C.

Yakovleva, I. Y., Kornilova, G. D., Tarasov, I. K., Alekseyev, V. N. (1982): Results of studies of cosmonauts' vestibular function and spatial perception. Kosm Biologiya 16:20-26.

Yamanobe, S., Taira, S., Morizono, T., Yagi, T., Kamio, T. (1990): Eye movement analysis system using computerized image recognition. Archives of Otolaryngology--Head & Neck Surgery 116:338-341.

Young, L. R., Meiry, J. L. (1975): A revised dynamic otolith model. Aerospace Medicine 39:606-608.

Young, L. R., Sheena, D. (1975): Eye-movement measurement techniques. American Psychologist 30:315-330.

Young, L. R., Lichtenberg, B. K., Arrott, A. P., Crites, T. A., Oman, C. M., Edelman, E. R. (1981): Ocular torsion on earth and in weightlessness. Annals of the New York Academy of Sciences 374:80-92.

Young, L. R. (1984): Perception of the body in space: mechanisms. (Chapter 22) Handbook of Physiology - The Nervous System III, American Physiological Society, Smith, Ian Darian, ed. 1023-1066.

Young, L. R., Oman, C. M., Watt, D. G. D., Money, K. E., Lichtenberg, B. K., Kenyon, R. V., Arrott, A. P. (1986a): MIT/Canadian vestibular experiments on the Spacelab-1 mission: 1. Sensory adaptation to weightlessness and readaptation to one-g: an overview. Experimental Brain Research 64:291-298.

Young, L. R., Shelhamer, M., Modestino, S. (1986b): MIT/Canadian vestibular experiments on the Spacelab-1 mission: 2. Visual vestibular tilt interaction in weightlessness. Experimental Brain Research 64:299-307.

Zeevi, Y. Y., Ish-Shalom, J. (1982): Measurement of eye movement with a ferromagnetic contact ring. IEEE Transactions on Biomedical Engineering Vol. BME-29, No. 7:511-522.